

ZooKeys anniversary: 10 years of leadership toward open-access publishing of zoological data and establishment at Pensoft of like-minded sister journals across the biodiversity spectrum

Terry Erwin¹, Pavel Stoev^{2,3}, Lyubomir Penev^{3,4}

1 National Museum of Natural History, Smithsonian Institution, Washington DC, USA **2** National Museum of Natural History, Bulgarian Academy of Sciences, Sofia, Bulgaria **3** Pensoft Publishers, Sofia, Bulgaria **4** Institute of Biodiversity and Ecosystem Research, Bulgarian Academy of Sciences, Sofia, Bulgaria

Corresponding author: *Lyubomir Penev* (info@pensoft.net)

Received 2 July 2018 | Accepted 2 July 2018 | Published 4 July 2018

<http://zoobank.org/ECBF809C-179A-49ED-AFD7-CB36C1C3D874>

Citation: Erwin T, Stoev P, Penev L (2018) ZooKeys anniversary: 10 years of leadership toward open-access publishing of zoological data and establishment at Pensoft of like-minded sister journals across the biodiversity spectrum. *ZooKeys* 770: 1–8. <https://doi.org/10.3897/zookeys.770.28105>

Today we publish issue 770 of our dear cutting-edge journal ZooKeys! It has been exactly ten years since the launch of the journal on 4 July 2008 that emanated from a delightful breakfast at the Entomological Society of America meeting in December 2007 in San Diego, California, when our Managing Editor and founder of Pensoft, Lyubomir Penev, proposed the idea to Terry Erwin, our Editor-in-Chief. The journal's tenth birthday is a great occasion to trace back its development and achievements since then, which has exceeded far beyond that initial breakfast dream of two colleagues enjoying the southern California sun.

ZooKeys was the first of Pensoft's open-access journals, set up to accelerate research and free information exchange in taxonomy, phylogeny, biogeography and evolution of animals. Starting as a taxonomic journal, it quickly expanded to other zoology-related sciences, such as ecology, molecular biology, genomics, evolutionary biology, palaeontology, behavioural science, bioinformatics etc. Later, ZooKeys was followed by the journals PhytoKeys and MycoKeys in the field of plant and fungal

systematics, which are now also amongst the most popular titles in their respective domains. The journal has been thriving since its inception and is currently considered as one of the most prolific and liked Open Access journals in zoology. ZooKeys started with merely 32 published papers in 2008 and just in a few years time became a mega-journal, publishing 466 papers in 2011. The number has been increasing since reaching its maximum in 2016–581 (Table 1, Fig. 1). To date, the journal has received more than 5200 submissions (no accurate data available for 2008–2010) and published 4103 articles, including 110 monographs. The number of published pages increased from 657 in 2008 to 16582 in 2016. The average rejection rate for the period 2016–2017 was around 25%, which we believe is optimal and sustainable for a primarily taxonomic journal.

Table 1. Total number of submitted manuscripts published articles, and printed pages since 2008. No accurate data for number of submissions 2008–2010.

Year	Submitted manuscripts	Published articles	Published pages
2008		32	657
2009		155	3738
2010		180	4871
2011	510	466	11145
2012	442	435	12205
2013	505	488	13382
2014	554	525	14178
2015	674	501	12634
2016	713	581	16582
2017	841	482	14091
2018 (as of 27 June 2018)	460	258	7250
Total	4904	4103	110733

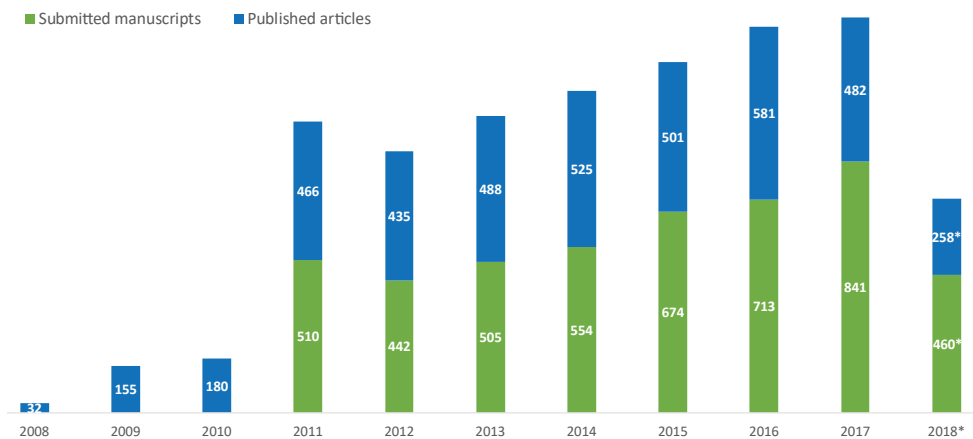


Figure 1. Growth of submitted manuscripts and published articles in ZooKeys from 2008 to 2018 (*until 27.6.2018).

The number of all authors publishing in ZooKeys is 5720 (ZooBank, courtesy of Richard Pyle, Bishop Museum, Honolulu) from altogether 131 countries. The highest numbers come first from China, then United States of America, followed by Brazil, Italy, Germany and Canada in that order. The Impact Factor of ZooKeys continues to grow, starting at 0.517 and currently it is 1.079.

Altogether, 8977 new species-group, 650 new genus-group and 45 new family-group taxa have been published in the journal since its launch (Table 2, Fig. 2) (Zoo-

Table 2. New taxa published in ZooKeys, registered in ZooBank (courtesy of Richard Pyle).

Year	Family	Genus	Species
2008	0	3	24
2009	1	51	360
2010	4	42	384
2011	12	90	840
2012	3	52	851
2013	3	75	1660
2014	3	71	1445
2015	2	50	911
2016	4	86	1035
2017	6	85	935
2018	7	45	532
Total	45	650	8977

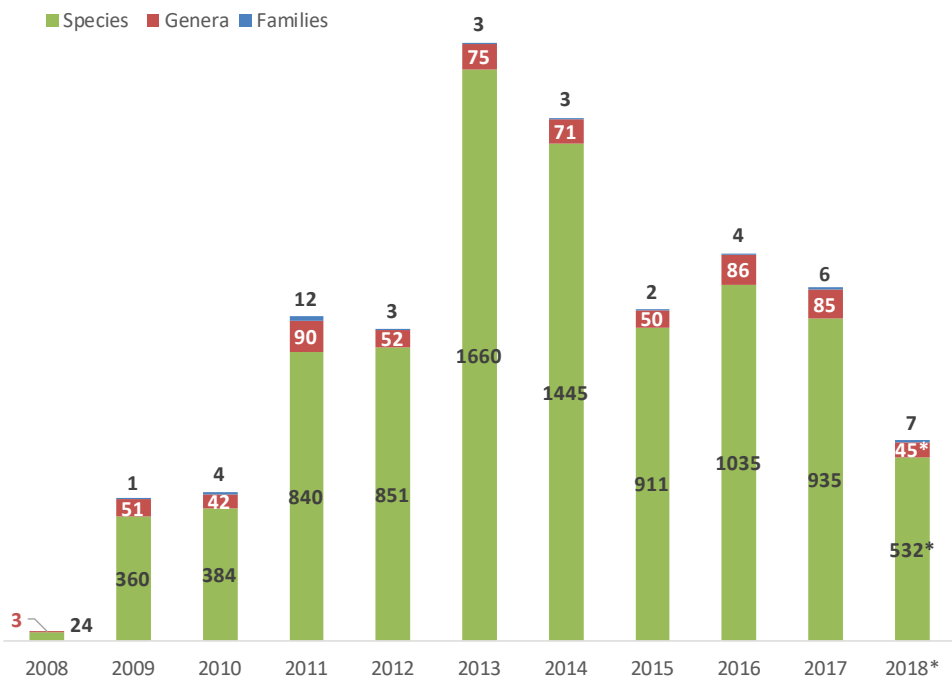


Figure 2. New taxa published in ZooKeys, registered in ZooBank (courtesy of Richard Pyle; *until 27.6.2018).

Bank, 29 June 2018, courtesy of Richard Pyle). This makes 9672 new taxa in total or 967.2 new taxa per year. This places ZooKeys as the second most prolific journal in Zoological Systematics after Zootaxa which began publishing in 2001.

Pensoft has been heavily investing in the technological advancement of its journals. A list of the most significant technologies implemented by its flagship ZooKeys in the recent years to facilitate editors, reviewers and authors is available in Table 3.

Over the past ten years, ZooKeys published a variety of papers on systematic zoology, including several world records, such as the deepest cave-dwelling centipede, the tiniest free-living insect and the smallest land snail. The journal also served as a platform for many of the world's first-of-a-kind, like the first insect description solely from photographs, the first study supported by crowd-funding in Japan, the first-of-a-kind footage of shrimp filter-feeding at depth of a 4826 m in the Mariana Trench, the first amphibious centipede and the second fossil beetle found on Antarctica. While ZooKeys is regularly featured in the annual "Top 10 species" by the International Institute for Species Exploration, in 2017, there were two species published in the journal, which appeared on the list: the world's second leggiest millipede – the 414-legged *Illacme tobini* and the first known amphibious centipede *Scolopendra cataracta*.

Table 3. New technological solutions implemented in the journal.

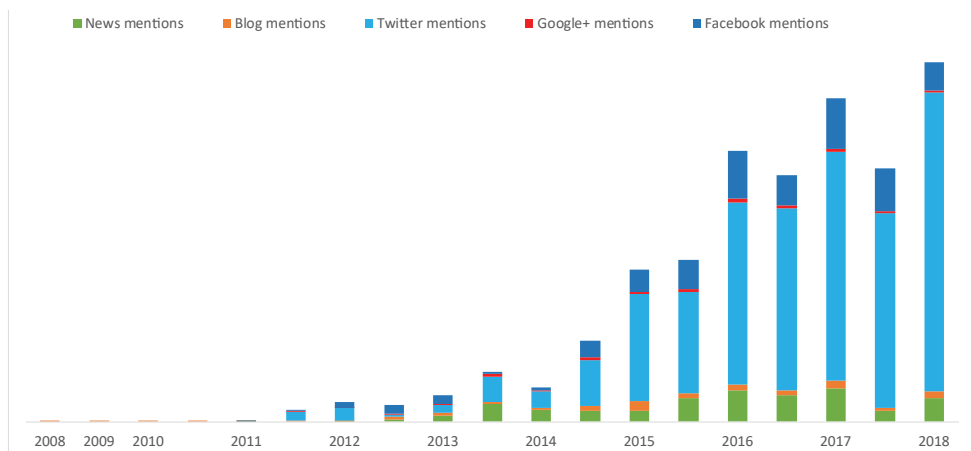
Feature	For the benefit of:	Link	Use
Automatic registrations of reviews at Publons	Reviewers and Editors	https://publons.com	Publons helps reviewers and editors get recognition for every review they make for the journal.
Dimensions	Authors, editors, administrators, publisher	https://www.dimensions.ai	Powerful tracker of citations; provides ranking of given research in a given field
Scopus CiteScore Metrics	Authors, editors, administrators, publisher	https://www.scopus.com/sourceid/19700170477	Interactive tool providing information on journal's performance
Export of published figures & supplementary materials to Biodiversity Literature Repository at ZENODO	Authors, data scientists, community in general	https://zenodo.org/communities/biosyslit/?page=1&size=20	Increases visibility and traceability of article and sub-article elements
Hypothes.is	Authors, readers	http://hypothes.is	Annotations on selected texts from the published article

The ten most viewed ZooKeys articles can be seen in Table 4.

Thanks to the collaboration between Pensoft and Altmetric, it is possible to track the popularity of each article published in ZooKeys within the public domain (Fig. 3). Provided the DOI link of a paper is included in an online publication, its citations from across a diverse range of both conventional and social online media platforms, including news outlets, blogs, Twitter, Facebook, Google+,

Table 4. ZooKeys articles by number of views.

Article	Nr of uniques views	Nr of total views
Helgen et al. (2013) Taxonomic revision of the olingos (<i>Bassaricyon</i>), with description of a new species, the Olinguito	56191	62724
Ledford et al. (2012) An extraordinary new family of spiders from caves in the Pacific Northwest (Araneae, Trogloraptoridae, new family)	51668	55952
Bouchard et al. (2011) Family-Group Names In Coleoptera (Insecta)	32446	36687
Nazari (2016) Review of <i>Neopalpa</i> Povolný, 1998 with description of a new species from California and Baja California, Mexico (Lepidoptera, Gelechiidae)	24654	33103
Sereno (2012) Taxonomy, morphology, masticatory function and phylogeny of heterodontosaurid dinosaurs	27168	30394
Hagedorn et al. (2011) Creative Commons licenses and the non-commercial condition: Implications for the re-use of biodiversity information	27173	29685
Winterton et al. (2012) A charismatic new species of green lacewing discovered in Malaysia (Neuroptera, Chrysopidae): the confluence of citizen scientist, online image database and cybertaxonomy	25329	28429
Laciny et al. (2018) <i>Colobopsis explodens</i> sp. n., model species for studies on “exploding ants” (Hymenoptera, Formicidae), with biological notes and first illustrations of males of the <i>Colobopsis cylindrica</i> species-group	22795	28258
Hamilton et al. (2016) Taxonomic revision of the tarantula genus <i>Aphonopelma</i> Pocock, 1901 (Araneae, Mygalomorphae, Theraphosidae) within the United States	14515	25536
Wizen and Gasith (2011) Predation of amphibians by carabid beetles of the genus <i>Epomis</i> found in the central coastal plain of Israel	24477	14876
Total	281087	282920

**Figure 3.** Total number of ZooKeys mentions in social media and popular magazines (Altmetric, June 2018).

Reddit etc., are all visible in the article menu to give our readers a clear insight into the attention and interest which the research published in the journal brings about beyond academia.

The description of a species of moth named after then US President-elect Donald Trump is an excellent example for a study with remarkable popularity across platforms (available from <https://doi.org/10.3897/zookeys.646.11411>). While as many as 964 tweets have been registered (likely many more, given that the count only registers the tweets featuring the DOI link to the paper), a total of 124 international news outlets (again, many have gone unaccounted) ran the story, including The Washington Post, FOX News, CNN, BBC News, The Independent, The Huffington Post, Ria.RU (RIA Novosti), Gazeta.ru, Wired (Italy), Le Figaro, Die Welt, Spiegel, National Geographic Australia, The Japan Times and The Hindustan Times.

A more recent study describing a new species of exploding ant was not only featured in 89 news stories by news outlets from around the world, such as National Geographic, The New York Times, FOX News, BBC News, Sky News, The Guardian, ABC, Gazeta.ru, Publico, Stern, El Pais, The Hindu, but also tweeted along with its DOI as many as 52 times. In fact, the remarkable species was even ‘assigned’ with its own hashtag (#ExplodingAnts) to trigger further discussion and engagement over the social media platform.

Table 5 shows the top ten ZooKeys papers, which attracted the largest media interest, according to data available from the global science news service EurekAlert.

Table 5. The top ten ZooKeys papers that attracted largest media interest.

Article	Press release	Media coverage
Brannoch and Svenson (2016) A new genus and species (<i>Cornuocollis</i> gen. n. <i>masoalensis</i> sp. n.) of praying mantis from northern Madagascar (Mantodea, Iridopterygidae, Tropicodantinae)	A new species and genus of ‘horned necked’ praying mantis from a French museum collection	Science Daily, Physorg, Health Medicine Network
Chen et al. (2017) <i>Oreoglanis hponkanensis</i> , a new sisorid catfish from north Myanmar (Actinopterygii, Sisoridae)	Chinese scientists discover a new species of catfish in Myanmar	Science Newline, Physorg, Health Medicine Network, I4U News
Laciny et al. (2018) <i>Colobopsis explodens</i> sp. n., model species for studies on “exploding ants” (Hymenoptera, Formicidae), with biological notes and first illustrations of males of the <i>Colobopsis cylindrica</i> species-group	New ant species from Borneo explodes to defend its colony	New York Times, The Guardian, Galileo, Gazeta.ru, New York Daily News
Van Dam et al. (2016) Four new species of <i>Trigonopterus</i> Fauvel from the island of New Britain (Coleoptera, Curculionidae)	New curiously scaled beetle species from New Britain named after ‘Star Wars’ Chewbacca	The Scientist Magazine, Fox News, Science News
Savary and Bryson Jr (2016) <i>Pseudouroctonus maidu</i> , a new species of scorpion from northern California (Scorpiones, Vaejovidae)	A new scorpion from California reveals hidden biodiversity in the Golden State	Science Daily, Physorg, Health Medicine Network
Hamilton et al. (2016) Taxonomic revision of the tarantula genus <i>Aphonopelma</i> Pocock, 1901 (Araneae, Mygalomorphae, Theraphosidae) within the United States	New tarantula named after Johnny Cash among 14 spider species found in the United States	CNN, BBC News, CBS News, The Guardian, The Columbian, Spiegel, Gazeta.ru
Guayasamin et al. (2017) A marvelous new glassfrog (Centrolenidae, Hyalinobatrachium) from Amazonian Ecuador	New species of frog from the Neotropics carries its heart on its skin	BBC Focus Science & Technology, Science News, Gazeta.ru, Science Daily

Article	Press release	Media coverage
Nazari (2017) Review of <i>Neopalpa</i> Povolný, 1998 with description of a new species from California and Baja California, Mexico (Lepidoptera, Gelechiidae)	New species of moth named in honor of Donald Trump ahead of his swearing-in as president	CNN, CBS News, The Straits Times, The Independent, Gazeta.ru, Focus, Galileo
Goto and Ishikawa (2016) <i>Borniopsis mortoni</i> sp. n. (Heterodonta, Galeommatoidea, Galeommataeidae sensu lato), a new bivalve commensal with a synaptid sea cucumber from Japan	Living together in mud: New bivalve species dwelling on a sea cucumber discovered in Japan	Nature World News, Health Medicine Network, Physorg
Marek et al. (2016) A new species of <i>Illacme</i> Cook & Loomis, 1928 from Sequoia National Park, California, with a world catalog of the Siphonorhinidae (Diplopoda, Siphonophorida)	New species of extremely leggy millipede discovered in a cave in California	New York Times, Washington Post, Gizmodo, Nature World News, Le Point

Apart from their remarkable findings, some of our authors have also been given a place in the spotlight by the news media. A Skype interview with Dr Chris Hamilton – the discoverer of the Johnny Cash tarantula – was aired live on Sky News, while Dr Vazrick Nazari, who added the name *Neopalpa donaldtrumpi* to the scientific records, was interviewed on BBC Radio 5. A podcast with Alice Laciny, the lead author of the study describing the exploding ant *Colobopsis explodens*, where she explains the curious behaviour of the new species and in the background, the ant is seen to actually defend itself against a larger offender, was made available on BBC News.

New species described in ZooKeys enjoy the attention of their celebrity namesakes, as well. Earlier this year, shortly after a water beetle discovered in Borneo was named after the famous actor and environmentalist Leonardo DiCaprio, the insect appeared on his profile photo on Facebook – an act, which was itself reported by several news outlets, including the Daily Mail, W Magazine and La Republica.

The success of ZooKeys would not be possible without the help of our authors, reviewers, subject editors, and readers, to whom we are very very thankful!

References

- Bouchard P, Bousquet Y, Davies A, Alonso-Zarazaga M, Lawrence J, Lyal C, Newton A, Reid C, Schmitt M, Slipinski A, Smith A (2011) Family-Group Names In Coleoptera (Insecta). ZooKeys 88: 1–972. <https://doi.org/10.3897/zookeys.88.807>
- Brannoch SK, Svenson GJ (2016) A new genus and species (*Cornucollis* gen. n. *masoalensis* sp. n.) of praying mantis from northern Madagascar (Mantodea, Iridopterygidae, Tropicodrominae). ZooKeys 556: 65–81. <https://doi.org/10.3897/zookeys.556.6906>
- Chen X-Y, Qin T, Chen Z-Y (2017) *Oreoglanis hponkanensis*, a new sisorid catfish from north Myanmar (Actinopterygii, Sisoridae). ZooKeys 646: 95–108. <https://doi.org/10.3897/zookeys.646.11049>

- Goto R, Ishikawa H (2016) *Borniopsis mortoni* sp. n. (Heterodonta, Galeommatoidea, Galeommatidae *sensu lato*), a new bivalve commensal with a synaptid sea cucumber from Japan. ZooKeys 615: 33–45. <https://doi.org/10.3897/zookeys.615.8125>
- Guayasamin JM, Cisneros-Heredia DF, Maynard RJ, Lynch RL, Culebras J, Hamilton PS (2017) A marvelous new glassfrog (Centrolenidae, Hyalinobatrachium) from Amazonian Ecuador. ZooKeys 673: 1–20. <https://doi.org/10.3897/zookeys.673.12108>
- Hagedorn G, Mietchen D, Agosti D, Penev L, Berendsohn W, Hobern D (2011) Creative Commons licenses and the non-commercial condition: Implications for the re-use of biodiversity information. ZooKeys 150: 127–149. <https://doi.org/10.3897/zookeys.150.2189>
- Hamilton CA, Hendrixson BE, Bond JE (2016) Taxonomic revision of the tarantula genus *Aphonopelma* Pocock, 1901 (Araneae, Mygalomorphae, Theraphosidae) within the United States. ZooKeys 560: 1–340. <https://doi.org/10.3897/zookeys.560.6264>
- Helgen K, Pinto M, Kays R, Helgen L, Tsuchiya M, Quinn A, Wilson D, Maldonado J (2013) Taxonomic revision of the olingos (*Bassaricyon*), with description of a new species, the Olinguito. ZooKeys 324: 1–83. <https://doi.org/10.3897/zookeys.324.5827>
- Laciny A, Zettel H, Kopchinskiy A, Pretzer C, Pal A, Salim KA, Rahimi MJ, Hoenigsberger M, Lim L, Jaitrong W, Druzhinina IS (2018) *Colobopsis explodens* sp. n., model species for studies on “exploding ants” (Hymenoptera, Formicidae), with biological notes and first illustrations of males of the *Colobopsis cylindrica* group. ZooKeys 751: 1–40. <https://doi.org/10.3897/zookeys.751.22661>
- Ledford J, Griswold C, Audisio T (2012) An extraordinary new family of spiders from caves in the Pacific Northwest (Araneae, Trogloraptoridae, new family). ZooKeys 215: 77–102. <https://doi.org/10.3897/zookeys.215.3547>
- Marek PE, Krejca JK, Shear WA (2016) A new species of *Illacme* Cook & Loomis, 1928 from Sequoia National Park, California, with a world catalog of the Siphonorhinidae (Diplopoda, Siphonophorida). ZooKeys 626: 1–43. <https://doi.org/10.3897/zookeys.626.9681>
- Nazari V (2017) Review of *Neopalpa* Povolný, 1998 with description of a new species from California and Baja California, Mexico (Lepidoptera, Gelechiidae). ZooKeys 646: 79–94. <https://doi.org/10.3897/zookeys.646.11411>
- Savary WE, Bryson Jr RW (2016) *Pseudouroctonus maidu*, a new species of scorpion from northern California (Scorpiones, Vaejovidae). ZooKeys 584: 49–59. <https://doi.org/10.3897/zookeys.584.6026>
- Sereno P (2012) Taxonomy, morphology, masticatory function and phylogeny of heterodontosaurid dinosaurs. ZooKeys 226: 1–225. <https://doi.org/10.3897/zookeys.226.2840>
- Van Dam MH, Laufa R, Riedel A (2016) Four new species of *Trigonopterus* Fauvel from the island of New Britain (Coleoptera, Curculionidae). ZooKeys 582: 129–141. <https://doi.org/10.3897/zookeys.582.7709>
- Winterton S, Guek H, Brooks S (2012) A charismatic new species of green lacewing discovered in Malaysia (Neuroptera, Chrysopidae): the confluence of citizen scientist, online image database and cybertaxonomy. ZooKeys 214: 1–11. <https://doi.org/10.3897/zookeys.214.3220>
- Wizen G, Gasith A (2011) Predation of amphibians by carabid beetles of the genus *Epomis* found in the central coastal plain of Israel. ZooKeys 100: 181–191. <https://doi.org/10.3897/zookeys.100.1526>

Red Sea Opisthobranchia 5: new species and new records of chromodorids from the Red Sea (Heterobranchia, Nudibranchia, Chromodorididae)

Nathalie Yonow¹

¹ Swansea Ecology Research Team, Department of Biosciences, Swansea University, Singleton Park, Swansea SA2 8PP, Wales, United Kingdom

Corresponding author: *Nathalie Yonow* (N.Yonow@swansea.ac.uk)

Academic editor: *B.W. Hoeksema* | Received 2 May 2018 | Accepted 22 June 2018 | Published 4 July 2018

<http://zoobank.org/C9EE5B4A-F377-4B49-824A-D4DE9F8FE92F>

Citation: Yonow N (2018) Red Sea Opisthobranchia 5: new species and new records of chromodorids from the Red Sea (Heterobranchia, Nudibranchia, Chromodorididae). *ZooKeys* 770: 9–42. <https://doi.org/10.3897/zookeys.770.26378>

Abstract

This is the fifth publication describing species of sea slug heterobranchs, originally based on collections from the Red Sea by the author on four expeditions carried out in 1983 and 1990, with the addition of specimens subsequently collected by underwater photographers who were stimulated by the book "Sea Slugs of the Red Sea". So much material has been amassed that only the new species and new Red Sea records of chromodorids are described in this paper, with an appendix listing specimens of previously recorded species. Three new species are described in detail and illustrated, belonging to three different genera: *Doriprismatica kyanomarginata* sp. n., *Glossodoris kahlbrocki* sp. n., and *Goniobranchus pseudodecorus* sp. n. One western Pacific species is recorded for the first time in the Red Sea, *Goniobranchus collingwoodi* (Rudman, 1987). The nomenclature of *Verconia sudanica* is discussed and stabilised.

Keywords

Biogeography, nomenclature, sea slug, taxonomy, western Indian Ocean

Introduction

This series of papers is based on the author's collections in the Red Sea during four expeditions in 1983 and 1990. Subsequent material was provided by underwater photographers and scientists who collected in the Egyptian Red Sea. The first two papers based on these collections dealt with the families Phyllidiidae (Yonow 1988) and Chromodorididae (Yonow 1989), while the third dealt with the families Polyceridae, Gymnodorididae, Discodorididae, and Hexabanchidae as well as a few Sacoglossa and Aglajidae (Yonow 1990). A fourth publication described some non-nudibranch sea slugs, the Cephalaspidea, Anaspidea, and Pleurobranchida, as well as the dendronotid and aeolid nudibranchs (Yonow 2000). The book "Sea Slugs of the Red Sea" (Yonow 2008) provided some further photographic evidence (some with specimens) of described and undescribed species, as well as a detailed checklist of species with all records (pp 59–61 for chromodorids), and a section entitled *Incertae Sedis* with photographs of unidentified chromodorids (p 275). Finally, new records and a new species are illustrated in Yonow (2015).

This paper deals with a number of specimens collected by the author but also includes specimens collected more recently by Johann Hinterkircher, Sven Kahlbrock, Ernesto Mollo, and Ángel Valdés in the northern Red Sea. One species each of the genera *Chromodoris*, *Diversidoris*, *Doriprismatica*, *Glossodoris*, *Hypselodoris*, *Miamira*, and *Verconia*, and two species of *Goniobranchus* are described. All species are illustrated with colour figures of living specimens, and any literature relating to the species in question is included in the synonymy for each species, focusing on the Red Sea, Arabian Sea, Persian Gulf, and the wider north-western Indian Ocean.

An appendix lists the additional material pertaining to species already described in the previous papers by this author on the Red Sea, with additional notes and illustrations.

Materials and methods

The materials and methods employed in the field (for the author's own collections) and in the laboratory have been described previously and are not repeated here (Yonow 1989, 1998, 1990, 2000). The material collected by Sven Kahlbrock and Johann Hinterkircher was not always measured or relaxed before preservation, but it was almost always accompanied by series of colour photographs. As soon as the material arrived, it was processed in the laboratory by microscope examination, and measurements, notes, and drawings were made of most preserved specimens; specimens were then placed in vials of 70% alcohol with labels. In the 'Material' section of each species and in the appendix, specimen refers to a collected animal which has been preserved, registered, and lodged in the Senckenberg Museum, Frankfurt, Germany, while individual refers to an animal which was photographed, some measured alive, but not collected or preserved.

The images of preserved specimens, or their parts, were taken with a Kodak M530 camera and/or an Olympus BX40F4 dissecting microscope. The buccal mass of each specimen was extracted and processed in 10% sodium hypochlorite solution for 1–2 minutes to dissolve connective and muscle tissue, leaving only the radula and the jaws. The features of the radulae and jaws of each species were analysed under the stereomicroscope and scanning electron microscope (JSM). Specimens, SEM stubs, colour slides, and digital images of the material included in this paper will be deposited in the Senckenberg Museum.

Species accounts

Chromodoris strigata Rudman, 1982

Plates 1, 2

Chromodoris strigata Rudman, 1982: 229–231, figs 17E, 26, 27 (Queensland, Australia; Madagascar); Yonow 2008: 60, 177 (Gulf of Eilat, Red Sea); Tibiriçá et al. 2017: 20, fig. 4C (Mozambique).

Material. Al Fanadir, near Hurghada, Egypt, 26 May 2009, two specimens 16 and 11 mm (preserved), leg. and photograph S Kahlbrock; numerous photographs from northern Egypt, S Kahlbrock and J Hinterkircher; numerous photographs from the Creek, Jeddah, Saudi Arabia, 1970–1994, W Pridgen.

Description. Photographs of the two specimens depict the typical pattern of this species in the Red Sea (Plate 1): there are five black lines on the dorsum, which are broken in the larger specimen. These have the characteristic blurring behind the rhinophores, mid-body, and in front of the gills where the white in-between the black is darker. The middle black line runs anteriorly between the rhinophores. There is a submarginal white band completely encircling the notum followed by a thicker yellow-orange margin. The dorsal surface of the foot is white with an orange margin and two black lines that do not meet on the tip of the tail. The rhinophores are either the same colour as the mantle margin or more orange. The 7–9 gills are the same colour as the rhinophores and bear white pinnules.

The body is elongate and the mantle is raised just in front of the gills. The foot is long and pointed, nearly 1/3 to 1/4 longer than the body length. The rhinophores are long and pointed, usually held out over the sides of the body in a characteristic manner. The gills are simply pinnate, arranged in a circle that is not closed posteriorly; the last gills are smaller than the others.

Distribution. These are the first specimen records from the Red Sea but an individual had been photographed in the Jeddah area of the Red Sea as early as the 1970's (W Pridgen pers. comm., Plate 2). There are subsequent records from the northern Red Sea (Yonow 2008) although it was never collected by the author. *Chromodoris strigata* is a western Pacific species with one record in the Indian Ocean, from Mozam-



Plate 1. *Chromodoris strigata* Rudman, 1982, photograph S Kahlbrock.



Plate 2. *Chromodoris strigata* Rudman, 1982, photograph E Pridgen.

bique (Tibirić et al. 2017). The records from India as *C. strigata* (and *C. colemani*, Sreeraj et al. 2012) are most likely *C. cf. hamiltoni* Rudman, 1977 as are the records from Mozambique of *Chromodoris* sp. 1 (Tibirić et al. 2017).

***Diversidoris flava* (Eliot, 1904)**

Plate 3

Chromodoris flava Eliot, 1904: 399 (Zanzibar).

Noumea flava – Rudman 1986c: 379, figs 1–4, 17 (GBR, Australia); Yonow 2008: 61, 199 (Red Sea).

Material. Sha'ab steel tank, Hurghada, Egypt, 01 Aug 2009, 35 m depth on sand, one specimen 4.5 × 2.5 mm (preserved), leg. and photographs S Kahlbrock; photographs only, vicinity of Hurghada, Egypt, 08 Nov 2013, 13 July 2015, S Kahlbrock.

Description. This species is unmistakable with its lemon yellow body bordered by a deep red line along the margin (Plate 3). The rhinophores and unipinnate gills are also lemon yellow. The tiny specimen was damaged, and missing most of its right rhinophore. The left rhinophore bears 12 lamellae, the edges of which are opaque white in life.

The mantle margin of the preserved specimen is of uniform thickness, as is its edge despite the implications of the red line along the margin in life, which is thicker at intervals in the photographs.

Remarks. *Diversidoris flava* was originally described in *Noumea* but it has been shown by Johnson and Gosliner (2012) that it belongs to the genus *Diversidoris*, separated from *Noumea* (= *Verconia*; see Remarks below for *Verconia sudanica*).

Distribution. This is the first specimen record of *Diversidoris flava* in the Red Sea; it was previously recorded by a series of photographs also from Eilat in the northern Red Sea no earlier than 2005 (Eilat, Yonow 2008: 199; <http://www.seaslugforum.net/find/21083>). The distribution of this somewhat uncommon species is throughout the Indo-Pacific Ocean; its recent arrival in the Red Sea may be due to shipping.

***Doriprismatica kyanomarginata* sp. n.**

<http://zoobank.org/3BA982AA-5F86-4089-8D8B-9534A07F6284>

Figure 1, Plate 4

Colourful sea slugs – Dipper and Woodward 1989: 58.

Glossodoris cincta – Yonow 2008: 60, 188 (lower left large and upper small photographs only, Egypt) (**non** *Casella cincta* Bergh, 1888).

Type material. HOLOTYPE SMF 349566: Egypt, Sept/Oct 1995, one specimen 21 × 13 mm preserved (still retains dorsal mottling, marginal bands clearly broad ochre, light blue line, black margin on both sides), leg. Á Valdés & E Mollo (HU-M7), radula already dissected, used for SEM.



Plate 3. *Diversidoris flava* (Eliot, 1904), photograph S Kahlbrock.



Plate 4. *Doriprismatica kyanomarginata* sp. n., photograph G Brown (non-type).

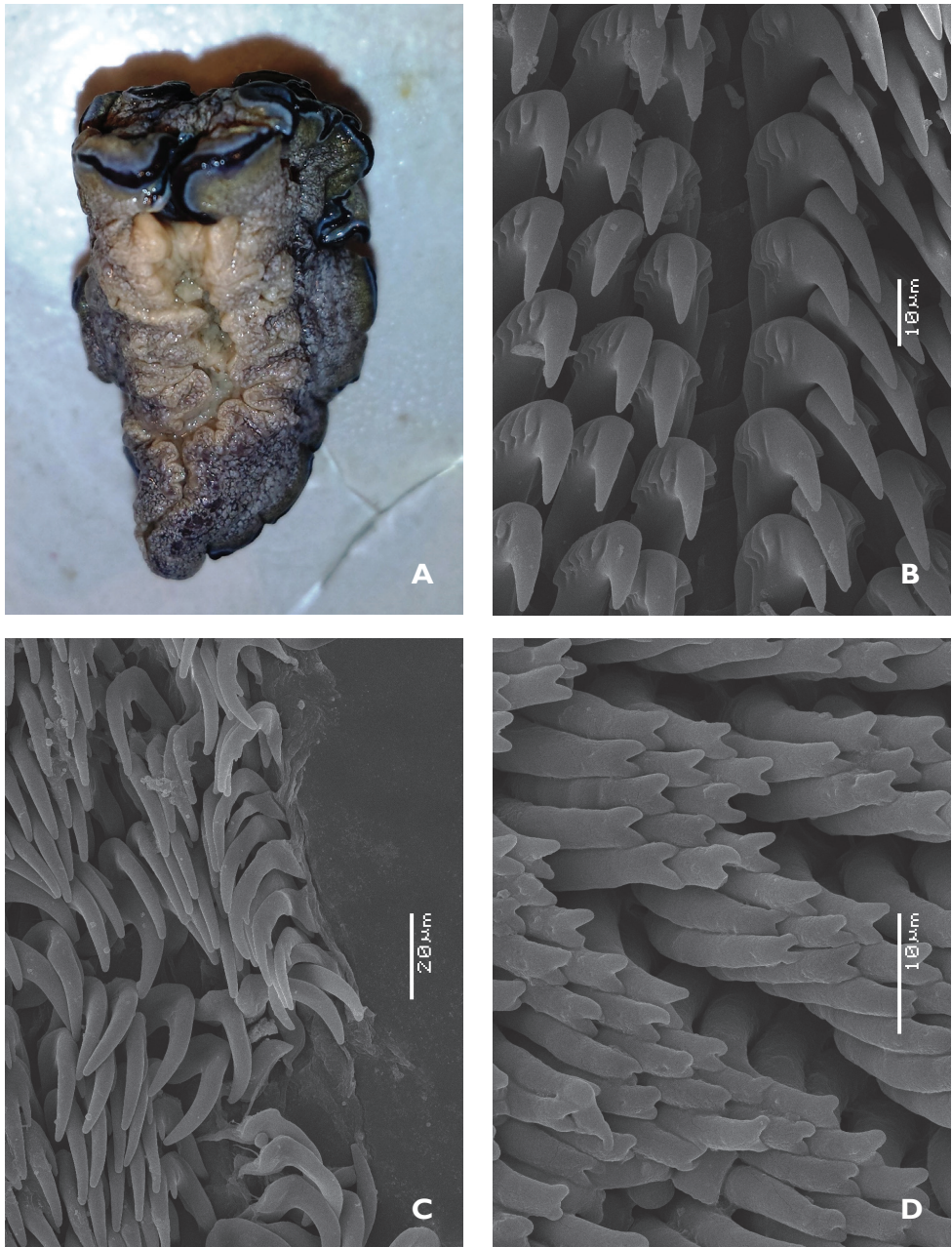


Figure 1. *Doriprismatica kyanomarginata* sp. n. **A** ventral view of whole specimen showing colours of the preserved specimen, including the anterior section of the mantle margin **B** midline area from the anterior portion of the radula **C** lateral teeth from the posterior section of the radula **D** jaw rodlets.

Other material. The Creek, Jeddah, Saudi Arabia, 1980s, photographs of one individual, J Kuchinke (Yonow 2008: 189, uppermost small photograph on right); one individual, photograph G Brown (Plate 4); Egypt, 1990s, photograph of one individual, J Hinterkircher; Egypt, 28 Sept 1995, intertidal, photograph of one individual, Á Valdés & E Mollo (HU-015).

Diagnosis. While the body shape and colour are similar to those of *Glossodoris cincta*, the marginal banding is diagnostic: the diffuse yellow innermost band has a sharp outer line bordering the distinct sky blue band, which is followed by a pitch-black margin visible on both sides of the mantle edge.

Description. This species is distinctive with its fleshy body thrown into four primary and multiple secondary folds. The approximately 20 gills are simply pinnate but whorled around the anal papilla. The rhinophores issue from low raised sheaths, which may bear tiny white spots around the margin, and carry in the region of 21 lamellae.

The body is cream with beige irregularities; this may be somewhat darker centrally in some individuals (Plate 4). The banding on the margin is distinctive: the creamy beige dorsum abruptly becomes more yellow, producing a band that is diffuse on the inside but abruptly demarcated on the outside. It is followed by a light blue line and the mantle margin is marked by a thick black line. This colour pattern is also present on the hyponotum. The gills have a beige-brown line up both sides, which meets over the top of each gill. The pinnules are opaque white. The rhinophores have a mottled beige stalk and the lamellate club is rather rounded. There is a white line up both sides and along the edges of the lamellae.

The coloured banding remains on the preserved specimens (Figure 1A). Ventrally, it is creamy beige, with the top of the foot a little darker but not as dark as the hyponotum. There are no coloured bands on the margin of the foot. The anterior margin of the foot is thickened, and the radula was already dissected upon reception.

The radular formula is $>73 \times$ approx. 50.0.50. There is no median thickening or rhachidian tooth present, but a small space in the middle (Figure 1B). The first marginal tooth on each side bears four or five denticles on each side of the cusp. The cusp becomes much longer at approximately tooth 4 or 5, and the four or five denticles also become a little larger. The outermost teeth in the row are undifferentiated but somewhat reduced in cusp and root sizes; the denticles are also reduced in both size and number (Figure 1C).

The jaw rodlets are curved and bicuspid at the tips, 20–25 μm long (Figure 1D).

Remarks. Originally considered a colour form of *Glossodoris cincta* by Rudman (1986a) and Yonow (2008), this species is rarely recorded in the Red Sea compared to the common reddish *G. cincta* with the ochre-black-white mantle margin: in fact, there are only four photographic records of this new species from Jeddah and Egypt since the 1970s (see Material above) compared to the many others of *G. cincta*. There are also no records of *D. kyanomarginata* sp. n. from the Red Sea on SeaSlugForum (<http://www.seaslugforum.net/showall/glosinc>) nor the internet. There is, however, one photograph of a pair of this new species in a book on the Persian Gulf (Dipper and Woodward 1989) but there are no further records from the Gulf.

The Indian Ocean form of *Glossodoris cincta* is similar to this species, but has a darker body with a similar fading towards the margin and only two coloured marginal bands, a bright yellow submarginal line and a black marginal line: there is no blue. Additionally, the radular and jaw elements differ substantially. There are many more denticles on the teeth of the western Indian Ocean specimen, approximately 8–13 compared to the 4–5 present on the teeth of this new species. The formula of a 55 mm living specimens is $134 \times 64.1.64$ with a distinct median thickening (Rudman 1986a: 149). The jaws of *Glossodoris cincta* also differ, with most being unicuspid; in *G. kyanomarginata* sp. n. the rodlets are bifid without exception, similar to those of the *G. atromarginata* group of species as defined in Rudman (1986a) but currently attributed to *Doriprismatica* (MolluscaBase 2018).

The body shapes differ from both *Doriprismatica atromarginata* (Cuvier, 1804) and *D. plumbea* (Pagenstecher, 1877) as illustrated by Rudman (1986a) and Yonow (1989) (both as *Glossodoris*) in being much more convoluted with secondary undulations. This is relevant, as the marginal banding of *D. plumbea* is similar in colour, and can often be blue. However, the body colour is much more yellow and darker in *D. plumbea*: Gohar and Abul-Ela (1959) described *D. plumbea* (as *Casella atromarginata*) in detail and subsequently Gohar and Soliman (1967) described the Indian Ocean form of *Glossodoris cincta* (as *Casella obsoleta*) and its development from the Egyptian Red Sea, comparing the two species' very different modes of development. Clearly, there are morphological, radular, and developmental differences between the two genera.

Distribution. Possibly endemic to the Red Sea. Only one unconfirmed published record from the Persian Gulf.

Derivatio nominis. The specific epithet is built by combining the Greek *κρᾶνός* and Latin *marginata*, referring to the cerulean blue submargin.

***Glossodoris kahlbrocki* sp. n.**

<http://zoobank.org/F69F9509-8562-4FA8-AF72-19D7DADB173E>

Figure 2, Plate 5

Glossodoris sp. 10 Debelius and Kuitert 2007: 189 (El Quseir, Egyptian Red Sea).

Glossodoris sp. 6 Gosliner et al. 2008: 238 (Red Sea).

Glossodoris sp. nov. Yonow 2015: fig. 540, fig. 21 (holotype; Hurghada, Red Sea).

Type material. HOLOTYPE SMF 349567: Dahara Wadi Gimal, near Hurghada, Egypt, 18 May 2010, 13 m depth, one specimen 25×10 mm preserved, leg. and photographs S Kahlbrock. **PARATYPE SMF 349568:** Dahara Wadi Gimal, near Hurghada, Egypt, 10 Jul 2012, 10 m depth, one specimen approx. 40 mm alive (27×10 mm preserved, bent), leg. and photographs S Kahlbrock (SK # 6). **PARATYPE SMF 349569:** Dahara Wadi Gimal, near Hurghada, Egypt, 13 Oct 2016, 12 m depth on rock during night dive, one spcm 15×9 mm preserved, leg. and photographs S Kahlbrock (SK # 3; radular and jaw preparations).



Plate 5. *Glossodoris kahlbrocki* sp. n., photograph E Pridgen (non-type).

Other material. The Creek, Jeddah, Saudi Arabia, 1970s, photographs of one individual only, W Pridgen (Plate 5).

Diagnosis. Uniformly white to cream mantle with no markings. Mantle colour bleeding into a more opaque white submargin. Bright blue border same thickness as opaque white band with clear distinct boundaries on both sides. Thin marginal line deep blue to black, present on both dorsal and ventral surfaces. Gills and rhinophores white, gill lamellae may tend to ochre.

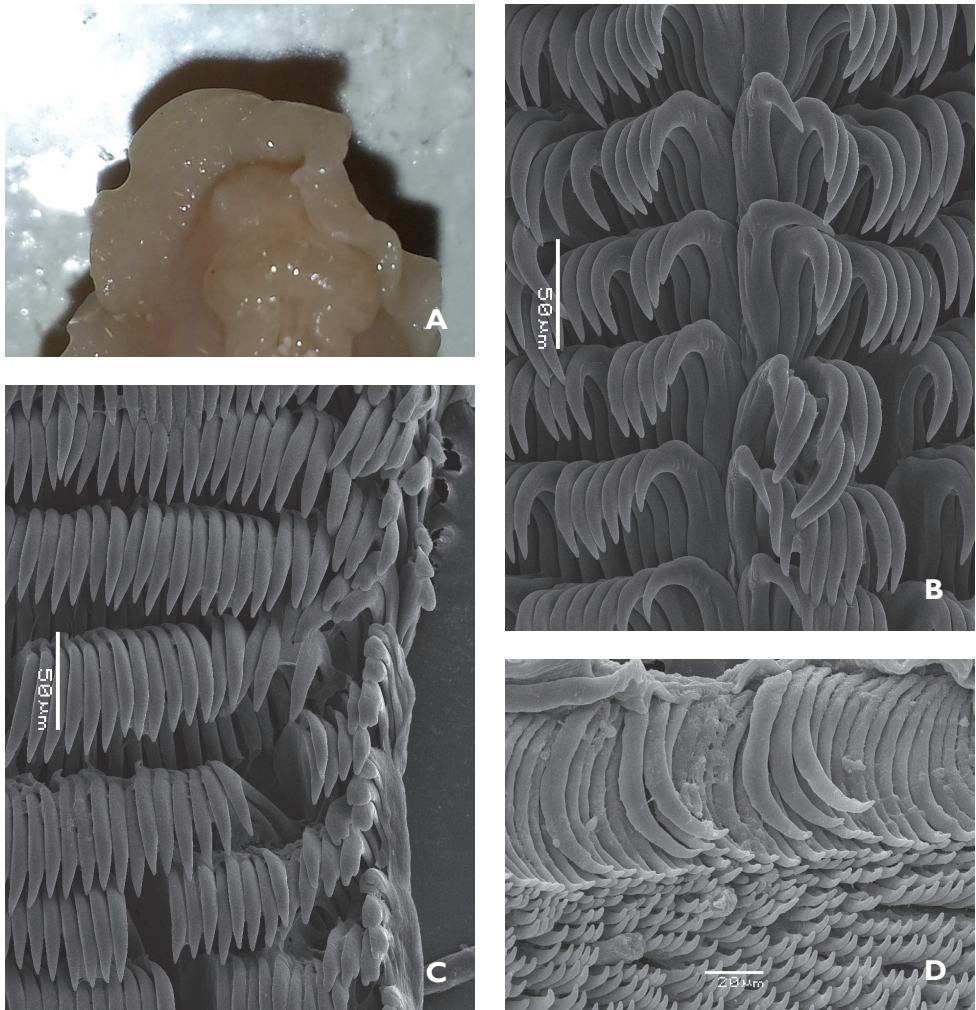


Figure 2. *Glossodoris kahlbrocki* sp. n. **A** ventral view of anterior showing head, oral tentacles, and foot margin **B** midline area from the posterior portion of the radula **C** lateral teeth from the middle section of the radula **D** jaw rodlets.

Description. This distinctive glossodorid is essentially white with a bright blue margin. The marginal pigmentation is identical in all three specimens (and the few available photographs, see Material above), and present on both sides of the mantle margin: an opaque creamy white band is followed by a light blue band and a deep blue to black marginal line. The gills are retracted into a small pocket in all but one photograph: in only one photograph of a series of photographs of the paratype specimen, the nine gills are extended: they are unipinnate with white rachides and ochre lamellae; in Plate 5 they are also extended and number at least five. They are arranged in a circling and the last two gills are smallest. The rhinophores are tall and parallel-sided, white

with faintly ochre lamellae: there are 21 lamellae in the paratype and 18 lamellae can be counted on the photograph of the 2016 non-type specimen. The rim of the rhinophore pocket is barely raised above the notum.

The body is solid and the thick mantle margin is held in three permanent folds. The hyponotum and top of the foot are identical in colour to the mantle, and there is no colour what-so-ever on the foot margin or oral tentacles.

The preserved holotype is fairly well relaxed and soft. It is elongated and slightly tapered at each end. The dorsum is of almost equal width and height. The mantle margin is very thin and flexible, with the permanent folds visible in the photographs present only as undulations. The foot is much longer than the mantle, and the posterior end is curled over the dorsum. The gill and rhinophore pockets are visible only as puckered holes. Viewed dorsally, the notum is pale pinkish white, the mantle margin is translucent cream. The digestive gland is visible as a dark patch halfway along the body to the left. In ventral view, it is visible as a large sphere spanning the width and depth of the body, therefore visible both dorsally and ventrally. The anterior margin of the foot is rounded and bilaminate; neither lamina is notched. The oral tentacles are two simple swellings each with a terminal nipple (Figure 2A). The type specimens are identical in their preserved states, but the smallest third specimen has a proportionately larger mantle margin. There is no hint of the blue margins on any of the preserved specimens except where the mantle was folded over in the paratype. Mantle glands are visible in a submarginal band on the posterior half of the mantle of the paratype (which also has the front of the foot and head partly damaged).

The reproductive organs of the small 15 mm preserved specimen dissected for the radula preparation were in a relatively underdeveloped state. This is not unexpected as the type specimens are twice the size.

The radular formula of the small specimen is $55 \times \sim 60.0 \sim 60$. There is no central tooth in the row; the first tooth in each row bears five or six small rounded denticles on the inner face of the curved cusp (Figure 2B). The remaining teeth have a straight root, longer than the cusp, and a small projection on the top. The teeth are the same shape and dimensions along the row until the last four or five, where they become very reduced in size and stacked in a line (Figure 2C).

The jaws comprise curved rodlets that are conical at the tips, which taper abruptly. They are relatively long, nearly 80 μm in length (Figure 2D).

Remarks. There is absolutely no species of chromodorid resembling this new species, in either the Red Sea or the western Indian Ocean: the pure white dorsum with startling blue marginal bands is unique.

Distribution. Endemic to the Red Sea. The first photograph of this species was taken in the 1970s, in the vicinity of Jeddah, Saudi Arabia (see Material above). Since then, it has only been photographed a few times, indicating its rarity in the Red Sea: the collected specimens are from the same locality years apart. Despite the numerous books and websites on nudibranchs, there are no records of this distinctive species anywhere else in the world.

Derivatio nominis. This species is in honour of Sven Kahlbrock, who searched many years for specimens of this beautiful but rare species. In addition, he has tirelessly supplied photographic records and many specimens in the last eight years.

***Goniobranchus collingwoodi* (Rudman, 1987)**

Figure 3, Plate 6

Chromodoris collingwoodi Rudman, 1987: 358–364, figs 23E-F, 32–35 (eastern Australia, Solomon Islands, Hong Kong); Baba 1989: 23, fig. 2; Rudman and Darvell 1990: 58, pl. 6B (Hong Kong); Wells and Bryce 1993: 117, fig. 144 (western Australia); Yonow 2001: 11, pl. 1 fig. 1 (Indonesia); Hervé 2010: 233 (New Caledonia).

Material. Rosalie Moller wreck, near Hurghada, Egyptian Red Sea, 28 Apr 2015, 40 m depth, 50–60 mm alive, 21 × 10 mm preserved leg. and photographs S Kahlbrock (SK # 3).

Description. The photographs perfectly fit the description of this species by Rudman (1987) (Plate 6). The dorsum is cream with a purple margin. Inside the



Figure 3. *Goniobranchus collingwoodi* (Rudman, 1987) ventral view of anterior showing head, oral tentacles, and foot margin.



Plate 6. *Goniobranchus collingwoodi* (Rudman, 1987), photograph S Kahlbrock.

purple margin is a broad opaque white band containing many yellow spots on the outside and very few purple spots on the inside. There is an ochre zone linking the white band to the dorsal hump, which is covered in brown patches and purple spots, and both are overlain with white spots. The rhinophores are brown with the edges of the lamellae being white. The quadrangular gills have a more complicated colour pattern, translucent with a dark brown or grey line down the edges of the pinnules on both their outer and inner sides, the pigmentation extending onto both sides of the pinnules. Some of the gills are branched or forked, and they are numerous, arranged in a double spiral around the anal papilla. The foot extends a short distance behind the mantle and is white with many round yellow spots and a purple patch on the margin.

Ventrally, the preserved specimen is monochromatic. The margins of the mantle and foot are contracted and the anterior margin of the foot is bilaminate (Figure 3).

Remarks. This is the first record of this well-known western Pacific species from the Red Sea. There are no literature records of this species from the Indian Ocean (e.g., Tibirićá et al. 2017, SeaSlugForum, http://seaslugs.free.fr/nudibranche/a_intro.htm). It remains to be seen if this is a one-off introduction or whether the species will establish itself in the either the Red Sea and/or the western Indian Ocean.

***Goniobranchus pseudodecorus* sp. n.**

<http://zoobank.org/228548FD-C48D-4CB8-A63F-018E6B72D1A8>

Figure 4, Plate 7

Chromodoris maculosa – Eliot 1908: 108–109 (the beacon, Khor Dongola, Suakin, Sudan) (**non** *Chromodoris maculosa* Pease, 1871).

Chromodoris cf. *decora* Yonow, 1989: 294, pl. 4 (Creek, Jeddah, Saudi Arabia, Red Sea); Perrone and Doneddu 2001: 121–130, pl. 1 figs C, D (Naama Bay, Sharm el Sheikh, Egypt, Red Sea).

Glossodoris sp. 10 Debelius & Kuitert, 2007: 149 (Eilat, Israel, Red Sea).

Chromodoris sp. Yonow, 2008: 60, 186 (Jeddah, Eilat, Red Sea).

Type material. **HOLOTYPE SMF 349570:** Hotel Zabargad, 120 km south of Marsa Alam, Egypt, Feb 2003, 16 mm alive (9 × 4 mm preserved), leg. and photographs J Hinterkircher. **PARATYPE SMF 349571:** Balena wreck, Hurghada, Egypt, 02 Aug 2012, 9 m depth, approx. 15 mm alive (10 × 3 mm preserved), leg. S Kahlbrock (SK # 19).

Other material. Quseir, Egypt, July 2000, approx. 10 mm alive (6 × 2.5 mm preserved), leg. and photographs J Hinterkircher (jaw and radular preparations); Jeddah, Saudi Arabia, photographs only from 1980's, Pam Kemp, J Kuchinke, G Smith; Eilat, Israel, 18 Feb 2005, O Ledermann; near Hurghada, Egypt, 07 July 2012, 12 June 2016, S Kahlbrock.

Diagnosis. Body shape rounded oblong anteriorly and rounded posteriorly. Opaque white pointed tail always longer than mantle. Dorsum translucent rose centrally and whiter marginally, with meandering longitudinal opaque white lines and round rose spots. Margin translucent orange with elongated opaque white patches.

Description. The shape of this species is very distinctive: all photographs depict an elongated oval body of which the anterior margin is oblong and the posterior end is rounded (Plate 7). The pointed tail extends beyond the mantle, and is translucent white with an opaque white triangular marking centrally. The mantle is translucent rose with longitudinal interrupted opaque white lines and round pink spots that are ocellated with deeper rose. Around this area is a band of white patches that may be confluent, followed by a translucent orange band containing discrete white patches. The rhinophores are translucent orange with two inner opaque white areas; there are up to 12 lamellae and the translucent stalks issue from translucent, slightly raised sheaths. The 6–8 unipinnate gills are arranged in a simple circle; they are also translucent with opaque white cores; the orange pigment in the tips is within the translucent area.

The preserved specimens are not totally contracted, and still retain the opaque white lines on the dorsum; however, no coloured spots remain on any of the specimens. The almost black digestive gland within is clearly visible. The edges of the foot are slightly crumpled, squared anteriorly, and the oral tentacles are visible as swollen nipples (Figure 4A). The anterior margin of the foot does not appear to be bilaminar. The 2012 specimen from Hurghada is aberrant in having two left rhinophores.



Plate 7. *Goniobranchus pseudodecorus* sp. n., photograph S Kahlbrock (non-type).

The notes made on the paratype on arrival read as follows: “dorsum dense, opaque dirty orange, glistening white lines, coloured areas still visible on rhinophores and gills (the latter were darker). Two left rhinophores but one right. Mantle margin distinct, separate, mantle glands visible posteriorly. Ventrally, the hyponotum a darker orange, foot lighter. Foot anterior margin angular with a slight median dent, large swollen oral tentacles.”

The reproductive system is developed in the 6 mm specimen (collected in the summer), despite its being smaller than the types and the average recorded length, with ducts and glands clearly visible as well as the bursa copulatrix.

This same specimen has a radular formula of $27-28 \times 28-33.1.33-28$. There is a small (up to $15 \mu\text{m}$ long) central triangular tooth medially, crowded by the first lateral teeth (Figure 4B). The first lateral is twisted on itself, with one or two large denticles medially and a row of four small saw-like denticles laterally (Figure 4B). The length of the cusp increases quickly to approximately tooth 9 as does the number of denticles, also to nine. In this region, the twist of the cusp is still pronounced and forms a small knob at the top of the root/cusp junction. At approximately tooth number 13–15 until the last five teeth, the cusps are somewhat straighter on the root with a pronounced knob on the top (Figure 4C); the denticles are saw-like. The last five teeth are stacked together and very reduced in size, flattened plates tapering towards the end with few denticles (Figure 4C).

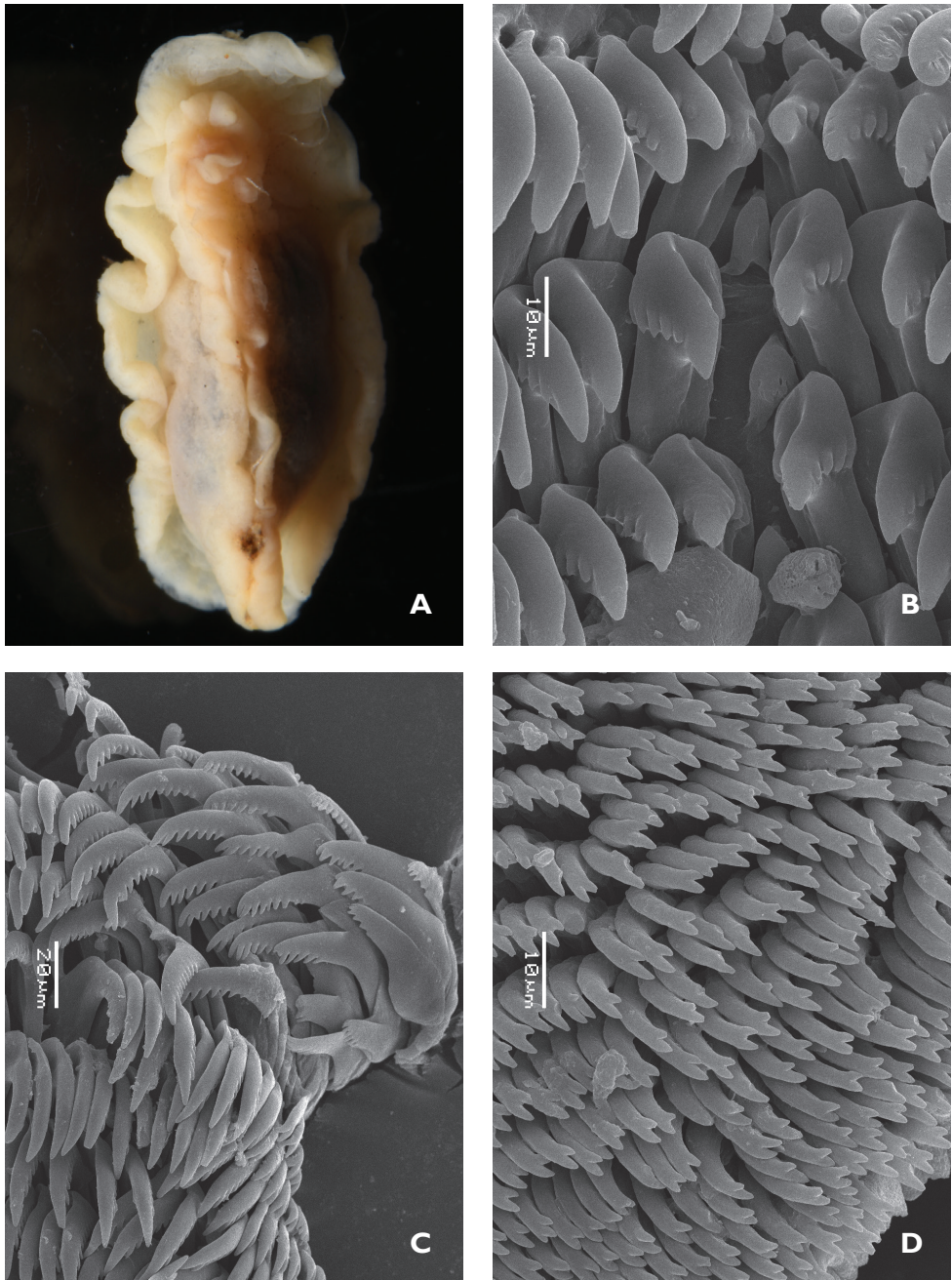


Figure 4. *Goniobranchus pseudodecorus* sp. n. **A** ventral view of anterior showing head, oral tentacles, and foot margin **B** midline area from the anterior portion of the radula **C** lateral teeth from the anterior section of the radula **D** jaw rodlets.

The jaws are composed of curved rodlets. These are bifid on the tip, with one denticle being much smaller than the other (Figure 4D).

Remarks. Although Eliot (1908) compares his specimen to *Chromodoris maculosa* Pease, subsequent records have shown it to be quite different and consistently so over time. *Goniobranchus pseudodecorus* sp. n. has been recorded from the Red Sea a number of times (Yonow 1989, Perrone and Doneddu 2001, <http://www.seaslugforum.net/find/13213>, Yonow 2008). *Goniobranchus decorus* (Pease), to which this species has been compared, does not occur in the Red Sea but has a western Pacific distribution: it is similar to *G. pseudodecorus* sp. n. in having a translucent orange margin and pointed white foot, but there are different white markings on the dorsum, large purple patches in the orange and white marginal bands, and the rhinophore pigmentation is without banding. The body is not so obviously angular anteriorly as in *G. pseudodecorus* sp. n. The radular formula of a 16 mm-preserved specimen from Australia is 52 (+3) × 48.0.48 and the teeth vary similarly along the row (Rudman 1986b: 331).

Distribution. Endemic to the Red Sea. The first record of this species is by Eliot (1908) from the Sudanese Red Sea in which he describes the same obvious characters of shape and colour: “Elongated and rather flat: mantle broad, especially over head. Foot ends in sharp point projecting... Gills small and thick, seven in number, simply pinnate, the two hindmost smaller. ... Colour translucent greyish pink. ... broad undefined band of opaque white, and outside, bordering the mantle, a broad transparent orange-yellow line interrupted by opaque white spots along the edge.” The species is clearly endemic to the Red Sea, and I suspect that the Maldives locality of the second photograph in Debelius and Kuitert (2008) is erroneous.

Derivatio nominis. An unimaginitive name alluding to the similarities with *Goniobranchus decorus*.

Hypselodoris dollfusi (Pruvot-Fol, 1933)

Figure 5, Plate 8

Glossodoris dollfusi Pruvot-Fol, 1933: 126, pl. I figs 7, 8; fig. 40 (Red Sea).

Hypselodoris dollfusi – Gosliner and Behrens 2000: 116, Figs 1B, 4, 5 (Oman); Yonow 2008: 60, 192 (Red Sea).

Material. Wreck of ‘Rosalie Moller’, near Hurghada, Egypt, 01 Aug 2012, 33 m depth, one specimen approx. 50 mm (approx. 25 × 15 mm preserved, curled), leg. and photographs S Kahlbrock.

Description. This specimen represents the first and nearest record to its type locality for a species originally described from the Red Sea 80 years ago, and is thereby removed from its *incertae sedis* status of Yonow (1989). It is clearly distinct and recognisable from all the Red Sea chromodorids: the body is very large, firm, and with a high profile. It is pale to dark yellow with series of large and small spots, which can be shades of red and pink, often with a red margin, and a yellow margin encircling the mantle (Plate 8).



Plate 8. *Hypselodoris dollfusi* (Pruvot-Fol, 1933), photograph S Kahlbrock.

The preserved specimen is beige (examined 2013) with an orange margin. The patches and spots remain visible as red or faded red. There are red spots also present on the gill pocket, on the gills, around the margin of the hyponotum (large), and on the top of the foot (small, fading). The gonopore is surrounded by a red ring. The rhinophore pockets are white and retain their red margins. The mantle glands are visible as a series of darker yellow patches at the very posterior of the margin (Figure 5A).

Ventrally, the body is swollen, cream-coloured, and the red spots visible as opaque white slightly raised spots (Figure 5A). The head is rounded, the tentacles just visible. The anterior margin of the foot is very angular, bilaminar, with both laminae notched.

The reproductive system of the single specimen preserved in the summer is well developed.

Its radular formula is $> 65 \times 71.0.71$. There is a clear space in the middle of the complete length of the radula. The first laterals on each side are identical and asymmetrical: all the teeth are clearly bicuspid but the first lateral has an additional small sharp cusp on its inner face (Figure 5B). The remaining laterals are typically hypselodorid and regular along the row. The last 15 or so teeth become rapidly reduced in size with the addition of a line of 3–5 denticles on the lower cusp (Figure 5C). Along the posterior portion of the radula, from approximately tooth 30 (if not earlier) the teeth are secondarily denticulate (Figure 5D).

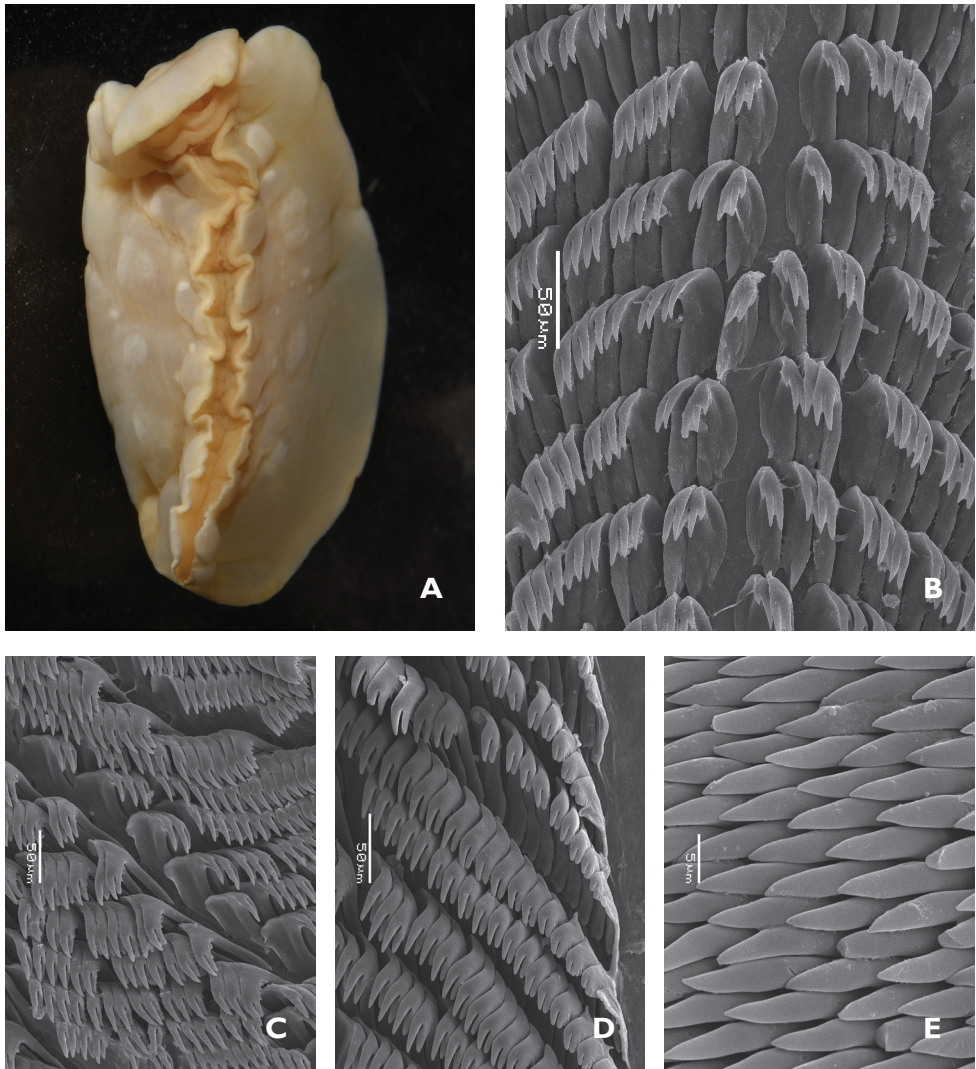


Figure 5. *Hypselodoris dollfusi* (Pruvot-Fol, 1933) **A** ventral view of the whole specimen showing head, oral tentacles, and deep hyponotum with raised spots **B** midline area from the anterior portion of the radula **C** lateral teeth from the posterior portion of the radula **D** lateral teeth from the middle section of the radula **E** jaw rodlets.

The jaws of *Hypselodoris dollfusi* are simple pointed rods with a slight curve (Figure 5E).

Remarks. It is remarkable that this species was described in 1933 and then not seen again until 1999. Gosliner and Behrens (2000) rediscovered the species based on specimens from the Persian Gulf. Although there is only one specimen from the Red Sea, there have been numerous photographic records from the northern gulfs of Eilat and Suez since Yonow (2008). It has since been photographed with some regularity but appears to be more common in the Persian Gulf (<http://www.seaslugforum.net/find/hypsdoll>, https://www.facebook.com/pg/uaebranchers/photos/?ref=page_internal).

White (1951) described a specimen from the Bannwarth Collection (NHM) as "...resembling a young individual of *Glossodoris luteorosea*...". While she does not describe any remaining pigment, the only species in the Red Sea with large red spots similar to the Mediterranean species is *H. dollfusi*. However, White describes nine gills (while there are ten in Gosliner and Behrens (2000) and eight in this specimen; one is bifurcated) and "... cream coloured, soft and semi-transparent. The mantle edge is undulating." This does not agree at all with the preserved specimen of *H. dollfusi* described here. Additionally, she describes a radular formula of $54 \times 30.0.30$ in an 11 mm-long preserved specimen ($66 \times 88.0.88$ in a non-measured specimen in Gosliner and Behrens 2000), and $> 65 \times 71.0.71$ in this 25 mm-long preserved specimen. Not only does the formula differ considerably, but also the form of the teeth differs in that the first lateral has two denticles and the second lateral has one denticle.

Distribution. The species is known only from the northern Red Sea (Yonow 2008), the Persian Gulf (Glazer et al. 1984, Dipper and Woodward 1989, Gosliner et al. 2008), and the Gulf of Oman (Gosliner and Behrens 2000).

Miamira magnifica Eliot, 1910

Figure 6, Plate 9

Miamira magnifica Eliot, 1910: 432, pl. 25 figs 10, 11 (Seychelles); Yonow 1994: 123 (Maldive Islands); Yonow 2008: 61, 206 (Red Sea); Tibirićá et al. 2017: 40, fig. 11G, H (Mozambique).

Material. Marine Biological Laboratory, Eilat, Israel, 09 Aug 1983, 10 m depth, one specimen 31×16 mm (preserved), leg. and photographs J Dafni.

Description/remarks. There is so much confusion surrounding this species that the Red Sea specimen is here described and illustrated in detail to enable clear recognition. As succinctly stated by Rudman (2007), a review of the genus by Valdés and Gosliner (1999) which synonymised several genera actually omitted two crucial species, and so the confusion continues. In concurrence with Rudman, *Miamira magnifica* is here reported as having an Indian Ocean distribution, including the Red Sea (also in Yonow 2008: 206). This is a correction of Yonow (1994) who stated that it had an Indo-West Pacific distribution because *flavicostata* from Australia and Japan had been included as a possible synonym.

Despite much searching, this remains the only specimen record of *Miamira* from the Red Sea. The specimen was examined and drawn by the author when it was moribund: it was pale green with white nodules, each of which were encircled by two or three blue rings (Plate 9); the central two nodules were the largest. The shape of this central green area was like a cross of Lorraine, a longitudinal central line with two crossbars. Outside this region, the mantle was white with raised orange spots, which also were present on the slightly raised tubercles covering the sides and white hyponotum of the specimen. The demarcation between the mantle and the sides was clearly marked by orange dots. The shape of the mantle was very regular and its texture firm, the foot extended beyond it.

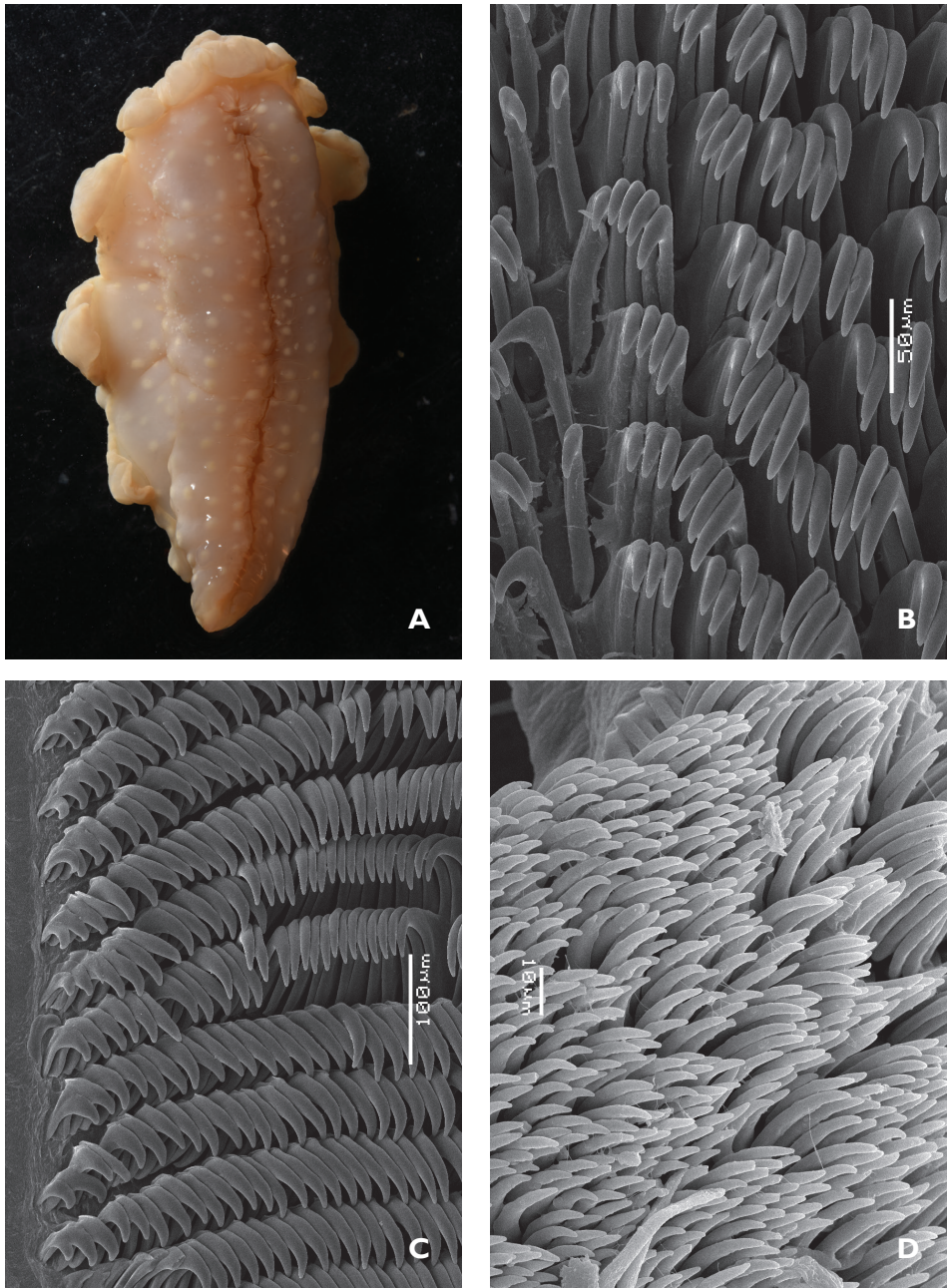


Figure 6. *Miamira magnifica* Eliot, 1910 **A** ventral view of whole specimen **B** midline area from the anterior portion of the radula **C** lateral teeth from the anterior section of the radula **D** jaw rodlets.

The preserved specimen retains much of the original shape, albeit somewhat contracted, and the spots are clearly visible (Figure 6A). The reproductive system of the single specimen was developed when it was collected in the summer.



Plate 9. *Miamira magnifica* Eliot, 1910, photograph J Dafni.

The radula comprises at least 80 rows of simply hooked teeth; there are approximately 100 teeth in a row. There is no rhachidian and the last few teeth in each row are greatly reduced in size and stacked together (Figure 6B, C). This compares well with those of a Maldives specimen measuring a very similar 30 mm having a radular formula of $102 \times$ approx. 90.0.90 (Yonow 1994).

The jaws are simple rodlets with pointed tips and a slight curve (Figure 6D).

Distribution. Northern Red Sea, tropical western Indian Ocean (Yonow 1994, Tibirićá et al. 2017, <http://www.seaslugforum.net/showall/ceramagn>).

Verconia sudanica (Rudman, 1985)

Plate 10

Noumea sudanica Rudman, 1985: 254, figs 1e, 7b, 8 (Red Sea); Yonow 2008: 61, 200 (Red Sea).

Material. South of Hurghada, Egypt, 22 Jan 2009, 2–4 m depth on rocks during night dive, four specimens 15–20 mm alive approx. (6.5, 7, 7, 8 mm preserved); leg. and photographs S Kahlbrock; photographs of numerous individuals, the Creek, Jeddah, Saudi Arabia, 1970–1994, W Pridgen, D & S Sharabati; photographs only, vicinity of Hurghada, Egypt, 13 Aug 2012, S Kahlbrock; photographs of the type specimen, Suakin, Sudan, 25 April 1980, leg. and photographs C Todd (Australian Museum C.131570).



Plate 10. *Verconia sudanica* Rudman, 1985, photograph S Kahlbrock.

Description. Since Rudman's (1985) and Yonow's (2008) records, *Verconia sudanica* has been recorded somewhat more frequently in the Red Sea (<http://www.seaslugforum.net/showall/noumsuda>, <https://www.inaturalist.org/taxa/126112-Noumea-sudanica>). It is described here from specimens collected in the northern Red Sea. The excellent series of photographs depict five individuals, of which three are grouped together (four specimens were collected). In the photograph of the group, the rhinophores and nine plumose but simply pinnate gills are all pure white. The edges of the rhinophore lamellae (numbering 9–11) and main axes of the gills (facing outwards) are opaque white. In photographs of a single animal, the apical one third of the rhinophore is very faintly orange, with opaque white edges to the 9–11 lamellae. All five animals have a white dorsum with pits and a narrow yellow margin, which is faintly darker orange at the edge (Plate 10). In two individuals, the pits are slightly yellow and in a third one, there are small conical papillae dotted on the surface. The foot is also white, and the tip is bordered with a yellow line; one photograph from the side shows that the margins of the foot are white.

The preserved specimens are identical, opaque cream with a thickened but slightly lighter coloured margin containing single round mantle glands that are semi-translucent. The gill pocket is large and slightly raised and in two specimens, the unipinnate gills barely protrude. The foot extends beyond the mantle slightly in all but one specimen. The foot is angular anteriorly, and the large oral tentacles are clearly visible.

Remarks. There are no similar species in the Red Sea; only the western Pacific *Verconia simplex* (Pease, 1871) is equally small, white to pale pink, with a bright orange margin; however, there are no specimen records further to the two photographs in Yonow (2008) so these records remain unconfirmed. *Verconia simplex* has bright orange tips to both the rhinophores and the gills.

Some comments are necessary on the generic placement of this species. Gosliner and Johnson (2012: 6) found that *Noumea* was not monophyletic but its species were distributed in two clades (and within other genera): “*Noumea* consists of two separate clades (both pp = 1.00) that are poorly supported as a combined clade in the analysis when variable positions are included (pp = 0.61). Although this support is not sufficient, all of the species in both of these clades are currently named *Noumea* and will retain this name in order to maintain stability.”

With this, they synonymised *Verconia*, a monotypic genus containing *V. verconis* (Basedow & Hedley, 1905). However, they failed to recognise that *Noumea* was preoccupied. WoRMS has a small note to that effect and *Verconia* (as a synonym) should be the correct generic designation (<http://www.marinespecies.org/aphia.php?p=notes&cid=279974>) despite its type species being morphologically different: “*Noumea* Risbec, 1928 (Mollusca: Gastropoda) is a junior homonym of *Noumea* Fauvel, 1874 (Arthropoda: Coleoptera), a name in current use. *Verconia* Pruvot-Fol, 1931 was recognized as a synonym of *Noumea* Risbec by Johnson and Gosliner (2012) and is here used for species of the chromodoridid group previously known as *Noumea*.”

Examination of Rudman’s (1984) review of the chromodorid genera and his descriptions of species of *Noumea* (Rudman 1986a, b) show that these two genera are in fact similar, but because the external morphology of *Verconia verconis* is so distinctive, it has historically been considered in its own genus. The radular formulae and teeth shapes are very similar, as are some morphological characters (although these are also similar to other chromodorid genera). The reproductive systems vary a little within the group described as *Noumea* by Rudman (1984, 1986a, b although some species belonging to a second clade have been re-assigned to *Diversidoris*) and in some cases are more similar to that of *V. verconis* (see also Rudman 1986b: 402). As it is very unlikely that the specimens of *V. verconis* used in the molecular analysis by Johnson and Gosliner (2012) were misidentified, the synonymy must be accepted, but it is unfortunate that these authors did not examine the literature and, as a result, the species they assigned to *Noumea* must now be reassigned to *Verconia*.

Distribution. Endemic to the Red Sea.

Conclusions

It is unfortunate that the photographic records of the chromodorids included in "Sea Slugs of the Red Sea" (Yonow 2008) and of *Diversidoris aurantionodulosa* in Yonow (2015) could not be substantiated by specimen collections. This paper completes the identification of all the available chromodorid specimens in the author’s collections

from the Red Sea; forty-one species of chromodorids has been recorded from the Red Sea to date, but there are an additional dozen species known from the literature (see checklist in Yonow 2008) or only from photographs (Yonow 2008, 2012; pers. obs.).

In the event that some species groups, such as the ‘*Glossodoris cincta*’ group, need further work, all available specimens will have been identified, described, and lodged in the Senckenberg Museum. The appendix lists material of six species commonly found in the Red Sea and recorded previously, and these are also deposited in the Museum.

While the length of time taken to publish some of these records has been substantial, one benefit has been that a vast number of photographs from various sources could be analysed to trace and date first records of ‘new’ species records. Hence, while the newly described species have been present in the Red Sea for the last four or five decades at least, *G. collingwoodi* and *D. flava* are almost certainly more recent introductions. I suspect it will be with the aid of ‘citizen scientists’ that more records of these species, and their establishment or not within the Red Sea, or at least the northern part of it, will be made.

Acknowledgements

I would like to thank Johann Hinterkircher and Sven Kahlbrock who have generously provided their photographs and collected specimens over the years, and have been enthusiastic about this research. Jacob Dafni saved a specimen for me with photographs when I visited Eilat in 1983, both of which are included here with grateful thanks and happy memories. Á Valdés & E Mollo kindly provided some of their collection of specimens, notes, and/or photographs of their trip to the Red Sea in September 1995 for which I am grateful. Woody Pridgen has spent the last few years scanning his million slides in search of nudibranchs, and has turned up some amazing records, which are documented in this work – I am so grateful. I would like to sincerely thank Benoît Dayrat, Kathe Jensen, Heike Wägele, and the subject editor Bert Hoeksema for their constructive comments.

Once again, this series of publications would not have been possible without the early inspirations of Dr. Tom Thompson, Doreen and Issam Sharabati, and Gunnar Bemert.

This research has received no special funding.

References

- Baba K (1989) Taxonomical study on two species of the “*aureopurpurea*” color group of *Chromodoris* from Japan (Nudibranchia: Chromodorididae). *Venus* 48(1): 21–26.
- Debelius H, Kuitert RH (2007) Nudibranchs of the world. IKAN-Unterwasserarchiv, Frankfurt, 359 pp.
- Dipper F, Woodward T (1989) *The Living Sea*. Motivate Publishing, United Arab Emirates, 95 pp.

- Eliot CNE (1904) On some nudibranchs from East Africa and Zanzibar. Part IV. Proceedings of the Zoological Society, London 1: 380–406. <https://doi.org/10.1111/j.1469-7998.1904.tb08295.x>
- Eliot CNE (1908) Reports on the marine biology of the Sudanese Red Sea XI. Notes on a collection of nudibranchs from the Red Sea. Journal of the Linnean Society (Zoology) 31: 86–122. <https://doi.org/10.1111/j.1096-3642.1908.tb00457.x>
- Eliot CNE (1910) Nudibranchs collected by Mr. Stanley Gardiner from the Indian Ocean in H.M.S. Sealark. Transactions of the Linnean Society, London 13: 411–438. <https://doi.org/10.1111/j.1096-3642.1910.tb00082.x>
- Glazer B, Glazer DT, Smythe KR (1984) The marine Mollusca of Kuwait, Arabian Gulf. Journal of Conchology 31: 311–330.
- Gohar HAF, Aboul-Ela IA (1959) On the biology and development of three nudibranchs. Publications of the Marine Biological Station of Ghardaqa 10: 41–62.
- Gohar HAF, Soliman GN (1967) The direct development of the nudibranch *Casella obsoleta* (Rüppell & Leuckart) (Gastropoda, Nudibranchiata). Publications of the Marine Biological Station of Ghardaqa 14: 149–166.
- Gosliner TM, Behrens DW (2000) Two new species of Chromodorididae (Mollusca: Nudibranchia) from the tropical Indo-Pacific, with a redescription of *Hypselodoris dollfusi* (Pruvot-Fol, 1933). Proceedings of the California Academy of Sciences 52(10): 111–124.
- Gosliner TM, Behrens DW, Valdés A (2008) Indo-Pacific Nudibranchs and Sea Slugs. A field guide to the world's most diverse fauna. Sea Challengers Natural History Books and the California Academy of Sciences, USA, 426 pp.
- Hervé J-F (2010) Guide des Nudibranches de Nouvelle-Calédonie et autres Opisthobranches. Editions Catherine Ledru, Nouméa, 404 pp.
- Johnson RE, Gosliner TM (2012) Traditional taxonomic groupings mask evolutionary history: A molecular phylogeny and new classification of the chromodorid nudibranchs. PLoS ONE 7(4): e33479. <https://doi.org/10.1371/journal.pone.0033479>
- MolluscaBase (2018) *Doriprismatica atromarginata* (Cuvier, 1804). Accessed through: World Register of Marine Species. <http://www.marinespecies.org/aphia.php?p=taxdetails&id=558499> [accessed: 15 June 2018]
- Perrone AS, Doneddu M (2001) Pattern convergence in Nudibranchia of the genus *Chromodoris* Alder & Hancock, 1855 (Opisthobranchia) from the Red Sea and Polycladida (Platyhelminthes) from the Mediterranean Sea. Vita Marina 47(4): 121–130.
- Pruvot-Fol A (1933) Mission Robert Dollfus en Egypte. Opisthobranchiata. Memoirs de l'Institut d'Egypte 21: 89–159.
- Rudman WB (1982) The Chromodorididae (Opisthobranchia, Mollusca) of the Indo-West Pacific: *Chromodoris quadricolor*, *C. lineolata* and *Hypselodoris nigrolineata* colour groups. Zoological Journal of the Linnean Society 76(3): 183–241. <https://doi.org/10.1111/j.1096-3642.1982.tb02182.x>
- Rudman WB (1984) The Chromodorididae (Opisthobranchia, Mollusca) of the Indo-West Pacific: a review of the genera. Zoological Journal of the Linnean Society 81: 115–273. <https://doi.org/10.1111/j.1096-3642.1984.tb01174.x>

- Rudman WB (1985) The Chromodorididae (Opisthobranchia, Mollusca) of the Indo-West Pacific: *Chromodoris aureomarginata*, *C. verrieri* and *C. fidelis* colour groups. Zoological Journal of the Linnean Society 83(3): 241–299. <https://doi.org/10.1111/j.1096-3642.1985.tb00875.x>
- Rudman WB (1986a) The Chromodorididae (Opisthobranchia, Mollusca) of the Indo-West Pacific: the genus *Glossodoris* Ehrenberg (= *Casella* Hancock and A. Adams). Zoological Journal Linnean Society 86(2): 101–184. <https://doi.org/10.1111/j.1096-3642.1986.tb01810.x>
- Rudman WB (1986b) The Chromodorididae (Opisthobranchia: Mollusca) of the Indo-West Pacific: *Noumea purpurea* and *Chromodoris decora* colour groups. Zoological Journal of the Linnean Society 86(4): 309–353. <https://doi.org/10.1111/j.1096-3642.1986.tb01814.x>
- Rudman WB (1986c) The Chromodorididae (Opisthobranchia, Mollusca) of the Indo-West Pacific: *Noumea flava* colour group. Zoological Journal of the Linnean Society 88(4): 377–404. <https://doi.org/10.1111/j.1096-3642.1986.tb02254.x>
- Rudman WB (1987) The Chromodorididae (Opisthobranchia, Mollusca) of the Indo-West Pacific: *Chromodoris epicuria*, *C. aureopurpurea*, *C. annulata*, *C. coi* and *Risbecia tryoni* colour groups. Zoological Journal of the Linnean Society 90(4): 305–407. <https://doi.org/10.1111/j.1096-3642.1987.tb01357.x>
- Rudman WB (2007, Apr 30) Is *Ceratosoma magnifica* (Eliot, 1910) a good species? [Message in] Sea Slug Forum. <http://www.seaslugforum.net/find/19854>
- Rudman WB, Darvell BW (1990) Opisthobranchs of Hong Kong part I: Goniodorididae, Onchidorididae, Triophidae, Gymnodorididae, and Chromodorididae (Nudibranchia). Asian Marine Biology 7: 31–79.
- Sreeraj CR, Sivaperuman C, Raghunathan C (2012) Addition to the Opisthobranchiate (Opisthobranchia, Mollusca) fauna of Andaman and Nicobar Islands, India. Galaxea, Journal of Coral Reef Studies 14: 105–113. <https://doi.org/10.3755/galaxea.14.105>
- Tibirică Y, Pola M, Cervera JL (2017) Astonishing diversity revealed: an annotated and illustrated inventory of Nudipleura (Gastropoda: Heterobranchia) from Mozambique. Zootaxa 4359(1): 1–133. <https://doi.org/10.11646/zootaxa.4359.1.1>
- Valdés A, Gosliner TM (1999) Reassessment of the systematic status of *Miamira* Bergh, 1875 and *Orodoris* Bergh, 1875 (Nudibranchia; Chromodorididae) in light of phylogenetic analysis. Journal of Molluscan Studies 65: 33–45. <https://doi.org/10.1093/mollus/65.1.33>
- Wells FE, Bryce CW (1993) Sea Slugs of Western Australia. Western Australian Museum, Perth, Australia, 184 pp.
- White KM (1951) On a collection of molluscs, mainly nudibranchs, from the Red Sea. Proceedings of the Malacological Society, London 28: 241–253. <https://doi.org/10.1093/oxfordjournals.mollus.a064590>
- Yonow N (1988) Red Sea Opisthobranchia. 1. The family Phyllidiidae (Mollusca, Nudibranchia). Fauna of Saudi Arabia 9: 138–151.
- Yonow N (1989) Red Sea Opisthobranchia. 2. The family Chromodorididae (Mollusca, Nudibranchia). Fauna of Saudi Arabia 10: 290–309.
- Yonow N (1990) Red Sea Opisthobranchia. 3. The orders Sacoglossa, Cephalaspidea, and Nudibranchia: Doridacea (Mollusca, Opisthobranchia). Fauna of Saudi Arabia 11: 286–299.

- Yonow N (1994) Opisthobranchs from the Maldive Islands, including descriptions of seven new species (Mollusca: Gastropoda). *Revue française d'Aquariologie / Herpétologie* 20(4): 97–130.
- Yonow N (2000) Red Sea Opisthobranchia 4: The Orders Cephalaspidea, Anaspidea, Notaspidea, and Nudibranchia: Dendronotacea and Aeolidacea. *Fauna of Arabia* 18: 87–131.
- Yonow N (2001) Results of the Rumphius Biohistorical Expedition to Ambon (1990). Part 11. Doridacea of the families Chromodorididae and Hexabanchidae (Mollusca, Gastropoda, Opisthobranchia, Nudibranchia), including additional Molukkan material. *Zoologische Mededelingen, Leiden* 75(1–15): 1–50.
- Yonow N (2008) Red Sea Sea Slugs. Pensoft Publications, Sofia/Moscow, 304 pp.
- Yonow N, (2015) Sea Slugs: unexpected biodiversity and distribution. In: Rasul NMA, Stewart ICF (Eds) *The Red Sea – The Formation, Morphology, Oceanography and Environment of a Young Ocean Basin*. Springer-Verlag, Berlin/Heidelberg, 531–550. https://doi.org/10.1007/978-3-662-45201-1_30

Appendix I

Additional specimen and photographic records of species of Chromodorididae previously described in Yonow (1988)

Chromodoris africana Eliot, 1904

- Near Garden, near Sha'arm el Sheikh, Egypt, 24 Dec 1990, 18 m depth (sandy rubble substrate with boulders), 37 × 9 mm alive, leg. and photographs N Yonow (NY # 109) [2 black lateral stripes, 2 white with faint blue tinge, broad mantle margin with white margin; orange pocket rims; fine white gill pinnules].
- Ras umm Sid, near Sha'arm el Sheikh, Egypt, 25 Dec 1990, 25 m depth (sandy rubble substrate with boulders), 40 × 8 mm alive, leg. and photographs N Yonow (NY # 113) [black laterally with 2.5 blue lines, thin stripe between rhino (does not widen like in *quadricolor*), less blue than *quadricolor*. Large gill pocket, ten gills, orange pocket rim and anal papilla].
- Wreck, Ras Mohammed, Egypt, 27 Dec 1990, 10 m depth, 62 × 10 mm alive, leg. and photographs N Yonow (NY # 117) [white margin, wide orange submargin + narrower white + wide black; broken dorsal black; 10+ gills + rhino dark orange'. Large gill pocket, orange rim also rhino pocket].
- Egypt, 24 Sept 1995, 30 m depth, two specimens 13 mm relaxed and min. 25 mm bent, both preserved (HU-02), leg. Á Valdés & E Mollo.
- Egypt, Sept/Oct 1995, one specimen min. 11 mm preserved, dissected, and dried out at some point (HU-M5), leg. Á Valdés & E Mollo.
- The creek, Jeddah, Saudi Arabia, 1970–1994, numerous photographs of numerous individuals, Pam Kemp, G Bemert, W Pridgen.



Plate 11. *Chromodoris africana* Eliot, 1904, photograph E Pridgen.

***Chromodoris quadricolor* (Rüppell & Leuckart, 1830)**

- South side Tiran Island, Ras Mohammed, 13 m depth (sandy gravelly substrate with isolated large boulders covered in epifauna), 23 Dec 1990, leg. and photographs N Yonow (NY # 110) [3 black lateral stripes, 3 blue, 13+ gills. More svelte than *africana*. Orange blur behind rhino. Orange gill + rhinophore pockets]; two individuals not collected (NY # 105, NY # 106), 17 × 5 mm and 40 × 8 mm [both perfect *C. quadricolor*].
- Near Garden, near Sha'arm el Sheikh, Egypt, 24 Dec 1990, 9 m depth (sandy rubble substrate with boulders), 25 × 5 mm, leg. N Yonow (NY # 114) [blurry, three black strips laterally].
- Ras umm Sid, near Sha'arm el Sheikh, Egypt, 25 Dec 1990, 25 m depth (sandy rubble substrate with boulders), 12 × 7 mm alive, leg. and photographs N Yonow (NY # 115).
- The creek, Jeddah, Saudi Arabia, 1970–1994, numerous photographs of numerous individuals, Pam Kemp, G Bemert, W Pridgen, N Yonow.
- Egyptian Red Sea, 1995–2001, numerous photographs of numerous individuals, J Hinterkircher.

***Glossodoris cincta* (Bergh, 1888)**

- Jeddah, Saudi Arabia, 1970–1980, photographs of three individuals, P Kemp.
- The creek, Jeddah, Saudi Arabia, 1970–1994, numerous photographs of numerous individuals, W Pridgen [common], Plate 13.



Plate 12. *Chromodoris quadricolor* (Rüppell & Leuckart, 1830), photograph E Pridgen.



Plate 13. *Glossodoris cincta* (Bergh, 1888), photograph E Pridgen.

- Egyptian Red Sea, 1995–2001, numerous photographs of numerous individuals, J Hinterkircher; 2009–2016, S Kahlbrock.

All photographs depicting individuals with the wide yellow-ochre submarginal band, blue-black marginal line, and the very edge marked in white.

***Glossodoris bikuereensis* (Pruvot-Fol, 1954)**

- Egypt, 29 Sept 1995, 25 m depth, photograph of one individual (HU-023), Á Valdés & E Mollo.
- Marsa Alam, Egypt, Feb/March 2001, photographs of one individual, J Hinterkircher; 2009–2016, S Kahlbrock. Plate 14.

***Hypselodoris maridadilus* Rudman, 1977**

- Egypt, 26 Sept 1995, intertidal, one specimen 14 × 7 mm preserved (HU-019), leg. Á Valdés & E Mollo.
- Jeddah, Saudi Arabia, 1970–1980, photographs of three individuals, P Kemp.
- The creek, Jeddah, Saudi Arabia, 1970–1994, photographs of two individuals, W Pridgen.
- Egyptian Red Sea, summer 1995, photographs of one individual, J Hinterkircher; 2009–2016, numerous photographs of several individuals, S Kahlbrock. Plate 15.

***Risbecia pulchella* (Rüppell & Leuckart, 1830)**

- Ufornakes reef, 20 km s of Hurghada, Egypt, 15 Aug 1965, one specimen 18 mm long × 13 mm high preserved, leg. Linsenmair [like T Paulus MSS # 7 but with slightly raised spots like SK # 5].
- Wreck, Aqaba, Jordan, Mar 1990, one specimen 37 mm long × 13 mm high preserved (MSS # 7), leg. and photo T Paulus [no markings or spots cf. recent specimen S Kahlbrock # 5].
- Egypt, 24 Sept 1995, one specimen 27 × 7 mm preserved (HU-01), leg. and photograph Á Valdés & E Mollo [had dried out in the past, brittle].
- MS Balena, Hurghada, Egypt, Apr 2015, 9 m depth, two specimens 48 mm long × 23 mm high and 46 mm long × 22 mm high preserved (SK # 5), leg. and photographs S Kahlbrock [opaque raised spots].
- The creek, Jeddah, Saudi Arabia, 1970–1994, numerous photographs of numerous individuals, many in mating pairs, W Pridgen.
- Egypt, 1995–2001, numerous photographs of numerous individuals, J Hinterkircher; 2009–2016, S Kahlbrock. Plate 16.



Plate 14. *Glossodoris hikuensis* (Pruvot-Fol, 1954), photograph S Kahlbrock.



Plate 15. *Hypselodoris maridadilus* Rudman, 1977, photograph S Kahlbrock.

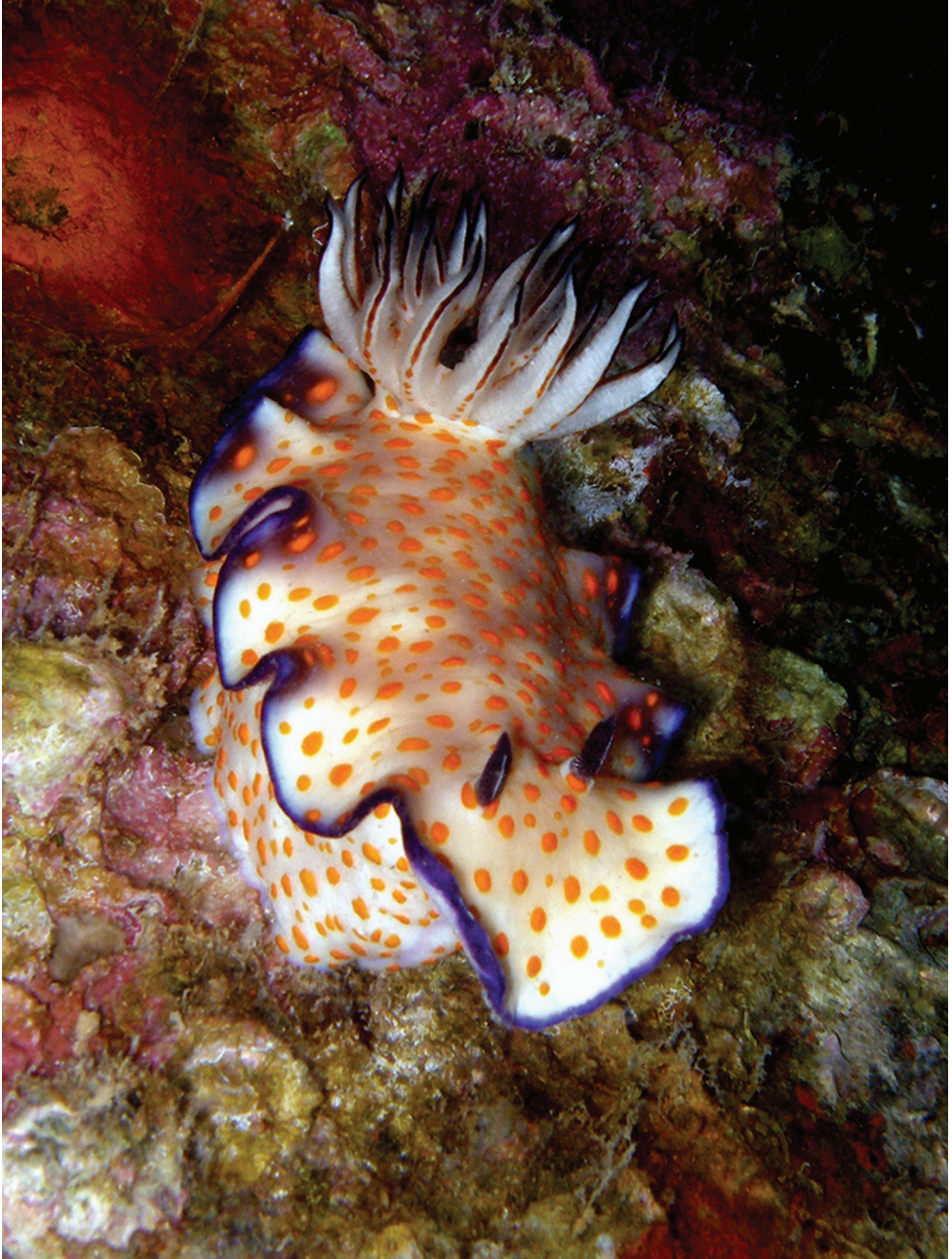


Plate 16. *Risbecia pulchella* (Rüppell & Leuckart, 1830), photograph S Kahlbrock.

A late Pleistocene gastropod fauna from the northern Caspian Sea with implications for Pontocaspian gastropod taxonomy

Thomas A. Neubauer^{1,2}, Sabrina van de Velde²,
Tamara Yanina³, Frank P. Wesselingh²

1 Department of Animal Ecology and Systematics, Justus Liebig University, Heinrich-Buff-Ring 26–32 IFZ, 35392 Giessen, Germany **2** Naturalis Biodiversity Center, P.O. Box 9517, 2300 RA Leiden, The Netherlands **3** Moscow State University, Faculty of Geography, Leninskie Gory, 1, 119991 Moscow, Russia

Corresponding author: *Thomas A. Neubauer* (thomas.a.neubauer@allzool.bio.uni-giessen.de)

Academic editor: *M. Haase* | Received 29 March 2018 | Accepted 20 May 2018 | Published 4 July 2018

<http://zoobank.org/4D984FDD-9366-4D8B-8A8E-9D4B3F9B8EFB>

Citation: Neubauer TA, van de Velde S, Yanina T, Wesselingh FP (2018) A late Pleistocene gastropod fauna from the northern Caspian Sea with implications for Pontocaspian gastropod taxonomy. *ZooKeys* 770: 43–103. <https://doi.org/10.3897/zookeys.770.25365>

Abstract

The present paper details a very diverse non-marine gastropod fauna retrieved from Caspian Pleistocene deposits along the Volga River north of Astrakhan (Russia). During time of deposition (early Late Pleistocene, late Khazarian regional substage), the area was situated in shallow water of the greatly expanded Caspian Sea. The fauna contains 24 species, of which 16 are endemic to the Pontocaspian region and 15 to the Caspian Sea. The majority of the species (13) belongs to the Pyrgulinae (Hydrobiidae), a group famous for its huge morphological variability in the Pontocaspian region. The phenotypic diversity has led to an inflation of genus and species names in the literature. New concepts are proposed for many of the genera and species found in the present material, with implications for the systematics and taxonomy of the entire Pontocaspian gastropod fauna. *Laevicaspia vinarskii* sp. n. is described as a new species. This contribution is considered a first step in revising the Pontocaspian gastropod fauna.

Keywords

biodiversity, endemism, long-lived lakes, non-marine Gastropoda, Quaternary

Introduction

The Caspian Sea is Earth's largest inland water body. With an area of 378,100 km² it covers about 40% of the world's continental surface water (Dumont 1998, Lehner and Döll 2004). The endorheic Caspian Basin is situated at the crossroads between Europe and Asia and borders Azerbaijan, Iran, Kazakhstan, Russia, and Turkmenistan. Today, its water balance is strongly controlled by the rivers Volga (Russia) and Ural (Kazakhstan) entering from the north and the Kura River (Azerbaijan) flowing in from the southwest and by evaporation from the sea and the adjacent Kara Bogaz Gol (Dumont 1998). The Caspian Sea is a mesohaline lake with an average salinity of about 12.8‰. Steep salinity gradients exist in the northern Caspian Sea from near freshwater conditions at the Volga River delta in the north to a maximum of 13.8‰ in the southeast (Dumont 1998).

During the Pleistocene, several major transgressive–regressive cycles caused recurrent connections between Black Sea and Caspian basins, which were accompanied by dramatic changes in lake size, salinity and biotic assemblages (e.g., Dumont 1998, Yanko-Hombach et al. 2007, Svitoch 2008, 2012, Shkatova 2010, Forte and Cowgill 2013, Van Baak et al. 2013, Yanina 2013, 2014, Taviani et al. 2014). In spite of the major environmental fluctuations over the geological past, the Caspian Sea Basin hosted a succession of anomalohaline to freshwater lakes since the late Pontian (late Messinian, late Miocene; Popov et al. 2006, Van Baak et al. 2013). The extensive duration facilitated the accumulation of diverse and highly endemic (“Pontocaspian”) biota in this long-lived lake (sensu Gorthner 1994), especially since the Early Pleistocene. As to the recent mollusk fauna, 92 species of gastropods and 35 species of bivalves are listed in latest systematic catalogues (e.g., Kantor and Sysoev 2005, 2006, Kantor et al. 2010, Vinarski and Kantor 2016). As for the gastropods, which are dominated by small-sized Hydrobiidae, 92.4% of them are endemic to the Caspian Sea (Neubauer et al. 2016a). Because of its high diversity, the Caspian Sea has been classified as a major biodiversity hotspot for anomalohaline gastropods (Neubauer et al. 2015a). However, the endemic mollusk fauna is at present severely suffering from the expansion of a number of invasive species (Kosarev and Yablonskaya 1994, Grigorovich et al. 2003, Orlova et al. 2005, Therriault et al. 2004, Riedel et al. 2006, Heiler et al. 2010, Albrecht et al. 2014). Since the early 20th century, human activity has led to a massive increase in the rate of establishment of non-indigenous aquatic species compared to preceding natural colonization (Grigorovich et al. 2003). Additional environmental pressure is exerted on the resident fauna by the increasing concentrations of heavy metals and pesticides (e.g., Agusa et al. 2004, Anan et al. 2005).

In order to predict future biodiversity loss as a response to natural or anthropogenically induced environmental change, it is vital to document and understand the species richness and development of the endemic fauna over longer temporal scales. For this purpose, a sound taxonomic framework is required. The extreme morphological variability of many of the described species complicates taxonomy and, thereby, hampers reliably diversity assessments. Preceding taxonomic studies carried out in the 19th and 20th century have produced a plethora of available species names, partly based on minor morphological deviations. Taxonomic works are hampered by (1) the inadequate



Figure 1. Geographic overview of the Pontocaspian region, with indication of the extent of the late Khazarian (early Late Pleistocene) transgression. The star marks Selitrennoye. Paleo-lake level was modeled in ESRI ArcGIS 10.4 based on Yanina (2014), who suggested an absolute lake level of 10 m b.s.l. at that time. Considering the present Caspian base level of 27 m b.s.l., this estimate corresponds to a lake level rise of 17 m. (Note that the model is restricted to the Pontocaspian catchment area and disregards potential topographic differences.) The bathymetry ranges are based on the GEBCO_2014 model (version 20150318) for present-day (Weatherall et al. 2015); shown isobaths equal to 100, 500 and 1000 m below current lake level.

nature of descriptions and illustrations, (2) the apparent loss of much of the material, (3) the few and hugely variable morphological characters in some of the groups, and (4) the apparent recent loss of many of the species, which makes combined morphological and molecular approaches impossible. Presently, the statuses of most Caspian endemic gastropods, especially of the numerous representatives of the Pyrgulinae (Hydrobiidae), are poorly resolved.

The present contribution details a diverse gastropod fauna from upper Khazarian (Upper Pleistocene) deposits from the northwestern part of the Caspian Basin, at that time witnessing a major transgressive event (Svitoch 2012; Fig. 1). We provide descriptions, illustrations and comparisons of the so far mostly poorly known species, and suggest nomenclatural and taxonomic rectifications. Since we could examine little of the type material of the discussed species (mostly because the whereabouts are

unknown), we limit our conclusions on former concepts and potential synonymies to taxa that have been thoroughly described and/or adequately illustrated (e.g., Kantor and Sysoev 2006). One particular focus of the present work is the revision of genus concepts that have been applied to Pontocaspian Hydrobiidae.

Materials and methods

The studied mollusk fauna derives from deposits exposed near the small village of Selitrennoye (also as Selitrennoe; *Russ.* Селитренное) along the left bank of the Akhtuba River, a tributary of the Volga River (Russia) (Fig. 1). The locality is situated about 100 km NNW of the city of Astrakhan in the administrative division of the same name (47°10'21.19"N, 47°26'25.41"E, WGS84). The investigated section of 14 m height spans the upper Khazarian to Khvalynian regional substages, which correlates to the early Late Pleistocene (Svitoch 2012, Yanina 2013, 2014). The base of the Quaternary outcrop, which lies 19 m below sea level, is formed by 2.5 m of upper Khazarian sands with common dispersed shells, including shell lenses (Fig. 2). This layer contains the here described gastropod fauna and several species of Lymnocardiinae bivalves. Upsection follows a 1-m-thick interval of horizontally alternating sandy and silty layers containing a diverse assemblage of bivalves of the genera *Monodacna*, *Didacna*, and *Dreissena*. Above it, 4 m of clays containing siltstones and sand layers were deposited. Overlying the interval, 3 m of lower Khvalynian sands are present, containing species of *Didacna* and *Dreissena*, followed by 1 m of brown silty clays ("chocolate clays"). The top of the Pleistocene deposits is marked by 1 m of upper Khvalynian sands and sandy loams barren of fossils, topped by a late Holocene soil complex rich in archeological remains.

Approximately 5 kg of sediment were collected by F.W. in September 2015 and were washed over a 0.5 mm sieve before sorting. All material is stored at the Faculty of Geography of the Moscow State University under collection numbers LV 201501–201530 and 201731–201750 and at the Naturalis Biodiversity Center, Leiden, The Netherlands, under collection numbers RGM 1309784–1309793, 1309797–1309856, 1310190–1310249, and 1310252–1310258.

Macro-photographs of the specimens were taken with a Leica M165 C stereomicroscope with attached DFC420 camera, using the focus stacking function of the Leica Application Suite software v. 4.4.0 at the Naturalis Biodiversity Center, Leiden. SEM images were acquired on a JEOL JSM-6480LV at the same institute. Specimens were coated with a 20 nm thick platinum-palladium alloy in a Quorum Q150T S coater.

For every species, a number of specimens was measured as representatives of its morphological spectrum. Shell measurements for *Theodoxus* are given as height × largest width (perpendicular to height) × second-largest width (perpendicular to both other axes); for all other species, measurements are given as height × width. Counting of protoconch whorls follows the method used by Verduin (1977) (Fig. 3). Descriptions and information on the whereabouts of type material are only indicated for Pontocaspian species; a brief account on the non-indigenous species detected herein is provided



Figure 2. Geographic position and log of the sampled section at Selitrennoye village. The star marks the layer of which the fauna derives. The stratigraphy was established based on the occurrence of *Lymnocar-diinae* bivalves, following the biostratigraphic scheme of Yanina (2013).

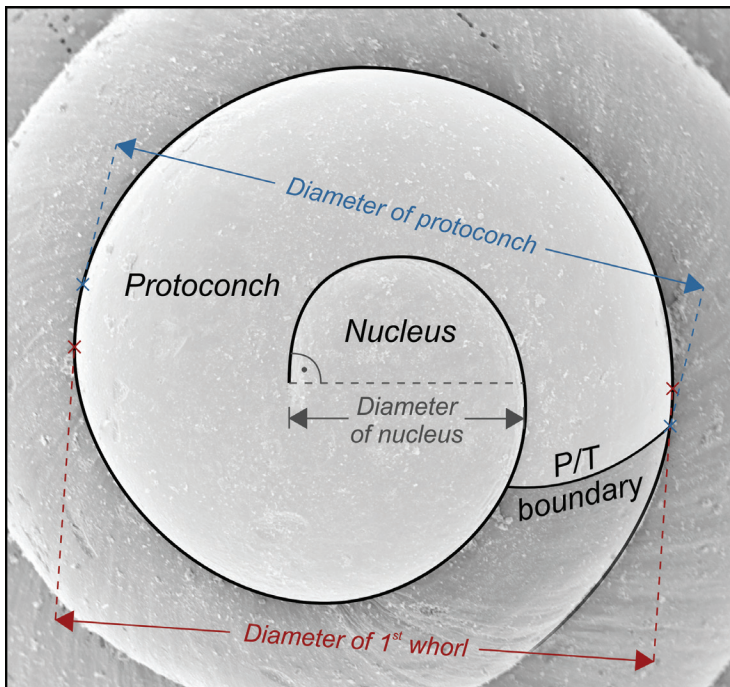


Figure 3. Sketch of the measurements made on the protoconch. The method for counting whorls follows Verduin (1977).

at the end of the Systematic Paleontology section. Synonymy lists comprise original descriptions, records providing illustrations and entries in systematic catalogues referring to Caspian records (e.g., Kantor and Sysoev 2006, Vinarski and Kantor 2016). The systematic classification follows Bouchet et al. (2017) and MolluscaBase (2017).

Abbreviations used are:

P/T	protoconch/teleoconch;
MSU	Moscow State University, Moscow, Russia, Faculty of Geography;
RGM	Naturalis Biodiversity Center, Leiden, The Netherlands, coll. Fossil Mollusca (formerly Rijksmuseum van Geologie en Mineralogie);
ZIN	Zoological Institute of the Russian Academy of Sciences, St. Petersburg, Russia.

Systematic paleontology

We tried to locate the depository of type specimens for all identified species, but this was successful only for a part of the fauna. In particular, much of the type material of the species described by Logvinenko and Starobogatov (1969) could not be located, since these authors did not provide information on the depository of the types or the localities they were retrieved at. According to Kantor et al. (2010), the types should be stored in ZIN but few have been found, since large parts of Starobogatov's collection have not been entirely inventoried as yet.

Class Gastropoda Cuvier, 1795

Subclass Neritimorpha Golikov & Starobogatov, 1975

Order Cycloneritimorpha Frýda, 1998

Superfamily Neritoidea Rafinesque, 1815

Family Neritidae Rafinesque, 1815

Subfamily Neritinae Poey, 1852

Genus *Theodoxus* Montfort, 1810

Type species. *Theodoxus lutetianus* Montfort, 1810 [currently considered as a synonym of *Theodoxus fluviatilis* (Linnaeus, 1758)]; by original designation. Recent; Europe.

Theodoxus pallasii Lindholm, 1924

Fig. 4A–F

1838 *Neritina liturata* m. Eichwald: 156–157 [non *Neritina liturata* Schultze, 1826].

1841 *Neritina liturata* m. – Eichwald: 258–260, pl. 38, figs 18–19 [non Schultze, 1826].

1855 *Neritina liturata* m. – Eichwald: 307–308 [non Schultze, 1826].

- 1887 *Neritina liturata* Eichw. sp. – W. Dybowski: 56–60 [non Schultze, 1826].
 1888 [*Neritina*] *liturata* Eichw. – W. Dybowski: 79, pl. 2, fig. 10 [non Schultze, 1826].
 * 1924 *Theodoxus pallasi* nom. nov.; Lindholm: 33, 34.
 1952 *Theodoxus pallasi* Lindh. – Zhadin: 208–209, fig. 124.
 1969 *Theodoxus pallasi* Ldh. – Logvinenko & Starobogatov: 343, pl. 5, figs 5–6, text-fig. 356.
 1994 *Theodoxus atrachanicus* Starobogatov in Starobogatov et al.: 8–9, fig. 1 (1–2).
 1994 *Th.[eodoxus] pallasi* Ldn. – Starobogatov et al.: 8–9, fig. 1 (3–4).
 2006 *Theodoxus pallasi* Lindholm, 1924. – Kantor & Sysoev: 45, pl. 20, fig. C.
 2006 *Theodoxus atrachanicus* Starobogatov in Starobogatov et al., 1994. – Kantor & Sysoev: 44, pl. 21, fig. C
 2009 *Theodoxus pallasi* Lindholm, 1924. – Filippov & Riedel: 70, 72, 74, 76, figs 4g–i.
 2011 *Theodoxus astrachanicus* Starobogatov in Starobogatov, Filchakov, Antonova et Pirogov, 1994. – Anistratenko et al.: 54–55, fig. 1 (6).
 2012 *Theodoxus pallasi* Lindholm, 1924. – Welter-Schultes: 29, unnumbered textfig.
 2016 *Theodoxus (Theodoxus) astrachanicus* Starobogatov in Starobogatov et al., 1994. – Vinarski & Kantor: 155–156.
 2016 *Theodoxus (Theodoxus) pallasi* (Lindholm, 1924). – Vinarski & Kantor: 156–157.
 2017 *Theodoxus pallasi* Lindholm, 1924. – Anistratenko et al.: 221, figs 4, 7, 10, 11 [cum syn.].

Material. 294 specimens (RGM 1309841, RGM 1309843, RGM 1310190–1310193, LV 201510).

Type material. Lectotype: ZIN 54547/63, designated by Starobogatov et al. (1994).

Type locality. “Inter Fucos littoris Derbendensis viva” (living among algae on the shores of Derbent), Dagestan, Russia.

Dimensions. 5.95 × 6.62 × 4.81 mm (RGM 1310191, Fig. 4A–C); 4.52 × 5.59 × 4.05 mm (LV 201510, Fig. 4D–F); 6.62 × 7.31 × 5.30 mm (RGM 1310192, Fig. 4I); 6.63 × 7.53 × 4.99 mm (RGM 1310190).

Description. Near globular shell with up to 2.7 whorls. Protoconch consists of about half a whorl; diameter of about 570 μm; nucleus measures ca. 250 μm in diameter; surface mostly corroded; P/T transition indistinct, marked by onset of growth lines. Apex weakly raised. Last whorl passes from upper suture over weakly inclined ramp with shallow concavity into broadly, regularly rounded flank that is near semi-circular in profile; relative length of ramp increases with ontogeny. Aperture inclined, regularly semicircular. Callus moderately thickened, glossy, edentate; right margin bulging, symmetrically sinuate, with near straight-sided lower and upper thirds and broad, shallow indentation in central third; left margin extends sinuate over base of penultimate whorl, with small adapical indentation, formed by slightly protruding peristome margin. Peristome sharply edged throughout ontogeny from adapical tip to where it passes into callus margin at base of penultimate whorl. Adapically, peristome margin forms steep crest towards callus, sometimes accompanied by thin, shallow furrow at the transition. Color pattern already starts on early teleoconch as widely spaced,

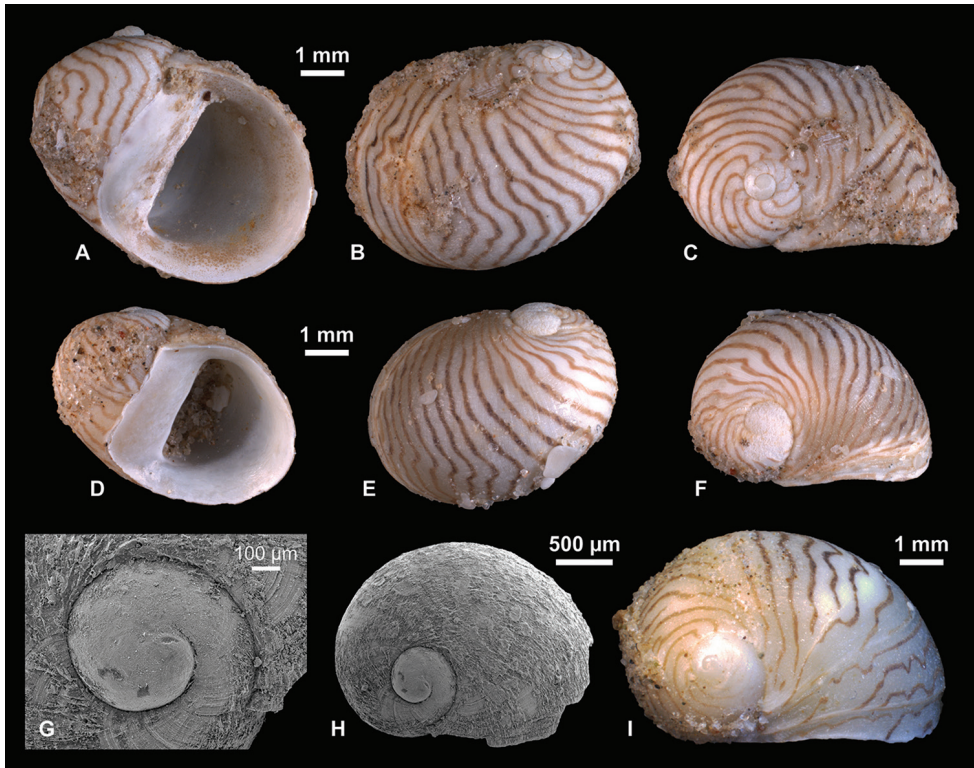


Figure 4. Neritidae. **A–C** *Theodoxus pallasi* Lindholm, 1924, RGM 1310191 **D–F** *T. pallasi*, LV 201510 **G, H** *T. pallasi*, RGM 1309843 **I** *T. pallasi*, RGM 1310192.

dark yellow to brown curved lines, which pass into slightly irregular zigzag lines with partly dichotomizing branches on last whorl; line width, density, amplitude, color and raggedness varies among specimens and partly within the same individual.

Discussion. The regular, widely spaced zigzag pattern is characteristic of the species. Comparable patterns occur in *T. danubialis* (Pfeiffer, 1828) and occasionally in *T. fluviatilis* (Linnaeus, 1758), but in these species lines are finer and more closely spaced. They furthermore differ in their less elongated shells. Similarly, *T. euxinus* (Clessin, 1886) from the Black Sea is more globular and shows a much denser and finer color pattern (Kantor and Sysoev 2006, Welter-Schultes 2012). *Theodoxus schultzei* (Grimm, 1877) has traditionally been distinguished from *T. pallasi* by its rounder shell and the massively expanded aperture (Zettler 2007). Currently, the whole group is under study using genetic data. Preliminary results suggest that both *T. pallasi* and *T. schultzei* may be grouped with the Armenian species *T. major* Issel, 1865, and possibly a major name change for *T. pallasi* is due (A.F. Sands, pers. commun. 05/2018).

Theodoxus astrachanicus Starobogatov in Starobogatov et al., 1994 from the Azov Sea and Volga delta is claimed to differ from *T. pallasi* in size and rate of whorl expansion (Starobogatov et al., 1994). However, both species correspond well in terms of shell shape and, in particular, the typical zigzag pattern (see also Kantor and Sysoev

2006). We therefore agree with Anistratenko et al. (2017) to treat *T. astrachanicus* as a junior synonym of *T. pallasii*.

Distribution. Presently living in the Caspian Sea, the Sea of Azov and the Aral Sea; records from Armenia and the Ural River need confirmation (Anistratenko et al. 2017). In the Pleistocene, the species also dwelled in river deltas entering the Black Sea, where it probably became extinct during the Neoeuxinian/late Pleistocene (Anistratenko et al. 2017).

Subclass Caenogastropoda Cox, 1960

Order Littorinimorpha Golikov & Starobogatov, 1975

Superfamily Truncatelloidea Gray, 1840

Family Hydrobiidae Stimpson, 1865

Subfamily Caspiinae B. Dybowski, 1913

Discussion. The genus *Caspia* has been widely used for species with small ovoid shells, occasionally with spiral or reticulate teleoconch sculpture. Based on the expression of sculpture, some authors have divided the species among the (sub)genera *Caspia* s.s., with a single spiral line below the suture, and *Clathrocaspia* Lindholm, 1930, exposing a reticulate pattern (e.g., Anistratenko and Prisyazhniuk 1992, Anistratenko 2013, Boeters et al. 2015, Büyükmeriç and Wesselingh 2018). Species lacking teleoconch sculpture were grouped under the new taxon *Ulskia* by Logvinenko and Starobogatov (1969). While those authors considered it a subgenus of *Pyrgula*, W. Dybowski (1887) originally treated its type species (*Caspia ulskii* Clessin & W. Dybowski in W. Dybowski, 1887, see below) as a sculpture-less form of *Caspia*.

Ulskia ulskii is available in the present material, and we have investigated the type species of *Clathrocaspia* (*Caspia pallasii* Clessin & W. Dybowski in W. Dybowski, 1887) obtained from Holocene deposits of the northern and southern Caspian Sea. However, the type species of *Caspia*, *Caspia baerii* Clessin & W. Dybowski in W. Dybowski, 1887, is unknown to us. The original description suggests that it is similar to *Ulskia* and *Clathrocaspia* in terms of size and shape, yet to differ in the presence of a single line below to suture, demarcating a narrow subsutural ramp. All three genera are probably closely related, which is also suggested by the similar protoconchs of *Ulskia* and *Clathrocaspia* (pers. obs. T.A.N.). Since *Ulskia* and *Clathrocaspia* can be easily distinguished based on the presence of sculpture, we propose to treat them as distinct genera. The status of *Caspia* remains doubtful until the type species is properly re-investigated.

The *Caspia*–*Clathrocaspia*–*Ulskia* species group can be well delimited from the larger, elongate-conical or -ovoid *Turricaspia* auct. and *Pyrgula* auct. Moreover, unpublished molecular data suggest that the group is unrelated to Pyrgulinae (T. Wilke, pers. comm. 04/2018). We follow Anistratenko (2013) and Bouchet et al. (2017), who listed the Caspiinae as separate subfamily.

Genus *Ulskia* Logvinenko & Starobogatov, 1969

Type species. *Caspia ulskii* Clessin & W. Dybowski in W. Dybowski, 1887; by original designation. Caspian Sea, Recent.

Ulskia ulskii (Clessin & W. Dybowski in W. Dybowski, 1887)

Fig. 5A–K

*1887 *Caspia Ulskii* nob.; W. Dybowski: 38–39.

1888 [*Caspia*] *Ulskii* n. sp. – W. Dybowski: 79, pl. 3, fig. 8.

1952 *Caspia ulskii* W. Dyb., 1888. – Zhadin: 205, fig. 205.

1969 *Pyrgula* [(*Ulskia*)] *nana* Logvinenko & Starobogatov: 379, fig. 367 (12).

1969 *Pyrgula* [(*Ulskia*)] *schorygini* Logv. et Star. sp. n.; Logvinenko & Starobogatov: 379, fig. 367 (11).

1969 *Pyrgula* [(*Ulskia*)] *ulskii* (Cless. et W. Dyb.). – Logvinenko & Starobogatov: 379, figs 367 (10).

2006 *Pyrgula nana* Logvinenko et Starobogatov, 1968. – Kantor & Sysoev: 101, pl. 47, fig. D.

2006 *Pyrgula schorygini* Logvinenko et Starobogatov, 1968. – Kantor & Sysoev: 103, pl. 45, fig. E.

2006 *Pyrgula ulskii* (Clessin et W. Dybowski in W. Dybowski, 1888). – Kantor & Sysoev: 104, pl. 45, fig. F.

2016 *Pyrgula nana* Logvinenko et Starobogatov, 1968. – Vinarski & Kantor: 240–241.

2016 *Pyrgula schorygini* Logvinenko et Starobogatov, 1968. – Vinarski & Kantor: 242.

2016 *Pyrgula ulskii* (Clessin et W. Dybowski in W. Dybowski, 1888). – Vinarski & Kantor: 244.

Material. 19 specimens (RGM 1309790, RGM 1309810, RGM 1309856, RGM 1310208, LV 201506).

Type material. “Probable syntype”: ZIN 4608/1. Holotype of *P. schorygini*: ZIN 4357/1. Holotype of *P. nana* not traced.

Type locality. “Kaspi-See” (Caspian Sea, no further details mentioned). Type locality of *P. schorygini*: Caspian Sea; off Apsheron Peninsula, 40°07.5'N, 50°57.5'E, WGS84, 88 m (after Vinarski and Kantor 2016). Type locality of *P. nana*: western part of the Caspian Sea, 70–120 m.

Dimensions. 2.05 × 1.13 mm (RGM 1309810, Fig. 5A, F, H, I); 2.16 × 1.16 mm (LV 201506, Fig. 5B, C, G); 2.12 × 1.10 mm (RGM 1309856, Fig. 5D, E); 2.12 × 1.23 mm (RGM 1309790, Fig. 5J, K).

Description. Slender ovoid shell with up to 4.7 whorls. Protoconch broad, low dome-shaped, comprising 1.25 whorls that measure 365 µm; nucleus is ca. 105 µm wide; protoconch surface finely but strongly malleate; pattern irregular on initial part and only partly present on nucleus; P/T transition marked by thin axial line and slight

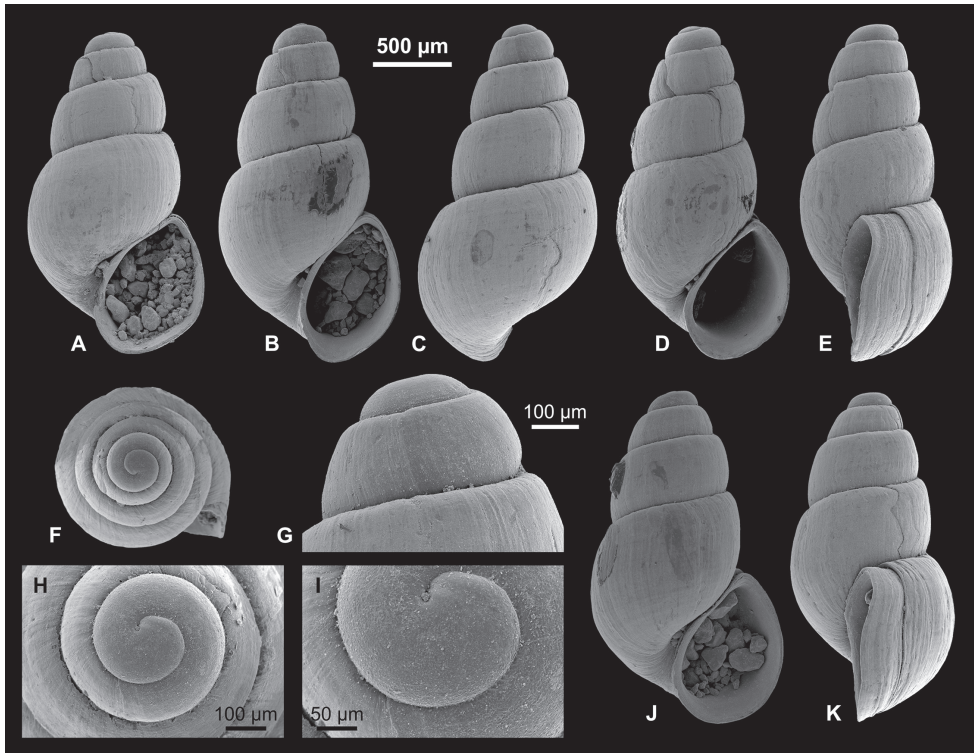


Figure 5. Caspiinae. **A, F, H, I** *Ulskia ulskii* (Clessin & W. Dybowski in W. Dybowski, 1887), RGM 1309810 **B, C, G** *U. ulskii*, LV 201506 **D, E** *U. ulskii*, RGM 1309856 **J, K** *U. ulskii*, RGM 1309790.

step in the upper suture. Teleoconch whorls slightly ton-shaped, weakly convex in abapical half and straight-sided or almost so in adapical half, followed by pronounced convexity at upper suture, producing slightly stepped spire. Last whorl attains ca. 61–66%, descends into steep, straight base. Aperture slender ovoid, slightly inclined, with faint adapical notch at contact to penultimate whorl. Peristome slightly thickened and expanded. In lateral view, outer lip exposes marked adapical indentation and very weak abapical indentation; columellar lip straight. Umbilicus narrow but always open. Growth lines weak but distinctly sigmoidal, with opisthocyrt upper half and prosocline lower half. In addition, faint spiral threads are visible on some shells.

Discussion. *Pyrgula schorygini* Logvinenko & Starobogatov, 1969 and *P. nana* Logvinenko & Starobogatov, 1969, both of which were also originally included in the subgenus *Ulskia*, closely resemble this species. Logvinenko and Starobogatov (1969) did not discuss similarities or differences among the species involved, but their descriptions suggest they considered minor differences in whorl profile and suture depth sufficient to discriminate species. A similar range of variability is present in our sample as well and might rather reflect intraspecific variation. We thus consider the three species synonymous.

Two more species were attributed to the subgenus *Ulskia* by Logvinenko and Starobogatov (1969). The shell of *Caspia derzhavini* (Logvinenko & Starobogatov,

1969) is more slender and has more whorls. *Caspia behningi* (Logvinenko & Starobogatov, 1969) differs in its broader and distinctly conical shape.

Distribution. Endemic to the Caspian Sea, reported from water depths between 45 and 120 m (Logvinenko and Starobogatov 1969).

? Subfamily Horatiinae Taylor, 1966

Genus *Andrusovia* Brusina in Westerlund, 1902a

Type species. *Andrusovia dybowskii* Brusina in Westerlund, 1902a; by original designation. Caspian Sea, Recent.

Discussion. The subfamily placement of the genus follows Vinarski and Kantor (2016: 214) and is based on the resemblance with species of the genus *Horatia* Bourguignat, 1887 (see also discussion in Starobogatov 2000). A recent molecular phylogeny including the Hydrobiidae suggests the Horatiinae to be distinct from the Belgrandiinae (Wilke et al. 2013; see also Bank 2017). We follow Starobogatov (2000) and regard *Caspiohoratia* Logvinenko & Starobogatov, 1969 as a junior synonym of *Andrusovia*.

Andrusovia brusinai Starobogatov, 2000

Fig. 6F–K, M–N

*2000 *Andrusovia brusinai* Starobogatov, sp. nov.; Starobogatov: 41, fig. 1C.

2006 *Andrusovia brusinai* Starobogatov, 2000. – Kantor & Sysoev: 83, pl. 40, fig. C.

2016 *Andrusovia brusinai* Starobogatov, 2000. – Vinarski & Kantor: 214.

Material. 39 specimens (RGM 1309839, RGM 1309840, RGM 1310206, LV 201509).

Type material. Holotype: ZIN (no number).

Type locality. Eastern part of the middle Caspian Sea (42°42.5'N, 51°32.5'E, WGS84), at 80 m.

Dimensions. 1.52 × 1.44 mm (RGM 1309840, Fig. 6F, G); 1.54 × 1.55 mm (LV 201509, Fig. 6H, K, N); 1.81 × 1.80 mm (RGM 1309839, Fig. 6I, J, M); 1.71 × 1.52 mm; 1.67 × 1.69 mm; 1.83 × 1.55 mm; 1.64 × 1.51 mm.

Description. Shell broad trochiform, about as high as wide, with up to 4 whorls. Rarely specimens with slightly elevated spire occur. Protoconch high domical, about semicircular in profile; initial part immersed; consists of 1.1 whorls, measures 300 µm in diameter; nucleus about 90 µm wide; protoconch surface finely but strongly malleate near lower suture, rest appears to be irregularly granulate, but that might be due to poor preservation; P/T boundary sharp, marked by massive growth constrictions near lower suture. Teleoconch whorls highly convex, with maximum convexity in adapical half, producing slightly stepped spire. Last whorl attains 74–81% of shell height. Aperture broadly drop-shaped, slightly inclined, with faint adapical notch at

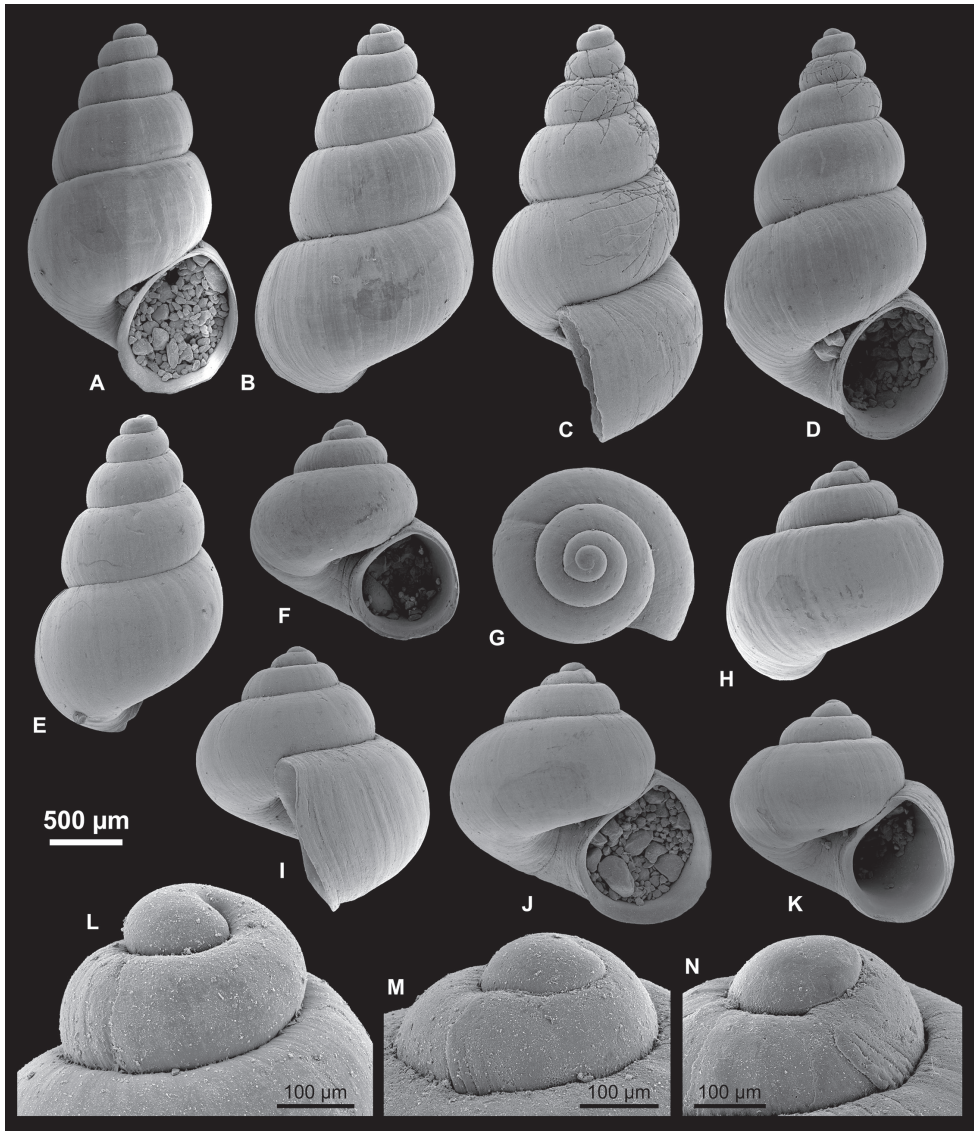


Figure 6. Hydrobiinae and Horatiinae. **A, B, L** *Ecriobia* cf. *grimmi* (Clessin in W. Dybowski, 1887), LV 201508 **C, D** *E.* cf. *grimmi*, RGM 1309845 **E** *E.* cf. *grimmi*, RGM 1309847 **F, G** *Andrusovia brusinaei* Starobogatov, 2000, RGM 1309840 **H, K, N** *A. brusinaei*, LV 201509 **I, J, M** *A. brusinaei*, RGM 1309839.

contact to penultimate whorl. Peristome slightly thickened and expanded at columella and base; sinuate in lateral view, with weakly protruding central part and weak adapical indentation. Umbilicus wide, deep. Fine prosocline growth lines cover shell. On one specimen, traces of spiral threads occur on base.

Discussion. The Caspian congeners *Andrusovia dybowskii* Brusina in Westerlund, 1902a (sensu Starobogatov 2000) and *A. andrusovi* Starobogatov, 2000 differ from

the present species in their much lower spires. *Andrusovia marina* (Logvinenko & Starobogatov, 1969) is smaller and has a shorter spire. Starobogatov (2000) based the distinction from *A. brusinai* on minor differences in shell ratios but these are strongly affected by the varying number of whorls and shell size; it might well be that *A. marina* and *A. brusinai* are just different growth stages of the same species. Since we have not seen the type material of Logvinenko and Starobogatov (1969), we tentatively accept the distinction of both taxa by Starobogatov (2000). Further comparison with the Logvinenko and Starobogatov material is essential to assess whether the two names refer indeed to distinct species.

Andrusovia brusinai resembles several recent species of *Horatia* Bourguignat, 1887, *Hauffenia* Pollonera, 1898 and *Islamia* Radoman, 1973 in terms of shell shape and protoconch surface. These differ from the present species in the either straight-sided (*Hauffenia*, *Islamia*; Arconada and Ramos 2006, Eröss and Petro 2008) or abapically (instead of adapically) sinuated peristome (*Horatia*; Szarowska 2006, Szarowska and Falniowski 2014). Shells of several species of *Pontohoratia* Vinarski, Palatov & Glöer, 2015 and *Motsameti* Vinarski, Palatov & Glöer, 2015 resemble *Andrusovia* species in terms of size and shape. They all differ in the more regularly shaped protoconchs, which show large nuclei and lack the massive growth constrictions.

Distribution. Endemic to the Caspian Sea, reported from middle and south Caspian Sea at depths between 47 and 311 m (Starobogatov 2000).

Subfamily Hydrobiinae Stimpson, 1865

Genus *Ecrobia* Stimpson, 1865

Type species. *Turbo minutus* Totten, 1834; by original description. United States, Recent.

Ecrobia cf. *grimmi* (Clessin in W. Dybowski, 1887)

Fig. 6A–E, L

cf. * 1887 *Hydrobia Grimmi* Cless.; W. Dybowski: 55–56.

cf. 1888 [*Hydrobia*] *Grimmi* Clessin. – W. Dybowski: 79, pl. 3, fig. 2.

cf. 1952 *Hydrobia grimmi* (Clessin) W. Dyb., 1888. – Zhadin: 225, fig. 147.

cf. 1969 *Pyrgohydrobia grimmi* (Cless. et W. Dyb.) – Logvinenko & Starobogatov: 249, fig. 358 (11).

cf. 2006 *Caspihydrobia grimmi* (Clessin in W. Dybowski, 1888). – Kantor & Sysoev, 91–92, pl. 43, fig. E.

cf. 2009 *Caspihydrobia grimmi* (Clessin et Dybowski, 1888). – Filippov & Riedel: 70–72, 74–76, figs 4a–d.

cf. 2016 *Caspihydrobia grimmi* (Clessin et W. Dybowski in W. Dybowski, 1888). – Vinarski & Kantor: 229.

Material. 345 specimens (RGM 1309845, RGM 1309847, RGM 1310207, LV 201508).

Type material. Not traced.

Type locality. “Kaspi-See” (Caspian Sea, no further details mentioned).

Dimensions. 2.56 × 1.45 mm (LV 201508, Fig. 6A, B, L); 2.83 × 1.54 mm (RGM 1309845, Fig. 6C, D); 2.19 × 1.30 mm (RGM 1309847, Fig. 6E); 3.88 × 2.26 mm; 3.48 × 1.97 mm; 3.77 × 1.99 mm; 3.50 × 1.89 mm; 3.26 × 1.79 mm; 3.33 × 1.66 mm.

Description. Shell shape highly variable, ranging from broad ovoid to slender conical, comprising up to 6.5 whorls. Protoconch consisting of about one whorl, with nucleus immersed; initial part slightly raised, producing acute apex; surface weakly granular to malleate; P/T transition clear. Protoconch and teleoconch whorls highly convex, sometimes slightly flattened centrally in later whorls; suture deep. Size of last whorl varies between 55–62%, descends into straight-sided base. Aperture regularly ovoid, slightly inclined, touching base of penultimate whorl, leaving wide umbilicus. Peristome simple, sometimes weakly expanded. Surface smooth except for very fine prosocline growth lines.

Discussion. The shells of *Ecrobia* can only be reliably identified on the species-level using molecular data (Haase et al. 2010). Therefore, we tentatively assign the detected specimens to *Ecrobia grimmi*, which is the only *Ecrobia* species occurring in the Caspian Sea today (Haase et al. 2010).

Most of the species presently assigned to *Caspiohydrobia* Starobogatov, 1970, including its type species, *Pyrgohydrobia eichwaldiana* Golikov & Starobogatov, 1966, range within the morphological variability of this species. Previous examination of both reproductive systems (Sitnikova et al. 1992) and juvenile shells (Filippov and Riedel 2009) did not yield criteria supporting interspecific differentiation. Very likely all of the thirty *Caspiohydrobia* species listed by Kantor and Sysoev (2006) are morphotypes of a single species, probably *E. grimmi*. Given the problems of using shell morphology to identify *Ecrobia*, taxonomic conclusions on the synonymy of the *Caspiohydrobia* species require molecular data.

Note on species authority. W. Dybowski (1887: 7) noted that all diagnoses were drafted by Clessin and himself and most new species were therefore marked with “nob.” (Lat. *nobis*, “us”). However, W. Dybowski obviously made exceptions. In case of the new genus *Clessinia*, he marked the authority with “m.” (Lat. *meus*, “mine”). For *Hydrobia grimmi*, the authority is clearly indicated with “Cless.,” making Clessin the sole author of the species (unlike indicated by several authors).

Distribution. Caspian Sea; Lake Sawa, Iraq (Haase et al. 2010); salt lakes near Chelyabinsk, Russia (Shishkoedova 2010). Subfossil records derive from Holocene deposits of the Aral Sea (Filippov and Riedel 2009).

Subfamily Pyrgulinae Brusina, 1882

1882 Pyrgulinae Brusina: 230.

1914 Micromelaniidae B. Dybowski & Grochmalicki: 276.

1915 Turricaspiinae B. Dybowski & Grochmalicki: 103.

2017 Pyrgulinae Brusina, 1882. – Bouchet et al.: 212, 346 [cum syn.].

Discussion. The Caspian Pyrgulinae (sensu lato) encompasses 64 species that are considered accepted in the current literature (Vinarski and Kantor 2016). However, most of them are poorly known, documented by insufficient descriptions and drawings; for many, the type material has not been found (Kantor and Sysoev 2006, Vinarski and Kantor 2016). The extreme morphological variability of several representatives, such as those detected in the material from Selitrennoye, led previous authors to introduce numerous species based on shells with only minor deviations in shape, size or whorl outline. The Caspian Pyrgulinae therefore requires careful revision using molecular and anatomical data as far as available.

In addition to the problems associated with distinguishing species, genus-level classification is poorly resolved as well. Several attempts have been made to categorize this vast variability, and genus concepts have changed tremendously (e.g., B. Dybowski and Grochmalicki 1915, 1917, Zhadin 1952, Logvinenko and Starobogatov 1969, Kantor and Sysoev 2006, Vinarski and Kantor 2016). Twelve genus names have been described for members of the Caspian Pyrgulinae, based on quite different concepts of traits considered diagnostic. Currently, all species are classified within *Caspia* Clessin & W. Dybowski, 1887, *Pyrgula* De Cristofori & Jan, 1832 and *Turricaspia* B. Dybowski & Grochmalicki, 1915 (Kantor and Sysoev 2006, Vinarski and Kantor 2016). This scheme unites quite a variety of different morphologies under the same genus names, while at the same time similar species are assigned to different genera (e.g., Kantor and Sysoev 2006). Unfortunately, hardly any previous study provided explanations for their genus classifications or systematic concepts in general.

A thorough revision of all Caspian Pyrgulinae is beyond the scope of this study, but we discuss and revise the concepts that have been applied to the species studied herein.

Vinarski and Kantor (2016) listed 38 species of the genus *Pyrgula* for the Caspian Sea. The type species of *Pyrgula* De Cristofori & Jan, 1832, *P. annulata* (Linnaeus, 1758), lives in freshwater lakes and springs in Italy and Dalmatia (Welter-Schultes 2012). Shell morphology, anatomy and protoconch characteristics are very similar to Pontocaspian Pyrgulinae, e.g., some species of *Turricaspia* (compare also discussion in Riedel et al. 2001). However, molecular evidence suggests that *Pyrgula annulata* is only distantly related to the Pontocaspian species flock within the Pyrgulinae, with the last common ancestor dating back to the late Miocene (Wilke et al. 2007). Therefore, Pontocaspian species should not be attributed to *Pyrgula*, despite apparent morphological congruence, especially of some of the keeled Pontocaspian Pyrgulinae. A separation on subfamily level as proposed by B. Dybowski and Grochmalicki (1915) is opposed by the latest phylogeny of rissoidan gastropods, which suggests a rather close relationship (Wilke et al. 2013).

Turricaspia B. Dybowski & Grochmalicki, 1915 (type species: *Micromelania turricula* B. Dybowski & Grochmalicki, 1915) was introduced for species with turritiform, elongate shells with numerous whorls. Presently, the genus includes 22 Caspian species, encompassing elongate and broad, conical and ovoid, and sculptured and smooth species (Kantor and Sysoev 2006, Vinarski and Kantor 2016). Many species assigned to *Pyrgula* by Kantor and Sysoev (2006) and Vinarski and Kantor (2016) actually re-

semble *Turricaspia turricula* with respect to the turritiform, conical shell. This similarity also regards the type species of the genera *Caspiopyrgula* Logvinenko & Starobogatov, 1969 (type species: *Turricaspia nossovi* Kolesnikov, 1947), *Eurycaspia* Logvinenko & Starobogatov, 1969 (*Micromelania pseudodimidiata* B. Dybowski & Grochmalicki, 1917), *Oxypyrgula* Logvinenko & Starobogatov, 1969 (*Pyrgula pseudospica* Logvinenko & Starobogatov, 1969), and *Trachycaspia* B. Dybowski & Grochmalicki, 1917 (*Rissoa dimidiata* Eichwald, 1838). After examination of descriptions and illustrations of the type species (e.g., Kantor and Sysoev 2006), we conclude that these genera should be considered as junior synonyms of *Turricaspia*.

Some of the species classified as *Turricaspia* by Kantor and Sysoev (2006) and Vinnarski and Kantor (2016) differ considerably from *Turricaspia* s.s. in shell shape. This contains the type species of the genera *Caspiella* Thiele, 1928 (*Rissoa conus* Eichwald, 1838), *Clessiniola* Lindholm, 1924 (*Paludina variabilis* Eichwald, 1838), and *Laevicaspia* B. Dybowski & Grochmalicki, 1917 (*Rissoa caspia* Eichwald, 1838). In turn, some species presently attributed to the genus *Euxinipyrgula* Sitnikova & Starobogatov, 1999 (type species: *Pyrgula milachevitchi* Golikov & Starobogatov, 1966) closely resemble species of the *Laevicaspia*–*Caspiella* group (compare Anistratenko et al. 2011).

Based on a review of the Pontocaspian species formerly attributed to these genera and illustrated in the literature (Golikov and Starobogatov 1966, Logvinenko and Starobogatov 1969, Alexenko and Starobogatov 1987, Kantor and Sysoev 2006, Anistratenko 2008), we propose to distinguish the genera *Clessiniola* and *Laevicaspia* from *Turricaspia*, and to treat *Caspiella* and *Euxinipyrgula* as junior synonyms of *Laevicaspia*.

Clessiniola species can be easily distinguished from species attributed to other genera based on their broad shells with a large body whorl and aperture. The situation for the *Laevicaspia*–*Caspiella*–*Euxinipyrgula* is more difficult. The three type species (see above) share the ovoid shape with cyrtocooid spire, the high whorl accretion rate, the shape, inclination, lateral situation and thickening of the aperture, and the extent and sculpture of the protoconch (e.g., Kantor and Sysoev 2006, Anistratenko 2008, and this study). The only differences are shell size and whorl convexity, which we do not consider sufficient to distinguish genera. The adapical thickening of the aperture resulting from downward growing of the shell in late ontogeny as stated in the diagnosis of the genus *Euxinipyrgula* by Sitnikova and Starobogatov (1999) is also shown for species that have been attributed to *Caspiella* (see below). The features of the soft-part anatomy considered diagnostic by these authors need to be rechecked and compared to live material from the Caspian Sea to reevaluate the position of *Euxinipyrgula*. Sitnikova and Starobogatov (1999) also discussed the similarities between *Caspiella* and *Euxinipyrgula*, concluding that *Caspiella* should perhaps be included in the genus *Euxinipyrgula*, possibly as a separate subgenus (which would be nomenclaturally invalid however).

The ovoid shape, lateral situation and thickening of the aperture typical for the *Laevicaspia*–*Caspiella*–*Euxinipyrgula* group are also found among species of the genus *Prososthenia* Neumayr, 1969 from the middle Miocene of the Dinaride Lake System (e.g., Neubauer et al. 2016b). These species, however, differ in the granulate protoconch making up less than one whorl.

Species of *Turricaspia* differ from *Laevicaspia* in the slower, regular whorl accretion, producing a conical spire and a higher number of whorls at the same size. In addition, *Turricaspia* species have usually more fragile shells, thinner peristomes and often more strongly sinuate growth lines.

The genus *Caspia* is listed among Pyrgulinae in latest catalogues (Kantor and Sysoev 2006, Vinarski and Kantor 2016), but it has been shown to be unrelated to that subfamily (Anistratenko 2013, Bouchet et al. 2017; see discussion of the Caspiinae above).

Finally, several Pontocaspian Pyrgulinae have been previously assigned to the genus *Micromelania* Brusina, 1874 (e.g., W. Dybowski 1887, B. Dybowski and Grochmalicki 1917). Its type species, *Micromelania cerithiopsis* Brusina, 1874 (subsequent designation by Dollfus 1912), derives from late Miocene deposits of Lake Pannon. It differs considerably from Pontocaspian Pyrgulinae regarding the presence of 2–4 noded keels and the small size (4.5 × 1.33 mm after Brusina 1874) compared to the rather high number of eight whorls.

Genus *Clessiniola* Lindholm, 1924

1887 *Clessinia* W. Dybowski: 41 [non Doering, 1875].

1924 *Clessiniola* Lindholm: 32–33, 34.

1928 *Clessinola* Strand: 68 [junior objective synonym of *Clessiniola*].

Type species. *Paludina variabilis* Eichwald, 1838; by typification of replaced name (*Clessinia* W. Dybowski, 1887). Volga delta and Caspian Sea, Quaternary to Recent.

Clessiniola variabilis (Eichwald, 1838)

Fig. 7A–I

*1838 *Paludina variabilis* m.; Eichwald: 151–152.

1841 *Paludina variabilis* m. – Eichwald: 253–254, pl. 38, figs 6–7.

1853 *Pal.[udina] variabilis* m. – Eichwald: 285.

1887 *Clessinia variabilis* Eichw. sp. – W. Dybowski: 41–42.

1888 [*Clessinia*] *variabilis* Eichw. sp. – W. Dybowski: 79, pl. 2, fig. 6.

1952 *Clessiniola variabilis* (Eichwald, 1841). – Zhadin: 255, fig. 199.

1966 *P.[yrgula] (Clessiniola) variabilis*. – Golikov & Starobogatov: 356, fig. 2 (2).

1969 *Pyrgula [(Clessiniola)] variabilis* (Eichw.) – Logvinenko & Starobogatov: 377, fig. 367 (1).

1987 *T.[urricaspia] variabilis* (Eichw.). – Alexenko & Starobogatov: 34, fig. 5.

2006 *Turricaspia variabilis* (Eichwald, 1838). – Kantor & Sysoev: 111, pl. 49, fig. J.

2011 *Turricaspia variabilis* (Eichwald, 1838). – Anistratenko et al.: 85, fig. 3 (15).

2014 *Turricaspia variabilis*. – Taviani et al.: 4, fig. 3b.

2016 *Turricaspia variabilis* (Eichwald, 1838). – Vinarski & Kantor: 251.

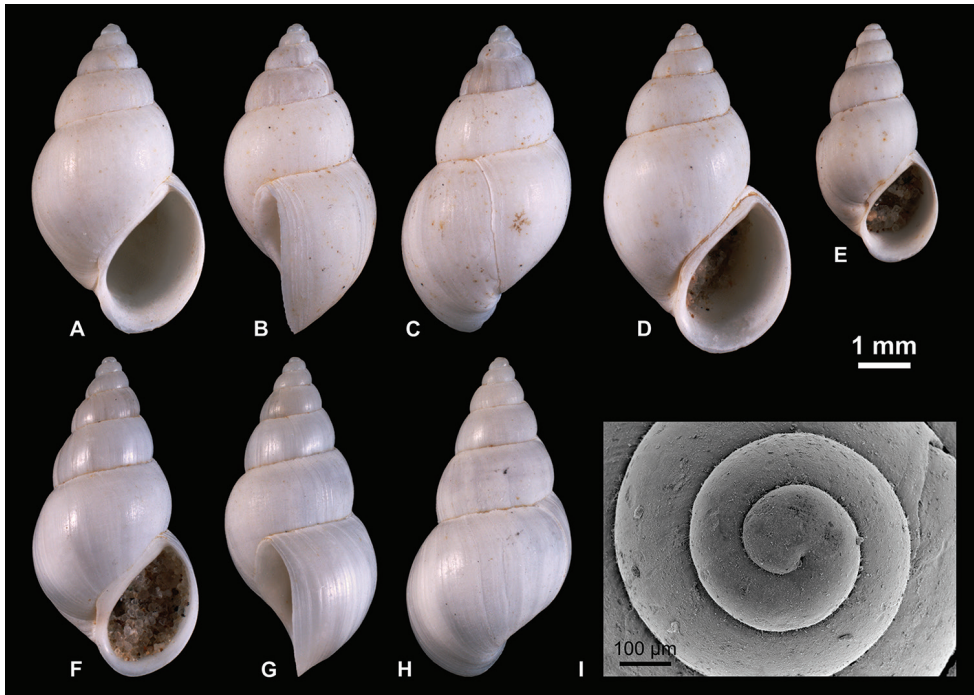


Figure 7. Pyrgulinae. **A–C** *Clessiniola variabilis* (Eichwald, 1838), LV 201507, broad morphotype **D** *C. variabilis*, RGM 1310246, broad morphotype **E** *C. variabilis*, RGM 1310245, slender morphotype **F–H** *C. variabilis*, RGM 1310243, slender morphotype **I** *C. variabilis*, RGM 1309827.

Material. 4867 specimens (RGM 1309815, RGM 1309826, RGM 1309827, RGM 1309831, RGM 1310243–1310247, LV 201507).

Type material. Not traced.

Type locality. “In Volgae ostio prope Astrachanum, et versus mare Caspium; etiam fossili in calcatio lapide conglutinato recentissimo Dagesthanici littoris” (at the Volga river mouth near Astrakhan, and towards the Caspian Sea; also in recently lithified fossil limestone at the shores of Dagestan).

Dimensions. 5.91 × 3.31 mm (LV 201507, Fig. 7A–C); 6.31 × 3.59 mm (RGM 1310246, Fig. 7D); 4.60 × 2.35 mm (RGM 1310245, Fig. 7E); 6.08 × 3.18 mm (RGM 1310243, Fig. 7F–H); 6.85 × 3.89 mm (RGM 1310244).

Description. Broadly drop-shaped to rarely conical shell of up to six whorls. Protoconch insufficiently preserved to specify extent and surface sculpture; P/T transition indistinct; first whorl measures ca. 340 µm in diameter. Teleoconch whorls moderately and regularly convex; sometimes, spire is very faintly stepped; suture narrow. In many specimens, shells starts to grow stronger in abapical direction in course of last (two) whorl(s), producing non-parallel suture and relatively higher penultimate whorl. Rarely, forms with comparatively slender shape and regularly increasing whorls (and thus relatively smaller last and penultimate whorls) occur. Both types are linked via intermediates. Aperture regularly ovoid, inclined; inner lip glossy, weakly to sometimes more

prominently thickened; strongly adnate, sheet-like expanded over base of penultimate whorl and columella, rarely leaving very narrow umbilicus; broad, shallow spout occurs at transition between columella and base; outer lip mainly thin, sometimes weakly thickened at anterior notch. Growth lines very faint, with prosocline upper third and near orthocline lower two-thirds.

Discussion. This species displays a large morphological variability within our ample material. Shell shape ranges between slender conical to broadly ovoid, sometimes with weakly irregular growth. Likewise, shell size, whorl convexity, and number of whorls vary considerably. Yet, these features intergrade without clear boundary, rendering a distinction of species unreasonable.

The morphological variability is not restricted to our material but a general feature of *Clessiniola*. It was documented by several previous authors, partly for specimens from the same localities (e.g., Eichwald 1838, Issel 1865, W. Dybowski 1887–1888, Golikov and Starobogatov 1966, Logvinenko and Starobogatov 1969, Alexenko and Starobogatov 1987, Anistratenko et al. 2011). The species concepts applied by the different authors, however, varied greatly. The present material includes shells that have been variably attributed to the species *C. variabilis* (Eichwald, 1838), *C. triton* (Eichwald, 1838) and *C. martensii* (Clessin & W. Dybowski in W. Dybowski, 1887). The *triton*-morphotype sensu Eichwald characterizes broad specimens with slightly detached aperture (see also Kantor and Sysoev 2006); these forms are rarely represented in our material. Eichwald (1838, 1841) himself confirmed the rarity of the form, also stating that he did not find a living representative (in contrast to *C. variabilis*). The *martensii*-morphotype was introduced for similarly broad morphologies. (Note that Clessin and W. Dybowski used a different concept of *C. triton*, there having a rather elongate conical shell.)

Because of the fluent morphological transition between forms traditionally referred to as *C. variabilis*, *C. triton* and *C. martensii*, as well as their joint occurrence in several localities in the Pontocaspian region, one might consider all of them synonymous. Personal observations on Holocene material from Dagestan area, however, indicate indeed distinguishable morphotypes without intermediates. Moreover, frequent shell repair found in most of the Selitrennoye specimens additionally complicates an unbiased view on morphological diversity. A more in-depth investigation comparing undamaged material from different sites is thus required.

Given the large variability, the Caspian species *Clessiniola ovum* (Logvinenko & Starobogatov, 1969) and *C. trivialis* (Logvinenko & Starobogatov, 1969), as well as *C. pseudotriton* (Golikov & Starobogatov, 1966) from the Dniester River mouth (compare Kantor and Sysoev 2006), might too be considered as synonyms of *C. variabilis*. However, the original descriptions and drawings provided impede clarification of their statuses.

Clessinia ahngerii Westerlund, 1902 is often listed as junior synonym of *C. variabilis*, but without discussion (e.g., Logvinenko and Starobogatov 1969, Vinarski and Kantor 2016). The original description of *C. ahngerii* suggests close similarities indeed between both species claiming, however, that it differs from other congeners in the much larger spire (11 × 5 mm) and the slightly sinuate outer lip. Examination of Westerlund's (1902b) material is required to ascertain the alleged synonymy.

The record of “*Paludina Eichwaldi* Kryn.” Eichwald (1841) listed in synonymy of *C. variabilis* refers to a nomen nudum mentioned in a species list by Krynicki (1837).

Distribution. Endemic to the Pontocaspian region. Found in the Caspian Sea and the lower courses of rivers and freshwater parts of the Azov and Black seas (Anisratenko et al. 2011, Vinarski and Kantor 2016). Also reported from Neoeuxinian (late Pleistocene) deposits of the Marmara Sea (Taviani et al. 2014).

Genus *Laevicaspia* B. Dybowski & Grochmalicki, 1917

- ? 1902a *Thaumasia* Westerlund: 104 [non Perty, 1833; non Albers, 1850].
 1917 *Laevicaspia* B. Dybowski & Grochmalicki: 5.
 1928 *Caspiella* Thiele: 353, 381.
 1999 *Euxinipyrgula* Sitnikova & Starobogatov: 158, 162.

Type species. *Rissoa caspia* Eichwald, 1838; by subsequent designation by Logvinenko and Starobogatov (1969). Caspian Sea, Pleistocene.

Discussion. Lindholm (1922) studied the type material of *Buliminus goebeli* Westerlund, 1896 from Mangyschlak (Mangystau Peninsula, Kazakhstan) and concluded that is a junior synonym of “*Micromelania*” *caspia* (Eichwald, 1838). Westerlund (1902a), considering *Buliminus goebeli* as a member of terrestrial “Bulimoidea” (= Enidae), introduced the new genus *Thaumasia*, which would take precedence over *Laevicaspia* B. Dybowski & Grochmalicki, 1917. However, *Thaumasia* Westerlund, 1902 is invalid as a junior homonym of *Thaumasia* Perty, 1833 (Arachnida) and *Thaumasia* Albers, 1850 (Gastropoda, Subulinidae) (see also Lindholm 1925).

Laevicaspia caspia (Eichwald, 1838)

Fig. 8A–K

- *1838 *Rissoa caspia* m.; Eichwald: 154–155.
 1841 *Rissoa caspia* – Eichwald: 256–257, pl. 38, figs 14–15.
 1853 *Riss.[oa] caspia* m. – Eichwald: 273.
 non 1876 *Hydrobia caspia*, Eichw. – Grimm: 150–153, pl. 6, fig. 15.
 non 1877 *Hydrobia caspia*, Eichw. – Grimm: 79–80, pl. 7, figs 3a–d.
 non 1887 *Micromelania caspia* Eichw. sp. – W. Dybowski: 21.
 non 1888 *Micr.[omelania] caspia* Eichw. sp. – W. Dybowski: 78, pl. 1, fig. 1.
 ? 1896 *B.[uliminus] (Napaeus?) goebeli* Westerlund: 188.
 1914 *Micromelania* (?) *curta* Nalivkin: 21–22, 31, pl. 6, figs 1–2 [partim; non figs 3–4, 7, 9–14].
 1914 [*Micromelania* (?) *curta*] var. *plano-convexa* Nalivkin: 22, 31, pl. 6, figs 15–18.
 non 1914 *Micromelania caspia* Eichw. – Nalivkin: 22, 31, pl. 6, figs 5–6 [partim; non fig. 8].

non 1917 *Micromelania* (*Turricaspia*, *Laevicaspia*) *caspia* Eichw. – B. Dybowski & Grochmalicki: 5–8, 36–38, pl. 1, figs 1–3.

non 1969 *Pyrgula caspia* (Eichw.). – Logvinenko & Starobogatov: 369–370, fig. 364 (1).

1987 *T.[urricaspia] caspia* (Eichw.). – Alexenko & Starobogatov: 33, fig. 2.

2006 *Turricaspia caspia* (Eichwald, 1838). – Kantor & Sysoev: 106, pl. 49, fig. M.

2014 *Euxinipyrgula lincta*. – Taviani et al.: 4, fig. 3c [non *Micromelania lincta* Milashevich, 1908].

2016 *Turricaspia caspia* (Eichwald, 1838). – Vinarski & Kantor: 246.

Material. 300 specimens (RGM 1309788, RGM 1309789, 1309797, RGM 1309798, RGM 1310196, RGM 1310257, RGM 1310258, LV 201511).

Type material. Lectotype: ZIN (No. 1 in systematic catalogue), designated by Alexenko and Starobogatov (1987).

Type locality. “In eodem lapide calcario Dagesthanico, fossilis” (in the same limestone of Dagestan [referring to the previous species, also found in Dagestan], fossil).

Dimensions. 9.01 × 3.31 mm (RGM 1310257, Fig. 8A–C); 7.88 × 3.31 mm (RGM 1310258, Fig. 8D–F); 10.33 × 3.92 mm (LV 201511, Fig. 8I–K); 9.92 × 3.83 mm; 10.21 × 3.88 mm; 9.52 × 3.54 mm; 9.69 × 3.61 mm.

Description. Large, slender ovoid shell comprising up to 8.3 whorls. Protoconch large, measuring 535–600 μm at 1.15–1.2 whorls, with initial part inflated; nucleus almost immersed, 190–230 μm wide; nucleus and early protoconch bear intentions of malleate sculpture, which passes into granular surface after half a whorl accompanied by onset of spiral striae; P/T boundary indistinct. Whorl convexity decreasing rapidly: first teleoconch whorl moderately convex, second to last whorl low convex, sometimes almost straight-sided; maximum convexity is in lower half; whorls closely attached, suture narrow; a very small but marked convexity appears at upper suture, producing a faintly stepped spire; occasionally, it is accompanied by shallow abapical concavity. Last whorl makes up 46–50% of shell height, passing over regular but weakly convex to near straight-sided to slightly concave base. Aperture slender ovoid, inclined, closely attached to preceding whorl; in latest ontogeny, shell growth is more abapically directed, resulting in marked thickening at adapical tip. Peristome simple, thin, slightly expanded and indented at base; distinctly and regularly sigmoidal in lateral view, with upper half broadly indented and lower half broadly protruding; inner lip protrudes in lateral view, extending sheet-like over base of penultimate whorl; umbilicus mostly closed, rarely very narrow, slit-like. Growth lines weakly sigmoidal: strongly prosocline in upper half, weakly opisthocline in lower half. Several specimens show faint spiral threads on last and penultimate whorls.

Discussion. Different concepts of this species previously applied have led to considerable confusion about its real identity. This is partly rooted in the description and illustration provided by Eichwald (1838, 1841) that were insufficient to allow safe discrimination from similar species. For instance, *Micromelania caspia* sensu Grimm (1876, 1877), W. Dybowski (1887–1888) and B. Dybowski and Grochmalicki (1917) differs from the present species in the acute apex, the moderately convex whorls, the

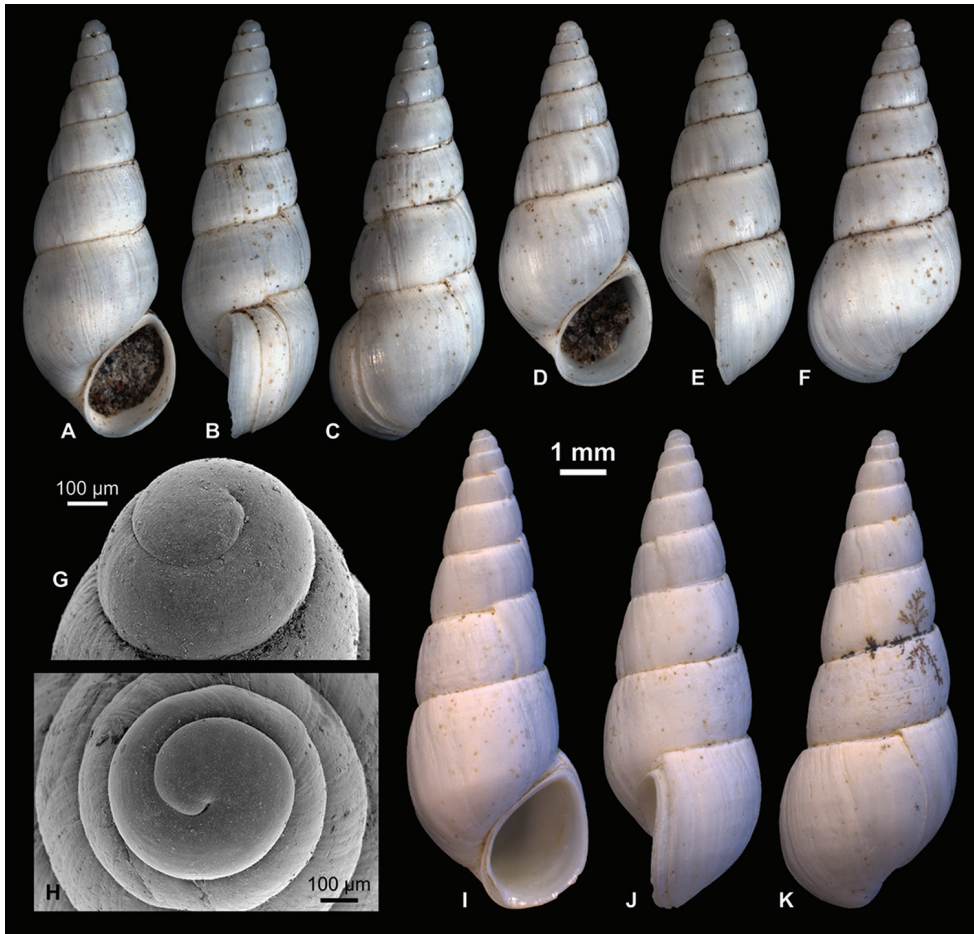


Figure 8. Pyrgulinae. **A–C** *Laevicaspia caspia* (Eichwald, 1838), RGM 1310257 **D–F** *L. caspia*, RGM 1310258 **G** *L. caspia*, RGM 1310197 **H** *L. caspia*, RGM 1310198 **I–K** *L. caspia*, LV 201511.

deep suture and the thin peristome. As already noted by Alexenko and Starobogatov (1987), it represents a different species, i.e., *Laevicaspia lincta* (Milashevich, 1908). That species was described from Lake Katlabukh near the Danube delta in Ukraine (lectotype, which matches Milashevich's description, is illustrated in Kantor and Sysoev 2006: 95, pl. 45, fig. D; as *Euxinipyrgula lincta*). Specimens from the Neoeuxinian (late Pleistocene) of the Marmara Sea identified as *E. cf. lincta* by Taviani et al. (2014) differ from that species in the near straight-sided whorls and thickened peristome; in fact, the material corresponds well to *L. caspia*.

Micromelania caspia sensu Nalivkin (1914) comprises at least two species, both being more elongate, having more whorls and relatively smaller last whorls than *L. caspia*. In turn, some of the illustrated syntypes of "*Micromelania*" *curta* Nalivkin, 1914 and the variety "*Micromelania*" *curta* var. *planoconvexa* Nalivkin, 1914 from Bakunian deposits of Shikhovo, Apsheron Peninsula, Azerbaijan, closely resemble the present spe-

cies and are thus (partly) considered synonymous. “*Micromelania*” *curta* encompasses a great variability of shapes, ranging from slender, elongate (*caspia*-type) to broad, conical shells. Since no holotype or lectotype have been designated, the status of this species is unresolved at present. Note that *Pyrgula curta* sensu Logvinenko and Starobogatov (1969) and Kantor and Sysoev (2006) does not correspond to Nalivkin’s species but rather to the specimens Nalivkin (1914) misidentified as *Micromelania caspia*.

Similarly, *Pyrgula caspia* sensu Logvinenko and Starobogatov (1969) is a quite different species, showing highly convex whorls and an inflated last whorl. It rather ranges within the morphological variability of *Turricaspia meneghiniana* (see below).

Alexenko and Starobogatov (1987) finally brought stability to the identity of *L. caspia* by designating a lectotype (see Kantor and Sysoev 2006: 106, pl. 49, fig. A; as *Turricaspia caspia*), which matches well our specimens. The label accompanying their specimen reads “Kaspiyskoye more” (“Caspian Sea”), which differs from the information provided by Eichwald (Dagestan) (see also discussion in Vinarski and Kantor 2016: 246). Inspection of the catalogue of the Zoological Institute, Russian Academy of Sciences, St. Petersburg (ZIN), however, confirmed that the lectotype is based on Eichwald’s original material.

The similar *Laevicaspia iljinae* (Golikov & Starobogatov, 1966) from Holocene deposits of the Crimean Peninsula can be distinguished in its more slender shape and the spruce-like whorl outline (i.e., steep, straight-sided upper two-thirds passing over convexity into flatter, convex lower third; see also Kantor and Sysoev 2006: 108, pl. 49, fig. D).

Distribution. Endemic to the Caspian Sea (Logvinenko and Starobogatov 1969 stated that the species occurs at a depth of 30–150 m in the middle and southern Caspian Sea, but these data have to be revised given their incorrect concept of *L. caspia*).

Laevicaspia cincta (Abich, 1859) comb. n.

Fig. 9A–H

*1859 *Rissoa cincta*; Abich: 57, pl. 2, fig. 6.

?1887 *Caspia Orthii* Clessin & W. Dybowski in W. Dybowski: 40.

?1888 [*Caspia*] *Orthii* n. sp. – W. Dybowski: 79, pl. 3, fig. 6.

1969 *Pyrgula* [(*Caspiella*)] *cincta* (Abich). – Logvinenko & Starobogatov: 372, fig. 366 (4).

2006 *Pyrgula cincta* (Abich, 1859). – Kantor & Sysoev: 98, pl. 47, fig. L.

2016 *Pyrgula cincta* (Abich, 1859). – Vinarski & Kantor: 236.

Material. 174 specimens (RGM 1309806, RGM 1309807, RGM 1310200, LV 201514).

Type material. Not traced.

Type locality. Abich (1859) specified the type locality on p. 12–13 as “Gulf of Baku”.

Dimensions. 3.83 × 1.93 mm (LV 201514, Fig. 9A, B); 4.05 × 1.89 mm (RGM 1309807, Fig. 9C–E); 4.41 × 2.10 mm (RGM 1309806, Fig. 9F–H); 4.73 × 2.11 mm; 4.59 × 2.10 mm; 4.58 × 2.17 mm.

Description. Slender ovoid shell with up to 6.5 whorls. Protoconch broad, low dome-shaped, consists of 1.2 whorls that measure 415 µm in diameter, with slightly

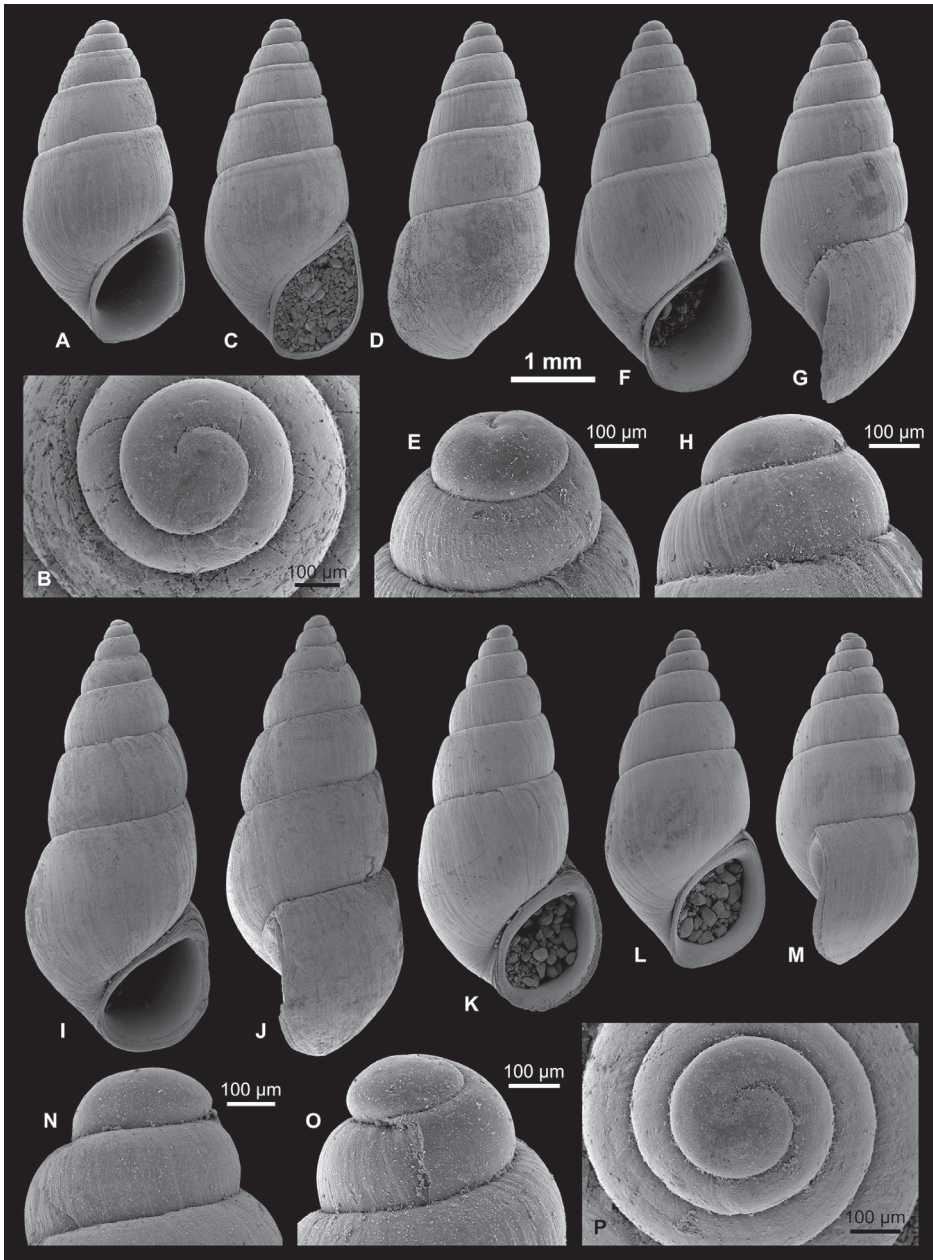


Figure 9. Pyrgulinae. **A, B** *Laevicaspia cincta* (Abich, 1859), LV 201514 **C–E** *L. cincta*, RGM 1309807 **F–H** *L. cincta*, RGM 1309806 **I, J** *L. cincta*, RGM 1309830 **K** *Laevicaspia conus* (Eichwald, 1838), LV 201515 **L–O** *L. conus*, RGM 1309829 **P** *L. conus*, RGM 1309828.

inflated initial part; nucleus 150 µm wide; protoconch surface weakly granulate, with intentions of striae on second half; P/T transition distinct, formed by sharp, thin axial line. Whorl convexity decreases steadily during ontogeny, with early teleoconch

whorls being moderately convex and penultimate and last whorl low convex to almost straight-sided. On third teleoconch whorl, weak subsutural band emerges that slightly enhances during ontogeny; band forms weak bulge throughout, with maximum convexity in its lower half and steep, almost straight-sided ramp in upper half; abapical demarcation clear, sometimes accompanied by thin groove. Last whorl attains 54–65% of shell height, passing from flattened whorl flank over marked convexity into steep, straight-sided base. Aperture near drop-shaped, inclined, with acute adapical angle, straight parietal margin, obtuse angle between parietal and columellar margins, sometimes slightly expanded palatal margin. Peristome not thickened, weakly expanded at columella and base; regularly sinuate in lateral view, with broad adapical indentation and about equally broad and high abapical protrusion. Umbilicus closed or very narrow. Growth lines weakly prosocline in upper half, near orthocline in lower half.

Discussion. The *Selitrennoye* specimens match with the original description in terms of size (shell height: 3–4 mm), the ovoid shell shape, the number of whorls, the rounded last whorl and the simple peristome margin; they differ in the expression of the subsutural band, which Abich indicated to be “weakly keeled”. We consider these differences to range within the intraspecific variability of this species.

Laevicaspia cincta can be readily distinguished from other Pontocaspian Pyrgulinae by its ovoid, slightly stepped shell with broad, blunt apex, subsutural band and flattened whorls in later ontogeny. *Laevicaspia abichi* (Logvinenko & Starobogatov, 1969) from the middle Caspian Sea, differs in the much larger size (6.8 × 3 mm), the conical shape, the narrower subsutural band and the larger aperture. The Caspian endemic species *Laevicaspia kowalewskii* (Clessin & W. Dybowski in W. Dybowski, 1887) resembles *L. cincta* very closely in terms of the slender ovoid shape with near straight-sided whorls, the closely attached aperture with thin peristome, and the lacking umbilicus; it differs in the lack of a subsutural band and the more elongate shape.

Caspia orthii Clessin & W. Dybowski in W. Dybowski, 1887 was synonymized with the present species by previous authors (e.g., Logvinenko and Starobogatov 1969, Kantor and Sysoev 2006, Vinarski and Kantor 2016). The original description matches well our specimens in terms of size (4.8 × 1.9 mm), number of whorls, expression of the subsutural band and shape of the aperture; the only difference is the “elongated-conical” shape compared to the ovoid shells of *L. cincta* described by Abich (1859) and represent by our material. Although not having seen W. Dybowski’s type material, we tentatively follow the previous assessment and consider *Caspia orthii* a junior synonym of *Laevicaspia cincta*.

Note that *Rissoa cincta* Deshayes, 1861 (p. 404, pl. 24, figs 4–6), described from the Eocene (Bartonian) of the Paris Basin, is a junior primary homonym of this species and thus invalid. At present, this species is classified in the genus *Pseudotaphrus* Cossman, 1888 (Ponder 1984: 96).

Distribution. Endemic to the Caspian Sea, in the southern part at a depth of >250 m (Parr et al. 2007).

***Laevicaspia conus* (Eichwald, 1838) comb. n.**

Fig. 9I–P

*1838 *Rissoa Conus* m.; Eichwald: 155.1841 *Rissoa Conus* m. – Eichwald: 257, pl. 38, figs 16a–b [wrongly given as “figs 16–17” on p. 257; see also corrigendum at the end of Eichwald’s work].1853 *Riss.[oa] conus* m. – Eichwald: 273.non 1876 *Eulima conus*, Eichw?. – Grimm: 154–156, pl. 6, fig. 14.1887 *Nematurella conus* Eichw. sp. (non Grimm). – W. Dybowski: 45.1888 [*Nematurella*] *conus* Eichw. sp. – W. Dybowski: 78, pl. 2, fig. 3.? 1896 *Prosostenia* [sic] *conus* Eichw. – Sinzov: 49–50, pl. 1, figs 30–33.1926 ?*Nematurella conus* (Eichwald). – Wenz: 2007.1952 *Caspiella conus* (Eichwald, 1841). – Zhadin: 259, fig. 211.1969 *Pyrgula* [(*Caspiella*)] *conus* (Eichw.). – Logvinenko & Starobogatov: 374, fig. 366 (5–6).non 2006 *Turricaspia conus conus* (Eichwald, 1838). – Kantor & Sysoev: 106, pl. 48, fig. J.2016 *Turricaspia conus conus* (Eichwald, 1838). – Vinarski & Kantor: 246–247.**Material.** 1135 specimens (RGM 1309828, RGM 1309829, RGM 1309830, RGM 1310199, RGM 1310226–1310228, LV 201515).**Type material.** Not traced.**Type locality.** “In eodem lapide calcareo, fossilis” (in the same limestone [referring to previous species, found in Dagestan], fossil).**Dimensions.** 5.14 × 2.19 mm (RGM 1309830, Fig. 9I, J); 4.60 × 2.18 mm (LV 201515, Fig. 9K); 4.02 × 1.91 mm (RGM 1309829, Fig. 9L–O); 3.87 × 1.87 mm (RGM 1309828, Fig. 9P); 4.60 × 2.23 mm (RGM 1310226); 5.12 × 2.37 mm (RGM 1310227); 4.17 × 2.14 mm (RGM 1310228).**Description.** Ovoid, glossy shell with up to 6.8 whorls. Shell outline variable, depending on growth stage: shells with up to 5 whorls are rather broad, nearly conical; in late ontogeny, shell growth is directed adapically, producing more elongate shapes with narrow, high last whorl; sometimes, these slender elongate morphotypes have slightly irregular shape. Protoconch consists of 1.2 whorls with 355 µm in diameter; nucleus almost immersed, 125 µm wide; surface faintly malleate or granulate, with intentions of spiral sculpture detected in some specimens; P/T boundary very distinct, marked by sharp, thin axial line. Teleoconch whorls weakly to moderately convex, sometimes adapically flattened. Last whorl attains between 55–63% of total height, grades into straight-sided or weakly convex base. Aperture drop-shaped, inclined, closely attached to base of preceding whorl, usually covering or rarely leaving slit-like umbilicus. Peristome slightly expanded, thin or thickened all around, especially at adapical tip; regularly sinuate in lateral view, with broad adapical indentation and about equally broad and high abapical protrusion. Growth lines weak, prosocline in upper half, orthocline in lower half.

Discussion. Logvinenko and Starobogatov (1969) listed “*Rissoa conus* Eichwald, 1841, partim” in synonymy of *Pyrgula kolesnikoviana* Logvinenko & Starobogatov in Golikov & Starobogatov, 1966 (now classified in *Laevicaspia*; see below), but without any explanation. The synonymy list was expanded as “*Rissoa conus* sensu Eichwald, 1841, partim, non Eichwald, 1838” by Kantor and Sysoev (2006) and Vinarski and Kantor (2016), yet again without discussion. The synonymy is not mentioned in the original description of *Laevicaspia kolesnikoviana* in Golikov and Starobogatov (1966). Very likely, the synonymy roots in the ambiguous description of Eichwald (1838, 1841), summarizing two different morphologies. Eichwald referred to the typical form as having a conical shell with seven, gently increasing whorls, whereas the last two are much broader; the size was indicated as 2×1 lin., which corresponds to 4.2×2.1 mm (given Eichwald used the Russian *liniya*). In addition, he mentioned rarer, slightly longer (3 lin.) specimens, with deeper suture and straight-sided whorls. In 1841, Eichwald illustrated one of these rare specimens. The description in the 1841-work, however, is almost identical to the original description. In this light, it remains unclear why Kantor and Sysoev (2006) and Vinarski and Kantor (2016) referred to as “*Rissoa conus* sensu Eichwald, 1841, partim, non Eichwald, 1838” in their synonymy lists of *L. kolesnikoviana*. To complete confusion, the specimen illustrated in Kantor and Sysoev (2006) is not *L. conus*, differing in the broad, blunt apex and the near straight-sided whorls; it rather resembles *L. kowalewskii* (Clessin & W. Dybowski in W. Dybowski, 1887).

The holotype of *L. kolesnikoviana* illustrated by Kantor and Sysoev (2006, pl. 47, fig. N) corresponds to the description and illustration of the rare, slender morphology of *Laevicaspia conus* sensu Eichwald in terms of the number of whorls and the near straight-sided whorls; it differs only in the considerably smaller size (3.7 mm vs. 6.3 mm). Yet, Golikov and Starobogatov (1966) and Logvinenko and Starobogatov (1969) indicate larger sizes for *L. kolesnikoviana* (5.5 mm and 6.5 mm, respectively), suggesting a great variability in size. On the other hand, the two morphologies delineated by Eichwald also match our own observations on *L. conus*. In late ontogeny, growth is directed almost entirely abapically, resulting in more elongate shells with an additional whorl. These larger morphologies correspond completely to the smaller, relatively bulkier shells in all other aspects, which is why we consider them as morphotypes rather than species-group taxa. Without Eichwald’s material at hand it is difficult to arrive at a conclusion on this matter.

The species has affinities with several representatives of the Azov and Black seas. *Pyrgula (Caspiella) lindholmiana* Golikov & Starobogatov, 1966, today considered as a subspecies of *L. conus* (e.g., Vinarski and Kantor 2016), has a larger and broader shell. Similarly, *Laevicaspia milachevitchi* (Golikov & Starobogatov, 1966) and *Laevicaspia boltovskoji* (Golikov & Starobogatov, 1966) are broader than *L. conus*, while *Laevicaspia lincta* (Milashevich, 1908) and *Laevicaspia limanica* (Golikov & Starobogatov, 1966) are more slender and larger.

“*Eulima conus* Eichwald” as described and illustrated by Grimm (1876, 1877) has little resemblance to actual *L. conus*. He illustrated a very elongate, conical shell with many more and almost perfectly straight-sided whorls. This fact was already noticed by

Clessin and W. Dybowski a few years later, and they introduced *Micromelania grimmi* Clessin & W. Dybowski in W. Dybowski, 1887 for the misidentified species.

The illustrations of specimens from the Kuyalnikian (late Pliocene to early Pleistocene) of the Odessa region identified as *Prososthenia conus* by Sinzov (1896) show shells with similar shape, proportions and whorl convexity. A more detailed examination of material from the region is required to assess whether it is indeed conspecific with *L. conus*.

Distribution. Endemic to the Caspian Sea, reported from depths between 0 and 120 m (Logvinenko and Starobogatov 1969).

***Laevicaspia kolesnikoviana* (Logvinenko & Starobogatov in Golikov & Starobogatov, 1966) comb. n.**

Fig. 10A–E, K, N

*1966 *P.[yrgula]* (*Caspiella*) *kolesnikoviana* Logvinenko et Starobogatov; Golikov & Starobogatov: 357, fig. 2 (8–9).

1969 *Pyrgula* [(*Caspiella*)] *kolesnikoviana* Logv. et Star. – Logvinenko & Starobogatov: 372, fig. 366 (1).

2006 *Pyrgula kolesnikoviana* Logvinenko et Starobogatov in Golikov et Starobogatov, 1966. – Kantor & Sysoev: 100, pl. 47, fig. N.

2016 *Pyrgula kolesnikoviana* Logvinenko et Starobogatov in Golikov et Starobogatov, 1966. – Vinarski & Kantor: 239.

Material. 514 specimens (RGM 1309816, RGM 1309818, RGM 1309819, RGM 1310212, RGM 1310221–1310225, LV 201516).

Type material. Holotype: ZIN 4462/1.

Type locality. Caspian Sea, N of Apsheron peninsula, NW from Kamni Dva Brata Island, 40°47'N, 49°42'E, 30 m (Vinarski and Kantor 2016).

Dimensions. 3.55 × 1.63 mm (RGM 1309816, Fig. 10A–C, K); 3.59 × 1.67 mm (LV 201516, Fig. 10D); 3.95 × 1.82 mm (RGM 1309819, Fig. 10E, N); 3.90 × 1.77 mm (RGM 1309818); 4.04 × 1.96 mm (RGM 1310222); 4.49 × 1.99 mm (RGM 1310223); 3.54 × 1.72 mm (RGM 1310224).

Description. Small, slender ovoid, shiny shell with up to 6.9 whorls. Protoconch consists of 1.2 whorls, measuring 355 µm in diameter; nucleus rather long, ca. 130 µm wide; surface finely granulate (maybe due to preservation; traces of finely malleate to irregularly striate pattern occurs on margins of nucleus and initial part); faint striae on last third; P/T boundary distinct. Whorl convexity of teleoconch whorls decreasing: first to second whorl moderately to highly convex, last whorl low to moderately convex. Faint subsutural band appears on later teleoconch whorls in some specimens, sometimes accompanied by weak concavity below. Last whorl attains 50–57% of shell height, passing via broad, regular convexity in to weakly convex base. Aperture ovoid, inclined, closely attached to preceding whorl; in latest ontogeny, shell growth is more abapically directed, resulting in marked thickening at adapical angle. Peristome thin

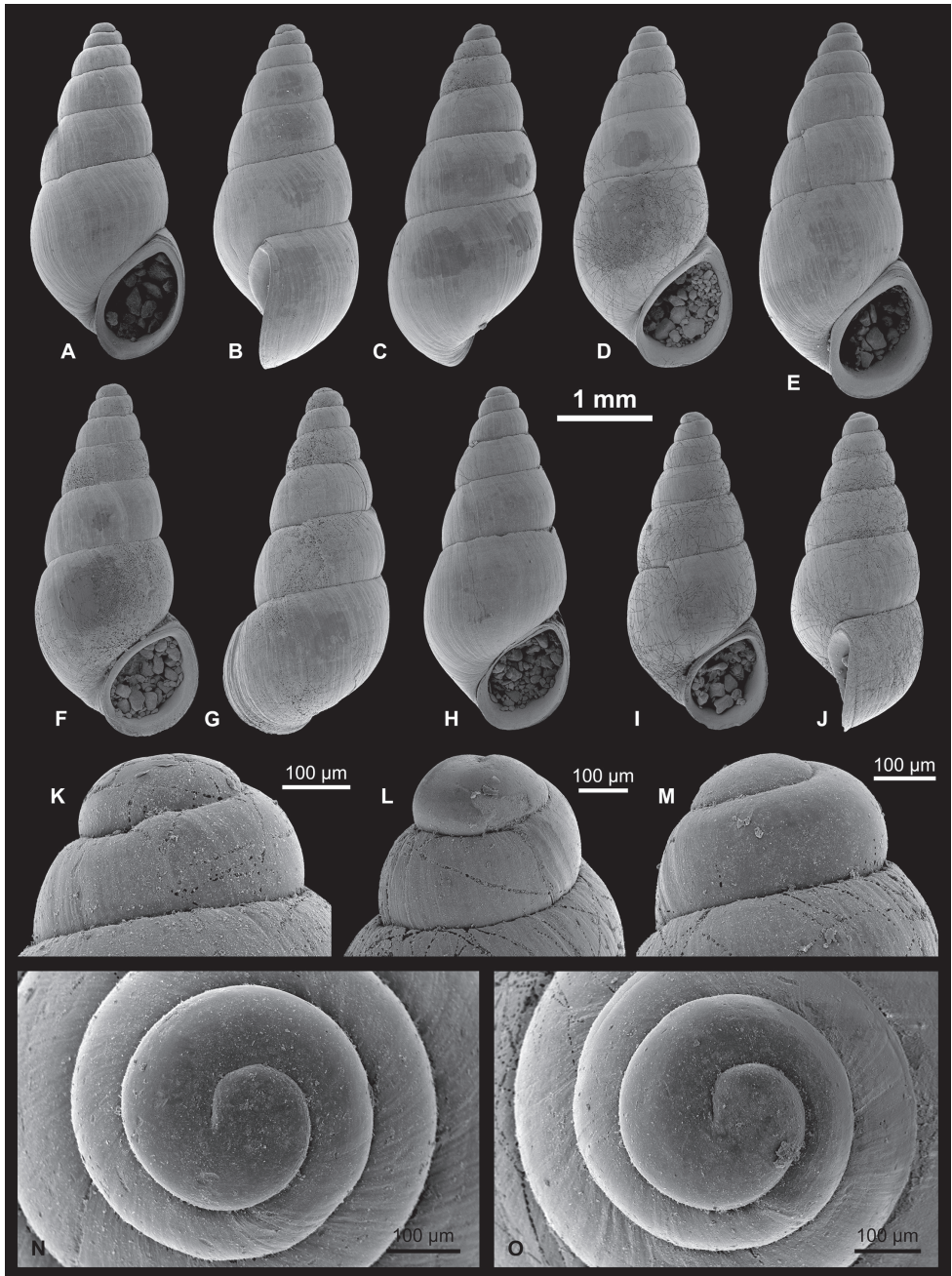


Figure 10. Pyrgulinae. **A–C, K** *Laevicaspia kolesnikoviana* (Logvinenko & Starobogatov in Golikov & Starobogatov, 1966), RGM 1309816 **D** *L. kolesnikoviana*, LV 201516 **E, N** *L. kolesnikoviana*, RGM 1309819 **F, G** *Laevicaspia vinarskii* sp. n., holotype, LV 201517 **H, O** *L. vinarskii* sp. n., RGM paratype, 1309805 **I, J, L, M** *L. vinarskii* sp. n., paratype, RGM 1309821.

or thickened all around, with parietal margin sometimes slightly expanded; weakly but regularly sinuate in lateral view, with broad adapical indentation and about equally broad and high abapical protrusion. Umbilicus usually closed or very narrow, slit-like. Growth lines weak, prosocline in upper half, orthocline in lower half. In addition, faint spiral furrows appear in some specimens.

Discussion. Co-occurring *Laevicaspia vinarskii* sp. n. differs in the consistently lower whorl expansion rate at the same size and the smaller aperture. *Laevicaspia kowalewskii* (Clessin & W. Dybowski in W. Dybowski, 1887) can be distinguished by its broader and larger shell.

Distribution. Endemic to the Caspian Sea, reported from depths between 25 and 180 m (Kolesnikov 1947, Logvinenko and Starobogatov 1969).

***Laevicaspia vinarskii* sp. n.**

<http://zoobank.org/8399A902-945D-444A-A8AD-136592F8E527>

Fig. 10F–J, L–M, O

Type material. Holotype: LV 201517; 3.70 × 1.72 mm (Fig. 10F–G). Paratypes: RGM 1309821; 3.34 × 1.48 mm (Fig. 10I, J, L, M). RGM 1309805; 3.61 × 1.54 mm (Fig. 10H, O). LV 201731; 4.14 × 1.93 mm.

Additional material. 5 specimens (RGM 1309793, LV 201732).

Type locality. Selitrennoye, Astrakhan, Russia; northern Caspian Basin; GPS coordinates: 47°10'21.19"N, 47°26'25.41"E (WGS84).

Age. Early Late Pleistocene (late Khazarian, MIS 5).

Etymology. In honor of Maxim Vinarski (Saint Petersburg State University) for his contributions to Malacology.

Diagnosis. Slender ovoid, imperforate shell with up to 6.5 moderately convex whorls, narrow suture, granulate–striate protoconch, high whorl expansion rate and small, adnate, inclined aperture.

Description. Slender ovoid shell with up to 6.5 whorls. Protoconch consists of 1.2 whorls measuring 375 µm; nucleus is 140 µm wide; surface strongly granulate on nucleus, less so on remaining protoconch, striae appear on last 0.25 whorls; P/T transition marked by distinct growth rim. Teleoconch whorls moderately convex, separated by narrow suture; whorls increase slowly in height, with the last attaining 53–57% of shell height, passing into weakly convex base. Weak subsutural band is observed in one specimen. Aperture small, inclined, closely attached to base of preceding whorl, leaving no or slit-like umbilicus. Peristome slightly thickened, especially at adapical tip; regularly sinuate in lateral view, with broad adapical indentation and about equally broad and high abapical protrusion. Distinct spiral furrows occur in well preserved specimens. Growth lines weak, prosocline in upper half, orthocline in lower half.

Discussion. The new species differs from co-occurring *Laevicaspia kolesnikoviana* in the higher whorl expansion rate at about the same size and the larger aperture. *Laevicaspia? ismailensis* (Golikov & Starobogatov, 1966) from lakes Yalpug and Kugur-

lu in the Danube river delta is more slender and larger (5.6 mm) at the same number of whorls and has a less inclined, rounder aperture (see holotype illustrated by Kantor and Sysoev 2006: pl. 50, fig. A).

Distribution. Endemic to the Caspian Sea Pleistocene, so far only known from Selitrennoye.

Genus *Turricaspia* B. Dybowski & Grochmalicki, 1915

- 1915 *Turricaspia* B. Dybowski & Grochmalicki: 105.
 1917 *Trachycaspia* B. Dybowski & Grochmalicki: 22.
 1969 *Pyrgula* (*Caspiopyrgula*) Logvinenko & Starobogatov: 366.
 1969 *Pyrgula* (*Eurycaspia*) Logvinenko & Starobogatov: 357.
 1969 *Pyrgula* (*Oxypyrghula*) Logvinenko & Starobogatov: 366.

Type species. *Micromelania turricula* B. Dybowski & Grochmalicki, 1915; by subsequent designation by Wenz (1939). Caspian Sea, Recent.

Turricaspia andrussowi (B. Dybowski & Grochmalicki, 1915)

Fig. 11A, B

- *1915 *Micromelania* (*Turricaspia*) *Andrussowi* nov. sp.; B. Dybowski & Grochmalicki: 125–126, pl. 3, figs 31a–b.
 1917 *Micromelania* (*Turricaspia*, *Trachycaspia*) *Andrussowi* nov. sp. – B. Dybowski & Grochmalicki: 26–27, pl. 4, fig. 39.
 1969 *Pyrgula* [(*Turricaspia*)] *andrussowi* [sic] (Dyb. et Gr.). – Logvinenko & Starobogatov: 365–366, fig. 362 (4) [partim].
 2006 *Turricaspia andrussowi* (B. Dybowski et Grochmalicki, 1915). – Kantor & Sysoev: 104–105, pl. 48, fig. A [partim].
 2016 *Turricaspia andrussowi* (B. Dybowski et Grochmalicki, 1915). – Vinarski & Kantor: 245 [partim].

Material. 3 spire fragments (RGM 1309814, RGM 1310205).

Type material. Lectotype: ZIN 4355/1 (specimen illustrated by B. Dybowski and Grochmalicki 1915, 1917), designated by Logvinenko and Starobogatov (1969), illustrated by Kantor and Sysoev (2006: pl. 48, fig. A).

Type locality. Caspian Sea (no locality specified).

Description. Available fragments indicate very slender, conical shell. Apex broad, blunt, bulbous. Whorl profile flattened, very weakly spruce-like, with straight-sided upper two-thirds passing over convexity into weakly convex lower third; in addition, broad, flat subsutural band appears, sometimes accompanied by very narrow concavity below. Umbilicus seems fully closed. Aperture not preserved in any specimen.

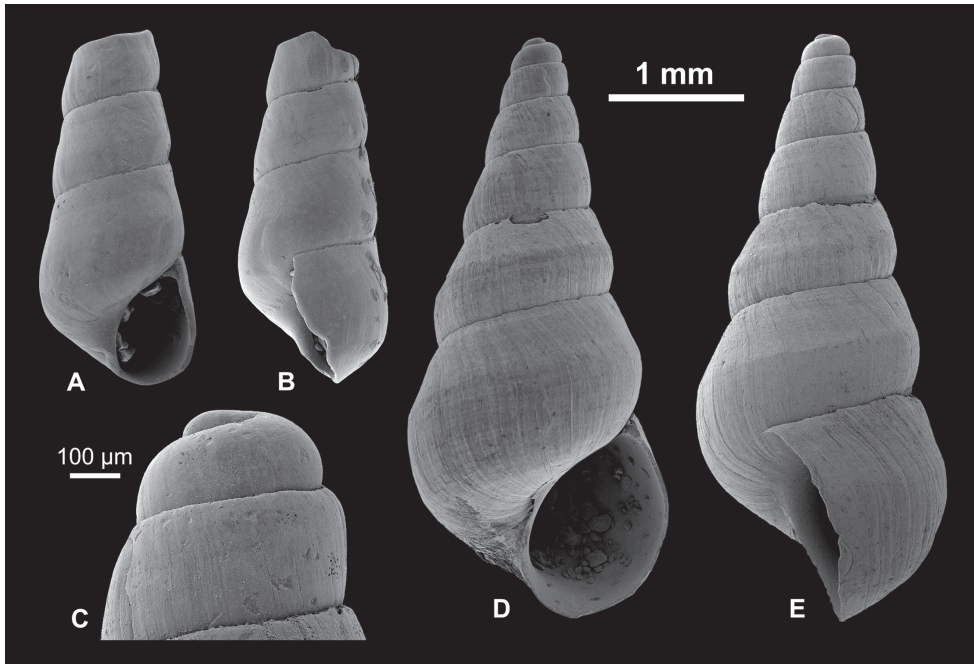


Figure 11. Pyrgulinae. **A–C** *Turricaspia* ? *dimidiata* (Eichwald, 1838), RGM 1309787 **D, E** *Turricaspia andrussowi* (B. Dybowski & Grochmalicki, 1915), RGM 1309814.

Discussion. The identification of the three spire fragments rests upon the strongly adpressed whorls with very narrow suture and the flattened, spruce-like whorl profile, and the large, bulbous protoconch. *Turricaspia eulimellula* (B. Dybowski & Grochmalicki, 1915) has a similarly slender spire with adpressed whorls, but it bears a basal keel and the maximum whorl convexity is around mid-height instead of in the lower third. *Turricaspia grimmi* (Clessin & W. Dybowski in W. Dybowski, 1887) differs in its perfectly straight-sided, rectangular, very weakly stepped whorl profile (see also B. Dybowski and Grochmalicki 1917, pl. 3, figs 34–35; Kantor and Sysoev 2006, pl. 46, fig. L).

A very similar species is *Pyrgula dubia* Logvinenko & Starobogatov, 1969 from the middle Caspian Sea, matching the present one in the weakly spruce-like whorl profile; in fact, it might just be a juvenile specimen of *T. andrussowi*. Similarly, *Pyrgula turkmenica* Logvinenko & Starobogatov, 1969, from the eastern part of southern Caspian Sea, corresponds to *T. andrussowi* in the weak subsutural band accompanied by an abapical concavity; it might as well be a juvenile representative of *T. andrussowi*.

Logvinenko and Starobogatov (1969) synonymized without discussion *Hydrobia spica* sensu Grimm, 1876, *Turricaspia elegantula* sensu B. Dybowski & Grochmalicki, 1915, *T. brusinae* (B. Dybowski & Grochmalicki, 1915), as well as several varieties of *T. spica* and *T. turricula* described by B. Dybowski & Grochmalicki (1915), with *T. andrussowi* (see also Kantor and Sysoev 2006, Vinarski and Kantor 2016). However, none of these taxa actually resembles *T. andrussowi*. This species can be well delimit-

ited from these alleged synonyms in its bulbous protoconch and the characteristic, weakly spruce-like whorl profile. (Note that the drawing provided by Logvinenko and Starobogatov 1969 shows a rather broad shell with acute apex; it has little in common with the lectotype designated by them).

Distribution. Endemic to the Caspian Sea (Logvinenko and Starobogatov 1969 indicated occurrences for the middle and southern Caspian Sea at depths of 25–80 m, but based on a much wider concept of the species).

***Turricaspia ? dimidiata* (Eichwald, 1838)**

Fig. 11C–E

?*1838 *Rissoa dimidiata* m.; Eichwald: 156.

? 1841 *Rissoa dimidiata* m. – Eichwald: 258, pl. 38, figs 17a–b [wrongly given as “figs 16–17” on p. 258; see also corrigendum at the end of Eichwald’s work].

? 1853 *Pal.[udina] dimidiata* m. – Eichwald: 285–286.

? 1887 *Micromelania dimidiata* Eichw. sp. – W. Dybowski: 31 [partim].

? 1888 *Micromelania dimidiata* Eichw. sp. – W. Dybowski: 78, pl. 1, figs 4a–f, 5 [partim].

? 1917 *Micromelania (Turricaspia) dimidiata* Eichw. – B. Dybowski & Grochmalicki: 32–33, pl. 4, figs 44–47 [partim].

? 1969 *Pyrgula dimidiata* (Eichw.). – Logvinenko & Starobogatov: 358–359, fig. 359 (1).

? 2006 *Pyrgula dimidiata* (Eichwald, 1838). – Kantor & Sysoev: 99, pl. 46, fig. K.

? 2016 *Pyrgula dimidiata* (Eichwald, 1838). – Vinarski & Kantor: 238.

Material. 1 subadult specimen (RGM 1309787).

Type material. Not traced.

Type locality. “In eodem lapide calcareo, fossilis” (in the same limestone [referring to the previous species, found in Dagestan], fossil).

Dimensions. 4.29 × 1.93 mm.

Description. Slender elongate shell with ca. 6.5 whorls preserved. Protoconch granulate, originally perhaps densely malleate. First teleoconch whorl straight-sided in profile, passing into weakly convex outline on 2nd–3rd whorl. Between 3rd and 4th whorl, broad, blunt central swelling emerges, grading into thin angulation on 5th whorl; no keel is developed. Whorl portion above swelling/angulation straight-sided, below weakly convex; directly above it, weak concavity is formed locally. Aperture ovoid, strongly adnate, leaving no umbilicus, with thin peristome. Growth lines rather distinct, with prosocline upper half and near orthocline lower half.

Discussion. A single subadult shell containing ca. 6.5 whorls (including the protoconch) is available. Size and number of whorls as well as the centrally placed angulation correspond well to Eichwald’s (1838, 1841) description and illustration of *T. dimidiata*. However, the central keel is very weakly expressed in our specimen and it starts not before the fourth whorl, which is why we only tentatively attribute it to this species.

Kantor and Sysoev (2006) illustrate a much more elongate specimen with cyrt-conoid spire and more abapically placed keel; it might represent a different species. *Turricaspia bakuana* (Kolesnikov, 1947), likewise described from Caspian Sea, too has a central keel, but differs in the much more slender shell and consistently strong keel from the second teleoconch whorl onwards (cf. Kantor and Sysoev 2006). *Turricaspia basalis* (B. Dybowski & Grochmalicki, 1915) has a broader conical habitus and the keel is placed near the lower suture. The subspecies *T. b. laticarinata* (Logvinenko & Starobogatov, 1969) only differs from *T. basalis* in the thickness of the keel and is herein considered a junior synonym of the nominal species.

Distribution. Endemic to the Caspian Sea, reported from middle and south Caspian Sea at depths between 35 and 200 m (Logvinenko and Starobogatov 1969).

Turricaspia lyrata (B. Dybowski & Grochmalicki, 1915)

Fig. 12A–K

- *1915 *Micromelania* (*Turricaspia*) *spica* Eichw. var. *lyrata* nov. var.; B. Dybowski & Grochmalicki: 117, pl. 2, fig. 18.
- 1915 *Micromelania* (*Turricaspia*) *spica* Eichw. var. *incisata* nov. var.; B. Dybowski & Grochmalicki: 117, pl. 2, fig. 19.
- 1915 *Micromelania* (*Turricaspia*) *spica* Eichw. var. *striata* nov. var.; B. Dybowski & Grochmalicki: 117, pl. 2, fig. 20.
- 1917 *Micromelania* (*Turricaspia*) *spica* Eichw. var. *lyrata* nov. var. – B. Dybowski & Grochmalicki: 17, pl. 3, fig. 25.
- 1917 *Micromelania* (*Turricaspia*) *spica* Eichw. var. *incisata* nov. var. – B. Dybowski & Grochmalicki: 18, pl. 3, fig. 26.
- 1917 *Micromelania* (*Turricaspia*) *spica* Eichw. var. *striata* nov. var. – B. Dybowski & Grochmalicki: 18, pl. 3, fig. 27.
- 1969 *Pyrgula* [(*Turricaspia*)] *lirata* [sic] (Dyb. et Gr.). – Logvinenko & Starobogatov: 365, fig. 362 (2).
- 2006 *Pyrgula lirata* [sic] (B. Dybowski et Grochmalicki, 1915). – Kantor & Sysoev: 101, pl. 46, fig. E.
- 2016 *Pyrgula lirata* [sic] (B. Dybowski et Grochmalicki, 1915). – Vinarski & Kantor: 240.

Material. 562 specimens (RGM 1309802, RGM 1309825, RGM 1310209, RGM 1310213, RGM 1310214, RGM 1310216, RGM 1310218–1310220, LV 201512, LV 201513).

Type material. Lectotype: ZIN 4552/1 (specimen illustrated by B. Dybowski and Grochmalicki 1915, 1917), designated by Logvinenko and Starobogatov (1969), illustrated by Kantor and Sysoev (2006: pl. 46, fig. E).

Type locality. Caspian Sea (no locality specified).

Dimensions. 7.68 × 2.59 mm (RGM 1310213, Fig. 12A–C); 7.99 × 2.42 mm (RGM 1310220, Fig. 12D); 7.34 × 2.28 mm (RGM 1310214, Fig. 12E); 7.54 ×

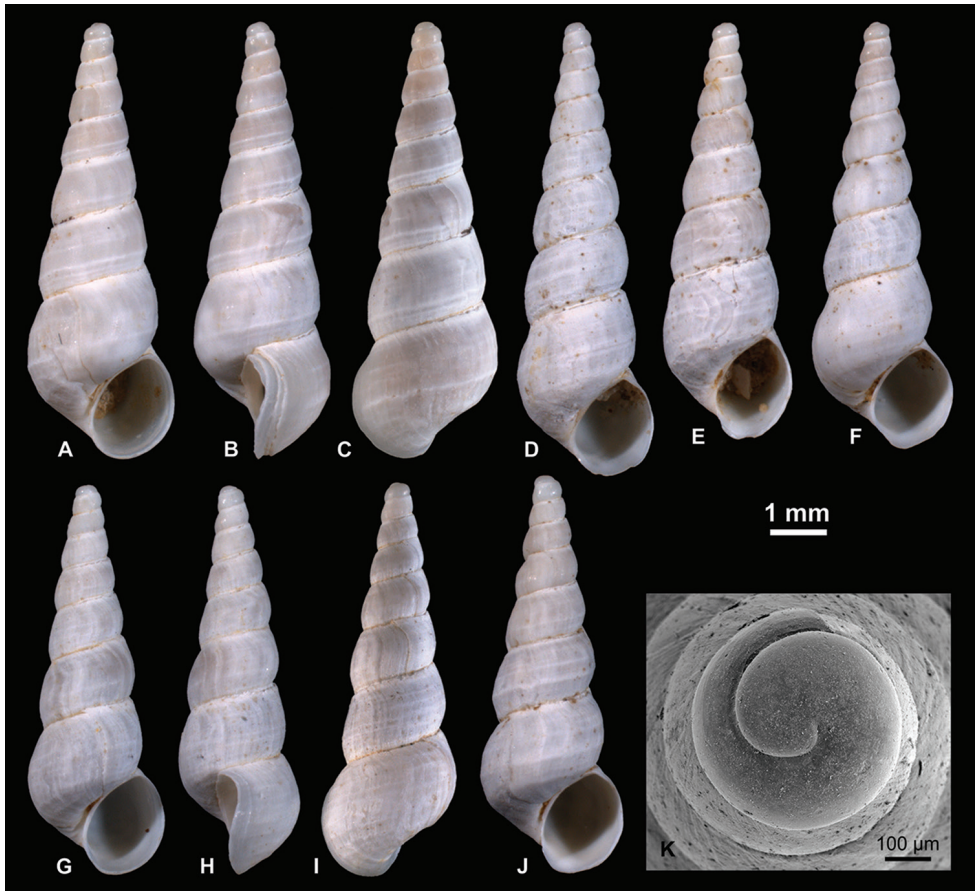


Figure 12. Pyrgulinae. **A–C** *Turrिकासpia lyrata* (B. Dybowski & Grochmalicki, 1915), RGM 1310213 **D** *T. lyrata*, RGM 1310220 **E** *T. lyrata*, RGM 1310214 **F** *T. lyrata*, LV 201512 **G–I** *T. lyrata*, LV 201513 **J** *T. lyrata*, RGM 1310218 **K** *T. lyrata*, RGM 1309802.

2.50 mm (LV 201512, Fig. 12F); 6.87 × 2.43 mm (LV 201513, Fig. 12G–I); 7 × 2.52 mm (RGM 1310218, Fig. 12J).

Description. Slender elongate shell of up to 9 whorls. Protoconch large, measuring about 485 µm in diameter; it forms bulbous cap on top of shell and comprises 1.25 whorls; surface weakly granulate, with striae on last 0.25 whorls; nucleus low, broad, ca. 170 µm in diameter; P/T transition very distinct, marked by sharp growth cessation. Teleoconch whorls low to moderately convex, often flattened or with straight-sided upper half, which creates spruce-like morphology. Sometimes, very weak and thin bulge appears below suture, producing faintly stepped spire. Most shells bear very low and somewhat irregular spirals, but expression varies considerably concerning its onset (mainly starts on lower whorls), strength (faint traces to distinct but blunt keels) and number of elements (one keel near base to several keels spread across whorl profile). Expression of sculpture varies in most specimens throughout ontogeny, which cre-

ates uneven, rugged appearance. Aperture comparatively small, in most cases regularly ovoid and weakly inclined, covering up umbilicus entirely or leaving very thin opening; peristome simple. Growth lines strongly sigmoidal, with prosocline upper third and opisthocline lower two-thirds.

Discussion. This species can be distinguished from its congeners in its large, bulbous protoconch and the typical, somewhat irregular sculpture. It is consistently larger, more massive and on average bears much stronger sculpture than co-occurring *T. ? spica*. The varieties “*Micromelania (Turricaspia) spica* var. *incisata*” and “*M. (T.) spica* var. *striata*” introduced by B. Dybowski and Grochmalicki (1915) only differ in the depth of the suture and the expression of the teleoconch sculpture, respectively. Given the variability of these features, we consider both of them synonymous with *T. lyrata*. Already Logvinenko and Starobogatov (1969) considered *incisata* and *lyrata* synonymous and, as first revisers, chose *lyrata* as the valid name of the species. The variety “*M. (T.) spica* var. *lordosa*” B. Dybowski & Grochmalicki, 1915 might also be a synonym of this species. However, the apex of the specimen illustrated in B. Dybowski and Grochmalicki (1915, 1917), which contains diagnostic characters, is not preserved. Nevertheless, *striata* and *lordosa* are certainly not synonymous with *T. andrussowi* as suggested by Logvinenko and Starobogatov (1969). That species differs from *T. lyrata* in the much slender whorls with spruce-like, near straight-sided profile.

Distribution. Endemic to the Caspian Sea (after Logvinenko and Starobogatov 1969, it occurs in the western part of the middle and southern Caspian Sea at a depth of 25–50 m; mind however that these authors used a slightly different concept of the species).

Turricaspia meneghiniana (Issel, 1865)

Fig. 13A–K

*1865 *Bythinia Meneghiniana*, Issel; Issel: 21, pl. 1, figs 12–13.

1866 *Bythinia Meneghiniana*, Issel. – Issel: 405, pl. 1, figs 12–13.

1917 *Micromelania (Turricaspia) caspia* Eichw. var. *inflata* nov. var. – B. Dybowski & Grochmalicki: 9, pl. 1, fig. 5.

? 1969 *Pyrgula caspia* (Eichw). – Logvinenko & Starobogatov: 369–370, fig. 364 (1).

? 1969 *Pyrgula meneghiniana* (Issel). – Logvinenko & Starobogatov: 370, fig. 365 (2).

non 1987 *T.[urricaspia] meneghiniana meneghiniana* (Iss.). – Alexenko & Starobogatov: 35, fig. 8.

2006 *Turricaspia meneghiniana* (Issel, 1865). – Kantor & Sysoev: 109, pl. 49, fig. E.

2016 *Turricaspia meneghiniana* (Issel, 1865). – Vinarski & Kantor: 248.

Material. 248 specimens (RGM 1309799, RGM 1309800, RGM 1310197, RGM 1310198, RGM 1310256, LV 201518).

Type material. Not traced.

Type locality. “Nei giacimenti fossiliferi di Baku” (from fossil deposits in Baku).

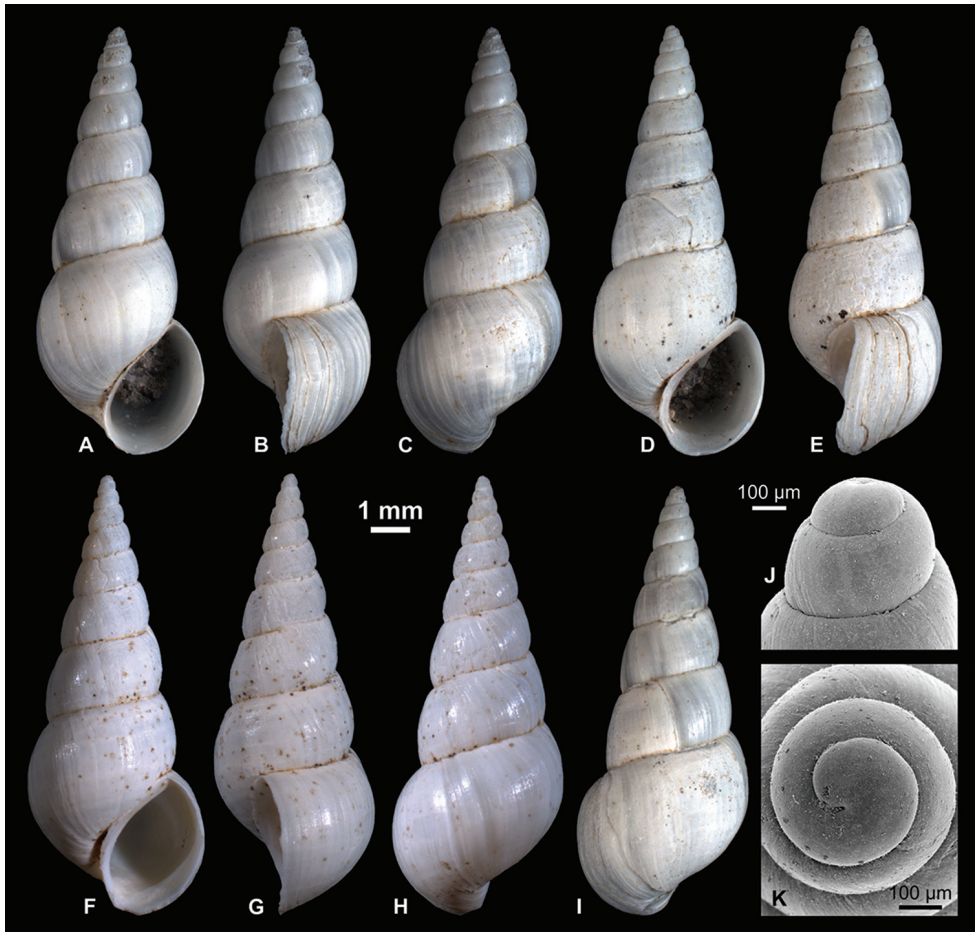


Figure 13. Pyrgulinae. **A–C** *Turricaspiia meneghiniana* (Issel, 1865), RGM 1310256 **D, E, I** *T. meneghiniana*, LV 201518 **F–H** *T. meneghiniana*, RGM 1310197 **J, K** *T. meneghiniana*, RGM1309799.

Dimensions. 10.86 × 4.27 mm (RGM 1310256, Fig. 13A–C); 10.91 × 4.36 mm (LV 201518, Fig. 13D, E, I); 11.17 × 4.50 mm (RGM 1310197, Fig. 13F–H); 10.82 × 4.14 mm; 11.23 × 4.40 mm; 11.65 × 4.49 mm.

Description. Conical shell with up to 9.3 whorls. Protoconch comprises 1.3 whorls, measuring 440 µm in diameter, with slightly inflated initial part; nucleus measures 150 µm in diameter; entire protoconch surface weakly granulate; indistinct spiral striae appear on second half; P/T transition distinct, formed by sharp, thin axial line. Teleoconch whorls increase slowly but regularly in height and width; whorls moderately convex, whereas convexity slightly decreases with ontogeny. Last whorl attains 45–48% of shell height, passes over perfect convexity into slightly convex base. Aperture ovoid, inclined, closely attached to base of preceding whorl across almost entire parietal margin. Peristome thin, not thickened, little expanded; weakly sigmoidal in lateral view, with broad, shallow indentation in upper half and broad, weak protrusion in lower half.

sion in lower half; inner lip protrudes in lateral view, extending sheet-like over base of penultimate whorl; umbilicus very narrow, slit-like. Growth lines weakly sigmoidal: strongly prosocline in upper half, weakly opisthocline in lower half. Several specimens show faint spiral threads on last and penultimate whorls.

Discussion. Our material matches well to the description of Issel (1865), corresponding in the conical shell shape, the regularly increasing whorls, the rounded last whorl with faint spiral striae, and the ovate, adapically angulated aperture; only his specimens (13.5 × 5 mm) are larger than ours and consist of more whorls. Compared to his description, Issel's illustration seem to overemphasize the relative height of the last whorl and underrepresent the pronounced whorl convexity. However, variability as to these characteristics is discernible also in our material.

Micromelania subulata Westerlund, 1902 is commonly listed as junior synonym of this species but always without discussion (e.g., Logvinenko and Starobogatov 1969, Kantor and Sysoev 2006, Vinarski and Kantor 2016). Westerlund's (1902b) description refers to a large (15 mm), elongate shell with 9.5–10 whorls and a thickened callus connecting the peristome margins. These features partly oppose Issel's description, which is why we tend to consider both taxa as separate, in contrast to most previous authors. Unfortunately, Westerlund's (1902b) type material of this species could not be traced, neither in the Göteborg Natural History Museum nor the Swedish Museum of Natural History in Stockholm, where the largest part of Westerlund's material is stored (Vinarski et al. 2013).

Another commonly cited synonym is *Micromelania caspia* var. *inflata* B. Dybowski & Grochmalicki, 1915, which indeed matches both Issel's description and our material.

Turricaspia meneghiniana differs from the similarly large *Laevicaspia caspia* (Eichwald, 1838) in its regularly conical profile, the higher number of whorls, and the higher whorl convexity. The drawings of "*Pyrgula meneghiniana* (Issel)" provided by Logvinenko and Starobogatov (1969) indicate a broader shell with low whorl convexity and might represent a different species. In contrast, *Pyrgula caspia* sensu Logvinenko and Starobogatov (1969) (non Eichwald 1838) resembles the present species in terms of the high shell convexity and regular growth rate and might be conspecific. *Turricaspia meneghiniana* sensu Alexenko and Starobogatov (1987), with few, low convex whorls and an angled base, is clearly a different species.

Distribution. Endemic to the Caspian Sea, reported from middle and south Caspian Sea at depths between 0 and 35 m (Logvinenko and Starobogatov 1969).

Turricaspia pulla (B. Dybowski & Grochmalicki, 1915)

Fig. 14A–J

*1915 *Micromelania* (*Turricaspia*) *caspia* Eichw. var. *pulla* nov. var.; B. Dybowski & Grochmalicki: 111, pl. 1, fig. 6a.

1917 *Micromelania* (*Turricaspia*) *caspia* Eichw. var. *pulla* nov. var. – B. Dybowski & Grochmalicki: 10, pl. 1, fig. 7.

- 1969 *Pyrgula* [(*Turricaspia*)] *pulla* (Dyb. et Gr.). – Logvinenko & Starobogatov: 361–362, fig. 360 (8).
 2006 *Pyrgula pulla* (B. Dybowski et Grochmalicki, 1915). – Kantor & Sysoev: 102, pl. 46, fig. C.
 2016 *Pyrgula pulla* (B. Dybowski et Grochmalicki, 1915). – Vinarski & Kantor: 242.

Material. 186 specimens (RGM 1309803, RGM 1309804, RGM 1309820, RGM 1310211, RGM 1310253–1310254, LV 201519).

Type material. Lectotype: ZIN 4422/1 (specimen illustrated by B. Dybowski and Grochmalicki 1915, 1917), designated by Logvinenko and Starobogatov (1969), illustrated by Kantor and Sysoev (2006: pl. 46, fig. C).

Type locality. Caspian Sea (no locality specified).

Dimensions. 4.88 × 2.10 mm (LV 201519, Fig. 14A–C); 5.17 × 2.11 mm (RGM 1310254, Fig. 14D, I, J); 4.77 × 1.90 mm (RGM 1310253, Fig. 14E–G); 5.84 × 2.16 mm (RGM 1309803); 5.54 × 1.97 mm (RGM 1309804).

Description. Slender conical shell with up to 8 whorls. Protoconch bulbous, weakly granulate, with striae on second half; diameter 410 µm, consists of 1.25 whorls; nucleus low, broad, 140 µm wide; transition to teleoconch distinct. Teleoconch whorls weakly convex, with maximum convexity at or slightly below midline of whorl profile; portion above maximum convexity almost straight-sided, portion below weakly convex. Whorls are separated by deep suture. Height of last whorl amounts 45% of total shell. Sometimes indentations of spiral lines appear on lower half of last whorl. Aperture ovoid, oblique, with weakly thickened and slightly expanded peristome; in lateral view, peristome is distinctly sigmoidal, with broad, shallow indentation in upper half and broad, weak protrusion in lower half. Umbilicus very narrow or closed. Growth lines sigmoidal, markedly prosocline in upper half, weakly opisthocline in lower half.

Discussion. The species can be easily distinguished from most other species of *Turricaspia* by its comparably broad conical shape, the low-convex whorls, and its small size. Juvenile specimens of *T. meneghiniana* remind of *T. pulla* but the former have broader shells with more convex whorls. *Turricaspia pullula* is likewise broader and exposes a characteristic tripartite whorl profile (see below).

Distribution. Endemic to the Caspian Sea, reported from middle and south Caspian Sea at depths between 15 and 75 m (Logvinenko and Starobogatov 1969).

Turricaspia pullula (B. Dybowski & Grochmalicki, 1915)

Fig. 14K, L

*1915 *Micromelania* (*Turricaspia*) *caspi* Eichw. var. *pullula* nov. var.; B. Dybowski & Grochmalicki: 111–112, pl. 1, fig. 7.

1917 *Micromelania* (*Turricaspia*) *caspi* Eichw. var. *pullula* nov. var. – B. Dybowski & Grochmalicki: 10–11, pl. 1, fig. 8.

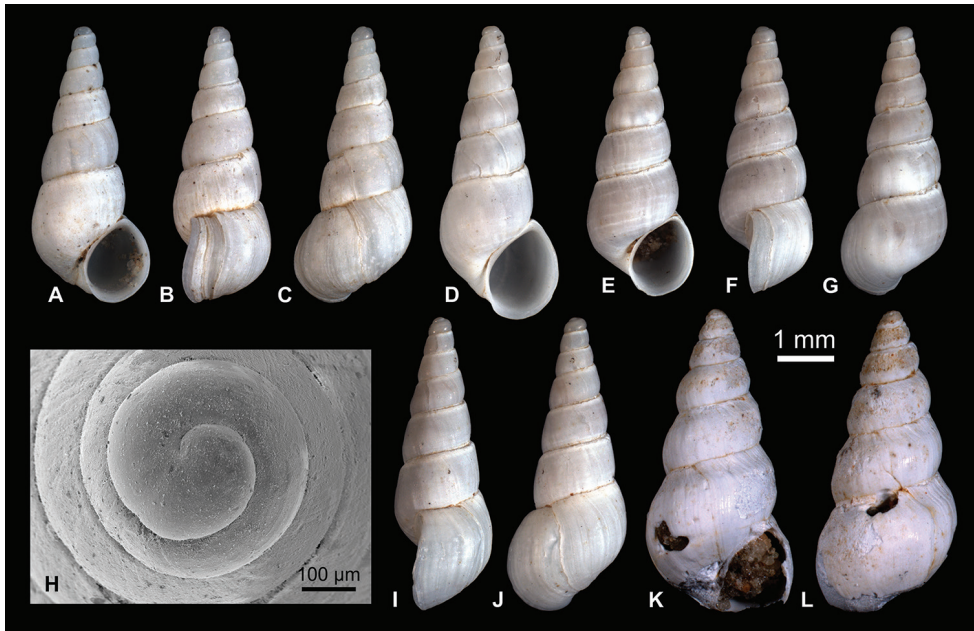


Figure 14. Pyrgulinae. **A–C** *Turrिकासpia pullula* (B. Dybowski & Grochmalicki, 1915), LV 201519 **D, I, J** *T. pullula*, RGM 1310254 **E–G** *T. pullula*, RGM 1310253 **H** *T. pullula*, RGM 1309820 **K, L** *Turrिकासpia pullula* (B. Dybowski & Grochmalicki, 1915), RGM 1310210.

1969 *Pyrgula* [(*Turrिकासpia*)] *pullula* (Dyb. et Gr.). – Logvinenko & Starobogatov: 366–367, fig. 363 (3).

2006 *Turrिकासpia pullula* (B. Dybowski et Grochmalicki, 1915). – Kantor & Sysoev: 109, pl. 50, fig. B.

2016 *Turrिकासpia pullula* (B. Dybowski et Grochmalicki, 1915). – Vinarski & Kantor: 249.

Material. 1 damaged specimen (RGM 1310210).

Type material. Lectotype: ZIN 4423/1 (specimen illustrated by B. Dybowski and Grochmalicki 1915, 1917), designated by Logvinenko and Starobogatov (1969), illustrated by Kantor and Sysoev (2006: pl. 50, fig. B).

Type locality. Caspian Sea (no locality specified).

Dimensions. 5.36 × 2.62 mm.

Description. A single incomplete specimen of about 6 whorls is preserved. Protoconch is corroded beyond recognition. Early teleoconch whorls are poorly convex to centrally flattened. Convexity strongly increases on about 3rd whorl. From 4th whorl onwards, whorl surface is partitioned into three zones: two lower zones are roughly straight-sided in profile, upper one slightly concave; middle zone slightly wider than other two; zones are separated by blunt angulations, whose expression varies between very faint to distinct (but no keel is formed). Aperture not preserved, but the tight coiling of the last preserved whorl suggests that umbilicus is absent. Growth lines strongly

prosocline in upper third, near orthocline in lower two-thirds; transition coincides with boundary between upper and middle zone.

Discussion. The available specimen corresponds well to the lectotype as illustrated by Kantor and Sysoev (2006). The very characteristic tripartite whorl profile is only discernible on the penultimate whorl of their specimen. Such a pattern is unknown for any other Pontocaspian Pyrgulinae.

Distribution. Endemic to the Caspian Sea, reported from the western part of the middle Caspian Sea at a depth of 60 m (Logvinenko and Starobogatov 1969).

Turricaspia ? *spica* (Eichwald, 1855)

Fig. 15A–R

- ? *1855 *Paludina spica* m.; Eichwald: 303–304, pl. 10, figs 8–9.
- ? 1887 *Micromelania spica* Eichw. sp. – W. Dybowski: 29–31.
- ? 1888 *Micr.[omelania] spica* Eichw. sp. – W. Dybowski: 78, pl. 1, figs 6a–c, pl. 3, figs 11a–d.
- ? 1917 *Micromelania (Turricaspia) spica* Eichw. – B. Dybowski & Grochmalicki: 16–17, pl. 3, figs 22–27.
- ? 1952 *Micromelania spica* (Eichwald, 1855). – Zhadin: 252–253, fig. 194.
- ? 1992 *Turricaspia spica*. – Anistratenko & Prisyazhniuk: 19, fig. 2d.
- ? 2006 *Turricaspia spica* (Eichwald, 1855). – Kantor & Sysoev: 110, pl. 49, fig. F.
- ? 2009 *Turricaspia cf. spica* (Eichwald, 1855). – Filippov & Riedel: 70, 72, 74, 76, figs 4e–f.
- ? 2016 *Turricaspia spica* (Eichwald, 1855). – Vinarski & Kantor: 250.

Material. 1420 specimens (RGM 1309784, RGM 1309785, RGM 1309786, RGM 1309811, RGM 1309812, RGM 1309813, RGM 1310229–1310231, RGM 1310233–1310237, RGM 1310239, RGM 1310240, LV 201501, LV 201502).

Type material. Not traced, most probably in ZIN (Vinarski and Kantor 2016).

Type locality. “Im kapischen Meere, am Ufer der Insel Tschetschnja, vorzüglich nordostwärts von der Insel im Meeresgrunde” (in the Caspian Sea, at the shores of Ostrov Chechen’, especially on the seafloor northeast of the island).

Dimensions. 6.40 × 2.18 mm (RGM 1310237, Fig. 15A–C); 5.93 × 2.27 mm (LV 201501, Fig. 15D–F); 6.13 × 2.19 mm (LV 201502, Fig. 15G–I); 6.36 × 2.21 mm (RGM 1310230, Fig. 15J–L); 6.01 × 1.90 mm (RGM 1310231, Fig. 15M–O); 5.88 × 2.00 mm (RGM 1310233, Fig. 15P); 5.55 × 1.97 mm (RGM 1310236, Fig. 15Q).

Description. Slender elongate shell, with up to nine convex whorls. Protoconch forms small bulbous cap, consisting of 1.3 whorls that measure 365 µm in diameter; surface weakly granulate, spiral striae set in after 0.5 whorls; nucleus is 140 µm wide; P/T boundary marked by thin, sharp axial line. Early teleoconch whorls have low convex profile. Two morphotypes are present: form A is broader, with whorls increasing slightly more in height (thus producing relatively larger last whorl) and little con-

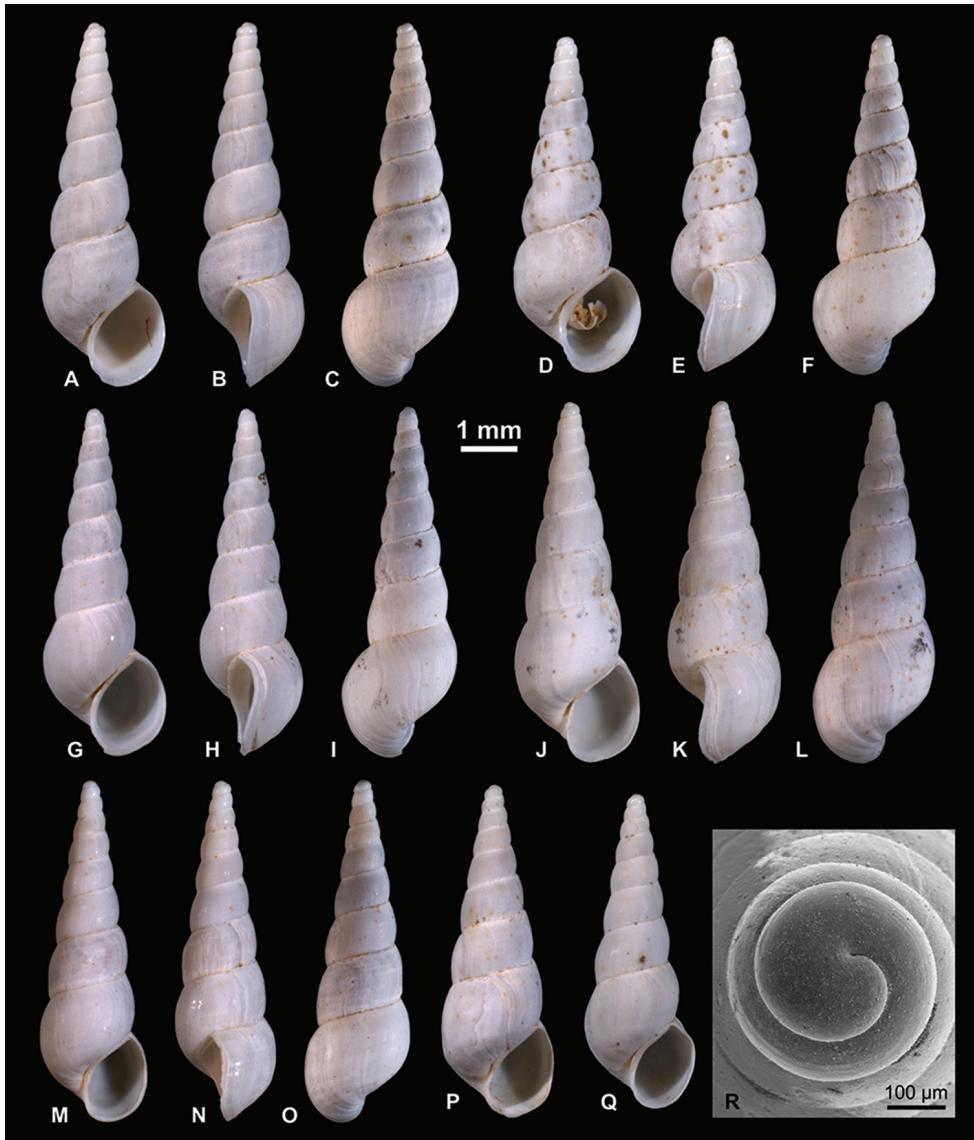


Figure 15. Pyrgulinae. **A–C** *Turricaspia ? spica* (Eichwald, 1855), form B, RGM 1310237 **D–F** *T. ? spica*, transitional form, LV 201501 **G–I** *T. ? spica*, form B, LV 201502 **J–L** *T. ? spica*, form A, RGM 1310230 **M–O** *T. ? spica*, form B, RGM 1310231 **P** *T. ? spica*, form A, RGM 1310233 **Q** *T. ? spica*, transitional form, RGM 1310236 **R** *T. ? spica*, RGM 1309813.

vex whorls; form B is more slender, whorls increase less fast in height in relation to width and whorl profile is stronger and more regularly convex. Both types are linked via intermediates. Generally, whorl profile varies between regularly convex (of varying strength), laterally flattened or bipartite (with near straight-sided upper half and convex lower half; rarely, transition between halves coincides with spiral thread). Suture

is narrow. In some specimens, last whorl is slightly inflated and aperture is expanded. Traces of spiral sculpture, ranging from faint lines to blunt keels of variable number occur on several shells. Aperture expansion and sculpture are found on both morphotypes, as well as in intermediates. Umbilicus mostly covered by inner lip; if open, it is very narrow. Growth lines markedly sigmoidal, with prosocline upper third and opisthocline lower two-thirds.

Discussion. The huge morphological variability with intergrading morphotypes complicates reasonable taxonomic distinctions within this taxon. Moreover, much of the shape variation (especially in later whorls) seems to be a result of shell repair after predator-induced damage.

The variability also hampers linking our material to an existing name. Several species (and varieties) have been introduced for slender elongate, multi-whorled shells from the Caspian Sea. While the sculptured representatives can be fairly well delimited, the smooth-shelled taxa have caused considerable confusion. Particularly challenging are the many small, slender species with pointy apex, moderately to strongly convex whorls and thin peristome. The group includes (aside from *T. spica*): *T. elegantula* (Clessin & W. Dybowski in W. Dybowski, 1887), *T. turricula* (B. Dybowski & Grochmalicki, 1915), *T. nossovi* (Kolesnikov, 1947), *T. concinna* (Logvinenko & Starobogatov, 1969), *T. spasskii* (Logvinenko & Starobogatov, 1969), *T. uralensis* (Logvinenko & Starobogatov, 1969) and *T. astrachanica* (Pirogov, 1971). *Turricaspia lyrata* (B. Dybowski & Grochmalicki, 1915), which was originally introduced as subspecies of *T. spica*, can be well delimited from that group because of its much larger, blunt apex.

A major problem in identifying and discriminating those species is that the concepts applied by later authors occasionally diverge largely from the original perceptions. This especially regards *T. spica* and the species described by B. Dybowski and Grochmalicki (1915). Unfortunately, the types for these species are not known for sure (Kantor and Sysoev 2006, Vinarski and Kantor 2016) and the original descriptions, drawings, and illustrations are mostly insufficient to allow distinction. Beyond that, different traits have been considered as diagnostic by different authors when describing new species, and morphological variability was hardly considered at all.

The identity of *Turricaspia spica* (sensu Eichwald) is dubious. The original description and illustration do not allow distinction from other similar species. The present specimens differ slightly from *T. spica* sensu Kantor & Sysoev, 2006, which is characterized by a faster whorl accretion rate and relatively higher whorls (including the last whorl). In contrast, our material largely fits the concept of *T. spica* as used by B. Dybowski and Grochmalicki (1917). We tentatively classify the Selitrennoye specimens in *Turricaspia spica*, being the oldest available name of the group. Many of the later proposed names might turn out to be junior synonyms. A more in-depth study is required to solve this problematic case.

Distribution. *Turricaspia spica* is endemic to the Caspian Sea. After Logvinenko and Starobogatov (1969), it occurs at a water depth between 0 and 30 m, but those authors applied a different concept of the species.

Hydrobiidae incertae sedis**Genus *Abeskunus* Kolesnikov in Logvinenko & Starobogatov, 1969**

Type species. *Paludina exigua* Eichwald, 1838; by original designation. Caspian Sea, Pleistocene.

Discussion. The genus *Abeskunus* and the species that have been attributed to it have caused considerable confusion. A detailed discussion of the taxonomic and nomenclatural problems associated with *Abeskunus*, considerations on its systematic placement, as well as a description of the type species will be provided in a forthcoming study. Preliminary work confirms classification of the species described below in *Abeskunus*.

***Abeskunus brusinianus* (Clessin & W. Dybowski in W. Dybowski, 1887)**

Fig. 16A–I

*1887 *Zagrabica Brusiniana* nob.; W. Dybowski: 52–53.

1888 *Zagrabica Brusiniana* n. sp. – W. Dybowski: 79, pl. 2, fig. 7.

1952 *Zagrabica brusiniana* W. Dyb., 1888. – Zhadin: 235, fig. 166 [partim].

1969 *Pseudamnicola* [*Abeskunus*] *brusiniana* (Cless. et W. Dyb.). – Logvinenko & Starobogatov: 381, fig. 367 (15).

2006 *Pseudamnicola brusiniana* (Clessin et W. Dybowski in W. Dybowski, 1888). – Kantor & Sysoev: 114, pl. 51, fig. J.

2016 *Pseudamnicola brusiniana* (Clessin et W. Dybowski in W. Dybowski, 1888). – Vinarski & Kantor: 222.

Material. 489 specimens (RGM 1309834, RGM 1309842, RGM 1310194, LV 201505).

Type material. Not traced.

Type locality. “Kaspi-See” (Caspian Sea, no further details mentioned).

Dimensions. 4.12 × 3.82 mm (RGM 1309834, Fig. 16A, F); 4.15 × 3.65 mm (LV 201505, Fig. 16B, C, I); 3.00 × 2.74 mm (RGM 1309842, Fig. 16D, E, G, H); 4.14 × 3.42 mm; 4.15 × 3.53 mm; 4.34 × 3.79 mm; 4.39 × 3.87 mm; 4.59 × 3.68 mm.

Description. Shell broadly conical, comprising up to 4.5 whorls. Protoconch broadly domical, with almost immersed initial part; consists of 1.25 whorls, measures 525 µm in diameter; nucleus is ca. 160 µm wide; nucleus surface covered with irregular elongated wrinkles; protoconch surface wrinkled, bearing thin, irregular spiral grooves on first third, passing over irregular pattern of faint spiral grooves and wrinkles into numerous, regularly parallel spiral furrows on last third; P/T transition without growth rim, marked by onset of growth lines. Teleoconch whorls highly convex, with maximum convexity in adapical half, producing slightly stepped spire. Last whorl attains 77–85% of shell height. Aperture drop-shaped, slightly inclined, with marked adapical notch at contact to penultimate whorl. Outer peristome margin not or slightly thickened, columellar and parietal margins weakly thickened; peristome slightly expanded towards columella (pro-

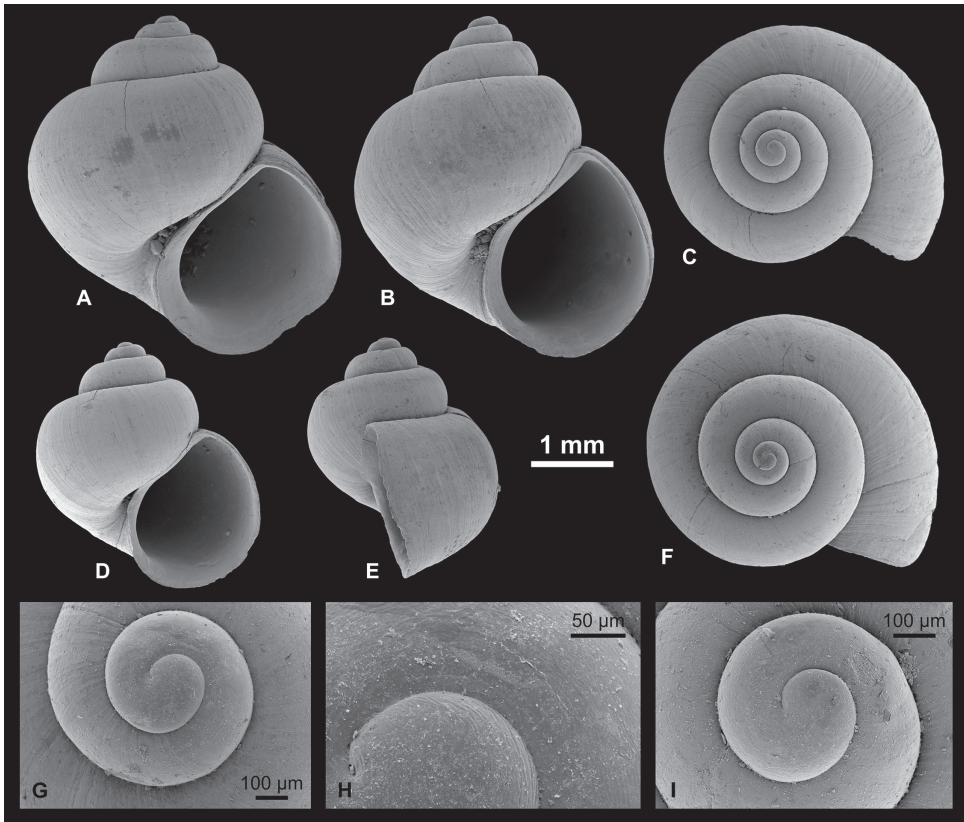


Figure 16. Hydrobiidae incertae sedis. **A, F** *Abeskunus brusinianus* (Clessin & W. Dybowski in W. Dybowski, 1887), RGM 1309834 **B, C, I** *A. brusinianus*, LV 201505 **D, E, G, H** *A. brusinianus*, RGM 1309842.

truding towards umbilicus in lateral view) and strongly towards base; weakly sinuate in lateral view, with broad but weak adapical protrusion and straight-sided abapical part. Umbilicus narrow, slit-like. Prosocline growth lines cover shell surface.

Discussion. The species differs from the type species *A. exiguus* (Eichwald, 1838) in the conical shell, the taller spire, the less inflated last whorl, and the distinct umbilicus. *Abeskunus brusinianus michelae* Tadjalli-Pour, 1977 is much more globular than *A. brusinianus*. The latter species strongly reminds of and might be conspecific with *A. exiguus*. *Pseudamnicola depressispira* Logvinenko & Starobogatov, 1969, which these authors also included in the subgenus *Abeskunus*, differs from the presumed congeners in the valvatoid shape with very wide umbilicus and small but distinct riblets.

Pseudamnicola? brusiniana Pavlović, 1903 is a junior secondary homonym of this species, for which Neubauer et al. (2015b) introduced *Pseudamnicola? babindolensis* as replacement name. Because of the revised classification, *P? brusinianus* [sic] Pavlović is reinstated as valid, with *P? babindolensis* as its junior objective synonym (ICZN 1999, Art. 59.4).

Distribution. Endemic to the Caspian Sea, in the southern and middle part at a depth of >250 m (Logvinenko and Starobogatov 1969, Parr et al. 2007).

Non-indigenous species

In addition to the Pontocaspian elements, six taxa including ubiquitous Palearctic species were identified. They all occur in low numbers and differ from Pontocaspian species in their preservation state. Shells of larger taxa (*Valvata*, *Esperiana*, and *Lithoglyphus*) are eroded and suggest transport. The smaller planorbids are better preserved but differ in their orange color indicating that they were not deposited along with the whitish shells of the Pontocaspian residents. Moreover, all six taxa are typical freshwater dwellers (e.g., Welter-Schultes 2012). They probably derive from rivers flowing into the northern Caspian Sea (Fig. 1).

Anisus cf. *spirorbis* (Linnaeus, 1758) (Fig. 17A–F). – 13 juvenile to semi-adult specimens have been found. They match *A. spirorbis* as depicted by Glöer (2002) and Welter-Schultes (2012) in size, the regularly striated surface, the slightly overlapping whorls, and the weakly asymmetrical lateral profile. However, whorls expand in relative width a bit more rapidly in the Selitrennoye specimens, which is why we only tentatively assign our material to this species.

Planorbis cf. *planorbis* (Linnaeus, 1758) (Fig. 17G–L). – Two juvenile specimens and one semi-adult are available, showing either a distinct or intentions of a keel on the periphery of the apical side, a feature typical of *P. planorbis* (Glöer 2002, Welter-Schultes 2012). In addition, shell size, whorl expansion and lateral profile fit well to this species. Since no adult specimen with fully developed keel have been found, we attribute our specimens to this species provisionally.

Bithynia sp. (Fig. 17M). – Four juvenile specimens are available, consisting of the protoconch and about one teleoconch whorl; the operculum is in-situ preserved in all specimens. The classification is based on the presence and shape of the operculum, the characteristics of the protoconch, as well as the shape of the aperture, all of which are features typical of the genus *Bithynia* (compare Glöer et al. 2005, Neubauer et al. 2016b).

Esperiana esperi (Férussac, 1823) (Fig. 17N). – The single fragmentary specimen matches well the specimens illustrated by Welter-Schultes (2012). The similar and often co-occurring *Microcolpia daudebartii acicularis* (Férussac, 1823) is more elongate and lacks the color pattern (Glöer 2002, Welter-Schultes 2012). In the Russian literature, *E. esperi* is commonly listed as member of the genus *Fagotia* Bourguignat, 1884 (e.g., Starobogatov et al. 2004, Vinarski and Kantor 2016), which is, however, invalid as a junior objective synonym of *Esperiana*. Starobogatov et al. (1992, 2004) listed numerous species of *Fagotia* for extant European water bodies and categorized them into several subgenera. All of them are presently considered junior synonyms of *Esperiana* and *E. esperi*, respectively (for a complete synonymy list, see Vinarski and Kantor, 2016). *Fagotia roseni* Starobogatov in Starobogatov et al., 1992 from Quaternary deposits of Georgia also ranges within the variability of *E. esperi* and is herewith considered synonymous.

Lithoglyphus naticoides (Pfeiffer, 1828) (Fig. 17O). – The shape of the sole specimen ranges well within the large morphological variability of Recent *L. naticoides* (e.g., Glöer 2002). Late Pleistocene *Lithoglyphus jahni* Urbański, 1975 has a relatively taller



Figure 17. Non-indigenous species. **A–D** *Anisus* cf. *spirorbis* (Linnaeus, 1758), LV 201503 **E–F** *A.* cf. *spirorbis*, RGM 1309801 **G–I** *Planorbis* cf. *planorbis* (Linnaeus, 1758), LV 201504 **J–L** *P.* cf. *planorbis*, RGM 1309835 **M** *Bithynia* sp., juvenile, RGM 1309853 **N** *Esperiana esperi* (Férussac, 1823), RGM 1309792 **O** *Lithoglyphus naticoides* (Pfeiffer, 1828), RGM 1309832 **P** *Valvata piscinalis* (Müller, 1774), RGM 1310249. Scale bar equals 1 mm unless indicated otherwise. Note that all Planorbidae are figured at the same scale to facilitate comparison.

conical shell and elevated spire (Kondrashov 2007). Coeval *Lithoglyphus pyramidatus* Möllendorff, 1873 is more elongate and lacks the stepped spire (Glöer 2002).

Valvata piscinalis (Müller, 1774) (Fig. 17P). – The eight, partly fragmented and corroded shells correspond well to Recent representatives of the species (Glöer 2002, Welter-Schultes 2012). Several of the *Valvata* species listed for the Volga delta region by Starobogatov et al. (1994, fig. 2) might be synonymous with this species. A conclusion on that matter requires examination of the material, which is unavailable to us.

Discussion

The current work provides a first insight into the magnitude of endemic Caspian gastropod biodiversity. The gastropod fauna of Selitrennoye is composed of 24 species, 16 of which are Pontocaspian endemic species and 15 exclusively Caspian. Six species are considered to be non-indigenous based on the combination of a truly freshwater autecology, a general wide spread palearctic distribution and a slightly different preservation from the bulk of the well preserved Caspian lacustrine species in the material. The non-Caspian gastropods are low in numbers, and we suspect they may have either floated into the Caspian Sea during periods of high river discharge or, more likely, were mixed in from underlying sediment layers through bioturbation. The Selitrennoye fauna was deposited in open lacustrine settings at a paleosalinity of approximately 10–11 psu as suggested by the general composition of the mollusk fauna (Yanina 2012). The presence of paired bivalves in the same sample indicates the in-situ character of the fauna. The shelly levels are located around 17 m b.s.l., and late Khazarian maximum sea levels are estimated as 10 m b.s.l. The presence of very sandy sediments with lenses suggests deposition above storm wave base. Altogether, this might translate into a sea floor at about 7 m water depth. The settings can be best compared with the present-day southernmost part of the northern Caspian Basin.

The taxonomy and systematics of Caspian gastropods is very much in need of an update. The abundant and well-preserved material presented here has given an indication about the generic placements of species and the magnitude of species richness. When compared to the latest inventory of Caspian gastropods by Vinarski and Kantor (2016), who presented 92 species for the entire Caspian Sea, our numbers (that represent a single locality) are still rather low. The synonymization of species we propose points in general to lower species numbers for Caspian gastropod faunas as reported before. However, the possibility exists that some of the species considered synonyms are sibling species. In order to test for that, we will require extensive new living material to perform combined genetic and morphometric analyses. In recent expeditions in the coastal areas of Azerbaijan and in the Caspian territory of Kazakhstan, we failed to detect living endemic Pyrgulinae gastropod species. All Caspian endemics are suffering badly from invasive species that have caused a total turnover of the fauna during the 20th century (Kosarev and Yablonskaya 1995, Grigorovich et al. 2003, Orlova et al. 2005, Therriault et al. 2004, Riedel et al. 2006, Heiler et al. 2010, Albrecht et

Table 1. List of species recovered from the late Khazarian deposits at Selitrennoye, with indication of their status as endemic to the Caspian Sea and the Pontocaspian region as a whole.

Species	Family	No. of specimens	Caspian endemic	Pontocaspian endemic
<i>Theodoxus pallasi</i> Lindholm, 1924	Neritidae	294		
<i>Ulskia ulskii</i> (W. Dybowski & Clessin in W. Dybowski, 1888)	Hydrobiidae	19	x	x
<i>Andrusovia brusinai</i> Starobogatov, 2000	Hydrobiidae	39	x	x
<i>Ecrobia</i> cf. <i>grimmii</i> (Clessin in W. Dybowski, 1888)	Hydrobiidae	345		
<i>Clessiniola variabilis</i> (Eichwald, 1838)	Hydrobiidae	4867		x
<i>Laevicaspia caspia</i> (Eichwald, 1838)	Hydrobiidae	300	x	x
<i>Laevicaspia cincta</i> (Abich, 1859)	Hydrobiidae	174	x	x
<i>Laevicaspia conus</i> (Eichwald, 1838)	Hydrobiidae	1135	x	x
<i>Laevicaspia kolesnikoviana</i> (Logvinenko & Starobogatov in Golikov & Starobogatov, 1966)	Hydrobiidae	514	x	x
<i>Laevicaspia vinarskii</i> sp. n.	Hydrobiidae	9	x	x
<i>Turricaspia andrussowi</i> (B. Dybowski & Grochmalicki, 1915)	Hydrobiidae	3	x	x
<i>Turricaspia</i> ? <i>dimidiata</i> (Eichwald, 1838)	Hydrobiidae	1	x	x
<i>Turricaspia lyrata</i> (B. Dybowski & Grochmalicki, 1915)	Hydrobiidae	562	x	x
<i>Turricaspia meneghiniana</i> (Issel, 1865)	Hydrobiidae	248	x	x
<i>Turricaspia pulla</i> (B. Dybowski & Grochmalicki, 1915)	Hydrobiidae	186	x	x
<i>Turricaspia pullula</i> (B. Dybowski & Grochmalicki, 1915)	Hydrobiidae	1	x	x
<i>Turricaspia</i> ? <i>spica</i> (Eichwald, 1855)	Hydrobiidae	1420	x	x
<i>Abeskunus brusinianus</i> (W. Dybowski & Clessin in W. Dybowski, 1888)	Hydrobiidae	489	x	x
<i>Valvata piscinalis</i> (Müller, 1774)	Valvatidae	8		
<i>Esperiana esperi</i> (Férussac, 1823)	Melanopsidae	1		
<i>Bithynia</i> sp.	Bithyniidae	4		
<i>Lithoglyphus naticoides</i> (Pfeiffer, 1828)	Lithoglyphidae	1		
<i>Anisus</i> cf. <i>spirorbis</i> (Linnaeus, 1758)	Planorbidae	13		
<i>Planorbis</i> cf. <i>planorbis</i> (Linnaeus, 1758)	Planorbidae	3		

al. 2014). This situation appears to complicate or even make it impossible to follow such an integrated approach. Especially for the genera *Clessiniola*, *Laevicaspia*, and *Turricaspia*, we think devoted taxonomic revisions will be required to assess the number of species and potential presence of siblings.

The present revision does elucidate generic concepts. Even though it is open for further improvement, it will provide a basis for the establishment of evolutionary relationships within genera by comparison with older (Bakunian/Apsheronian) and younger Caspian faunas. By understanding species richness and evolutionary relationships of Caspian faunas, we will be able to document the nature and severity of the Anthropocene biodiversity crisis in this long-lived lake.

Author contributions

FPW and TY conducted field work and collected the material; SV and FPW processed the material; TAN, SV, and FPW identified the species; TAN and FPW wrote the manuscript.

Acknowledgements

We are grateful to Vitaliy V. Anistratenko, Maxim Vinarski, Jan Johan ter Poorten, Anita Eschner, and Yuri Kantor for support during literature research. Maxim Vinarski is moreover thanked for inspection of the collection catalogue of the Zoological Institute of the Russian Academy of Sciences in St. Petersburg. We thank Ronald Pouwer and Marjan Helwerda for assistance in sample sorting. Our sincere thanks also go to Dietrich Kadolsky, Mathias Harzhauser, Peter Glöer, Diana Delicado, and Daniela Esu for sharing taxonomic considerations. Tom Wilke shared information on unpublished molecular data of the Caspian hydrobiids. Ted von Proschwitz and Anna Persson are thanked for their effort in trying to locate Westerlund's type material. Thomas Nichterl helped with Latin translations. The careful reviews by Vitaliy V. Anistratenko and Frank Riedel greatly improved the quality of this work. This paper contributes to the PRIDE Project ("Drivers of Pontocaspian Biodiversity Rise & Demise") funded by the European Union's Horizon 2020 research and innovation programme under the Marie Skłodowska-Curie grant agreement No. 642973. It also contributes to the FreshGEN Project ("Freshwater systems in the Neogene and Quaternary of Europe: Gastropod biodiversity, provinciality, and faunal gradients") funded by the Austrian Science Fund FWF (project no. P25365-B25). T.A.N. was supported by an Alexander-von-Humboldt Scholarship and a Martin Fellowship granted by Naturalis Biodiversity Center. T.Y. was supported by the Russian Science Foundation (grant no. 16-17-10103).

References

After Anistratenko (2013), the publication dates of W. Dybowski's "Die Gasteropoden-Fauna des Kaspischen Meeres" is not 1888 as indicated in the respective journal volume. Issue 1 (pp. 1–64, containing all descriptions) was published in 1887; issues 2 (pp. 65–79, summary and plate captions) and 3 (pls. 1–3) appeared in 1888.

B. Dybowski and Grochmalicki (1917) is a slightly altered version of B. Dybowski and Grochmalicki (1915). That work is a preprint initially destined to be published in the "Annuaire du Musée Zoologique de l'Académie impériale des Sciences de St Petersburg", vol. 20, but it was withdrawn from the volume by the editors. It is nonetheless nomenclaturally available. Since the authors thought their work had remained unpublished, they slightly emended it and re-published it in 1917, re-describing most of the

taxa they introduced in 1915 as new and adding new ones. Despite considerable effort, we were unable to obtain a copy of that rare work.

The publication date of Birshtein et al.'s comprehensive systematic account of the Caspian fauna, including the catalogue of Caspian mollusks by Logvinenko and Starobogatov, is usually given as “1968” and so it says in the book itself. According to Sysoev and Kantor (1992), however, the book was published in April 1969.

- Abich H (1859) Vergleichende chemische Untersuchungen der Wasser des Caspischen Meeres, Urmia- und Van-See's. Mémoires de l'Académie impériale des sciences de St.-Petersbourg, 6e série, Sciences mathématiques, physiques et naturelles 7: 1–57. <https://biodiversitylibrary.org/page/46467180>
- Agusa T, Kunito T, Tanabe S, Pourkazemi M, Aubrey DG (2004) Concentrations of trace elements in muscle of sturgeons in the Caspian Sea. *Marine Pollution Bulletin* 49(9–10): 789–800. <https://doi.org/10.1016/j.marpolbul.2004.06.008>
- Albers JC (1850) Die Heliceen, nach natürlicher Verwandtschaft systematisch geordnet. Enslin, Berlin, 262 pp.
- Albrecht C, von Rintelen T, Sereda S, Riedel F (2014) Evolution of ancient lake bivalves: the Lymnocardiiinae (Cardiidae) of the Caspian Sea. *Hydrobiologia* 739(1): 85–94. <https://doi.org/10.1007/s10750-014-1908-3>
- Alexenko TL, Starobogatov YaI (1987) Vidy *Caspia* i *Turricaspia* (Gastropoda, Pectinibranchia, Pyrgulidae) Azovo-Chernomorskogo basseyna. *Vestnik Zoologii* 21(3): 32–38.
- Anan Y, Kunito T, Tanabe S, Mitrofanov I, Aubrey DG (2005) Trace element accumulation in fishes collected from coastal waters of the Caspian Sea. *Marine Pollution Bulletin* 51(8–12): 882–888. <https://doi.org/10.1016/j.marpolbul.2005.06.038>
- Anistratenko VV (2008) Evolutionary trends and relationships in hydrobiids (Mollusca, Caenogastropoda) of the Azov-Black Sea Basin in the light of their comparative morphology and paleozoogeography. *Zoosystematics and Evolution* 84(2): 129–142. <https://doi.org/10.1002/zoos.200800001>
- Anistratenko VV (2013) On the taxonomic status of the highly endangered Ponto-Caspian gastropod genus *Caspia* (Gastropoda: Hydrobiidae: Caspiinae). *Journal of Natural History* 47(1–2): 51–64. <https://doi.org/10.1080/00222933.2012.742934>
- Anistratenko VV, Khaliman IA, Anistratenko OY (2011) Mollyuski Azovskogo morya. Naukova dumka, Kiev, 171 pp.
- Anistratenko VV, Prisyazhniuk VA (1992) Novyye dannyye o mollyuskakh golotsenovykh otlozheniy Chernogo morya na Ukraine. *Vestnik Zoologii* 5: 15–21.
- Anistratenko VV, Zettler ML, Anistratenko OY (2017) On the taxonomic relationship between *Theodoxus pallasii* and *T. astrachanicus* (Gastropoda: Neritidae) from the Ponto-Caspian region. *Archiv für Molluskenkunde* 146(2): 213–226. <https://doi.org/10.1127/arch.moll/146/213-226>
- Arconada B, Ramos MA (2006) Revision of the Genus *Islamia* Radoman, 1973 (Gastropoda, Caenogastropoda, Hydrobiidae) on the Iberian Peninsula and Description of Two New Genera and Three New Species. *Malacologia* 48(1/2): 77–132. <https://biodiversitylibrary.org/page/13115520>

- Bank R (2017) Horatiinae D.W. Taylor, 1966 – MolluscaBase. World Register of Marine Species. <http://molluscabase.org/aphia.php?p=taxdetails&id=1000097> [on 2018-02-01]
- Boeters HD, Glöer P, Georgiev D, Dedov I (2015) A new species of *Caspia* Clessin et W. Dybowski, 1887 (Gastropoda: Truncatelloidea: Hydrobiidae) in the Danube of Bulgaria. *Folia Malacologica* 23: 177–186. <https://doi.org/10.12657/folmal.023.014>
- Bouchet P, Rocroi J-P, Hausdorf B, Kaim A, Kano Y, Nützel A, Parkhaev P, Schrödl M, Strong EE (2017) Revised classification, nomenclator and typification of gastropod and monoplacophoran families. *Malacologia* 61(1–2): 1–526. <https://doi.org/10.4002/040.061.0201>
- Bourguignat JR (1884) Histoire des mélanien du système européen. *Annales de Malacologie* 2: 1–168. <https://biodiversitylibrary.org/page/16301109>
- Bourguignat JR (1887) Étude sur les noms génériques des petites paludinidées a opercule spirescent suivie de la description du nouveau genre *Horatia*. Tremblay, Paris, 56 pp. <https://doi.org/10.5962/bhl.title.10453>
- Brusina S (1874) Fossile Binnen-Mollusken aus Dalmatien, Kroatien und Slavonien nebst einem Anhang. Actienbuchdruckerei, Agram, 138 pp.
- Brusina S (1882) Le Pyrgulinae dell'Europa orientale. *Bollettino della Società Malacologica Italiana* 7(13–19)[1881]: 229–292. <https://biodiversitylibrary.org/page/39283992>
- Büyükeriç Y, Wesselingh FP (2018) New cockles (Bivalvia: Cardiidae: Lymnocardiinae) from Late Pleistocene Lake Karapinar (Turkey): Discovery of a Pontocaspian refuge? *Quaternary International* 465 (A): 37–45. <https://doi.org/10.1016/j.quaint.2016.03.018>
- Clessin S (1886) Binnenmollusken aus Rumänien. *Malakozoologische Blätter (Neue Folge)* 8: 49–56. <https://biodiversitylibrary.org/page/35594868>
- Cox LR (1960) Thoughts on the classification of the Gastropoda. *Proceedings of the Malacological Society of London* 33: 239–261.
- Cuvier G (1795) Second Mémoire sur l'organisation et les rapports des animaux à sang blanc, dans lequel on traite de la structure des Mollusques et de leur division en ordre, lu à la société d'Histoire Naturelle de Paris, le 11 prairial an troisième. *Magasin Encyclopédique, ou Journal des Sciences, des Lettres et des Arts* 2: 433–449.
- De Cristofori G, Jan G (1832) *Catalogus in IV. sectiones divisus rerum naturalium in museo exstantium Josephi De Cristofori et Georgii Jan plurium Acad. Scient. et Societ. Nat. Cur. Sodalium complectens adumbrationem oryctognosiae et geognosiae atque prodromum faunae et floriae Italiae Superioris. Sectio II. Conchyliologia. Pars I. Conspectus methodicus molluscorum. Fasc. 1. Testacea terrestria et fluviatilia. Carmignani, Parma, pp. 1–2 [unnumbered] [Dispositio methodica generum], pp. 1–8 [Conchyliia terrestria et fluviatilia], pp. 1–4 [Mantissa in secundam partem catalogi testaceorum exstantium in collectione quam possident], pp. 1–4 [Excerptum e primo nostre programmate], pp. 1–16 [Conchyliia fossilia]* <https://biodiversitylibrary.org/page/39520781>
- Deshayes GP (1861–1864) Description des animaux sans vertèbres découverts dans le bassin de Paris pour servir de supplément a la description des coquilles fossiles des environs de Paris comprenant une revue générale de toutes les espèces actuellement connues. Tome deuxième. – Texte. Mollusques Acéphalés Monomyairew et Brachiopodes. Mollusques céphalés. Première Partie. J.-B. Baillièere et Fils, Paris, 968 pp. <https://biodiversitylibrary.org/page/35623270>

- Doering A (1875) Estudios sistemáticos y anatómicos sobre los moluscos pulmoníferos de los países del Plata. *Periódico Zoológico* 1(3): 129–204.
- Dollfus GF (1912) Recherches critiques sur quelques genre et espèces d'*Hydrobia* vivants ou fossiles. *Journal de Conchyliologie* 59(3): 179–270. <https://biodiversitylibrary.org/page/16299461>
- Dumont HJ (1998) The Caspian Lake: History, biota, structure, and function. *Limnology and Oceanography* 43 (1): 44–52. <https://doi.org/10.4319/lo.1998.43.1.0044>
- Dunker W (1861) Beschreibung neuer Mollusken. *Malakozoologische Blätter* 8: 35–45. <https://biodiversitylibrary.org/page/15919848>
- Dybowski B (1913) Ueber Kaspische Schnecken aus der Abteilung Turricaspiinae subfam. nova, zum Vergleich mit den Turribaicaliinae subfam. nova. *Bulletin de l'Académie Impériale des Sciences de St.-Petersbourg, sixième série* 7 (16): 905–906. <https://biodiversitylibrary.org/page/4183344>
- Dybowski B, Grochmalicki J (1914) Beitrage zur Kenntnis der Baikalmollusken, I. Baicalidae, 1. Turribaicaliinae subfam. nova. *Annuaire du Musée Zoologique de l'Académie Impériale des Sciences de St. Pétersbourg* 18 (2): 268–316. <https://biodiversitylibrary.org/page/8508337>
- Dybowski B, Grochmalicki J (1915) Ueber kaspische Schnecken aus der Abteilung “Turricaspiinae” subfam. nova zum Vergleich mit den Turribaikalina nobis. *Petrograd*, 34 pp. [numbered 103–136], 3 pls.
- Dybowski B, Grochmalicki J (1917) Studien über die turmförmigen Schnecken des Baikalsees und des Kaspimeeres (Turribaicaliinae – Turricaspiinae). *Abhandlungen der Kaiserlich-Königlichen Zoologisch-Botanischen Gesellschaft in Wien* 9 (3): 1–55. <https://biodiversitylibrary.org/page/5550074>
- Dybowski W (1887–1888) Die Gasteropoden-Fauna des Kaspischen Meeres. Nach der Sammlung des Akademikers Dr. K. E. v. Baer. *Malakozoologische Blätter (Neue Folge)* 10(1–3): 1–64 [issue 1, 1887], 65–79 [issue 2, 1888], pl. 1–3 [issue 3, 1888]. <https://biodiversitylibrary.org/page/35483241>
- Eichwald E (1838) Faunae Caspii Maris primitiae. *Bulletin de la Société Impériale des Naturalistes de Moscou* 11 (2): 125–174. <https://biodiversitylibrary.org/page/41342125>
- Eichwald E (1841) Fauna Caspio-Caucasica nonnullis observationibus novis illustravit. *Nouveaux Mémoires de la Société Impériale des Naturalistes de Moscou* 7: 1–290. <https://biodiversitylibrary.org/page/33163057>
- Eichwald E (1853) *Lethaea Rossica ou Paléontologie de la Russie, décrite et figurée. Troisième volume. Dernière période.* Schweizerbart, Stuttgart, 533 pp. <https://biodiversitylibrary.org/page/36423437> [text], <https://biodiversitylibrary.org/page/39452522> [plates]
- Eröss ZP, Petró E (2008) A new species of the valvatiform hydrobiid genus *Hauffenia* from Hungary (Mollusca: Caenogastropoda: Hydrobiidae). *Acta Zoologica Academiae Scientiarum Hungaricae* 54 (2): 159–167.
- Férussac AEJPF d'A d (1823) Monographie des espèces vivantes et fossiles du genre mélanopside, *Melanopsis*, et observations géologiques à leur sujet. *Mémoires de la Société d'Histoire Naturelle de Paris* 1(1): 132–164. <https://biodiversitylibrary.org/page/3555191>

- Filippov A, Riedel F (2009) The late Holocene mollusc fauna of the Aral Sea and its biogeographical and ecological interpretation. *Limnologica* 39(1): 67–85. <https://doi.org/10.1016/j.limno.2008.04.003>
- Forte AM, Cowgill E (2013) Late Cenozoic base-level variations of the Caspian Sea: A review of its history and proposed driving mechanisms. *Palaeogeography, Palaeoclimatology, Palaeoecology* 386: 392–407. <https://doi.org/10.1016/j.palaeo.2013.05.035>
- Frýda J (1998) Higher classification of the Paleozoic gastropods inferred from their early shell ontogeny. In: Bieler R, Mikkelsen PM (Eds) 13th International Malacological Congress, Abstracts. Washington, DC, 108.
- Glöer P (2002) Die Tierwelt Deutschlands, 73. Teil: Die Süßwassergastropoden Nord- und Mitteleuropas. Bestimmungsschlüssel, Lebensweise, Verbreitung. ConchBooks, Hackenheim, 327 pp.
- Glöer P, Falniowski A, Szarowska M (2005) *Bithynia leachii* (Sheppard 1823) and *B. troschelii* (Paasch 1842), two distinct species? *Heldia* 6: 49–56.
- Golikov AN, Starobogatov YaI (1966) Ponto-kaspiyskiy bryukhonogiye mollyuski v Azovo-Chernomorskom basseyne. *Zoologicheskii Zhurnal* 45 (3): 352–362.
- Golikov AN, Starobogatov YaI (1975) Systematics of prosobranch gastropods. *Malacologia* 15 (1): 185–232.
- Gorthner A (1994) What is an ancient lake? In: Martens K, Goddeeris B, Coulter G (Eds) Speciation in Ancient Lakes. *Archiv für Hydrobiologie – Beiheft: Ergebnisse der Limnologie* 44 : 97–100.
- Gray JE (1840) Shells of molluscous animals. In: Synopsis of the contents of the British Museum (42th edn). G. Woodfall, London, 105–152.
- Grigorovich IA, Therriault TW, MacIsaac HJ (2003) History of aquatic invertebrate invasions in the Caspian Sea. *Biological Invasions* 5: 103–115. <https://doi.org/10.1023/A:1024050824073>
- Grimm OA (1876) Kaspiyskoye more i yego fauna. Tetrad' 1. *Trudy Aralo-Kaspiyskoy Ekspeditsii* 2: 1–168. http://www.cawater-info.net/library/rus/hist/2_grimm.pdf
- Grimm OA (1877) Kaspiyskoye more i yego fauna. Tetrad' 2. *Trudy Aralo-Kaspiyskoy Ekspeditsii* 2(2): 1–105. http://www.cawater-info.net/library/rus/hist/2_grimm.pdf
- Haase M, Naser MD, Wilke T (2010) *Ecrobia grimmii* in brackish Lake Sawa, Iraq: indirect evidence for long-distance dispersal of hydrobiid gastropods (Caenogastropoda: Rissooidea) by birds. *Journal of Molluscan Studies* 76: 101–105. <https://doi.org/10.1093/mollus/eyp051>
- Heiler KCM, Nahavandi N, Albrecht C (2010) A New Invasion Into an Ancient Lake – The Invasion History of the Dreissenid Mussel *Mytilopsis leucophaeata* (Conrad, 1831) and Its First Record in the Caspian Sea. *Malacologia* 53 (1): 185–192. <https://doi.org/10.4002/040.053.0112>
- ICZN (1999) International Code of Zoological Nomenclature. International Trust for Zoological Nomenclature, London, 306 pp. <http://www.nhm.ac.uk/hosted-sites/iczn/code/index.jsp>
- Issel A (1865) Catalogo dei molluschi raccolti dalla missione italiana in Persia aggiuntavi la descrizione delle specie nuove o poco note. Stamperia Reale, Torino, 55 pp. <http://magtecafi-ese.inera.it/unifi/opac/unifi/scheda.jsp?pid=mag:13023>

- Issel A (1866) Catalogo dei molluschi raccolti dalla missione italiana in Persia aggiuntavi la descrizione delle specie nuove o poco note. Memorie della Reale accademia delle scienze di Torino, 2. serie 23: 387–439. <https://biodiversitylibrary.org/page/31197934>
- Kantor YuI, Sysoev AV (2005) Katalog mollyuskov Rossii i sopredel'nykh stran. KMK Scientific Press, Moscow, 627 pp.
- Kantor YuI, Sysoev AV (2006) Morskiye i solonovatovodnyye bryukhonogiye mollyuski Rossii i sopredel'nykh stran: illyustrirovannyi katalog. KMK Scientific Press, Moscow, 372 pp., 140 pls.
- Kantor YuI, Vinarski MV, Schileyko AA, Sysoev AV (2010) Catalogue of the Continental Mollusks of Russia and Adjacent Territories. Version 2.3.1. http://www.ruthenica.com/documents/Continental_Russian_molluscs_ver2-3-1.pdf
- Kolesnikov VP (1947) Tablitsa dlya opredeleniya kaspyskikh gastropod. Byulleten' Moskovskogo Obshchestva Ispytateley Prirody, Otdel Geologicheskiiy 22(1): 105–112.
- Kondrashov PE (2007) New gastropod species from the Pleistocene of the Upper Don basin. Paleontological Journal 41 (5): 513–519. <https://doi.org/10.1134/S0031030107050061>
- Kosarev AN, Yablonskaya EA (1994) The Caspian Sea. SPB Academic Publishing, The Hague, 259 pp.
- Krynicky AJ (1837) Conchyliia tam terrestria, quam fluviatilia et e maribus adjacentibus Imperii Rossici indigena, quae pro mutua offeruntur historiae naturalis cultoribus commutatione. Bulletin de la Société Impériale des Naturalistes de Moscou 10(2): 50–64. <https://biodiversitylibrary.org/page/5521585>
- Lehner B, Döll P (2004) Development and validation of a global database of lakes, reservoirs and wetlands. Journal of Hydrology 296(1–4): 1–22. <https://doi.org/10.1016/j.jhydrol.2004.03.028>
- Lindholm VA (1922) Miscellaneous notes on palaeartic land and freshwater Mollusks. Ezhegodnik Zoologicheskogo Muzeya Imperatorskoy Akademii Nauk 23(3–4): 304–320. <https://biodiversitylibrary.org/page/8483531>
- Lindholm VA (1924) K nomenklature nekotorykh kaspyskikh gastropod. Russkiy Gidrobiologicheskiiy Zhurnal 3 (1–2): 32–34.
- Lindholm VA (1925) Beitrag zur Systematik und Nomenklatur der Familie Enidae (Buliminidae). Archiv für Molluskenkunde 57: 23–41. https://www.zobodat.at/pdf/Archiv-fuer-Molluskenkunde_57_0023-0041.pdf
- Lindholm VA (1930) Drei interessante Wasserschnecken (Gastropoda) aus dem westlichen Turkestan. Doklady Akademii Nauk SSSR 1929: 311–314.
- Linnaeus C (1758) Systema naturae per regna tria naturae, secundum classes, ordines, genera, species, cum characteribus, differentiis, synonymis, locis. Tomus I. Editio decima, reformata. Laurentius Salvius, Holmiae, 824 pp. <https://biodiversitylibrary.org/page/726886>
- Logvinenko BM, Starobogatov YaI (1969) Mollusca. In: Birshtein YaA, Vinogradov LG, Kondakov NN, Kuhn MS, Astakhova TV, Romanova NN (Eds) Atlas bespozvonochnykh Kaspyskogo morya. Pishchevaya Promyshlennost (Vsesoyuznyi Nauchno-issledovatel'skii Institut Morskogo Rybnogo Khozyaistva i Okeanografii), Moskva, 308–385.
- Milashevich KO (1908) Mollyuski, sobrannyye vo vremya ekskursii S.A. Zernova na minonostye No. 264 na r. Dunay s 28 iyunya po 3 iyulya 1907 goda. Bulletin de l'Académie Impériale des Sciences de St.-Petersbourg, sixième série 2(12): 991–996.

- Möllendorff Ov (1873) Beiträge zur Fauna Bosniens. Inauguraldissertation, Görlitz. <https://biodiversitylibrary.org/page/12924443>
- Montfort P Dd (1810) Conchyliologie systématique et classification méthodique de coquilles; offrant leurs figures, leur arrangement générique, leurs descriptions caractéristiques, leurs noms; ainsi que leur synonymie en plusieurs langues. Ouvrage destiné à faciliter l'étude des coquilles, ainsi que leur disposition dans les cabinets d'histoire naturelle. Coquilles univalves, non cloisonnées. Tome second. Schoell, Paris, 676 pp. <https://biodiversitylibrary.org/page/11065017>
- Nalivkin DV (1914) Mollyuski gory bakinskogo yarusa. Trudy Geologicheskogo Komiteta, novaya seriya 116: 1–32.
- Neubauer TA, Georgopoulou E, Harzhauser M, Mandic O, Kroh A (2016a) Predictors of shell size in long-lived lake gastropods. *Journal of Biogeography* 43(10): 2062–2074. <https://doi.org/10.1111/jbi.12777>
- Neubauer TA, Harzhauser M, Georgopoulou E, Kroh A, Mandic O (2015a) Tectonics, climate, and the rise and demise of continental aquatic species richness hotspots. *Proceedings of the National Academy of Sciences of the United States of America* 112(37): 11478–11483. <https://doi.org/10.1073/pnas.1503992112>
- Neubauer TA, Kroh A, Harzhauser M, Georgopoulou E, Mandic O (2015b) Taxonomic note on problematic Neogene European freshwater Gastropoda. *Annalen des Naturhistorischen Museums in Wien, Serie A* 117: 95–100. http://verlag.nhm-wien.ac.at/pdfs/117A_095100_Neubauer.pdf
- Neubauer TA, Mandic O, Harzhauser M (2016b) The freshwater mollusk fauna of the Middle Miocene Lake Drniš (Dinaride Lake System, Croatia): a taxonomic and systematic revision. *Austrian Journal of Earth Sciences* 108(2): 15–67. <https://doi.org/10.17738/ajes.2015.0013>
- Neumayr M (1869) Beiträge zur Kenntniss fossiler Binnenfaunen. *Jahrbuch der k. k. geologischen Reichsanstalt* 19: 355–382. <https://biodiversitylibrary.org/page/36221771>
- Orlova MI, Muirhead JR, Antonov PI, Shcherbina GK, Starobogatov YaI, Biochino GI, Theriault TW, MacIsaac HJ (2005) Range expansion of quagga mussels *Dreissena rostriformis bugensis* in the Volga River and Caspian Sea basin. *Aquatic Ecology* 38(4): 561–573. <https://doi.org/10.1007/s10452-005-0311-6>
- Parr TD, Tait RD, Maxon CL, Newton III FC, Hardin JL (2007) A descriptive account of benthic macrofauna and sediment from an area of planned petroleum exploration in the southern Caspian Sea. *Estuarine, Coastal and Shelf Science* 71(1–2): 170–180. <https://doi.org/10.1016/j.ecss.2006.07.018>
- Pavlović PS (1903) Građazapoznavanje tercijara u Staroj Srbiji. *Annales Géologiques de la Péninsule Balkanique* 6(1): 155–189. <https://archive.org/stream/geoloshkianalib00zavogoog#page/n176/mode/2up>
- Perty JAM (1833) Delectus animalium articulorum, quae in itinere per Brasiliam annis MDCCCXVII–MDCCCXX [1817–1820] jussu et auspiciis Maximiliani Josephi I Bavariae Regis augustissimi peracto, collegerunt Dr. J. B. de Spix et Dr. C. F. Ph. de Martius. Vol. 3. Friedrich Fleischer, Monachii, 224 pp., pl. 25–40. <https://biodiversitylibrary.org/page/47586617>

- Pfeiffer C (1828) Naturgeschichte deutscher Land- und Süßwasser-Mollusken. Dritte Abtheilung. Landes-Industrie-Comptoir, Weimar, 84 pp.
- Pirogov VV (1971) O nakhozhdenii novogo vida mollyuska iz roda *Pyrgula* Crist. et Jan. v avandel'tye reki Volgi. Trudy Astrakhanskogo Zapovednika imeni V.I. Lenina 13: 249–253.
- Poey F (1852) Introduccion a los Ciclostomas con generalidades sobre los moluscos gastropodos y particularmente sobre los terrestres operculados. Memorias sobre la historia natural de la isla de Cuba 1(8): 77–96. <https://biodiversitylibrary.org/page/2524896>
- Pollonera C (1898) Intorne ad alcune Conchiglie del Friuli. Bollettino dei Musei di Zoologi ed Anatomia comparata della Università di Torino 13: 1–4.
- Ponder WF (1984) A review of the Genera of the Rissoidae (Gastropoda: Mesogastropoda: Rissoacea). Records of the Australian Museum Supplement 4: 1–221. https://australian-museum.net.au/uploads/journals/16835/100_complete.pdf
- Popov SV, Shcherba IG, Ilyina LB, Nevesskaya LA, Paramonova NP, Khondkarian SO, Magyar I (2006) Late Miocene to Pliocene palaeogeography of the Paratethys and its relation to the Mediterranean. Palaeogeography, Palaeoclimatology, Palaeoecology 238(1–4): 91–106. <https://doi.org/10.1016/j.palaeo.2006.03.020>
- Radoman P (1973) New classification of fresh and brackish water Prosobranchia from the Balkans and Asia Minor. Prirodjnacki Muzej u Beogradu, Posebna Izdanja 32: 3–30.
- Rafinesque CS (1815) Analyse de la nature ou tableau de l'univers et des corps organisés. Privately published by author, Palermo, 223 pp. <http://gallica.bnf.fr/ark:/12148/bpt6k98061z>
- Riedel F, Audzijonyte A, Mugue N (2006) Aliens Associating with Caspian Sea Endemic Bivalves. Biological Invasions 8(5): 1067–1071. <https://doi.org/10.1007/s10530-005-5920-4>
- Riedel F, Healy JM, Röpsdorf P, Sitnikova TYa (2001) Ecology, Shell Morphology, Anatomy and Sperm Ultrastructure of Caenogastropod *Pyrgula annulata*, with a Discussion of the Relations between the 'Pyrgulidae' and Caspian and Baikalian Rissooideans. Limnologica 31: 289–302. [https://doi.org/10.1016/S0075-9511\(01\)80031-1](https://doi.org/10.1016/S0075-9511(01)80031-1)
- Schultze FTS (1826) Catalog der Conchylien-Sammlung des verstorbenen Herrn Ober-Einnehmers Freiherrn von der Malsburg, in deren Besitz sich jetzt befindet der Herr Kammerherr Baron v. d. Malsburg zu Escheberg bei Cassel in Cur-Hessen. Berlin, 199 pp.
- Shishkoedova OS (2010) Pervaya nakhodka mollyuskov roda *Caspihydrobia* (Mollusca: Gastropoda) v Chelyabinskoy oblasti. In: Ecology: from the southern mountains to the northern seas. Materials of the young scientists' meeting, 19–23 April, 2010, Yekaterinburg. Goschitsky Publisher, Yekaterinburg, 210–213.
- Shkatova VK (2010) Paleogeography of the Late Pleistocene Caspian Basins: Geochronometry, paleomagnetism, paleotemperature, paleosalinity and oxygen isotopes. Quaternary International 225: 221–229. <https://doi.org/10.1016/j.quaint.2009.05.001>
- Sinzov I (1896) Beschreibung einiger Arten neogener Versteinerungen, welche in den Gouvernements von Cherson und Bessarabien aufgefunden wurden. Zapiski novorossiiskoe obshchestvo estestvoispytatelei 21: 39–88. [In Russian]
- Sitnikova TYa, Starobogatov YaI (1999) Novyye rod semeystva Pyrgulidae (Gastropoda, Pectinibranchia) iz presnykh rod Azovo-Chernomorskogo basseyna (v svyazi s voprosom o Ponto-Kaspiyskikh vidakh v Azovo-Chernomorskogom basseyne). Zoologicheskii Zhurnal 78(2): 158–163.

- Sitnikova TYa, Starobogatov YaI, Anistratenko VV (1992) Anatomiya i sistematicheskoye polozheniye nekotorykh melkikh Pectinibranchia (Mollusca, Gastropoda) fauny Yevropy. Vestnik Zoologii 6: 3–12.
- Starobogatov YaI (1970) Fauna mollyuskov i zoogeographicheskoye rayonirovaniye kontinental'nykh vo do emov zemnogo shara [The mollusk fauna and zoogeographical regionalisation of continental waterbodies of the Earth]. Nauka, Leningrad, 372 pp.
- Starobogatov YaI (2000) Caspian endemic genus *Andrusovia* (Gastropoda Pectinibranchia Horatiidae). Ruthenica 10(1): 37–42.
- Starobogatov YaI, Alexenko TL, Levina OV (1992) Rody *Fagotia* i *Microcolpia* (Gastropoda Pectinibranchia Melanopsidae) i ikh predstaviteli v sovremennoj faune. Byulleten' Moskovskogo Obshchestva Ispytateley Prirody, Otdel biologicheskiiy 97(3): 57–72.
- Starobogatov YaI, Filchakov VA, Antonova LA, Pirogov VV (1994) Novyye dannyye o mollyuskakh i vysshikh rakoobraznykh delty Volgi. Vestnik Zoologii 4–5: 8–12.
- Starobogatov YaI, Prozorova LA, Bogatov VV, Sayenko EM (2004) Mollyuski. In: Tsalolikhin SJ (Ed.) Opredelitel' presnovodnykh bespozvonochnykh Rossii i sopredel'nykh territoriy. T. 6. Mollyuski, Polikhety, Nemertiny. Izdatel'stvo "Nauka", St. Petersburg, 9–491.
- Stimpson W (1865) Researches upon the Hydrobiinae and allied forms: chiefly made from materials in the Museum of the Smithsonian Institution. Smithsonian Miscellaneous Collections 7: 1–59.
- Strand E (1928) Miscellanea nomenclatorica zoologica et palaeontologica. I–II. Archiv für Naturgeschichte, Abteilung A 92(8): 30–75.
- Svitoch AA (2008) The Khvalynian Transgression of the Caspian Sea and the New-Euxinian Basin of the Black Sea. Water Resources 35 (2): 165–170. <https://doi.org/10.1134/S0097807808020048>
- Svitoch AA (2012) The Caspian Sea Shelf during the Pleistocene Regressive Epochs. Oceanology 52 (4): 526–539. <https://doi.org/10.1134/S0001437012030113>
- Sysoev AV, Kantor YI (1992) Names of Mollusca introduced by Ya.I.Starobogatov in 1957–1992. Ruthenica 2 (2): 119–159.
- Szarowska M (2006) Molecular phylogeny, systematics and morphological character evolution in the Balkan Rissoidae (Caenogastropoda). Folia Malacologica 14(3): 99–168. <https://doi.org/10.12657/fofmal.014.014>
- Szarowska M, Falniowski A (2014) *Horatia* Bourguignat, 1887: is this genus really phylogenetically very close to *Radomaniola* Szarowska, 2006 (Caenogastropoda: Truncatelloidea)? Folia Malacologica 22(1): 31–39. <https://doi.org/10.12657/fofmal.022.003>
- Tadjalli-Pour M (1977) Les Mollusques marins des côtes Iraniennes de la Mer Caspienne (Astara-Hachtpar). Journal de Conchyliologie 114(3–4): 87–117.
- Taviani M, Angeletti L, Çagatay MN, Gasperini L, Polonia A, Wesselingh FP (2014) Sedimentary and faunal signatures of the post-glacial marine drowning of the Pontocaspian Gemlik “lake” (Sea of Marmara). Quaternary International 345: 11–17. <https://doi.org/10.1016/j.quaint.2014.05.045>
- Taylor DW (1966) A Remarkable Snail Fauna from Coahuila, México. The Veliger 9(2): 152–228. <https://biodiversitylibrary.org/page/42521795>
- Therriault TW, Docker MF, Orlova MI, Heath DD, MacIsaac HJ (2004) Molecular resolution of the family Dreissenidae (Mollusca: Bivalvia) with emphasis on Ponto-Caspian species,

- including first report of *Mytilopsis leucophaeata* in the Black Sea basin. Molecular Phylogenetics and Evolution 30(3): 479–489. [https://doi.org/10.1016/S1055-7903\(03\)00240-9](https://doi.org/10.1016/S1055-7903(03)00240-9)
- Thiele J (1928) Revision des Systems der Hydrobiiden und Melaniiden. Zoologische Jahrbücher, Abteilung Systematik, Ökologie und Geographie der Tiere 55: 351–402.
- Totten JG (1834) Description of some new Shells, belonging to the coast of New England. American Journal of Science and Arts 26: 366–369. <https://biodiversitylibrary.org/page/15985663>
- Urbański J (1975) *Lithoglyphus jahni* n. sp. aus den mitteleuropäischen Ablagerungen des Mindel/Riss Interglazials nebst Bemerkungen über den nordbalkanischen *L. fuscus* (C. Pfeiffer 1828) (= *L. pyramidatus* Moellendorf 1873) – (Gastropoda, Prosobranchia, Hydrobiidae). Bulletin de la Société des Amis des Sciences et des Lettres de Poznan 15: 107–111.
- Van Baak CGC, Vasiliev I, Stoica M, Kuiper KF, Forte AM, Aliyeva E, Krijgsman W (2013) A magnetostratigraphic time frame for Plio-Pleistocene transgressions in the South Caspian Basin, Azerbaijan. Global and Planetary Change 103: 119–134. <https://doi.org/10.1016/j.gloplacha.2012.05.004>
- Verduin A (1977) On a remarkable dimorphism of the apices of sympatric closely-related marine gastropod species. Basteria 41(5-6): 91–95.
- Vinarski MV, Kantor Yul (2016) Analytical catalogue of fresh and brackish water molluscs of Russia and adjacent countries. A.N. Severtsov Institute of Ecology and Evolution of RAS, Moscow, 544 pp.
- Vinarski MV, Nekhaev IO, Glöer P, Proschwitz Tv (2013) Type materials of freshwater gastropod species described by C.A. Westerlund and accepted in current malacological taxonomy: a taxonomic and nomenclatorial study. Ruthenica 23(2): 79–108.
- Vinarski MV, Palatov DM, Glöer P (2014) Revision of ‘*Horatia*’ snails (Mollusca: Gastropoda: Hydrobiidae sensu lato) from South Caucasus with description of two new genera. Journal of Natural History 48(37-38): 2237–2253. <https://doi.org/10.1080/00222933.2014.917210>
- Welter-Schultes FW (2012) European non-marine molluscs, a guide for species identification. Planet Poster Editions, Göttingen, 679 pp.
- Wenz W (1926) Fossilium Catalogus I: Animalia. Gastropoda extramarina tertiaria. W. Junk, Berlin, vol. VII: 1863–2230.
- Wenz W (1938–1944) Gastropoda. Teil 1: Allgemeiner Teil und Prosobranchia. In: Schindewolf OH (Ed.) Handbuch der Paläozoologie, Band 6. Verlag Gebrüder Bornträger, Berlin, 1639 pp.
- Westerlund CA (1896) Neue centralasiatische Mollusken. Ezhegodnik Zoologicheskogo Muzeya Imperatorskoy Akademii Nauk 1(3): 181–198. <https://biodiversitylibrary.org/page/9006596>
- Westerlund CA (1902a) Methodus dispositionis Conchyliorum extramarinorum in Regione palaeartica viventium, familias, genera, subgenera et stirpes sistens. Rad Jugoslavenske akademije znanosti i umjetnosti 151: 82–139. <http://dizbi.hazu.hr/object/view/km6Jc2154m>
- Westerlund CA (1902b) Malacologische Bemerkungen und Beschreibungen. Nachrichtenblatt der Deutschen Malakozoologischen Gesellschaft 34: 35–47. <https://biodiversitylibrary.org/page/15598774>

- Wilke T, Albrecht C, Anistratenko VV, Sahin SK, Yildirim MZ (2007) Testing biogeographical hypotheses in space and time: faunal relationships of the putative ancient Lake Egirdir in Asia Minor. *Journal of Biogeography* 34: 1807–1821. <https://doi.org/10.1111/j.1365-2699.2007.01727.x>
- Wilke T, Haase M, Hershler R, Liu H-P, Misof B, Ponder W (2013) Pushing short DNA fragments to the limit: Phylogenetic relationships of ‘hydrobioid’ gastropods (Caenogastropoda: Rissooidea). *Molecular Phylogenetics and Evolution* 66: 715–736. <https://doi.org/10.1016/j.ympev.2012.10.025>
- Yanina TA (2013) Biostratigraphy of the Middle and Upper Pleistocene of the Caspian Region. *Quaternary International* 284: 85–97. <https://doi.org/10.1016/j.quaint.2012.02.008>
- Yanina TA (2014) The Ponto-Caspian region: Environmental consequences of climate change during the Late Pleistocene. *Quaternary International* 345: 88–99. <https://doi.org/10.1016/j.quaint.2014.01.045>
- Yanko-Hombach V, Gilbert AS, Panin N, Dolukhanov PM (Eds) (2007) *The Black Sea Flood Question: Changes in Coastline, Climate and Human Settlement*. Springer, Dordrecht, 971 pp. <https://doi.org/10.1007/978-1-4020-5302-3>
- Zettler ML (2007) A redescription of *Theodoxus schultzei* (Grimm, 1877), an endemic neritid gastropod of the Caspian Sea. *Journal of Conchology* 39(3): 245–251.
- Zhadin VI (1952) *Mollyuski presnykh i solonovatykh vod SSSR*. Izdatel'stvo Akademii Nauk SSSR, Moskva, Leningrad, 376 pp.

Ancient home or in exile? The easternmost species of genus *Starengovia* Snegovaya, 2010 found in China (Opiliones, Nemastomatidae, Nemastomatinae)

Chao Zhang¹, Jochen Martens^{2,3}

1 *The Key Laboratory of Invertebrate Systematics and Application, College of Life Sciences, Hebei University, Baoding, Hebei 071002, China* **2** *Institut für Organismische und Molekulare Evolutionsbiologie, D-55099 Mainz, Germany* **3** *Senckenberg Research Institute, Arachnology, Frankfurt am Main, Germany*

Corresponding author: *Chao Zhang* (opiliones@163.com)

Academic editor: *A. Kury* | Received 4 April 2018 | Accepted 18 May 2018 | Published 04 July 2018

<http://zoobank.org/3A5FA717-6819-4873-BBE4-F14974B8F879>

Citation: Zhang C, Martens J (2018) Ancient home or in exile? The easternmost species of genus *Starengovia* Snegovaya, 2010 found in China (Opiliones, Nemastomatidae, Nemastomatinae). ZooKeys 770: 105–115. <https://doi.org/10.3897/zookeys.770.25491>

Abstract

Starengovia quadrituberculata **sp. n.** is described and illustrated based on male and female specimens collected in Yunnan Province, China. The new species is distinct from the two other congeners, *S. kirgizica* Snegovaya, 2010 and *S. ivanloebli* Martens, 2017, in having two pairs of low submedian tubercles on abdominal areae III and IV; distal margin of the lateral foliate wing-like structures of the penis situated close to the glans base, the short rod-like stylus, the form and position of spines on the stylus of the penis, anvil-shaped tubercles mainly on front margin of prosoma. The occurrence of *Starengovia* in Yunnan, the second nemastomatine species in China, creates a huge distributional gap of roughly 2700 km distance to its closest neighbor *S. ivanloebli* in Northwest Pakistan. The historical relations of Chinese nemastomatines are discussed.

Keywords

East Palaearctic, genitalia, harvestmen, relict species, *Starengovia*, taxonomy, Yunnan Province

Introduction

The family Nemastomatidae Simon, 1872 is currently represented by two subfamilies (Ortholasmatinae Shear & Gruber, 1983, and Nemastomatinae Simon, 1872) and includes 23 genera and 138 species worldwide (Schönhofer 2013; Zhang and Zhang 2013; Martens 2006, 2016, 2017; Zhang, Zhao and Zhang 2018). Distribution of Nemastomatinae is predominantly West Palaearctic covering nearly all parts of Europe, and beyond Europe penetrating, e.g., to Kyrgyzstan and in the Pamir Mts. Recently, the first nemastomatine harvestman was discovered in China and assigned to a new genus, *Sinostoma* Martens, 2016, extending the distribution of nemastomatines to approximately 3000 km southeastwards. Here another minute nemastomatine harvestman species is described from China in the mountains of southern Yunnan Province.

Materials and methods

Taxonomic scheme follow the outline proposed by Gruber (2007). The specimens were preserved in 75% ethanol, examined, and drawn under a Leica M205A stereomicroscope equipped with a drawing tube. Photographs were taken using a Leica M205A stereomicroscope equipped with a DFC 450 CCD. The type specimens are deposited in the Museum of Hebei University, Baoding, China (MHBU). All measurements are given in mm.

Taxonomy

Nemastomatidae Simon, 1872

Nemastomatinae Simon, 1872

***Starengovia* Snegovaya, 2010**

Starengovia Snegovaya, 2010: 351–352; Schönhofer 2013: 47; Martens 2017: 187–188.

Type species. *Starengovia kirgizica* Snegovaya, 2010, original designation.

Diagnosis. Small species up to 1.7 mm, dorsal scutum with lines of anvil-shaped tubercles along margins of scutal areas. Pairs of para-median tubercles on opisthosomal areas of dorsal scutum. Truncus penis moderately slender, large muscle-containing inflated base, truncus in straight continuation of inflated base. Distal part of truncus with one large lateral wing on either side, glans inconspicuous, not well differentiated from truncus; armament of glans simple with symmetrical arrangement. Apophysis on basal cheliceral article of male well-marked, with a distad-directed hook, discharge area for secretion in a bowl-like excavation on medial side of apophysis (Martens 2017).

Distribution. China (Yunnan), Kyrgyzstan, Uzbekistan, Himalayas of Pakistan.

Key to the currently known species of *Starengovia*

- 1 Distributed in Yunnan, China, low para-median tubercles on opisthosomal areae III and IV (Figs 1, 8, 13, 26–27, 29–30), penis with alae of wings bent to ventral side (Figs 20–22)..... ***S. quadrituberculata* sp. n.**
- Distributed in Central Asia (Kyrgyzstan, Uzbekistan) and NW Pakistan; high slender or compact para-median tubercles on opisthosomal areae I–V; penis with alae of wings bent to ventral side or straight, not bent..... **2**
- 2 Distributed in Kyrgyzstan (one record also in Uzbekistan), tubercles of dorsal scutum conical and compact; penis with alae of wings bent to ventral side ...
.....***S. kirgizica***
- Distributed in northwestern Pakistan, tubercles of dorsal scutum slender, penis with alae of wings straight, not bent to ventral side***S. ivanloebli***

***Starengovia quadrituberculata* sp. n.**

<http://zoobank.org/3A5FA717-6819-4873-BBE4-F14974B8F879>

Figs 1–31

Diagnosis. Areae III–IV of opisthosomal region each with a pair of very low median tubercles inclined posteriorly. Basal segment of chelicerae dorso-distally with a triangular apophysis in male (in lateral view). Distal part of penis with extended lateral wing structure; width of the wings almost equivalent to length. Glans short, nearly cone-shaped; stylus short and conical. Scanty anvil-shaped tubercles confined to front margin of prosoma.

Type locality. CHINA, Yunnan Province: Baoshan City, Lujiang Town, Dahaoping, 24°57'42"N, 98°43'58"E, 2142 m ASL, evergreen forest, sifted from leaf litter.

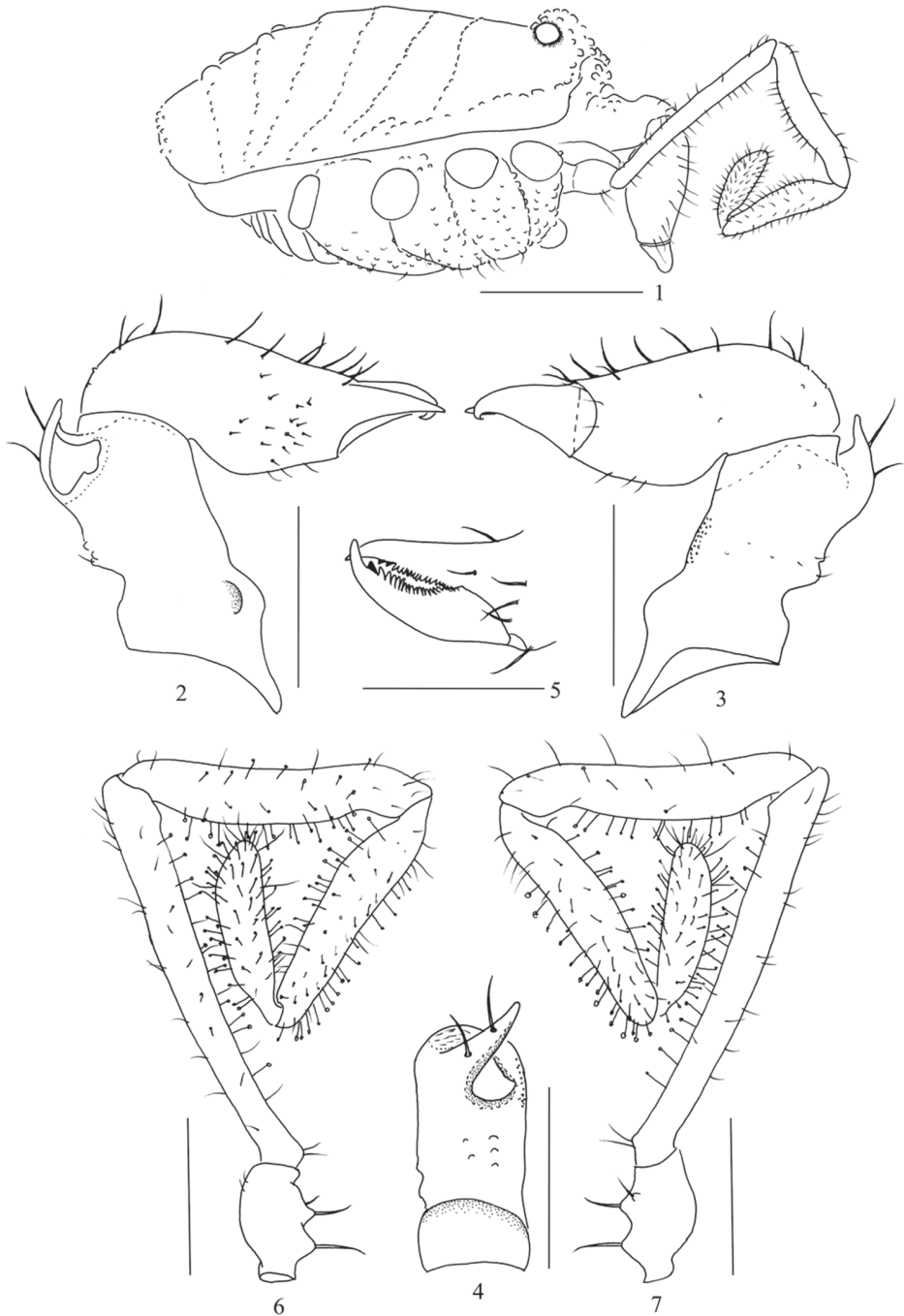
Type specimen. Holotype male (MHBU-Opi-20171208). Adult male preserved in 75% ethanol, with genitalia in a separate microvial. Original label: MHBU-Opi-20171208, CHINA: Yunnan Province, Baoshan City, Lujiang Town, Dahaoping, 24°57'42"N, 98°43'58"E, 2142 m ASL, 23 November 2017, Y.N. Mu leg.

Paratype. 1♀ (MHBU-Opi-20171209), same data as the holotype.

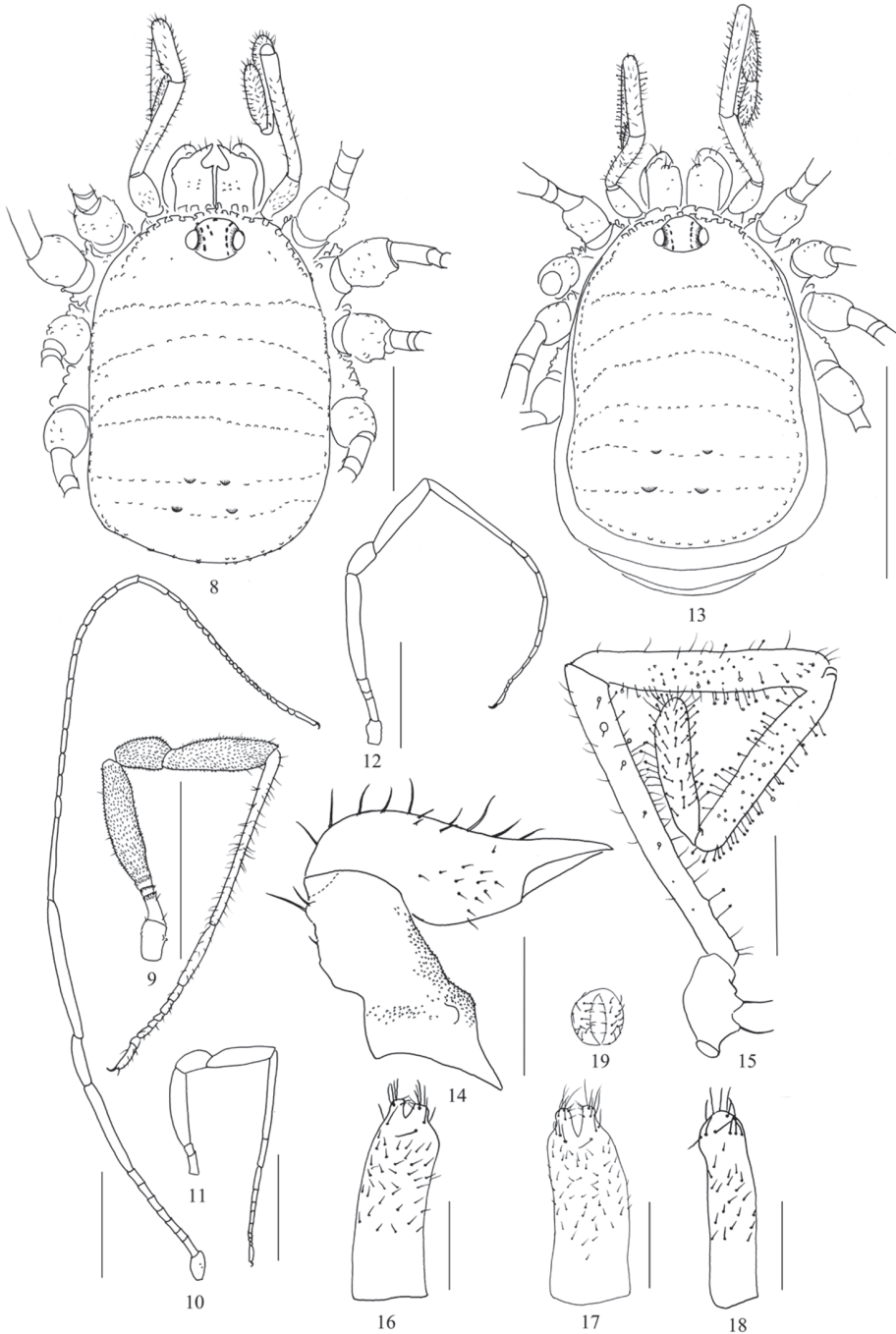
Etymology. The specific name is taken from the Latin *quadri-* (four) and *tuberculum* (tubercle, small apophysis), referring to the two pairs of small tubercles on opisthosomal areae III and IV.

Description of the male holotype. Habitus as in Figs 1, 8, 26–28. Coloration in alcohol: dorsum brown black, without silvery or golden markings (Fig. 26). Venter concolorous with the dorsum (Fig. 28), but intersegmental membranes whitish. Chelicerae and pedipalpi chestnut-brown. Legs deep black.

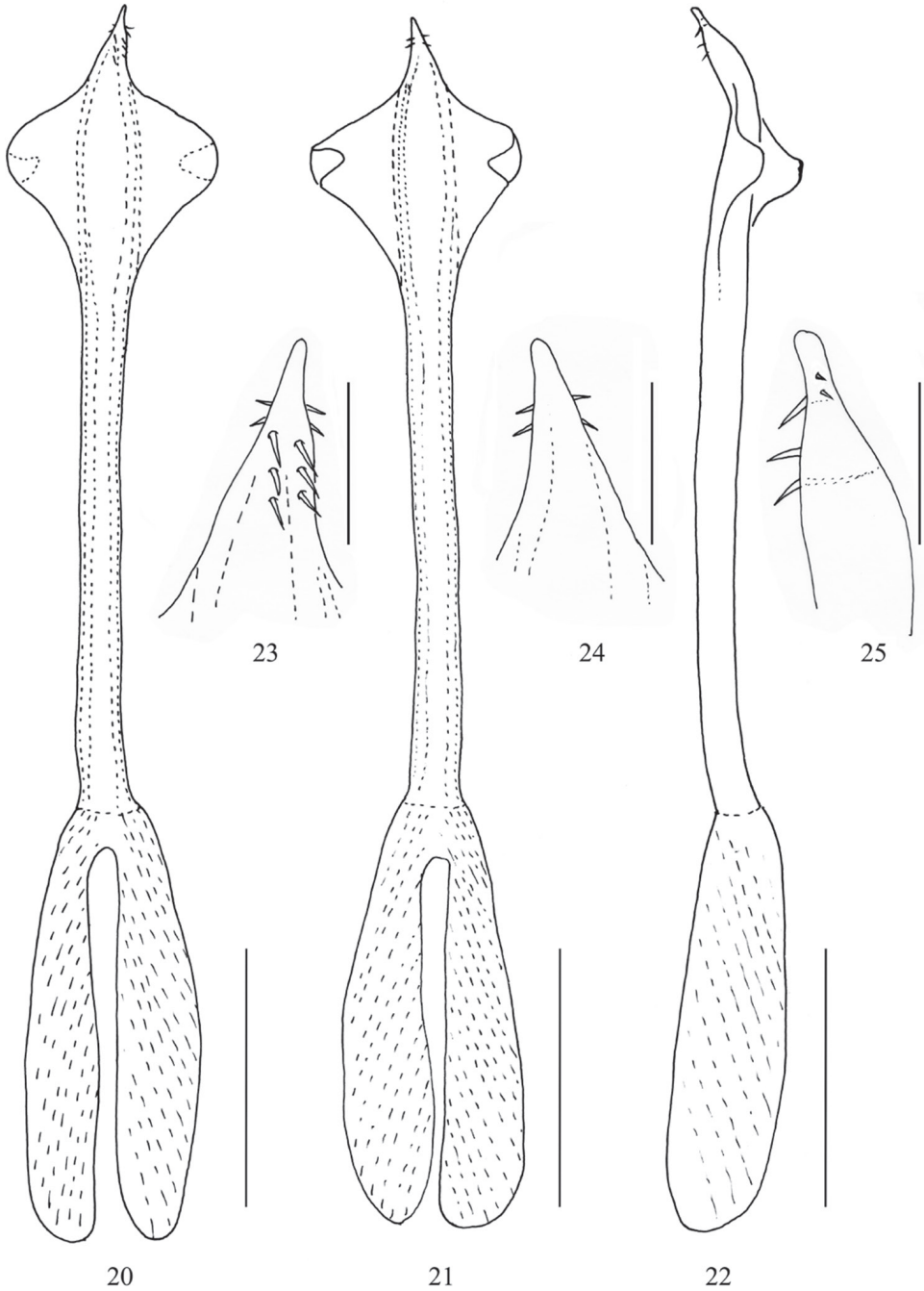
Dorsum (Figs 8, 26). Body small, strongly sclerotized. Dorsal scutum ovoid in shape. Anterior margin of the carapace nearly rounded, armed with a continuous row of anvil-shaped tubercles, posterior margin slightly rounded, more quadrangular. Ocularium slightly elevated, rising from frontal margin of scutum, irregularly covered



Figures 1–7. *Starengovia quadrituberculata* sp. n. male (holotype) **1** Body, lateral view **2** Left chelicera, medial view **3** Left chelicera, ectal view **4** Basal segment of left chelicera, dorsal view **5** Left cheliceral fingers, frontal view **6** Left pedipalp, medial view **7** Left pedipalp, ectal view. Scale bars 0.5 mm (**1**); 0.25 mm (**2–7**).



Figures 8–19. *Starengovia quadrituberculata* sp. n. **8** Body, male, dorsal view **9–12** Right legs, retrolateral view **9** Leg I **10** Leg II **11** Leg III **12** Leg IV **13** Body, female, dorsal view **14** Left chelicera, female, medial view **15** Left pedipalp, female, medial view **16** Ovipositor, ventral view **17** Ovipositor, dorsal view **18** Ovipositor, lateral view **19** Ovipositor, frontal view. Scale bars 1 mm (**9–13**); 0.5 mm (**8**); 0.25 mm (**14–18**).



Figures 20–25. *Starengovia quadrituberculata* sp. n. male (holotype) **20** Penis, dorsal view **21** Penis, ventral view **22** Penis, lateral view **23** Penis tip, dorsal view **24** Penis tip, ventral view **25** Penis tip, lateral view. Scale bars 0.25 mm (**20–22**); 0.05 mm (**23–25**).

with quadrangular tubercles. Supracheliceral lamellae consisting of three small sclerite plates. Metaplethridial area and opisthosomal region (areae I–V) separated by lines of quadrangular tubercles similar to those at peripheral margins of the scutum. Areae III–IV each with a pair of low median pegs inclined posteriorly. Free tergites not visible from above.

Venter (Fig. 28). Coxae with scattered low rounded tubercles on ventral surfaces and pro-laterally and retro-laterally with a row of quadrangular tubercles. Genital operculum short, almost tongue-shaped, surface with scattered tubercles. Free sternites with few tubercles at margins.

Chelicerae (Figs 2–5). Basal segment ventrally and medially each with a rounded hump at the base (medial view, Fig. 2), and dorso-distally with a triangular apophysis distinctly surpassing front margin of basal segment, approximately as long as high (in lateral view), medially compressed and spoon-shaped (medial view, Fig. 2); apophysis medially inclined dorso-distally projecting into a pointed hook, dorsally with two long setae; the medial excavation of apophysis harbouring the secretion porefield; a few tubercles laterally and dorsally on medial part of basal segment (Figs 3–4); a multitude of minute granules on the ventro-lateral surface of basal segment (Fig. 3). The second segment with a few tubercles laterally and dorsally at base. Many long dorsal setae and rows of short setae at base of fixed finger (Fig. 2). Fingers short, with diaphanous teeth and dark subapical teeth: one dark tooth on movable finger, two dark teeth on fixed finger (Fig. 5).

Pedipalpi (Figs 6–7). Trochanters with three ventral seta-tipped tubercles. Femora and patellae with normal straight setae mainly on dorsal and lateral sides. Femora slightly swollen distally and ventrally with sparse clavate setae. Patellae ventrally slightly thickened and medially, ventrally and laterally with sparse clavate setae. Tibiae and tarsi densely covered with clavate setae all round.

Legs (Figs 9–12). Femora, patellae, and tibiae of leg I, III and IV slightly inflated. Femora, patellae, and tibiae of all legs densely covered with stiff, short bristles (Fig. 9). Pseudoarticulations of femora I–IV: 2/7/2/3; pseudoarticulations of metatarsi I–IV: 0/13/1/3. Tarsal segments I–II with two tarsomere groups: 8 (6+2), 24 (22+2); III–IV with three each: 9 (5+2+2), 9 (5+2+2).

Penis (Figs 20–25). Moderately slender; no clear distinction between truncus, glans, and stylus. Basis forming a large inflated part (occupying approximately one third of whole penis length) and deeply split into two parts each bearing one large muscle portions, basis well differentiated from rest of truncus; truncus beyond basis parallel-sided, distal portion close to glans inconspicuously curved (lateral view). Ventro-lateral side of truncus sub-distally with two broad foliate wing-like structures forming a transparent membrane, triangular, free pointed end curled to ventral side. Glans extremely short, armament of glans with pairs of short spicule-like setae; three pairs on dorsal side, two pairs more distally on both “lateral” sides, stylus short and rod-like.

Female (Figs 13–15, 29–31). In appearance and coloration similar to the male, but body much larger (Figs 13, 29). Free tergites visible from above (Fig. 13). Basal segment of chelicerae dorso-distally with a hump covered with two long setae, and



Figures 26–31. *Starengovia quadrituberculata* sp. n. Photographs of holotype male and female paratype **26** Body and parts of appendages, male, dorsal view **27** Ditto, lateral view **28** Ditto, ventral view **29** Body and parts of appendages, female, dorsal view **30** Ditto, lateral view **31** Ditto, ventral view. Scale bars 0.5 mm.

ventrally with a multitude of minute granules, similar granules medially at the base (Fig. 14). Patellae of pedipalpi with many clavate hairs (Fig. 15). Pseudoarticulations of femora I–IV: 2/7/2/3–4; pseudoarticulations of metatarsi I–IV: 1/14/2/3. Tarsal segments I–IV: 9 (7+2), 15 (13+2), 8 (4+2+2), 10 (6+2+2).

Ovipositor (Figs 16–19). Short type (Martens et al. 1981, Suzuki 1974: 88), unsegmented. The apical furca bipartite, each bearing 16 setae in three groups: six long setae at the base of furca (Fig. 18), four short ones medially at the margin of apical lobe (Fig. 19), and six long ones between former two groups (Fig. 19).

Table 1. *Starengovia quadrituberculata* sp. n. Measurements of the pedipalp and legs of the male holotype, as length/depth.

	Trochanter	Femur	Patella	Tibia	Metatarsus	Tarsus	Total
Pedipalp	0.21/0.11	0.63/0.06	0.48/0.07	0.41/0.08		0.27/0.07	2.00
Leg I	0.22/0.14	0.91/0.16	0.37/0.17	0.59/0.17	1.15/0.06	1.01/0.05	4.25
Leg II	0.22/0.14	1.85/0.09	0.50/0.13	1.28/0.10	3.29/0.06	2.17/0.05	9.31
Leg III	0.22/0.14	1.01/0.16	0.34/0.18	0.56/0.14	1.13/0.06	0.96/0.05	4.22
Leg IV	0.22/0.14	1.40/0.14	0.36/0.17	0.79/0.15	1.65/0.06	1.20/0.05	5.62

Table 2. *Starengovia quadrituberculata* sp. n. Measurements of the pedipalp and legs of the female paratype, as length/depth.

	Trochanter	Femur	Patella	Tibia	Metatarsus	Tarsus	Total
Pedipalp	0.23/0.11	0.66/0.06	0.53/0.07	0.42/0.06		0.29/0.07	2.13
Leg I	0.22/0.14	0.89/0.15	0.37/0.16	0.59/0.15	1.13/0.06	1.02/0.05	4.22
Leg II	0.22/0.14	1.82/0.09	0.53/0.13	1.22/0.10	3.26/0.06	2.13/0.05	9.18
Leg III	0.22/0.14	0.91/0.14	0.35/0.17	0.53/0.14	1.15/0.06	0.91/0.05	4.07
Leg IV	0.22/0.14	1.36/0.13	0.37/0.17	0.70/0.12	1.60/0.06	1.19/0.05	5.44

Measurements. Male holotype (female paratype): Body 1.41 (1.75) long. 0.96 (1.26) wide at the widest portion. Ocularium 0.13 (0.18) long, 0.23 (0.23) wide. Basal segment of chelicerae 0.32 (0.30) long; second segment of chelicerae 0.45 (0.54) long. Penis 0.75 long (including glans), 0.05 wide at base, alate part 0.20 wide, fork 0.39 long. Ovipositor 0.60 long. Measurements of left pedipalp and right legs as in Tables 1, 2.

Habitat. The specimens were collected by leaf litter sieving in broad-leaved forest under dense canopy at an altitude of 2142 m ASL.

Distribution. Known only from the type locality in southern Yunnan Province, China.

Discussion

The discovery of a species of the genus *Starengovia* in Yunnan comes quite unexpectedly. *Starengovia* is known from Central Asian Kyrgyzstan and Uzbekistan only by a few localized records of *S. kirgizica* Snegovaya, 2010. *Starengovia ivanloebli* Martens, 2017 is known from the Himalayas of Northwest Pakistan, disjunct by 700 km. The present record of *S. quadrituberculata* sp. n. moves the distributional limit of nemastomatines by a second species by roughly 2700 km to the Southeast to southern Yunnan Province in China. The first nemastomatine ever discovered in China is *Sinostoma yunnanicum* Martens, 2016, only 380 km to the northeast of the present record, in Yunnan as well. Both are minute species less than 2 mm in body length, difficult to discover and apparently restricted to primeval mountain forests above 2000 m.

The few records of nemastomatines in East Asia hitherto known are restricted to two genera and appear to be remarkably disjunct from the European nemastomatine

core distributional area. Though more local Asian occurrences may be discovered in the future, these are rare harvestmen and probably relicts of old lineages which do not exist in the West Palaearctic and probably never occurred there. According to only punctual, disjunct distributional areas and morphological traits Central Asian and Chinese occurrences of nemastomatines seem to represent “ancient homes” rather than “recent exiles”, i.e., geographical outliers of the main prosperous and speciose West Palaearctic radiations. This is meant in a dynamic sense – not just static as marginal occurrences.

In accordance with this hypothesis, *Starengovia* and *Sinostoma* display rather plesiomorphic genitalic characters (Martens 2016, 2017) and may be basally derived members of the nemastomatine radiation. They will probably be placed at or near the base of the still incomplete molecular genetic tree (Schönhofer and Martens 2012).

Acknowledgements

For access to rare specimens we are deeply indebted to Yannan Mu, Zhaoyi Li and Zegang Feng. This work was supported by a grant of the National Natural Science Foundation of China (No. 31471956) to CZ. JM got grants from Feldbausch Foundation and Wagner Foundation at Fachbereich Biologie of Mainz University to carry out field work in Asia. CZ acknowledges financial support from the researcher alumni network senckenberg, Frankfurt am Main, Germany (FANS). Jürgen Gruber and Christopher Taylor critically commented on an earlier version of the manuscript and gave valuable input. We heartily thank all friends, colleagues, and institutions.

References

- Gruber J (2007) Nemastomatidae Simon, 1872. In: Pinto-da-Rocha R, Machado G, Giribet G (Eds) Harvestmen: The Biology of Opiliones. Harvard University Press, Cambridge and London, 148–151.
- Martens J (2006) Weberknechte aus dem Kaukasus (Arachnida, Opiliones, Nemastomatidae). *Senckenbergiana biologica* 86:145–210.
- Martens J (2016) *Sinostoma yunnanicum*, the first nemastomatine harvestman in China (Arachnida: Opiliones: Nemastomatidae). *Zootaxa* 4126: 444–450. <https://doi.org/10.11646/zootaxa.4126.3.9>
- Martens J (2017) On *Starengovia* Snegovaya, a genus of Asian nemastomatines (Arachnida: Opiliones: Nemastomatidae). *Revue Suisse de Zoologie* 124: 187–201. <https://doi.org/10.5281/zenodo.893462>
- Martens J, Hoheisel U, Götze M (1981) Vergleichende Anatomie der Legeröhren der Opiliones als Beitrag zur Phylogenie der Ordnung (Arachnida). *Zoologische Jahrbücher. Abteilung für Ontogenie und Anatomie der Tiere* 105: 13–76.
- Schönhofer AL (2013) A taxonomic catalogue of the Dyspnoi Hansen and Sørensen, 1904 (Arachnida: Opiliones). *Zootaxa* 3679: 1–68. <https://doi.org/10.11646/zootaxa.3679.1.1>

- Schönhöfer AL, Martens J (2012) The enigmatic Alpine opilionid *Saccarella schilleri* gen. n., sp. n. (Arachnida: Nemastomatidae) – isolated systematic placement inferred from comparative genital morphology. *Organisms Diversity & Evolution* 12: 409–419. <https://doi.org/10.1007/s13127-012-0073-7>
- Shear WA, Gruber J (1983) The opilionid subfamily Ortholasmatinae (Opiliones, Troguloidea, Nemastomatidae). *American Museum Novitates* 2757:1–65.
- Simon E (1872) Notices sur les arachnides cavernicoles et hypogés. *Annales de la Société Entomologique de France* 2: 215–244.
- Snegovaya NY (2010) New harvestman genus and species from Kyrgyz Republic (Kyrgyzstan) (Arachnida: Opiliones: Nemastomatidae). *Acta Zoologica Bulgarica* 62: 351–354.
- Suzuki S (1974) The Japanese species of the genus *Sabacon* (Arachnida, Opiliones, Ischyropsalididae). *Journal of Science of the Hiroshima University* 25: 83–108.
- Zhang C, Zhang F (2013) Description of a new *Cladolasma* (Opiliones: Nemastomatidae: Ortholasmatinae) species from China. *Zootaxa* 3691: 443–452. <https://doi.org/10.11646/zootaxa.3691.4.3>
- Zhang F, Zhao LK, Zhang C (2018) *Cladolasma ailaoshan*, a new species of the genus *Cladolasma* Suzuki, 1963 from China (Opiliones: Nemastomatidae: Ortholasmatinae). *ZooKeys* 748: 11–20. <https://doi.org/10.3897/zookeys.748.23273>

Sinodraconarius gen. n., a new genus of Coelotinae spiders from Southwest China (Araneae, Agelenidae)

Bing Li¹, Zhe Zhao², Chuntian Zhang¹, Shuqiang Li²

1 College of Life Science, Shenyang Normal University, Shenyang, Liaoning 110034, China **2** Institute of Zoology, Chinese Academy of Sciences, Beijing 100101, China

Corresponding author: Chuntian Zhang (chuntianzhang@aliyun.com); Shuqiang Li (lisq@ioz.ac.cn)

Academic editor: Y. Marusik | Received 23 November 2017 | Accepted 12 May 2018 | Published 4 July 2018

<http://zoobank.org/1402C2E7-6F94-4883-8F60-E34CF9B3D348>

Citation: Li B, Zhao Z, Zhang C, Li S (2018) *Sinodraconarius* gen. n., a new genus of Coelotinae spiders from Southwest China (Araneae, Agelenidae). ZooKeys 770: 117–135. <https://doi.org/10.3897/zookeys.770.22470>

Abstract

A new genus of the subfamily Coelotinae F.O. Pickard-Cambridge, 1893, *Sinodraconarius* gen. n., with four new species, *S. cawarongensis* sp. n. (♂♀), *S. muruoensis* sp. n. (♂♀), *S. sangjiuensis* sp. n. (♂♀, type species), *S. yui* sp. n. (♂♀) and *S. patellabifidus* (Wang, 2003) comb. n., ex. *Draconarius* Ovtchinnikov, 1999 is described. The genus is restricted to Southwest China. *Sinodraconarius* gen. n. is most similar to *Draconarius* but can be distinguished by the shape of the copulatory organs. The DNA barcodes of all species were documented for future use.

Keywords

Asia, taxonomy, new combination, new species

Introduction

The spider subfamily Coelotinae (Araneae, Agelenidae) comprises 694 valid species belonging to 27 genera worldwide (World Spider Catalog 2018), of which 88% of the species are restricted to Asia, 8% to Europe and 4% to North America. So far, 339 coelotine species in 21 genera are known from China, including three genera erected in recent years: *Flexicoelotes* Chen, Li & Zhao, 2015, *Papiliocoelotes* Zhao & Li, 2016 and *Sinocoelotes* Zhao & Li, 2016.

Draconarius Ovtchinnikov, 1999, with 246 named species, is the largest genus of Coelotinae. Recent molecular studies suggested that *Draconarius* is polyphyletic and requires taxonomic rearrangements (Zhao and Li 2017). Here, we described a new genus, *Sinodraconarius* gen. n., with four new species.

Material and methods

The specimens were examined with a LEICA M205C stereomicroscope. The photographs were captured with an Olympus C7070 wide zoom digital camera (7.1 megapixels) mounted on an Olympus SZX12 dissecting microscope and an Olympus BX51 compound microscope. Photos from multiple focal planes were combined using Helicon Focus (Version 3.00) photo stacking software. Epigynes and male palps were examined after dissection from the spiders' bodies. Epigynes were cleared by boiling in a 10% potassium hydroxide (KOH) water solution before taking photos of the vulva.

All measurements were obtained using a LEICA M205C stereomicroscope and are in millimeters. Eye sizes were measured as the maximum diameter from either the dorsal or frontal views. Leg measurements are given as: total length (femur, patellatibia, metatarsus, tarsus). The male palps depicted are the left ones. The terminology used in the text and figures follows Wang (2002). Abbreviations:

Morphological characters:

A	epigynal atrium;	E	embolus;
ALE	anterior lateral eye;	EB	embolic base;
AME	anterior median eye;	FD	fertilization duct;
AME–ALE	distance between AME and ALE;	LTA	retro-lateral tibial apophysis;
AME–AME	distance between AME and AME;	MA	median apophysis;
AME–PME	distance between AME and PME;	PA	patellar apophysis;
ALE–PLE	distance between ALE and PLE;	PLE	posterior lateral eye;
C	conductor;	PME	posterior median eye;
CD	copulatory duct;	PME–PLE	distance between PME and PLE;
CDA	conductor dorsal apophysis;	PME–PME	distance between PME and PME;
CF	cymbial furrow;	R	receptacle;
CO	copulatory opening;	RTA	retroventral tibial apophysis;
		ST	subtegulum;
		T	tegulum.

DNA barcodes were obtained for future use. A partial fragment of the mitochondrial cytochrome oxidase subunit I (COI) gene was amplified and sequenced for all species, using the following primers: Forward: LCO1490-oono

Table 1. Voucher specimen information.

Species	GenBank accession number	Sequence length	Collection localities
<i>S. cawarongensis</i> sp. n.	KY778914	1194bp	Zhowagoin Township, Zayü, Tibet, China
<i>S. muruoensis</i> sp. n.	KY778913	1194bp	Zhowagoin Township, Zayü, Tibet, China
<i>S. patellabifidus</i>	KY778910	1194bp	Liuku Township, Lushui, Yunnan, China
<i>S. sangjiuensis</i> sp. n.	KY778915	1194bp	Zhowagoin Township, Zayü, Tibet, China
<i>S. yui</i> sp. n.	KY778908	1194bp	Segula Mountain, Nyingchi, Tibet, China

(5'-CWACAAAYCATARRGATATTGG-3') and Reverse: C1-N-2776 (5'-GGA-TAATCAGAATANCGNCGAGG-3'). For additional information on extraction, amplification and sequencing procedures, see Zhao and Li (2017). All sequences were analyzed using BLAST and are deposited in GenBank. The accession numbers are provided in Table 1.

All of the specimens (including molecular vouchers) are deposited in the Institute of Zoology, Chinese Academy of Sciences (IZCAS), Beijing, China.

Taxonomy

Family Agelenidae C.L. Koch, 1837

Subfamily Coelotinae F.O. Pickard-Cambridge, 1893

Genus *Sinodraconarius* Z. Zhao & S. Li, gen. n.

<http://zoobank.org/8FD70171-B9AF-49D7-967B-74B3AEB9945E>

Type species. *Sinodraconarius sangjiuensis* Zhao & Li, sp. n.

Etymology. The generic name is derived from its similarity to *Draconarius* and the Latin adjective *Sino-* for Chinese referring to the main distribution region of the genus. The gender is masculine.

Diagnosis. The males of *Sinodraconarius* gen. n. are similar to those of *Draconarius* by having a patellar apophysis, two tibial apophyses (RTA and LTA) and a long median apophysis, but can be distinguished by the short cymbial furrow, less than 1/2 length of cymbium *vs.* long and generally more than 1/2 length of the cymbium in *Draconarius*; patellar apophysis bifurcate *vs.* not bifurcate in *Draconarius*. The females of *Sinodraconarius* gen. n. are similar to those of *Draconarius* by having a small epigynal atrium, with epigynal hoods located laterally, and the copulatory openings located centrally on the epigyne plate, but can be distinguished by lacking epigynal teeth; receptacles simple.

Description. Small to very large sized, with a total length of 6.90–17.60; body brownish to brown, with black setae. Carapace nearly pear-shaped, with longitudinal

fovea and radial grooves; sternum brownish, heart-shaped. Abdomen nearly oval, grey to dark grey, with 4–5 grey chevron-like markings. Chelicerae with three promarginal and two retromarginal teeth. Leg formula (4 > 1 > 2 > 3). Male palp with one bifurcate patellar apophysis; two tibial apophyses (RTA and LTA), RTA extending beyond the tibia; cymbial furrow short, less than 1/2 length of cymbium; conductor short, with dorsal conductor apophysis; the apex of conductor with small basal lamella; embolus short; median apophysis long, finger-like; tegulum broad. Tibia strongly bent and dorsal part of tibia and patella bent almost to a right angle, ventral part of tibia at 45° angle. Epigyne: with septum; teeth lacking; atrium small, length of atrium two times longer than width, heart-shaped; epigynal hoods located laterally; copulatory openings located centrally on epigynal plate; copulatory ducts short, extending mesad of receptacles; receptacles broad, widely separated.

Comments. In addition to morphological study, we analyzed the relationships of coelotine spiders using eight genes from 286 species in 19 genera (Zhao and Li 2017). The molecular topologies inferred by three different approaches all supported *Sinodraconarius* gen. n. as a monophyletic group that is closely related to *Draconarius*. For details, please see SD001, SD002, SD019, SD028 and ZZ300 (Southern *Coelotes* groups) in Figure 3 and supplementary figures S4–S6 of Zhao and Li (2017).

Distribution. So far, the genus is known from Tibet and Yunnan, China (Fig. 11).

***Sinodraconarius sangjiuensis* Z. Zhao & S. Li, sp. n.**

<http://zoobank.org/50956D57-E022-4FBB-8BE3-F73C258B3441>

Figs 1–2, 11

Type material. Holotype ♂ (IZCAS): China: Tibet: Zayü: Zhougoin Township, Sangjiu Village, Mingqi group, 16 km SE of Yakou, N28.72276°, E97.70598°, 3698 m, 1.IX.2014, Jincheng Liu leg. **Paratypes:** 3♂♂, 3♀♀ (IZCAS): same data as holotype; 3♂♂ (IZCAS): China: Tibet: Zayü: Zhougoin Township, Xiongjiu Village, N28.60677°, E97.28166°, 1938 m, 29.VIII.2014, Jincheng Liu leg.

Etymology. The specific name refers to the type locality, Sangjiu Village; adjective.

Diagnosis. The males can be easily distinguished from other *Sinodraconarius* gen. n. species by the patellar apophysis longer than the tibia *vs.* shorter than the tibia in other species (Fig. 1A–C). The females can be easily distinguished from other *Sinodraconarius* gen. n. species by the epigynal hoods in the center of the epigynal plate *vs.* anterolaterally in other species (Fig. 2A–B).

Description. Male (holotype). Total length 12.25. Carapace 5.75 long, 4.50 wide. Abdomen 6.50 long, 4.00 wide. Eye sizes and interdistances: AME 0.15, ALE 0.23, PME 0.20, PLE 0.23; AME–AME 0.10, AME–ALE 0.15, AME–PME 0.23, ALE–PLE 0, PME–PME 0.18, PME–PLE 0.20. Leg measurements: I 23.72 (7.69, 7.05, 5.77, 3.21); II 22.43 (7.69, 6.41, 5.45, 2.88); III 20.19 (6.73, 5.77, 5.13, 2.56); IV 24.67 (8.01, 7.05, 6.73, 2.88). Palp: patella longer than tibia; patellar apophysis

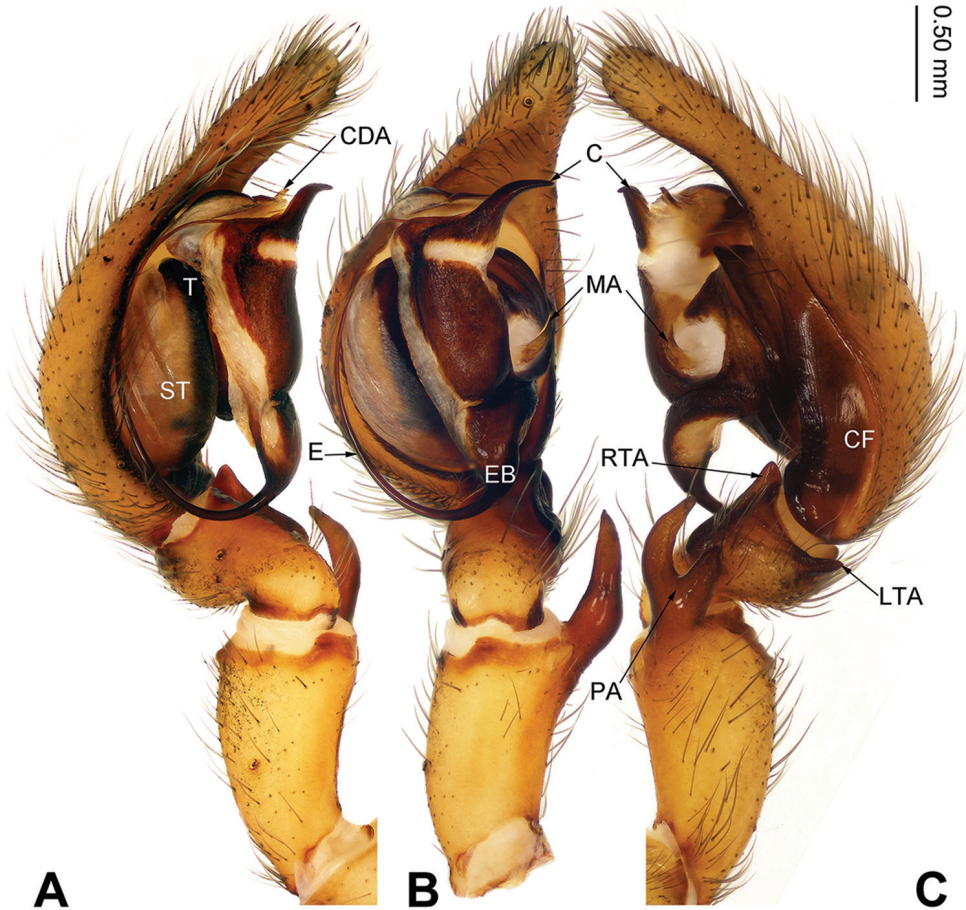


Figure 1. Left male palp of *Sinodraconarius sangjiuensis* sp. n., holotype. **A** Prolateral view **B** Ventral view **C** Retrolateral view. Scale bar: equal for **A, B, C**.

thin and long, about three times longer than wide, with two branches and ventral branch larger than dorsal one; anterior 1/3 of RTA extending beyond the tibia, apex of RTA slightly bent; LTA about half of the RTA length; conductor short, apex of conductor pointed and bent retrolaterally; apex of median apophysis pointed; dorsal conductor apophysis broad, the visible part (between conductor and tegulum) subtriangular; embolus beginning at 5:30 o'clock position (Fig. 1A–C).

Female (paratype). Total length 12.50. Carapace 6.00 long, 4.25 wide. Abdomen 6.50 long, 4.25 wide. Eye sizes and interdistances: AME 0.15, ALE 0.25, PME 0.20, PLE 0.26; AME–AME 0.10, AME–ALE 0.10, AME–PME 0.25, ALE–PLE 0, PME–PME 0.15, PME–PLE 0.30. Leg measurements: I 18.59 (6.41, 6.09, 3.84, 2.25); II 18.27 (6.41, 5.77, 3.84, 2.25); III 17.45 (6.09, 5.27, 3.84, 2.25); IV 21.15 (6.41, 6.41,

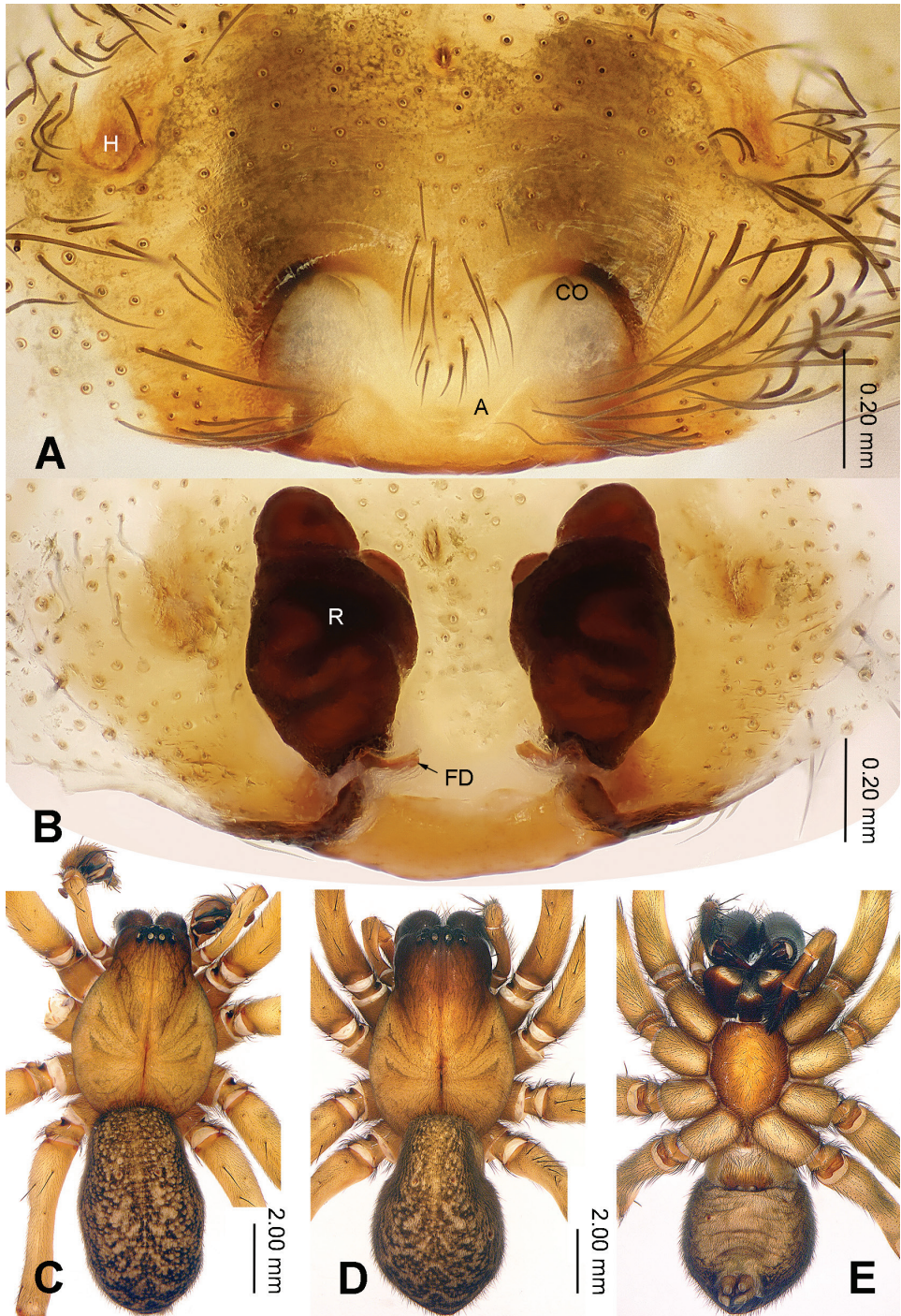


Figure 2. Epigyne and habitus of *Sinodraconarius sangjiuensis* sp. n. **A** Epigyne, ventral **B** Vulva, dorsal **C** Male habitus, dorsal **D** Female habitus, dorsal **E** Female habitus, ventral. Scale bar equal for **D** and **E**.

5.45, 2.88). Epigyne: apex of the V-shaped septum tapering; atrium two times longer than wide, occupying approx. 1/8 of epigyne plate; copulatory ducts hidden by receptacles in ventral view, hidden by epigyne in dorsal view; receptacles broad and separated by 1/2 width of receptacle; head of receptacles located anteriorly, broad and short, 1/4 length and 1/6 width of receptacles (Fig. 2A–B).

Variation. Total length of males 9.94–12.25 (n = 7) and of females 11.22–16.70 (n = 3).

Distribution. Known only from Zayü, Tibet (Fig. 11).

***Sinodraconarius cawarongensis* Z. Zhao & S. Li, sp. n.**

<http://zoobank.org/6A67E4D6-67A1-41BC-A22A-03D82C14E98F>

Figs 3–4, 11

Type material. Holotype ♂ (IZCAS): China: Tibet: Zayü: Cawarong Township, 3.5 km E of Jumuchang, N28.55227°, E98.19554°, 3145 m, 7.IX.2014, Jincheng Liu leg.

Paratypes: 13♂♂, 4♀♀ (IZCAS): same data as holotype; 9♂♂, 1♀ (IZCAS): China: Tibet: Zayü: Zhouwagoin Township, Ridong Village, N28.49183°, E98.11320°, 3495 m, 4.IX.2014, Jincheng Liu; 6♂♂, 2♀♀ (IZCAS): China: Tibet: Zayü: Zhouwagoin Township, 6 km N of Muruo Village, N28.59332°, E98.02774°, 3955 m, 5.IX.2014, Jincheng Liu leg.

Etymology. The specific name refers to the type locality, Cawarong Township; adjective.

Diagnosis. The males are similar to *S. patellabifidus* by having an indistinct LTA and a long median apophysis but can be differentiated by the branches of the patellar apophysis, with the ventral branch larger than the dorsal branch in retrolateral view *vs.* the ventral branch equal to the dorsal branch in *S. patellabifidus* (Figs 3A–C, 7A–C). The females can be differentiated from *S. sangjiuensis* sp. n. by having the head of receptacles located anteriorly *vs.* mediolaterally in *S. sangjiuensis* sp. n. and the septum indistinct (apex of the septum is tapering in *S. sangjiuensis* sp. n.) (Figs 2A–B, 4A–B, 8A–B).

Description. Male (holotype). Total length 8.45. Carapace 4.50 long, 3.35 wide. Abdomen 3.95 long, 2.65 wide. Eye sizes and interdistances: AME 0.12, ALE 0.18, PME 0.15, PLE 0.16; AME–AME 0.09, AME–ALE 0.05, AME–PME 0.15, ALE–PLE 0, PME–PME 0.13, PME–PLE 0.15. Leg measurements: I 14.86 (5.25, 4.81, 2.88, 1.92); II 13.99 (5.25, 4.25, 2.88, 1.61); III 13.73 (4.75, 3.85, 3.21, 1.92); IV 16.28 (5.45, 4.49, 4.10, 2.24). Palp: with one crescent-like bifurcate patellar apophysis, ventral branch is larger than dorsal branch of patellar apophysis; anterior 1/5 of RTA extending beyond the tibia; LTA indistinct; cymbial furrow less than 1/3 of cymbium length; apex of conductor pointed and bent retrolaterally; median apophysis finger-like, covered in short hairs; dorsal conductor apophysis broad, the visible part (between conductor and tegulum) subtriangular; embolus broad, beginning at position 8:30 o'clock (Fig. 3A–C).

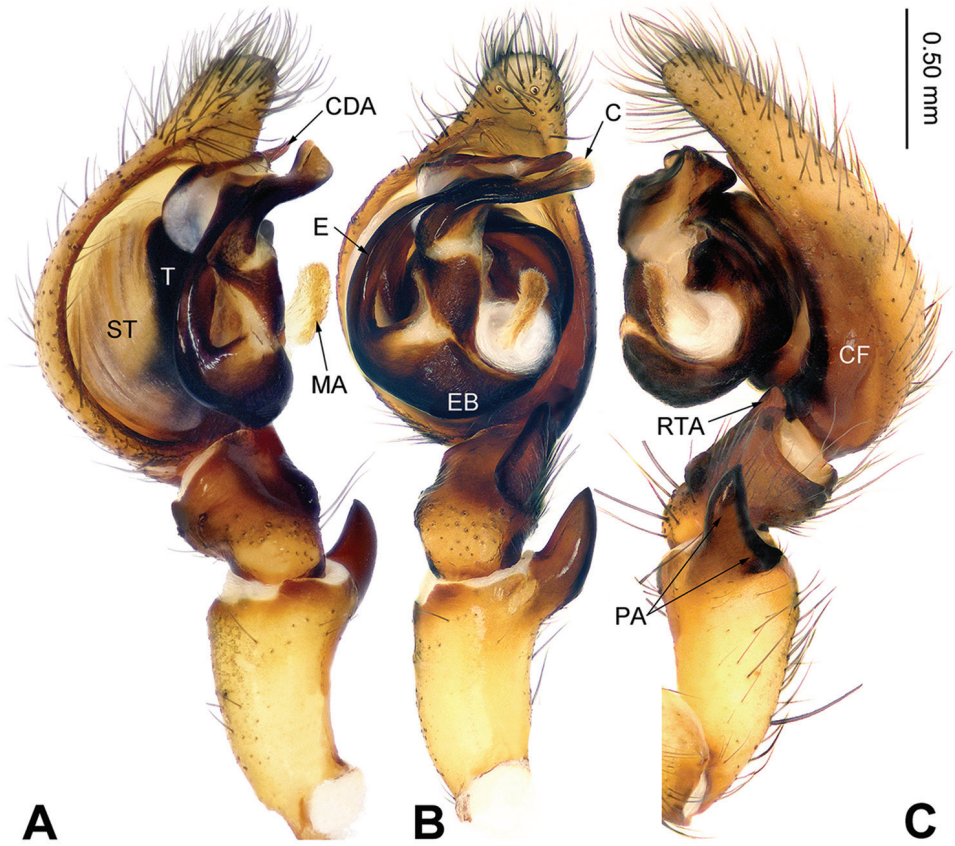


Figure 3. Left male palp of *Simodraconarius cawarongensis* sp. n., holotype. **A** Prolateral view **B** Ventral view **C** Retrolateral view. Scale bar equal for **A, B, C**.

Female (paratype). Total length 6.90. Carapace 3.40 long, 2.30 wide. Abdomen 3.50 long, 2.50 wide. Eye sizes and interdistances: AME 0.09, ALE 0.16, PME 0.14, PLE 0.15; AME–AME 0.08, AME–ALE 0.05, AME–PME 0.18, ALE–PLE 0, PME–PME 0.13, PME–PLE 0.14. Leg measurements: I 8.68 (3.30, 2.75, 1.66, 0.97); II 8.16 (3.05, 2.49, 1.66, 0.96); III 7.98 (3.15, 2.24, 1.61, 0.98); IV 9.82 (3.75, 2.75, 2.11, 1.21). Epigyne: rectangular; septum indistinct; hoods located anterolaterally on the plate; atrium 3 times longer than wide, anterior part slightly wider than posterior part, occupying about 1/8 of epigynal plate; receptacles broad, separated by a width of a receptacle; the head of receptacles located anteriorly (Fig. 4A–B).

Variation. Total length of males (n = 29) 7.69–10.26 and of females (n = 7) 6.90–8.34.

Distribution. Known only from Zayü, Tibet (Fig. 11).

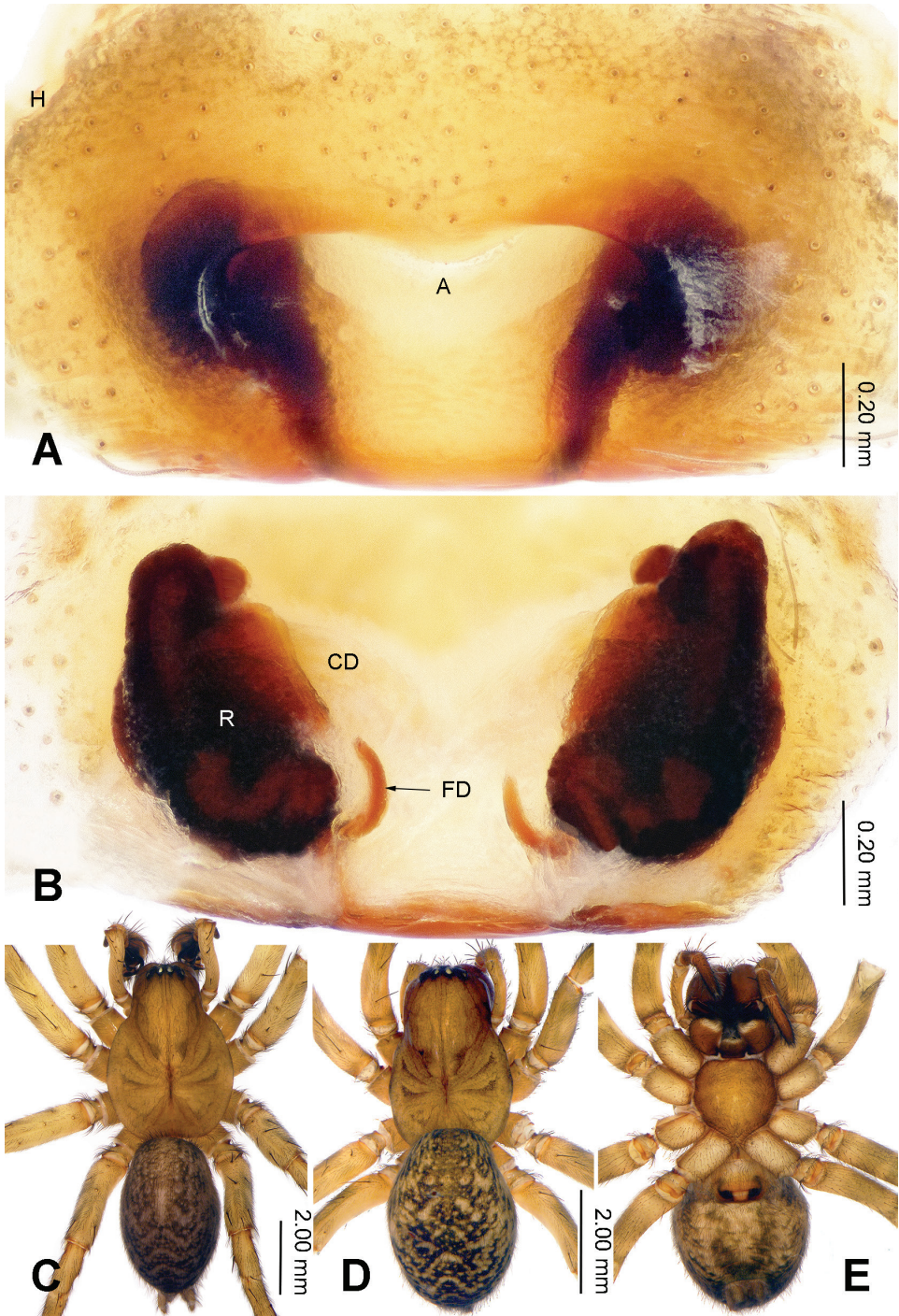


Figure 4. Epigyne and habitus of *Sinodraconarius cawarongensis* sp. n. **A** Epigyne, ventral **B** Vulva, dorsal **C** Male habitus, dorsal **D** Female habitus, dorsal **E** Female habitus, ventral. Scale bar equal for **D** and **E**.

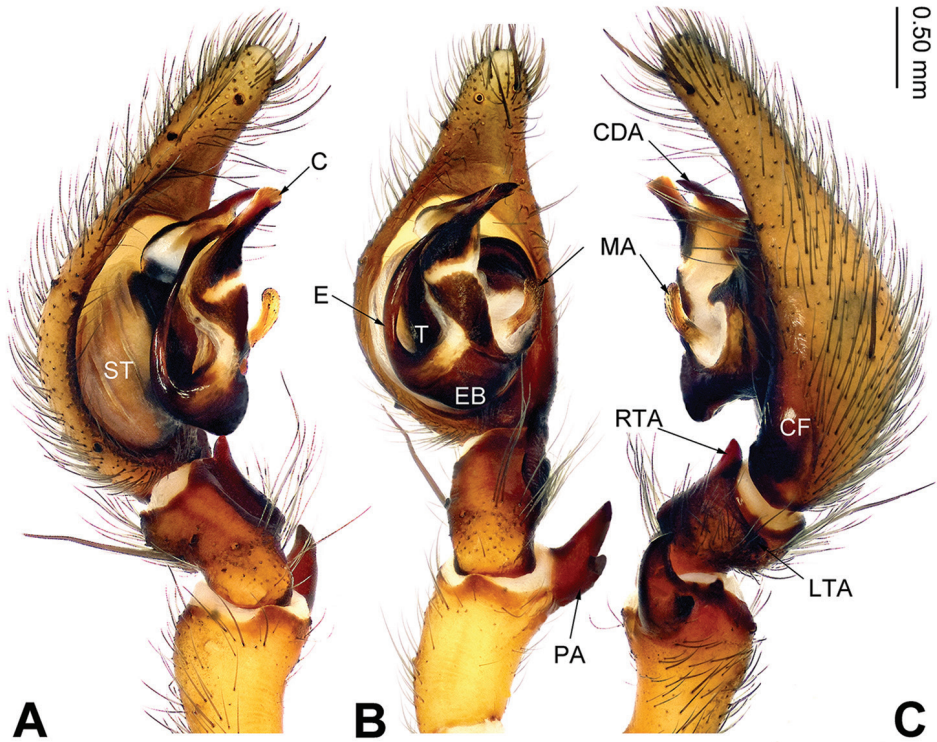


Figure 5. Left male palp of *Sinodraconarius muruoensis* sp. n., holotype. **A** Prolateral view **B** Ventral view **C** Retrolateral view. Scale bar equal for **A, B, C**.

***Sinodraconarius muruoensis* Z. Zhao & S. Li, sp. n.**

<http://zoobank.org/DBBFF4FB-ECD3-40E6-8BAC-663C0342FC89>

Figs 5–6, 11

Type material. Holotype ♂ (IZCAS): China: Tibet: Zayü: Zhougoin Township, Muruo Village, Gaoshan Mountain pasture, N28.62049°, E98.05035°, 4347 m, 5.IX.2014, Jincheng Liu leg. **Paratypes:** 5♂♂, 3♀♀ (IZCAS): same data as holotype; 1♂, 5♀♀ (IZCAS): China: Tibet: Zayü: Zhougoin Township, Muruo Village, Qimala Yakou, N28.62049°, E98.05035°, 4657 m, 2.IX.2014, Jincheng Liu leg.

Etymology. The specific name refers to the type locality, Muruo Village; adjective.

Diagnosis. The males of the new species are similar to these of *S. sangjiuensis* sp. n. by having a ventral branch of the patellar apophysis that is larger than the dorsal branch but can be easily distinguished from *S. sangjiuensis* sp. n. by the apex of conductor being straight *vs.* bent in *S. sangjiuensis* sp. n. (Figs 1A–C, 5A–C). The females of the new species are similar to *S. sangjiuensis* sp. n. by the apex of septum tapering but can be easily distinguished from by having the hoods and the head of the receptacles located anteriorly rather than medially (Figs 2A–B, 6A–B).

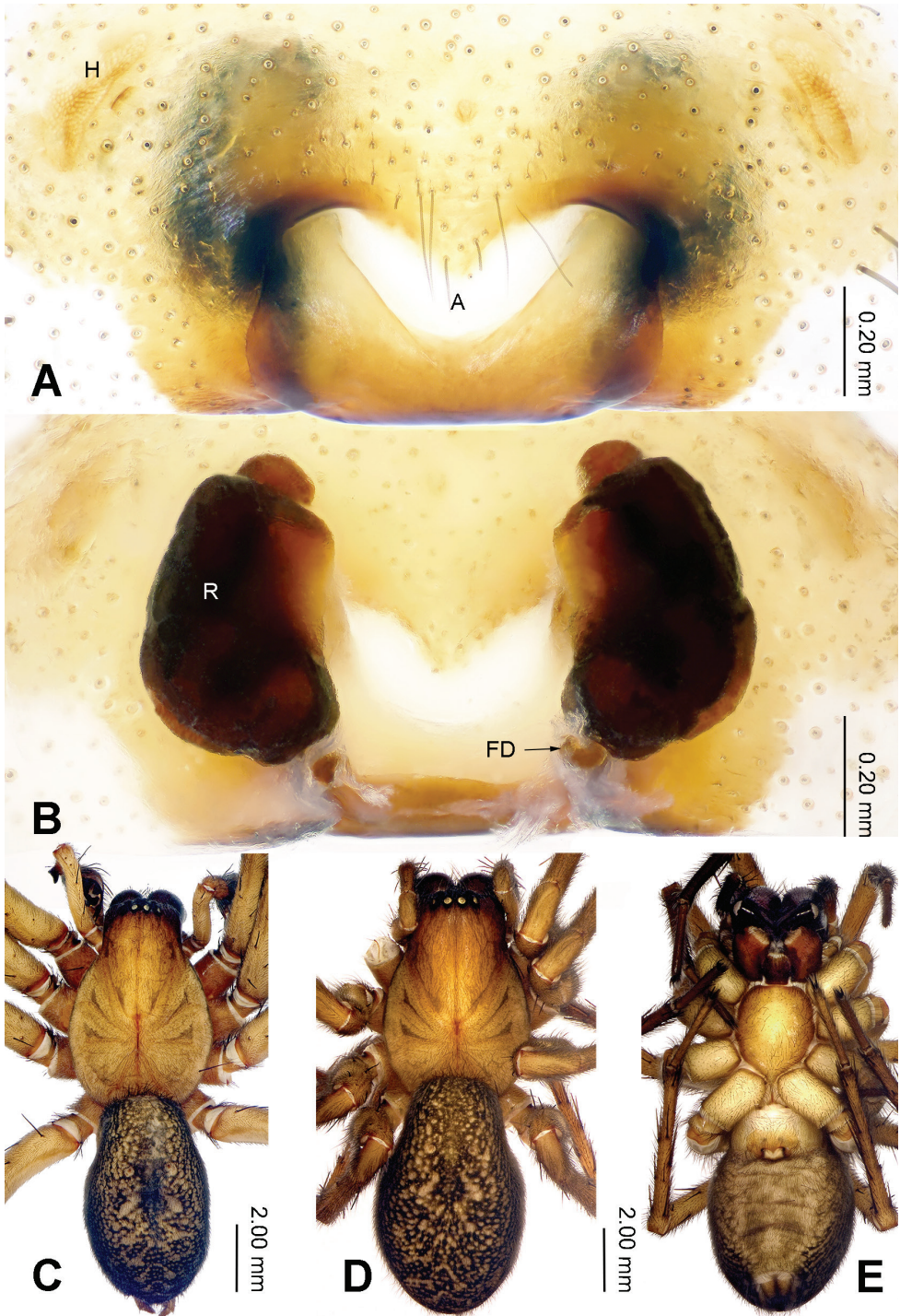


Figure 6. Epigyne and habitus of *Sinodraconarius muruoensis* sp. n. **A** Epigyne, ventral **B** Vulva, dorsal **C** Male habitus, dorsal **D** Female habitus, dorsal **E** Female habitus, ventral. Scale bar equal for **D** and **E**.

Description. Male (holotype). Total length 13.50. Carapace 6.50 long, 4.50 wide. Abdomen 7.00 long, 4.00 wide. Eye sizes and interdistances: AME 0.10, ALE 0.23, PME 0.20, PLE 0.25; AME–AME 0.13, AME–ALE 0.15, AME–PME 0.30, ALE–PLE 0, PME–PME 0.20, PME–PLE 0.15. Leg measurements: I 27.84 (8.64, 8.63, 6.73, 3.84); II 27.21 (8.63, 8.65, 6.41, 3.52); III 24.99 (8.01, 7.05, 6.41, 3.52); IV 29.48 (9.62, 8.02, 8.01, 3.83). Palp: with one bifurcate patellar apophysis (ventral branch of patellar apophysis larger than dorsal one) and one small apophysis; LTA indistinct; cymbial furrow short, about 1/5 of the of cymbial length; conductor short, extending anteriorly, the apex of conductor pointed and bending retro-anteriorly; median finger-like; dorsal the visible part of conductor apophysis (between conductor and regulum) subtriangular, shorter than conductor; embolus beginning at position 7:30 o'clock (Fig. 5A–C).

Female (paratype). Total length 11.00. Carapace 5.00 long, 4.00 wide. Abdomen 6.00 long, 4.00 wide. Eye sizes and interdistances: AME 0.15, ALE 0.22, PME 0.20, PLE 0.24; AME–AME 0.10, AME–ALE 0.10, AME–PME 0.15, ALE–PLE 0, PME–PME 0.15, PME–PLE 0.25. Leg measurements: I 16.88 (6.08, 5.44, 3.12, 2.24); II 15.69 (6.08, 4.48, 3.21, 1.92); III 15.40 (5.77, 4.49, 3.23, 1.91); IV 18.58 (6.73, 5.12, 4.81, 1.92). Epigyne: with V-shaped septum, apex of septum tapering; hoods located laterally; atrium two times wider than long, occupying approx. 1/7 of epigynal plate; receptacles separated by the width of a receptacle; the head of the receptacles broad, short, located anteriorly (Fig. 6A–B).

Variation. Total length of males (n = 7) 11.86–17.60 and of females (n = 8) 6.90–11.00.

Distribution. Known only from Zayü, Tibet (Fig. 11).

***Sinodraconarius patellabifidus* (Wang, 2003), comb. n.**

Figs 7–8, 11

Draconarius patellabifidus Wang 2003: 542, fig. 49A–D (♂♀); Wang et al. 2010: 81, figs 331–351 (♂♀); Zhu et al. 2017: 338, fig. 209A–D (♂♀).

Material examined. 2♀♀ (IZCAS): China: Yunnan Province: Nujiang Lisu Autonomous Prefecture: Lushui County, Liuku Township, N25.80797°, E98.84226°, 1220 m, 18.IX.2014, Jincheng Liu leg.; 1♂, 1♀ (IZCAS): China: Yunnan Province: Nujiang Lisu Autonomous Prefecture: Lushui County, Luzhang Township, Fengxue Yakou, N25.97244°, E98.68376°, 3150 m, 19.IX.2014, Jincheng Liu leg.

Diagnosis. The males can be differentiated from *S. sangjiuensis* sp. n. by the ventral branch of the patellar apophysis which is the same length as the dorsal branch *vs.* larger than dorsal one in *S. sangjiuensis* sp. n. (Figs 1A–C, 7A–C). The females can be differentiated from *S. sangjiuensis* sp. n. by the head of the receptacles located anteriorly *vs.* mediolaterally in *S. sangjiuensis* sp. n.; septum indistinct (apex of the septum is tapering in *S. sangjiuensis* sp. n.) (Figs 2A–B, 8A–B).

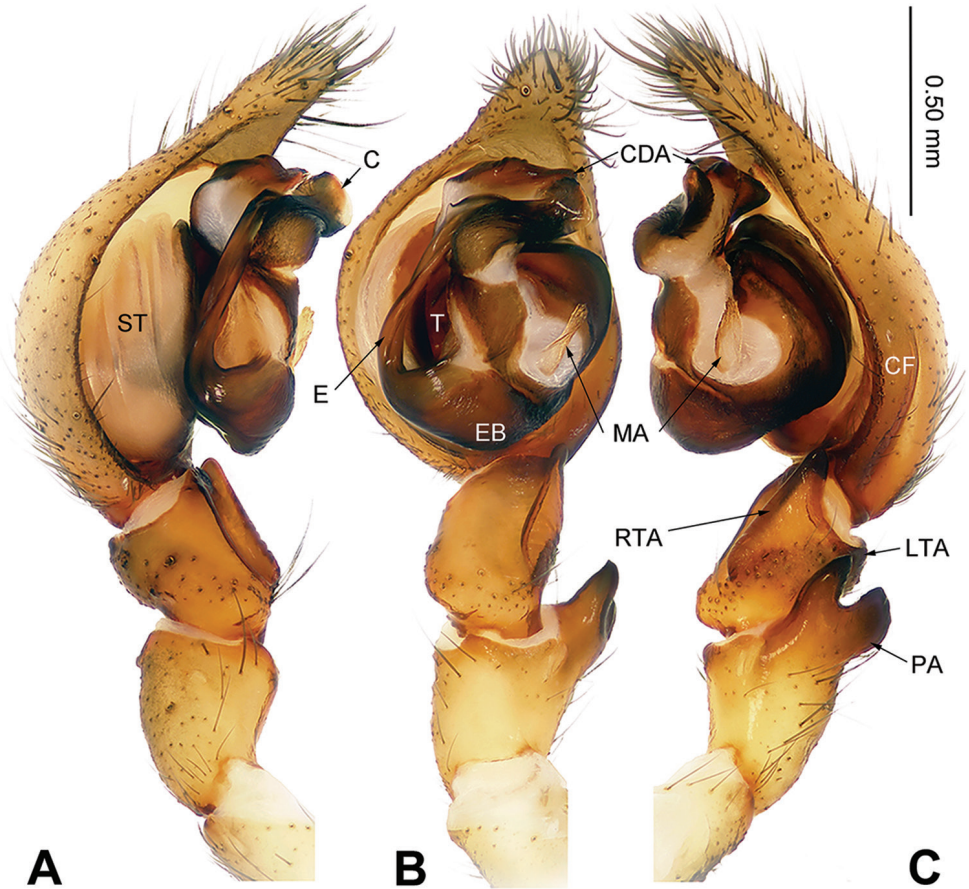


Figure 7. Left male palp of *Sinodraconarius patellabifidus* **A** Prolateral view **B** Ventral view **C** Retrolateral view. Scale bar equal for **A, B, C**.

Description. Described by Wang (2003).

Variation. Total length of females (n = 3) 8.75–11.80.

Distribution. Known only from Yunnan (Fig. 11; Wang 2003: map 17; Wang et al. 2010: 545).

***Sinodraconarius yui* Z. Zhao & S. Li, sp. n.**

<http://zoobank.org/1BB98FE5-7F5A-4CA3-8DDF-1D1C79E52CD8>

Figs 9–11

Coelotes himalayaensis Hu 2001: 134, fig. 45.3–4 (♂ only, ♀ mismatched).

Draconarius himalayaensis Wang 2003: 534 (♂ only, ♀ mismatched); Zhu et al. 2017: 289, fig. 166C–D (♂ only, ♀ mismatched)

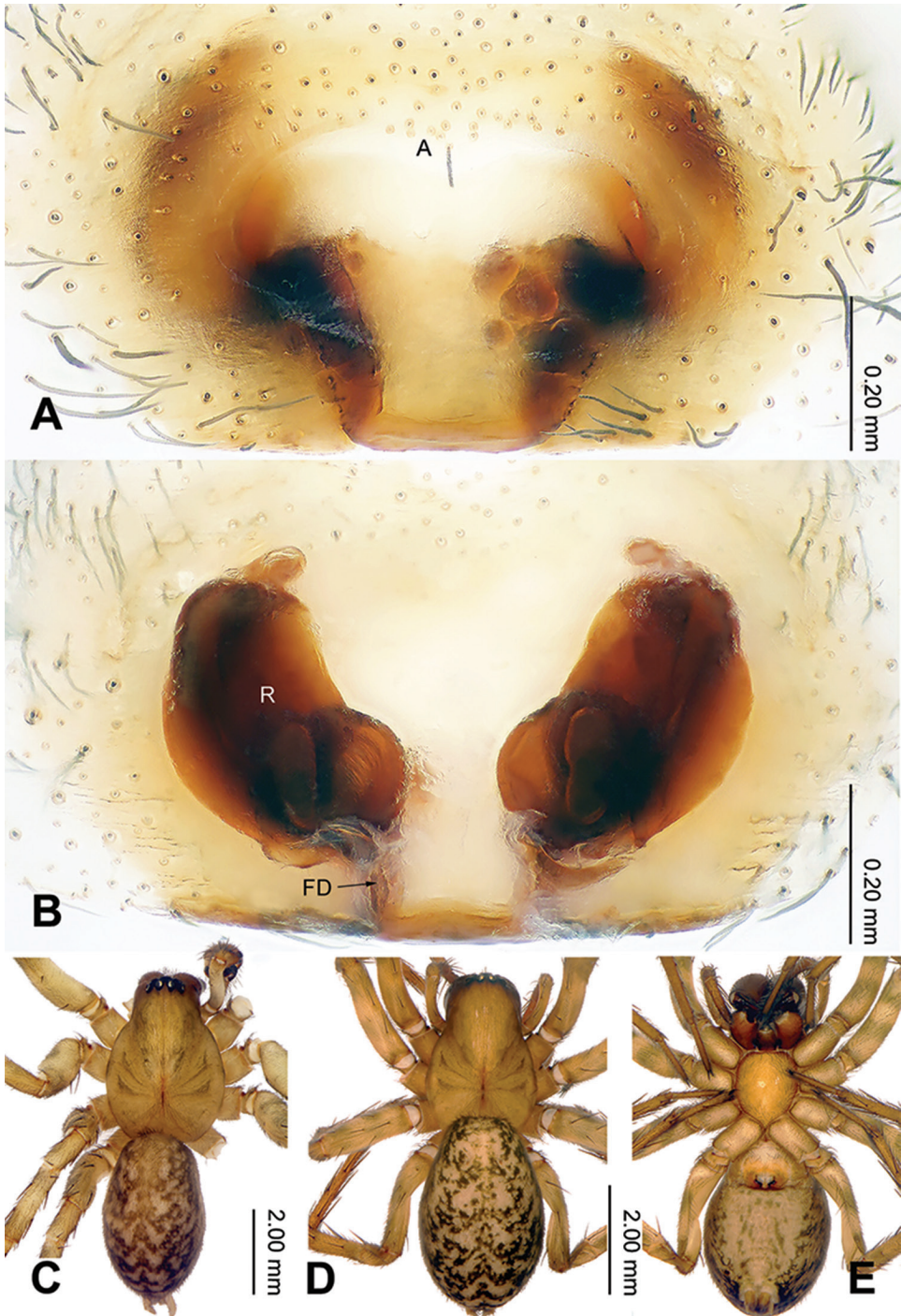


Figure 8. Epigyne and habitus of *Sinodraconarius patellabifidus* **A** Epigyne, ventral **B** Vulva, dorsal **C** Male habitus, dorsal **D** Female habitus, dorsal **E** Female habitus, ventral. Scale bar equal for **D** and **E**.

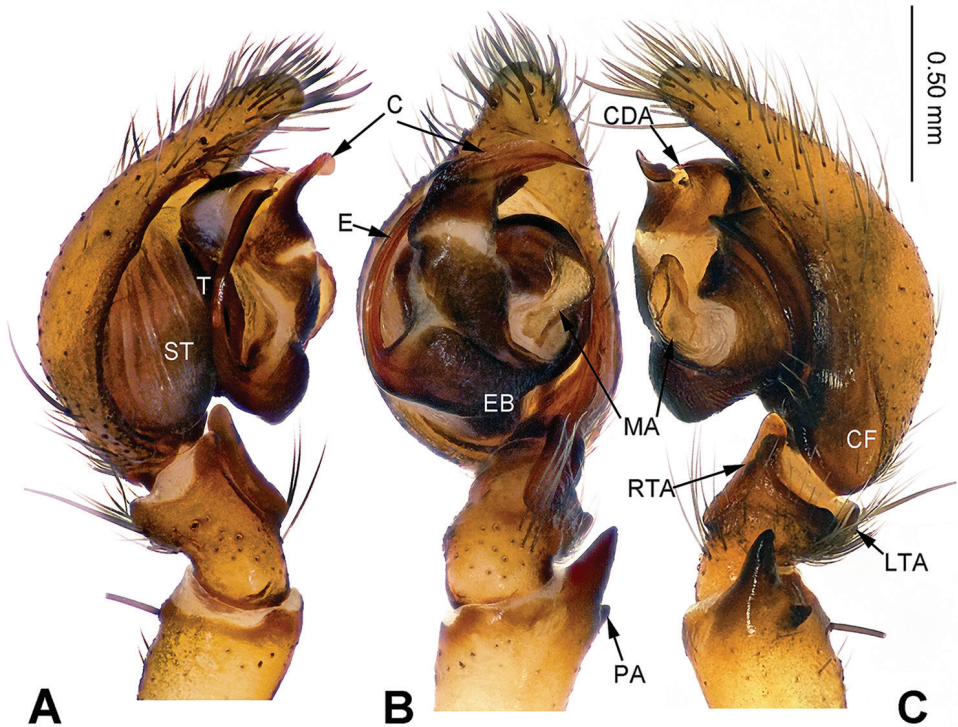


Figure 9. Left male palp of *Sinodraconarius yui* sp. n., holotype. **A** Prolateral view **B** Ventral view **C** Retrolateral view. Scale bar equal for **A, B, C**.

Type material. Holotype ♂ (IZCAS): China: Tibet: Nyingchi: Segula Mountain, N29.605017°, E94.609117°, 4184 ± 4 m, 11.X.2010, Hao Yu leg. **Paratypes:** 2♂♂ (IZCAS): same data as holotype; 1♀ (IZCAS): China: Tibet: Nyingchi: Positive face of Segula Mountain, N29.607583°, E94.608767°, 4190 ± 13 m, 12.VIII.2010, Hao Yu leg.

Etymology. The specific name is after Hao Yu, the collector of specimens used in this study; noun (name) in genitive case.

Diagnosis. The males are similar to these of *S. sangjiuensis* sp. n. by the ventral branch of the patellar apophysis larger than dorsal one and the apex of the conductor pointed and bent retrolaterally, but can be easily distinguished from *S. sangjiuensis* sp. n. by the short palp (Figs 1A–C, 9A–C). The females are similar to *S. sangjiuensis* sp. n. by having the apex of the septum tapering but can be easily distinguished from *S. sangjiuensis* sp. n. by the epigynal hoods located anterolaterally *vs.* mediolaterally in *S. sangjiuensis* sp. n. (Figs 2A–B, 10A–B).

Description. Male (holotype). Total length 7.59. Carapace 4.00 long, 2.60 wide. Abdomen 3.59 long, 2.56 wide. Eye sizes and interdistances: AME 0.09, ALE 0.20, PME 0.14, PLE 0.19; AME–AME 0.08, AME–ALE 0.05, AME–PME 0.16, ALE–PLE 0, PME–PME 0.09, PME–PLE 0.13. Leg measurements: I 12.15 (4.06, 4.00, 2.68, 1.41); II 10.22 (3.44, 3.50, 2.03, 1.25); III 9.99 (3.28, 3.00, 2.40, 1.31); IV

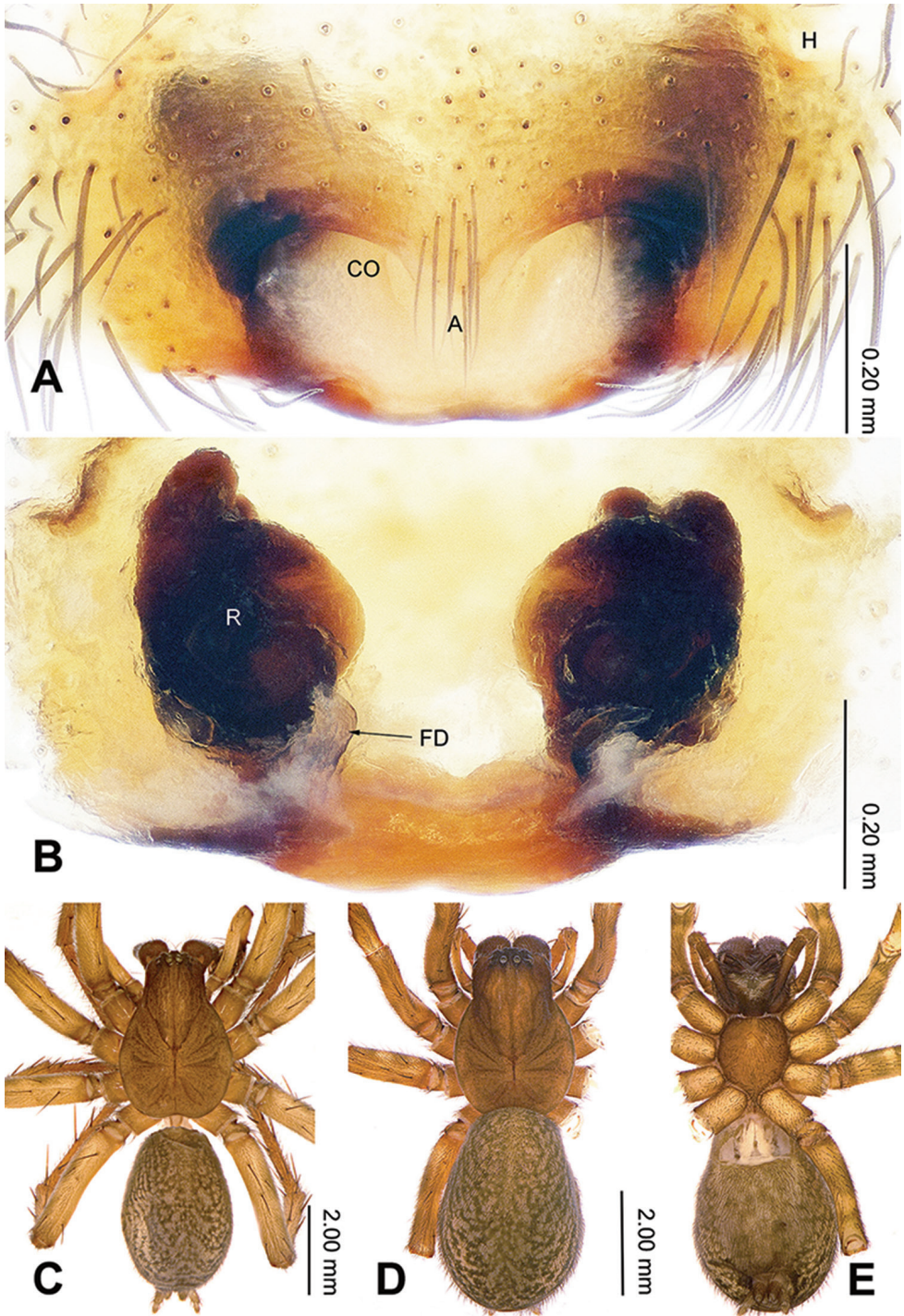


Figure 10. Epigyne and habitus of *Sinodraconarius yui* sp. n. **A** Epigyne, ventral **B** Vulva, dorsal **C** Male habitus, dorsal **D** Female habitus, dorsal **E** Female habitus, ventral. Scale bar equal for **D** and **E**.

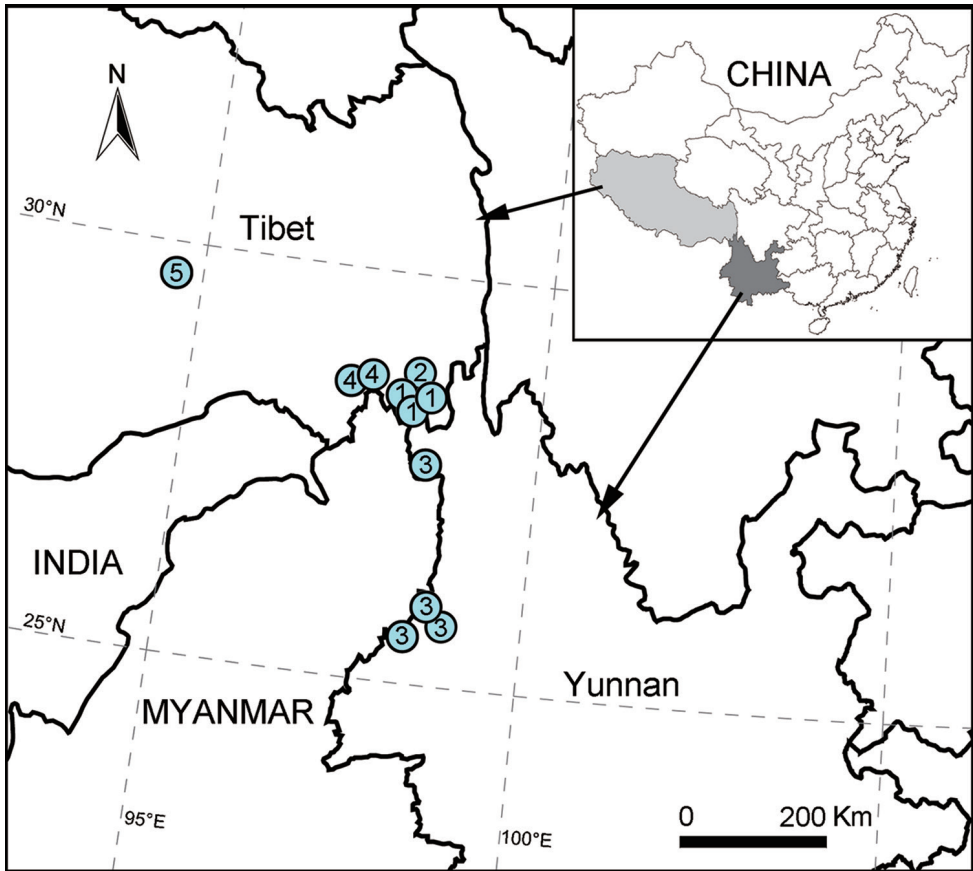


Figure 11. Localities of *Sinodraconarius* species in the Southwest China. 1 *S. cawarongensis* sp. n. 2 *S. muruoensis* sp. n. 3 *S. patellabifidus* 4 *S. sangjiuensis* sp. n. 5 *S. yui* sp. n.

12.82 (4.06, 3.80, 3.40, 1.56). Palp: ventral branch of patellar apophysis larger than dorsal one; anterior 1/5 part of RTA extending beyond the tibia; LTA obvious; cymbial furrow less than 1/4 of cymbium length; the apex of conductor concave and spiral; median apophysis conspicuous, finger-like, the apex of the median apophysis expanded and open; dorsal conductor apophysis broad, the visible part (between conductor and regulum) hidden by conductor in ventral view; embolus beginning at position 10 o'clock (Fig. 9A–C).

Female (paratype). Total length 7.89. Carapace 3.40 long, 2.40 wide. Abdomen 4.49 long, 2.40 wide. Eye sizes and interdistances: AME 0.10, ALE 0.18, PME 0.15, PLE 0.15; AME–AME 0.11, AME–ALE 0.06, AME–PME 0.15, ALE–PLE 0, PME–PME 0.10, PME–PLE 0.15. Leg measurements: I 9.17 (3.58, 2.88, 1.75, 0.96); II 8.66 (3.07, 2.88, 1.75, 0.96); III 8.47 (3.20, 2.56, 1.75, 0.96); IV 11.05 (3.59, 3.52, 2.50, 1.44). Epigyne: apex of the V-shaped septum tapering; hoods located laterally; atrium two times wider than long, occupying approx. 1/4 of epigynal plate; receptacles

spaced by the width of a receptacle; the head of the receptacles broad and short, located anteriorly (Fig. 10A–B).

Comments. The male of the new species was first described by Hu (2001) as the allotype of *Coelotes himalayaensis* and later transferred from *Coelotes* to *Draconarius* by Wang (2003). However, we found that the male and female of *D. himalayaensis* were mismatched. Therefore, the male is established as a new species here, and both sexes are described.

Variation. Total length of males (n = 3) 7.05–7.59.

Distribution. Known only from Nyingchi, Tibet (Fig. 11).

Acknowledgements

The manuscript benefitted greatly from comments by Yuri M. Marusik, Yanfeng Tong, Mykola Kovblyuk and Mikhail Omelko. Sarah Crews kindly checked English. Xiaoqing Zhang and Francesco Ballarin checked an early version of the manuscript. This study was supported by the National Natural Sciences Foundation of China (NSFC) to Zhe Zhao (NSFC-31772418), Chuntian Zhang (NSFC-31750002) and Shuqiang Li (NSFC-31530067, 31471960).

References

- Chen L, Li S, Zhao Z (2015) A new genus of Coelotinae (Araneae, Agelenidae) from southern China. *ZooKeys* 541: 41–56. <https://doi.org/10.3897/zookeys.541.6678>
- Chen L, Zhao Z, Li S (2016) *Sinocoelotes* gen. n., a new genus of the subfamily Coelotinae (Araneae, Agelenidae) from Southeast Asia. *ZooKeys* 614: 51–86. <https://doi.org/10.3897/zookeys.614.8663>
- Hu JL (2001) Spiders in Qinghai-Tibet Plateau of China. Henan Science and Technology Publishing House, 658 pp.
- Koch CL (1837) Übersicht des Arachnidensystems. Nürnberg, Heft 1, 1–39. <https://doi.org/10.5962/bhl.title.39561>
- Ovtchinnikov SV (1999) On the supraspecific systematics of the subfamily Coelotinae (Araneae, Amaurobiidae) in the former USSR fauna. *Tethys Entomological Research* 1: 63–80.
- Pickard-Cambridge FO (1893) Handbook to the study of British spiders (Drassidae and Agelenidae). *British Naturalist* 3: 117–170.
- Wang XP (2002) A generic-level revision of the spider subfamily Coelotinae (Araneae, Amaurobiidae). *Bulletin of the American Museum of Natural History* 269: 1–150. [https://doi.org/10.1206/0003-0090\(2002\)269<0001:AGLROT>2.0.CO;2](https://doi.org/10.1206/0003-0090(2002)269<0001:AGLROT>2.0.CO;2)
- Wang XP (2003) Species revision of the coelotine spider genera *Bifidocoelotes*, *Coronilla*, *Draconarius*, *Femoracoelotes*, *Leptocoelotes*, *Longicoelotes*, *Platocoelotes*, *Spiricoelotes*, *Tegecoelotes*, and *Tonsilla* (Araneae: Amaurobiidae). *Proceedings of the California Academy of Sciences* 54: 499–662.

- Wang XP, Griswold CE, Miller JA (2010) Revision of the genus *Draconarius* Ovtchinnikov 1999 (Agelenidae: Coelotinae) in Yunnan, China, with an analysis of the Coelotinae diversity in the Gaoligongshan Mountains. *Zootaxa* 2593: 1–127. <https://doi.org/10.11646/zootaxa.2593.1.1>
- World Spider Catalog (2018) Natural History Museum Bern. Version 18.5. <http://wsc.nmbe.ch> [accessed 4 January 2018]
- Zhao Z, Li S (2016) *Papiliocoelotes* gen. n., a new genus of Coelotinae (Araneae, Agelenidae) spiders from the Wuling Mountains, China. *ZooKeys* 585: 33–50. <https://doi.org/10.3897/zookeys.585.8007>
- Zhao Z, Li S (2017) Extinction vs. rapid radiation: the juxtaposed evolutionary histories of coelotine spiders support the Eocene–Oligocene orogenesis of the Tibetan Plateau. *Systematic Biology* 66(6): 988–1006. <https://doi.org/10.1093/sysbio/syx042>
- Zhu MS, Wang XP, Zhang ZS (2017) *Fauna Sinica: Invertebrata Vol. 59: Arachnida: Araneae: Agelenidae and Amaurobiidae*. Science Press, Beijing, 727 pp.

Systematics of the ant genus *Proceratium* Roger (Hymenoptera, Formicidae, Proceratiinae) in China – with descriptions of three new species based on micro-CT enhanced next-generation-morphology

Michael Staab^{1,2,*}, Francisco Hita Garcia^{3,*}, Cong Liu³,
Zheng-Hui Xu⁴, Evan P. Economo³

1 University of Freiburg, Faculty of Environment and Natural Resources, Nature Conservation and Landscape Ecology, Tennenbacherstr. 4, 79106 Freiburg, Germany **2** Freiburg Institute for Advanced Studies (FRIAS), University of Freiburg, Albertstraße 19, 79104 Freiburg, Germany **3** Biodiversity and Biocomplexity Unit, Okinawa Institute of Science and Technology Graduate University, 1919-1 Tancha, Onna-son, Okinawa, Japan **4** Key Laboratory of Forest Disaster Warning and Control in Yunnan Province, College of Biodiversity Conservation and Utilization, Southwest Forestry University, Kunming, Yunnan Province 650224, P.R. China

Corresponding author: Michael Staab (michael.staab@nature.uni-freiburg.de)

Academic editor: M. Borowiec | Received 8 March 2018 | Accepted 11 May 2018 | Published 4 July 2018

<http://zoobank.org/63FDA225-900E-42A6-9FD1-8B02D8CD1F44>

Citation: Staab M, Hita Garcia F, Liu C, Xu Z-H, Economo EP (2018) Systematics of the ant genus *Proceratium* Roger (Hymenoptera, Formicidae, Proceratiinae) in China – with descriptions of three new species based on micro-CT enhanced next-generation-morphology. ZooKeys 770: 137–192. <https://doi.org/10.3897/zookeys.770.24908>

Abstract

The genus *Proceratium* Roger, 1863 contains cryptic, subterranean ants that are seldom sampled and rare in natural history collections. Furthermore, most *Proceratium* specimens are extremely hairy and, due to their enlarged and curved gaster, often mounted suboptimally. As a consequence, the poorly observable physical characteristics of the material and its scarcity result in a rather challenging alpha taxonomy of this group. In this study, the taxonomy of the Chinese *Proceratium* fauna is reviewed and updated by combining examinations of traditional light microscopy with x-ray microtomography (micro-CT). Based on micro-CT scans of seven out of eight species, virtual 3D surface models were generated that permit in-depth comparative analyses of specimen morphology in order to overcome the difficulties to examine physical material of *Proceratium*. Eight Chinese species are recognized, of which three are newly described: *Proceratium bruelheidei* Staab, Xu & Hita Garcia, **sp. n.** and *P. kepingmai* **sp. n.** belong to the *P. itoi* clade

* Michael Staab and Francisco Hita Garcia contributed equally to this work.

and have been collected in the subtropical forests of southeast China, whereas *P. shobei* **sp. n.** belongs to the *P. stictum* clade and it is only known from a tropical forest of Yunnan Province. *Proceratium nujiangense* Xu, 2006 **syn. n.** is proposed as a junior synonym of *P. zhaoi* Xu, 2000. These taxonomic acts raise the number of known Chinese *Proceratium* species to eight. In order to integrate the new species into the existing taxonomic system and to facilitate identifications, an illustrated key to the worker caste of all Chinese species is provided, supplemented by species accounts with high-resolution montage images and still images of volume renderings of 3D models based on micro-CT. Moreover, cybertype datasets are provided for the new species, as well as digital datasets for the remaining species that include the raw micro-CT scan data, 3D surface models, 3D rotation videos, and all light photography and micro-CT still images. These datasets are available online (Dryad, Staab et al. 2018, <http://dx.doi.org/10.5061/dryad.h6j0g4p>).

Keywords

3D model, BEF-China, cybertype, Gutianshan National Nature Reserve, subtropical forest, taxonomy, tropical forest, Xishuangbanna

Introduction

Recent phylogenetic studies have clarified the evolutionary history of ant subfamilies and genera. One higher-level taxon consistently recovered is the subfamily Proceratiinae, which belongs to the poneroid clade (e.g. Brady et al. 2006, Moreau et al. 2006, Blanchard and Moreau 2017, Borowiec et al. 2017). This subfamily currently contains three valid extant genera and one fossil genus with eight fossil and 144 valid extant species, and one fossil genus with four species (Bolton 2018). *Proceratium* Roger, 1863 is the largest genus in the subfamily with 83 extant and six fossil species. However, based on recent molecular phylogenetic results, the monophyly of the genus appears doubtful (Borowiec et al. 2017). While globally distributed, with the majority of species occurring in warm and sufficiently wet climates, the geographic record is very patchy (Baroni Urbani and de Andrade 2003, Hita Garcia et al. 2014, Guénard et al. 2017). Specimens are only rarely collected, usually in leaf litter or soil samples. Colonies typically occur in low densities (but see Masuko 2010) and are small, having usually fewer than 100 workers (but see Onoyama and Yoshimura 2002, Fisher 2005). *Proceratium* have a cryptobiotic lifestyle with hypogeic foraging habits and nesting in leaf litter, rotting wood, top soil, or below stones (Baroni Urbani and de Andrade 2003). As far as it is known, they are specialized predators of the eggs of spiders and other arthropods, which can be stored in large quantities in the nest (e.g. Brown 1957, Brown 1979, Fisher 2005). Notably, some Japanese *Proceratium* species also display larval haemolymph feeding, a behavior otherwise only known from the ‘dracula ant’ subfamily Amblyoponinae (Masuko 1986). However, if this is a typical feature for the whole genus or restricted to a few congeners remains unknown and requires more in-depth natural history data than currently available.

The genus has been comprehensively revised on a global scale by Baroni Urbani and de Andrade (2003). The authors also refined the internal species clades originally erected by Brown (1958) and grouped the genus in eight internal clades that reflect the relationships of a morphology-based phylogeny (Baroni Urbani and de Andrade

2003). Nevertheless, the account on the genus is far from complete, as can be seen in the few single species descriptions (Fisher 2005, Liu et al. 2015a) and regional revisions published since then (Xu 2006, Hita Garcia et al. 2014, 2015). Considering the cryptic lifestyle and extreme rarity in collections, it is very likely that many more species await discovery and formal taxonomic treatment. In China, seven *Proceratium* species from three clades (*P. itoi* clade, *P. silaceum* clade, *P. stictum* clade) have been recorded so far (Xu 2000, Xu 2006, Liu et al. 2015b), albeit the geographic coverage within the country is poor (Guénard and Dunn 2012). The genus is only known from the provinces of Yunnan (six species), Hunan (two species), Zhejiang (one species), and the island of Taiwan (two species). There are no records from the other provinces in south and southeast China where *Proceratium* populations almost inevitably occur.

In the last decade, X-ray microtomography (micro-CT) technology has gained popularity among systematicists and is being increasingly employed in arthropod taxonomy. Micro-CT is a state-of-the-art imaging technology that facilitates the generation of high-resolution, virtual, and interactive three-dimensional (3D) reconstructions of whole specimens or of particular body parts (Hörnschemeyer et al. 2002, Friedrich and Beutel 2008). The virtual nature of such reconstructions enables non-destructive and comprehensive 3D analyses of anatomy and morphology (Faulwetter et al. 2013, Friedrich et al. 2014). Another crucial benefit of micro-CT is its application for virtual dissections and identification of new diagnostic characters (Deans et al. 2012), which has been successfully applied for lepidopterans (Simonsen and Kitching 2014), mayflies (Sartori et al. 2016), and recently ants (Hita Garcia et al. 2017a).

Despite its common usage in invertebrate paleontology, as well as functional and comparative morphology (e.g. Beutel et al. 2008, Berry and Ibbotson 2010, Barden and Grimaldi 2012), until very recently micro-CT was not applied to alpha taxonomy. In the last years, this situation is changing and micro-CT has become a powerful tool to visually enhance and support diagnostic species delimitations, from single species descriptions to revisions. While initially used for polychaetes (Faulwetter et al. 2013), myriapods (Stoev et al. 2013, Akkari et al. 2015), spiders (Michalik and Ramírez 2013), earthworms (Fernández et al. 2014), and flatworms (Carbayo and Lenihan 2016, Carbayo et al. 2016), micro-CT has evolved into a cutting-edge tool increasingly applied for ant taxonomy (Csősz 2012, Fischer et al. 2016, Sarnat et al. 2016, Agavekar et al. 2017, Hita Garcia et al. 2017a, 2017b). A detailed and critical assessment of the technology and its applications for ant taxonomy was provided by Hita Garcia et al. (2017b). Another key advantage of applying micro-CT for invertebrate taxonomy is the use of openly available cybertype datasets linked to the original, physical type material (Faulwetter et al. 2013, Akkari et al. 2015, Hita Garcia et al. 2017b).

In this study, we provide a review of the genus *Proceratium* in China, in which we describe three new species: *P. bruelheidei* sp. n. and *P. kepingmai* sp. n. from the *P. itoi* clade from subtropical southeast China and *P. shobei* sp. n. from the *P. stictum*

clade from the tropical south of Yunnan Province. The newly available insights from this study suggest that *P. nujiangense* Xu, 2006 is conspecific with *P. zhaoi* Xu, 2000. Thus, we treat *P. nujiangense* syn. n. as a junior synonym of *P. zhaoi*. To distinguish the new species from morphologically similar species, particularly in the *P. itoi* clade, and to ease future identifications, we provide an illustrated key to the Chinese fauna. We also give species accounts for all other valid species and add a locality record for *Proceratium longigaster* Karavaiev, 1935. Like in previous studies (Fischer et al. 2016, Sarnat et al. 2016, Agavekar et al. 2017, Hita Garcia et al. 2017a, 2017b), we continue using and exploring microtomography for ant taxonomy. In order to visually enhance the taxonomic descriptions, we provide still images and 3D videos based on surface volume renderings of micro-CT scans from all Chinese species (except for *P. longmenense* Xu, 2006). Since the treated species are rather hairy, often dirty, and too scarce for any physical specimen manipulations, we also use the 3D reconstructions for virtual in-depth examinations of surface morphology. Furthermore, the complete micro-CT datasets containing the scan raw data, 3D rotation videos, still images of 3D models, and 3D surfaces supplemented by color montage photos are made freely available online (Staab et al. 2018, <http://dx.doi.org/10.5061/dryad.h6j0g4p>) as cybertypes.

Materials and methods

Abbreviations of depositories

The collection abbreviations follow Evenhuis (2018). The material upon which this study is based is located or will be deposited at the following institutions:

BMNH	The Natural History Museum, London, UK
CASC	California Academy of Sciences, San Francisco, California, USA
MHNG	Muséum d'Histoire Naturelle de la Ville de Genève, Geneva, Switzerland
NIAES	National Institute for Agro-Environmental Sciences, Japan
NHMB	Naturhistorisches Museum Basel, Switzerland
OIST	Okinawa Institute of Science and Technology, Onna-son, Japan
SIZK	Schmalhausen Institute of Zoology, Kiev, Ukraine
SWFU	Southwest Forestry University, Kunming, Yunnan, PR China
TARI	Taiwan Agricultural Research Institute, Taichung, Taiwan
ZMBH	Museum für Naturkunde der Humboldt-Universität, Berlin, Germany

Specimens and imaging

The material of the new species was collected during recent ecological field work activities of the first author (see e.g. Staab et al. 2014, Staab et al. 2017) and others (see

Liu et al. 2016). All available worker specimens were mounted and measured with a Leica M125 stereo microscope under magnification of 80–100 \times . To compose montage images, we took raw image stacks with a Leica M205C microscope equipped with a Leica DFC450 camera and then assembled montage images with Helicon Focus (version 6) software. Additional material of previously described *Proceratium* species known to occur in China and of Asian species from the three *Proceratium* species clades containing Chinese species (*P. itoi* clade, *P. silaceum* clade, *P. stictum* clade) was also examined (see species and specimen data in Suppl. material 1: Table S1 for non-Chinese species). The other distributional data used for map generation was extracted from Antmaps.org (Janicki et al. 2016, Guénard et al. 2017).

Measurements and indices

The following measurements (all expressed in mm) and indices are based on Hita Garcia et al. (2014, 2015):

- EL** Eye length: maximum length of eye measured in oblique lateral view.
- HL** Head length: maximum measurable distance from the mid-point of the anterior clypeal margin to the mid-point of the posterior margin of head, measured in full-face view. Impressions on anterior clypeal margin and posterior head margin reduce head length.
- HLM** Head length with mandibles: maximum head length in full-face view including closed mandibles.
- HW** Head width: maximum head width directly above the eyes, measured in full-face view.
- MFeL** Metafemur length: maximum length of metafemur measured along its external face.
- MTiL** Metatibia length: maximum length of metatibia measured along its external face.
- MBaL** Metabasitarsus length: maximum length of metabasitarsus measured along its external face.
- LT3** Abdominal tergum III length: maximum length of abdominal tergum III (=length of abdominal segment III) in lateral view.
- LS4** Abdominal sternum IV length: maximum length of abdominal sternum IV in lateral view.
- LT4** Abdominal tergum IV length: maximum length of abdominal tergum IV in lateral view.
- PeL** Petiolar length: maximum length of the petiolar node in dorsal view including its anterior prolongation.
- PeW** Petiolar width: maximum width of petiole measured in dorsal view.
- SL** Scape length: maximum length of scape shaft excluding basal condyle.
- TL** Total body length: combined length of HLM + WL + PeL + LT3 + LT4.

- WL** Weber's length: diagonal length of mesosoma in lateral view from the anterior-most point of pronotal slope (excluding neck) to posteroventral margin of propodeal lamella or lobe.
- CI** Cephalic index: $HW / HL * 100$
- OI** Ocular index: $EL / HW * 100$
- SI** Scape index: $SL / HL * 100$
- MFeI** Metafemur length index: $MFeL / HW * 100$
- MTiI** Metatibia length index: $MTiL / HW * 100$
- MBaI** Metabasitarsus length index: $MBaL / HW * 100$
- DPeI** Dorsal petiole index: $PeW / PeL * 100$
- ASI** Abdominal segment index: $LT4 / LT3 * 100$
- IGR** Gastral reflexion index: $LS4 / LT4$

X-ray micro computed tomography and 3D images

We scanned all Chinese *Proceratium* species, except for *P. longmenense* from which no material was available for micro-CT analysis. For each of the new species, we scanned the holotype worker specimen, whereas for the remainder of the species we either scanned a paratype or non-type specimen, if no type material was available. An overview of scanning parameters and specimens used is provided in Table 1. All micro-CT scans were performed using a Zeiss Xradia 510 Versa 3D X-ray microscope operated with the Zeiss Scout-and-Scan Control System software (version 11.1.6411.17883). 3D reconstructions of the resulting scan raw data were done with the Zeiss Scout-and-Scan Control System Reconstructor (version 11.1.6411.17883) and saved in DICOM file format. Volume renderings, surface mesh generations, virtual examinations and dissections were performed with Amira software (version 6.3.0). Post-processing of mesh data in order to generate clean surfaces was done with Meshlab (version 1.3.3). The methodology for the virtual examinations of 3D surface models, generation of

Table 1. Overview of micro-CT scanning data presenting specimen data, scan settings, and voxel sizes for the resulting scans (all specimens are workers and all files are in DICOM format).

Species	Identifier	Type status	Magnification (x)	Exposure (s)	Voxel size (µm)	Source distance (mm)	Detector distance (mm)	Voltage (kV)	Power (W)	Amperage (µA)
<i>deelemani</i>	CASENT0790842	non-type	4	1.5	4.826	24.99	10	45.24	3.54	78.14
<i>kepingmai</i>	CASENT0790031	holotype	4	1.5	4.359	19.99	11	45.23	3.54	78.3
<i>bruelbeidei</i>	CASENT0790023	holotype	4	1.5	4.359	19.99	11	45.24	3.55	78.35
<i>itoi</i>	OKENT0016142	non-type	4	0.8	3.660	13	11	45.24	3.54	78.29
<i>japonicum</i>	CASENT0790834	non-type	4	0.8	3.897	14.99	11	45.24	3.54	78.17
<i>longigaster</i>	CASENT0790673	non-type	4	0.8	3.097	11	13	45.24	3.54	78.19
<i>nuijiangense</i>	CASENT0790672	paratype	4	1.5	2.534	12	19.99	45.24	3.54	78.19
<i>shobei</i>	CASENT0717686	holotype	4	1.5	4.193	17.99	11	45.24	3.53	78.05
<i>zhaoi</i>	CASENT0790671	paratype	4	1.5	2.252	11	22	45.24	3.54	78.33

3D rotation videos, and virtual dissections follow Hita Garcia et al. (2017a). For more details on micro-CT scanning and post-processing workflow pipeline, we refer to the exhaustive descriptions in Hita Garcia et al. (2017a, 2017b).

Data availability

All specimens used in this study have been databased and the data are freely accessible on AntWeb (<http://www.antweb.org>). Each specimen can be traced by a unique specimen identifier attached to its pin. The Cybertype datasets provided in this study consist of the full micro-CT original volumetric datasets (in DICOM format), 3D surface models (in STL and PLY formats), 3D rotation video files (in .mp4 format, see Suppl. material), all light photography montage images, and all image plates including all important images of 3D models for each species. All data have been archived and are freely available from the Dryad Digital Repository (Staab et al. 2018, <http://dx.doi.org/10.5061/dryad.h6j0g4p>). In addition to the cybertype data at Dryad, we also provide freely accessible 3D surface models of all treated species on Sketchfab (<https://sketchfab.com/arilab/collections/proceratium>).

Results

Synopsis of Chinese *Proceratium* species

Proceratium itoi clade

Proceratium bruelheidei Staab, Xu & Hita Garcia sp. n. [China: Jiangxi, Zhejiang]

Proceratium itoi (Forel, 1918) [China: Hunan, Zhejiang; Taiwan; Japan; South Korea; Vietnam]

Proceratium kepingmai Staab, Xu & Hita Garcia sp. n. [China: Jiangxi, Zhejiang]

Proceratium longmenense Xu, 2006 [China: Yunnan]

Proceratium zhaoi Xu, 2000 [China: Yunnan]

= *Proceratium nujiangense* Xu, 2006 [China: Yunnan] syn. n.

Proceratium silaceum clade

Proceratium japonicum Santschi, 1937 [China: Yunnan; Taiwan; Japan]

= *Proceratium formosicola* Terayama, 1985 [Taiwan]

Proceratium longigaster Karavaiev, 1935 [China: Hunan, Yunnan, Zhejiang; Vietnam]

Proceratium stictum clade

Proceratium shobei Staab, Xu & Hita Garcia sp. n. [China: Yunnan]

Identification key to Chinese *Proceratium* species (workers)

This key is partly derived from Baroni Urbani and de Andrade (2003) and Xu (2006).

- 1 In profile, petiolar node squamiform and rectangular, high and erect (Fig. 1A) **2**
- In profile, petiolar node never squamiform, either low, elongate, and barrel-shaped, or rounded-triangular (Fig. 1B) **3**

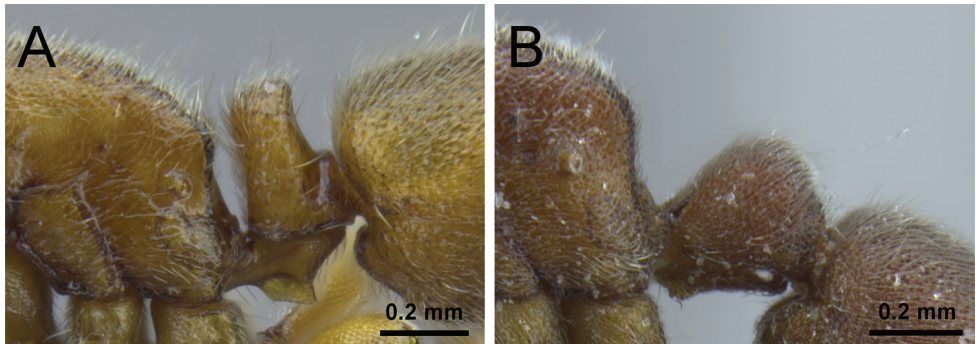


Figure 1. Petiole in profile view. **A** *P. japonicum* (CASENT0790834) **B** *P. itoi* (OKENT0016142).

- 2 In profile, petiolar node clearly narrowing dorsally, broader on the base than on the apex (Fig. 2A); in dorsal view, petiole at least 1.5× wider than long (DPeI ≥155); abundant long appressed shaggy hairs from LT3 project distinctly over the constriction between LT3 and LT4 (Fig. 2A) [China: Hunan, Yunnan, Zhejiang; Vietnam] ***P. longigaster***
- In profile, petiolar node not or only weakly narrowing dorsally, the base as or almost as broad as the apex (Fig. 2B); even if narrowing, petiole never 1.5× times wider than long in dorsal view (DPeI <150); no shaggy hairs protruding from LT3 over the constriction to LT4, if single longer hairs present, then not shaggy (Fig. 2B) [China: Yunnan; Taiwan; Japan] ***P. japonicum***

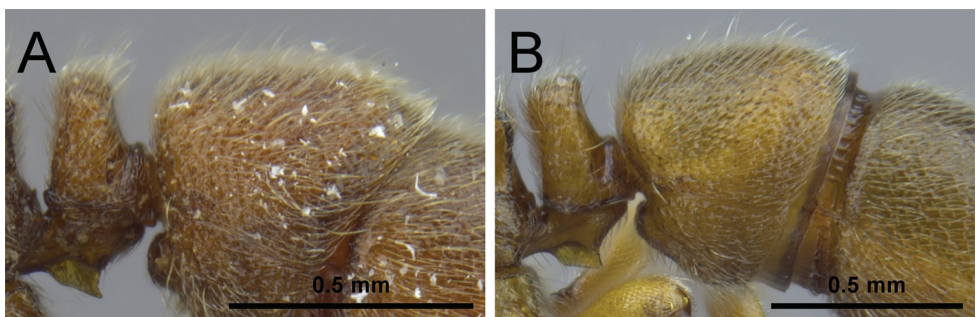


Figure 2. Petiole, abdominal segment III and anterior portion of abdominal segment IV in profile view. **A** *P. longigaster* (CASENT0790673) **B** *P. japonicum* (CASENT0790834).

- 3 Anterior clypeal margin with a distinct and broad notch (Fig. 3A); postero-dorsal corners of propodeum armed with conspicuous thick and acute teeth (Fig. 3C); head, mesosoma, petiole, and abdominal segment III strongly foveolate (Fig. 22) [China: Yunnan] *P. shobei*
- Anterior clypeal margin without a distinct and broad notch (Fig. 3B); postero-dorsal corner of propodeum bluntly rounded or angular (Fig. 3D), never with conspicuous teeth as above; head, dorsal mesosoma, petiole, and abdominal segment III usually granulate or punctate (Figs 8, 10, 12, 14, 15) 4

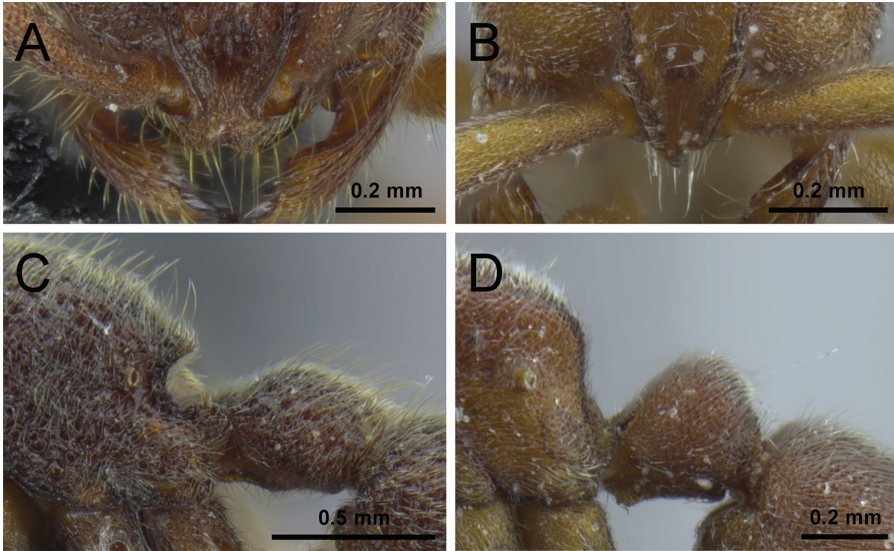


Figure 3. Anterior portion of cephalic dorsum, in full-face view (A, B), and propodeum and petiole, in profile view (C, D). A, C *P. shobei* (CASENT0717686) B, D *P. itoi* (OKENT0016142).

- 4 Frontal carinae weakly developed, short, little diverging above antennal insertions, and with narrow lateral lamellae; dorsal surface of body without erect hairs protruding from dense pubescence (Fig. 4A); smaller species (WL ≤ 0.80) with shorter legs (MFeI < 80 , MTiI < 65 , MBaI < 40) [China: Yunnan] *P. zhaoi*
- Frontal carinae better developed, long, diverging above antennal insertions, and usually with broad lateral lamellae; dorsal surface of body with erect hairs protruding from dense pubescence (Fig. 4B); larger species (WL > 0.95) with longer legs (MFeI > 80 , MTiI > 65 , MBaI > 50) 5

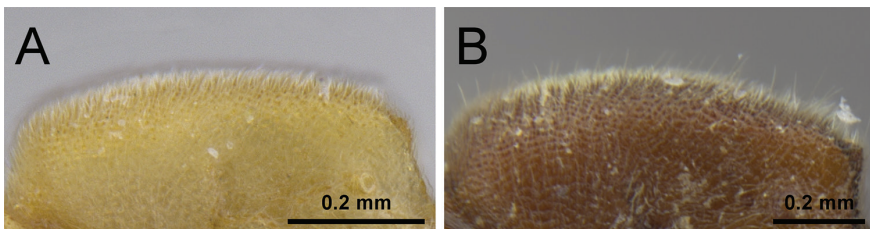


Figure 4. Mesosoma dorsum in profile view. A *P. zhaoi* (CASENT0790671) B *P. bruelheidei* (CASENT0790023).

- 5 In profile, posterodorsal corners of propodeum rounded (Fig. 5A) [China: Hunan, Zhejiang; Taiwan; Japan; South Korea; Vietnam].....*P. itoi*
 – In profile, posterodorsal corners of propodeum angular (Fig. 5B)6

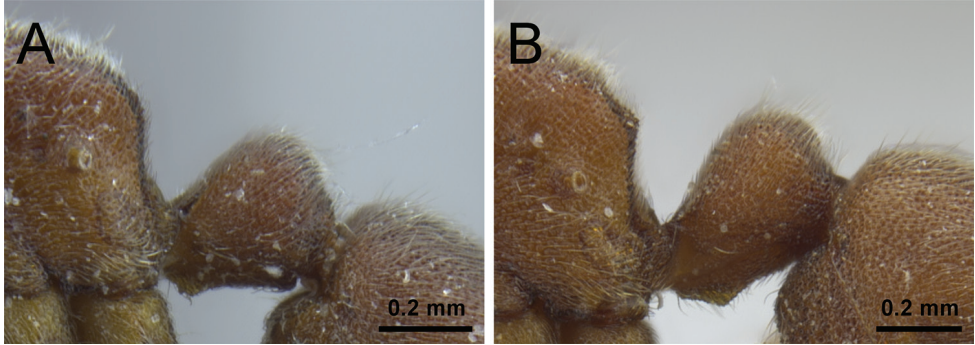


Figure 5. Propodeum and petiole in profile. **A** *P. itoi* (OKENT0016142) **B** *P. kepingmai* (CASENT0790031).

- 6 Scapes without erect hairs protruding from the dense pubescence; frontal carinae touching each other at their anteriormost level (Fig. 6A), their lateral lamellae relatively narrow, not conspicuously broader above antennal insertions; head (CI 85) and scapes (SI 68) relatively long [China: Yunnan]..... *P. longmenense*
 – Scapes with many erect hairs protruding from the dense pubescence; frontal carinae clearly separated at their anteriormost level, not touching each other, their lamellae broad, conspicuously extending laterally above antennal insertions (Fig. 6B); head relatively broad (CI ≥ 89) and scapes (SI ≤ 63) relatively short....7

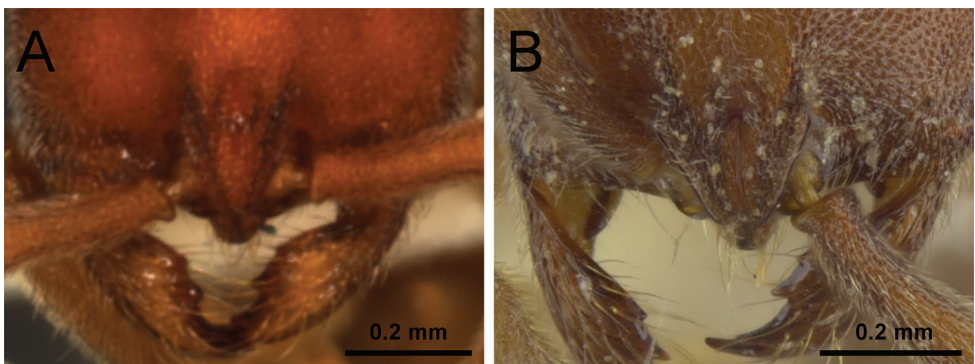


Figure 6. Anterior portion of cephalic dorsum in full-face view. **A** *P. longmenense* **B** *P. bruelheidei* (CASENT0790023).

- 7 Propodeal declivity punctured, mostly opaque; frontal furrow conspicuous and darker than anterior cephalic dorsum (Fig. 7A); posterior face of petiolar node in profile steeper than anterior face and about half as long as anterior face (Fig. 7C) [China: Jiangxi, Zhejiang] *P. kepingmai*
- Propodeal declivity very shiny, at most superficially punctured; frontal furrow inconspicuous and of same color than anterior cephalic dorsum (Fig. 7B); posterior face of petiolar node in profile as steep as anterior face and less than half as long as anterior face (Fig. 7D) [China: Jiangxi, Zhejiang] *P. bruelheidei*

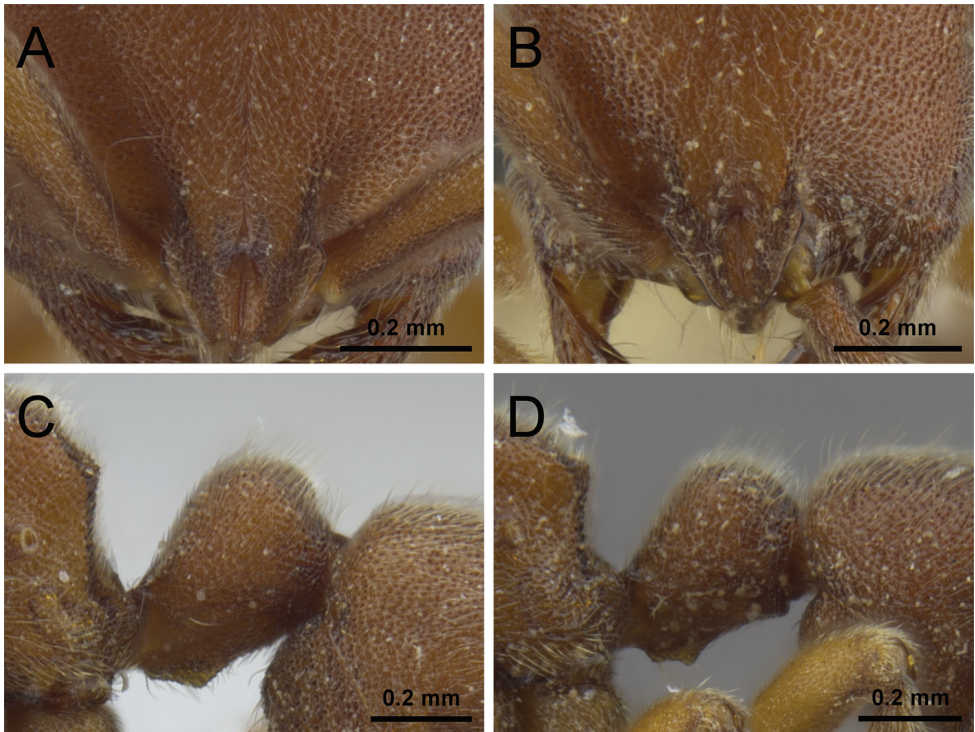


Figure 7. Anterior portion of cephalic dorsum in full-face view (**A, B**) and petiole in profile (**C, D**). **A, C** *P. kepingmai* (CASENT0790031) **B, D** *P. bruelheidei* (CASENT0790023).

Taxonomic species accounts of Chinese *Proceratium*

Proceratium itoi clade

Definition. Workers of this clade can be separated from all other *Proceratium* species by the combination of abdominal sternum IV protruding over the posterior end of abdominal sternum III, petiolar node nodiform, and body sculpture densely granulate to punctate (definition follows Baroni Urbani and de Andrade 2003).

Comments. This clade includes seven species and is restricted to east and southeast Asia. All species except *P. malesianum* de Andrade, 2003 and *P. williamsi* Mathew & Tiwari, 2000 occur in China. The species are morphologically similar, particularly in relative body proportions and indices, but can be safely separated with the identification key presented above. More detailed accounts on species delimitation and biology are reported at the species accounts below.

***Proceratium bruelheidei* Staab, Xu & Hita Garcia, sp. n.**

<http://zoobank.org/D5261D06-D21C-4149-B716-2347DC616BD5>

Figs 4B, 6B, 7B, 7D, 8, 9, 24

Type material. Holotype. Pinned worker from CHINA, Jiangxi Province, near the village Xingangshan, ca. 15 km SE of Wuyuan, 29°7'24"N / 117°54'25"E, 158 m asl, early successional tree plantation of the BEF-China experiment, Winkler leaf litter extraction, 26-IV-2015, leg. Merle Noack, label "MN290" (CASENT0790023), deposited in SWFU.

Paratypes. Seven pinned workers in total; one with same data as holotype except label "MN291" (CASENT0790025, in SWFU); one with same data as holotype except 29°7'24"N / 117°54'31"E, 204 m asl, 22-IV-2015, label "MN248" (CASENT0790024, in SWFU); one with same data as holotype except 29°7'33"N / 117°54'41"E, 246 m asl, 30-IV-2015, label "MN309" (CASENT0790029, in SWFU); one with same data as holotype except 29°7'33"N / 117°54'40"E, 239 m asl, 04-V-2015, label "MN371" (CASENT0790030, in SWFU); one with same data as holotype except 29°7'15"N / 117°54'22"E, 122 m asl, 12-V-2015, label "MN479" (CASENT0790028, in CASC); one with same data as holotype except 29°7'37"N / 117°54'25"E, 219 m asl, 20-V-2015, label "MN525" (CASENT0790026, in ZMBH); one from CHINA, Zhejiang Province, Gutianshan National Nature Reserve, ca. 35 km NW of Kaihua, 29°16'37"N / 118°5'26"E, 617 m asl, young secondary subtropical mixed forest, manual sifting of leaf litter, 11-VII-2008, leg. Andreas Schuldt, label "CSP 22" (CASENT0790027, in ZMBH).

Cybertype. Volumetric raw data (in DICOM format), 3D rotation video (in .mp4 format, see Suppl. material 3: Video 1), still images of surface volume rendering, and 3D surface (in PLY format) of the physical holotype (CASENT0790023) in addition to montage photos illustrating head in full-face view, profile and dorsal views of the body. The data is deposited at Dryad (Staab et al. 2018, <http://dx.doi.org/10.5061/dryad.h6j0g4p>) and can be freely accessed as virtual representation of the type. In addition to the cybertype data at Dryad, we also provide a freely accessible 3D surface model of the holotype at Sketchfab (<https://skfb.ly/6txMz>).

Diagnosis. *Proceratium bruelheidei* differs from the other members of the *P. itoi* clade by the following character combination: relatively large species (TL 3.61–4.00); sides of head straight to very weakly convex, posterior sides only narrowing dorsally, vertex convex; frontal carinae well developed, with large lamellae that extend laterally

above the antennal insertions; frontal furrow inconspicuous and of the same color as the surrounding anterior cephalic dorsum; posterodorsal corners of the propodeum broadly angular; propodeal declivity superficially punctured, but shiny; posterior face of petiolar node in profile as steep as anterior face and less than half as long as anterior face; apex of the petiolar node almost as long as broad in dorsal view; subpetiolar process roughly trapezoid and well developed (albeit with variable ventral outline); abdominal segment IV very strongly recurved (IGR 0.24–0.26); in addition to dense pubescence, abundant erect hairs present on scapes and dorsal surface of body, longest of those hairs longer than maximum dorsoventral diameter of metafemur.

Worker measurements. Holotype. TL 3.94; EL 0.04; SL 0.50; HL 0.84; HLM 1.09; HW 0.79; WL 1.06; MFeL 0.69; MTiL 0.54; MBaL 0.40; PeL 0.39; PeW 0.32; LT3 0.56; LS4 0.21; LT4 0.84; OI 4; CI 93; SI 59; MFeI 87; MTiI 69; MBaI 51; DPeI 81; IGR 0.25; ASI 150.

Paratypes (n = 7). TL 3.61–4.00; EL 0.03–0.04; SL 0.49–0.53; HL 0.79–0.86; HLM 0.96–1.08; HW 0.73–0.79; WL 1.03–1.10; MFeL 0.63–0.74; MTiL 0.54–0.58; MBaL 0.39–0.41; PeL 0.36–0.39; PeW 0.30–0.32; LT3 0.51–0.58; LS4 0.19–0.22; LT4 0.75–0.92; OI 4–5; CI 89–94; SI 60–63; MFeI 86–96; MTiI 69–74; MBaI 50–54; DPeI 82–84; IGR 0.24–0.26; ASI 145–159.

Worker description. In full-face view, head slightly longer than broad (CI 89–94), anterior sides straight to very weakly convex, posterior sides narrowing dorsally, vertex convex. Clypeus reduced and narrow, with a broadly triangular median anterior projection. Frontal carinae relatively short, moderately separated, slightly covering antennal insertions, constantly diverging posteriorly, lateral expansions of anterior part of frontal carinae developed as broad lamellae, raised, conspicuously and broadly extending laterally above antennal insertions; frontal area convex; frontal furrow developed as a raised carina, starting at the clypeal projection and extending over the anterior 2/5 of the cephalic dorsum, with a short gap at the level where the lamellae of frontal carinae are broadest, frontal furrow less conspicuous after the gap. Eyes reduced, minute (OI 4–5), consisting of one to four ommatidia and located on midline of head. Antennae 12-segmented, scapes short (SI 59–63), not reaching posterior head margin and thickening apically. Mandibles elongate and triangular, relatively slender, masticatory margin with four teeth in total, apical tooth long and acute, the other teeth smaller and decreasing in size from second to fourth tooth, gap between second and third tooth larger than between other teeth.

Mesosoma in profile slightly convex and as long as maximum head length including mandibles (WL 1.03–1.10 vs HLM 0.96–1.09). Lower mesopleurae (katepisterna) with well-demarcated sutures, upper mesopleurae (anepisterna) with inconspicuous sutures, no other sutures developed on lateral and dorsal mesosoma; lower mesopleurae weakly inflated posteriorly; posterodorsal corner of propodeum broadly angular, propodeal lobes weakly developed as bluntly rounded lamellae; propodeal declivity almost vertical, slightly inclined anteriorly; in posterodorsal view, sides of propodeum separated from declivity by distinct lamellate margins; in profile view, propodeal spiracle rounded, at mid height, opening of spiracle slightly facing posteriorly. Legs moderately

long (MFeL 0.63–0.74, MTiL 0.54–0.58, MBaL 0.39–0.41); all tibiae with a pectinate spur; calcar of strigil without a basal spine; pretarsal claws simple; arolia present.

Petiolar node in profile high, nodiform, with a straight and sloping anterior face, dorsum of node broadly rounded, posterior face as steep as anterior face and relatively short, less than half as long as anterior face; petiole in dorsal view longer than broad, apex of node almost as long as broad; ventral process of petiole well developed, with a roughly trapezoid projection of varying shape and ventral outline (see 'variation').

In dorsal view abdominal segment III anteriorly much broader than petiole; its sides convex; abdominal sternite III anteriomedially with a conspicuous depression marked by a thin rim. Constriction between abdominal segments III and IV deep. Abdominal segment IV very large, strongly recurved (IGR 0.24–0.26) and posteriorly rounded, with a lamella on its anterior border around the constriction to abdominal segment III, this lamella thicker ventrally than dorsally; abdominal tergum IV 1.5–1.6× longer than abdominal tergum III (ASI 145–159), remaining abdominal tergites and sternites inconspicuous and projecting anteriorly. Sting large and extended.

Whole body covered with dense mat of short, decumbent to suberect pubescent hairs; additionally, dorsal surfaces of body with abundant significantly longer suberect and erect hairs; such hairs also present on abdominal sternite III + IV, scapes (anterior faces of scapes with many hairs, posterior faces with fewer hairs) and legs (ventral faces of femora and tibiae with many hairs, dorsal faces with fewer hairs), the longest hairs on dorsal surface of body longer than the maximum dorsoventral diameter of metafemur. Mandibles striate; entire body densely punctate; on sides of pronotum punctures aligned in diffuse lines, appearing striate; punctures on antennae, legs, and abdominal segment IV finer than on rest of body; propodeal declivity shiny and at most superficially punctate; abdominal segments V–VII very superficially reticulate and shiny. Body color uniformly orange brown to reddish brown, vertex of head slightly darker, legs, antennal funiculus, and abdominal segments V–VII yellowish brown.

Etymology. The species epithet is a patronym in honor of the German botanist Prof. Helge Bruelheide and his efforts in establishing and promoting the BEF-China project. All specimens of this species were collected on BEF-China field sites.

Distribution and ecology. Most of the type series was collected during a leaf litter ant survey (Noack 2016) in the experimental tree plantations of the BEF-China Main Experiment (Bruelheide et al. 2014). No direct observations of biology and natural history are available. The trees under which the Winkler samples yielding seven of eight type specimens were collected were just six years old and had a mean diameter at breast height of 5.6 ± 2.5 cm ($n=7$) (Noack 2016). This may indicate that *P. bruelheidei* could prefer early successional forests with a relatively open soil, as the ground from which leaf litter was taken had a mean litter cover of $55 \pm 24\%$ ($n=7$). The single specimen (CASENT0790027) from the Gutianshan National Nature Reserve was likewise collected from an early successional forest stand that was clear-cut less than 20 years prior to the collection of the specimen. However, further sampling will be necessary to draw quantitative conclusions on habitat preferences.

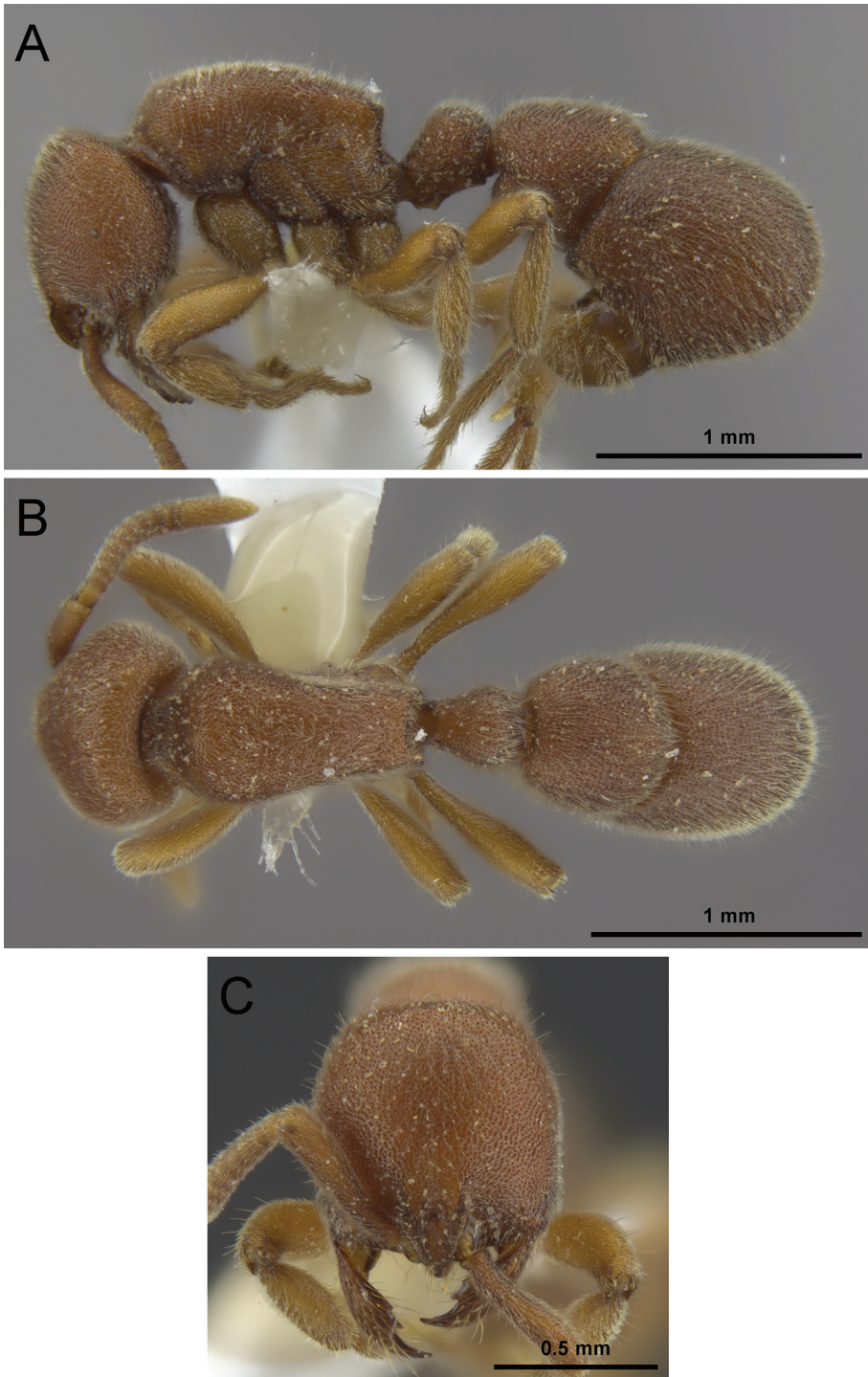


Figure 8. *Proceratium bruelheidei* sp. n. holotype worker (CASENT0790023). **A** Body in profile **B** Body in dorsal view **C** Head in full-face view.

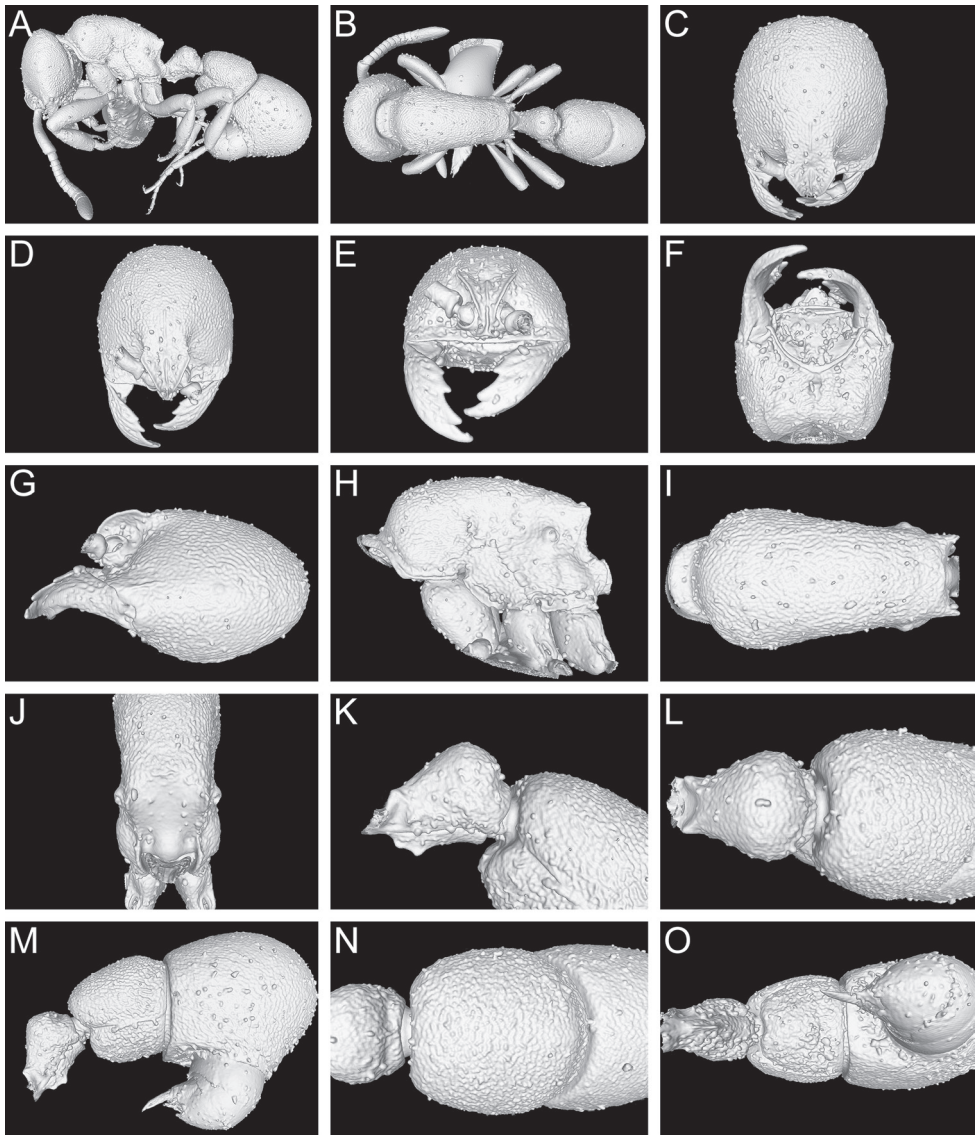


Figure 9. Still images from surface display volume renderings of 3D model of *Proceratium bruelheidei* sp. n. holotype worker (CASENT0790023). **A** Body in profile **B** Body in dorsal view **C** Head in dorsal view **D** Head in anterodorsal view **E** Head in anterior view **F** Head in ventral view **G** Head in profile **H** Mesosoma in profile **I** Mesosoma in dorsal view **J** Propodeum in posterodorsal view **K** Abdominal segment II and parts of III in profile **L** Abdominal segment II and parts of III in dorsal view **M** Abdominal segments II–VII in profile **N** Abdominal segment III and parts of II and IV in dorsal view **O** Abdominal segments II–VII in ventral view.

Taxonomic notes. *Proceratium bruelheidei* is most similar to *P. kepingmai*. From the other species of the *P. itoi* clade, *P. bruelheidei* can be separated by using the characters given in the ‘taxonomic notes’ of *P. kepingmai* below. From this species, *P. bruelheidei* dif-

fers by the shape of the head in full-face view with straight sides and a convex vertex (sides convex, broadest at level of eyes and vertex almost straight in *P. kepingmai*), the shiny propodeal declivity that is only superficially punctured (densely punctured and mostly opaque in *P. kepingmai*), the inconspicuous frontal furrow that has the same color as the surrounding anterior cephalic dorsum (frontal furrow conspicuous and dark in *P. kepingmai*), the posterior face of petiolar node as steep as the anterior face of the node and less than half as long as the anterior face (posterior face steeper than anterior face and about half as long in *P. kepingmai*), the apex of the petiolar node that is little broader than long (clearly broader than long in *P. kepingmai*), and the more strongly recurved abdominal segment IV (IGR 0.24–0.26) (IGR 0.30–0.32 in *P. kepingmai*). Additionally, *P. bruelheidei* has distinctly more and longer erect hairs protruding from the dense pubescence on the dorsum of the body and the ventral abdomen. While the number of hairs may be a treacherous character as hairs can break during specimen processing, the length of hairs can reliably be quantified. In *P. bruelheidei* the longest erect hairs on the dorsum of the petiole and on abdominal sternum III are longer than the maximum dorsoventral diameter of the metafemur (as long as or shorter than maximum diameter of metafemur in *P. kepingmai*).

Variation. The variation in body size is within the normal limits of other *Proceratium* species and the type specimens of *P. bruelheidei* show, with the notable exception of the subpetiolar process, no observable intraspecific differences. While the process is well developed and roughly trapezoid in all available specimens, its size, exact shape, and ventral outline vary. In the holotype (CASENT0790023) and several paratypes (CASENT0790025, CASENT0790026, CASENT0790029) the subpetiolar process has a distinct notch, so that it almost looks like an upside-down volcano. This notch is absent in other specimens (CASENT0790027, CASENT0790028, CASENT0790030), where the ventral outline of the process is straight. In one specimen (CASENT0790024) the ventral outline is also straight but with a row of minute denticles. It thus appears that this character, which is often used to delimitate *Proceratium* species (e.g. Baroni Urbani and de Andrade 2003, Hita Garcia et al. 2014), may be less suitable for species in the *P. itoi* clade, as also indicated by the variation in the subpetiolar process within the type series of *P. zhaoi* (Xu 2000).

***Proceratium itoi* (Forel, 1918)**

Figs 1B, 3B, 3D, 5A, 10, 11, 24

Sysphincta itoi Forel, 1918: 717 (w.), Japan

Proceratium itoi – Brown 1958: 247 (see also Baroni Urbani and de Andrade 2003: 267, Onoyama and Yoshimura 2002: 32)

Proceratium itoi – Ogata 1987: 107 (m.), Japan

Proceratium itoi – Onoyama and Yoshimura 2002: 35 (q.), Japan

Type material. Syntypes. Three pinned workers from JAPAN, Tokyo, leg. Ito (CASENT0907205, in MHNG) [images examined].

Non-type material examined. JAPAN, Fukuoka, Mt. Tachibana, 25-VII-1984, leg. S. Nomura (OKENT016137; OKENT016138; OKENT016139; OKENT016141; OKENT016142, all in OIST).

Virtual dataset. Volumetric raw data (in DICOM format), 3D rotation video (in .mp4 format, see Suppl. material 4: Video 2), still images of surface volume rendering, and 3D surface (in PLY format) of a non-type specimen (OKENT0016142) in addition to montage photos illustrating head in full-face view, profile and dorsal views of the body. The data is deposited at Dryad (Staab et al. 2018, <http://dx.doi.org/10.5061/dryad.h6j0g4p>) and can be freely accessed as virtual representation of the species. In addition to the data at Dryad, we also provide a freely accessible 3D surface model at Sketchfab (<https://skfb.ly/6txMM>).

Diagnosis. *Proceratium itoi* differs from the other members of the *P. itoi* clade by the following character combination: medium-sized species (TL 3.46–3.82); sides of head very weakly convex, almost straight, broadest at level of eyes and gently narrowing anteriorly and posteriorly, vertex weakly convex, almost straight; frontal carinae well developed, with large lamellae that extend laterally above the antennal insertions; frontal furrow inconspicuous; posterodorsal corners of propodeum rounded, propodeal declivity superficially punctured (more so dorsally) but largely shiny; posterior face of petiolar node in profile steeper as anterior face; petiole almost as broad as long (DPeI 86–93), apex of petiolar node broader than long in dorsal view; subpetiolar process developed and triangular (but may be small); in addition to dense pubescence abundant erect hairs present on scapes and dorsal surface of body, longest of those hairs shorter than maximum dorsoventral diameter of metafemur.

Distribution and ecology. This species is widely distributed, occurring from Japan (except Hokkaido) and South Korea to Vietnam. It has been recorded from Taiwan and the Chinese provinces Zhejiang and Hunan. Thus, we expect that it will be collected from the geographically intermediate provinces in the future. No direct biological observations from China are available, but the Japanese populations are comparatively well studied (Onoyama and Yoshimura 2002). Nests are found in the soil or rotting wood of various deciduous or evergreen forest types and workers forage hypogeic or in leaf litter. Mature colonies have 100–200 workers and densities can reach 0.3 colonies per m² (Masuko 2010). Larval hemolymph feeding has been observed (Masuko 1986).

Taxonomic notes. *Proceratium itoi* is a typical member of its clade of intermediate size (WL 0.96–1.04) and is similar to most other species in body proportions and indices. *Proceratium itoi* can be separated from *P. williamsi* and *P. zhaoi* by the presence of erect hairs on the dorsal body surface (absent in *P. williamsi* and *P. zhaoi*); from *P. longmenense* by the presence of erect hairs on the scape (absent in *P. longmenense*) and by the frontal carinae separated at their anteriormost level (touching each other at their anteriormost level in *P. longmenense*). In *P. itoi* the posterodorsal corners of propodeum are rounded and this character distinguishes this species from *P. bruelheidei* and *P. kepingmai* (posterodorsal corners of the propodeum angular), which are also larger species (WL 1.03–1.10 and 1.14–1.24). The rounded posterodorsal corners of propodeum are shared between *P. malesianum* and *P. itoi*, but *P. malesianum* is a smaller species

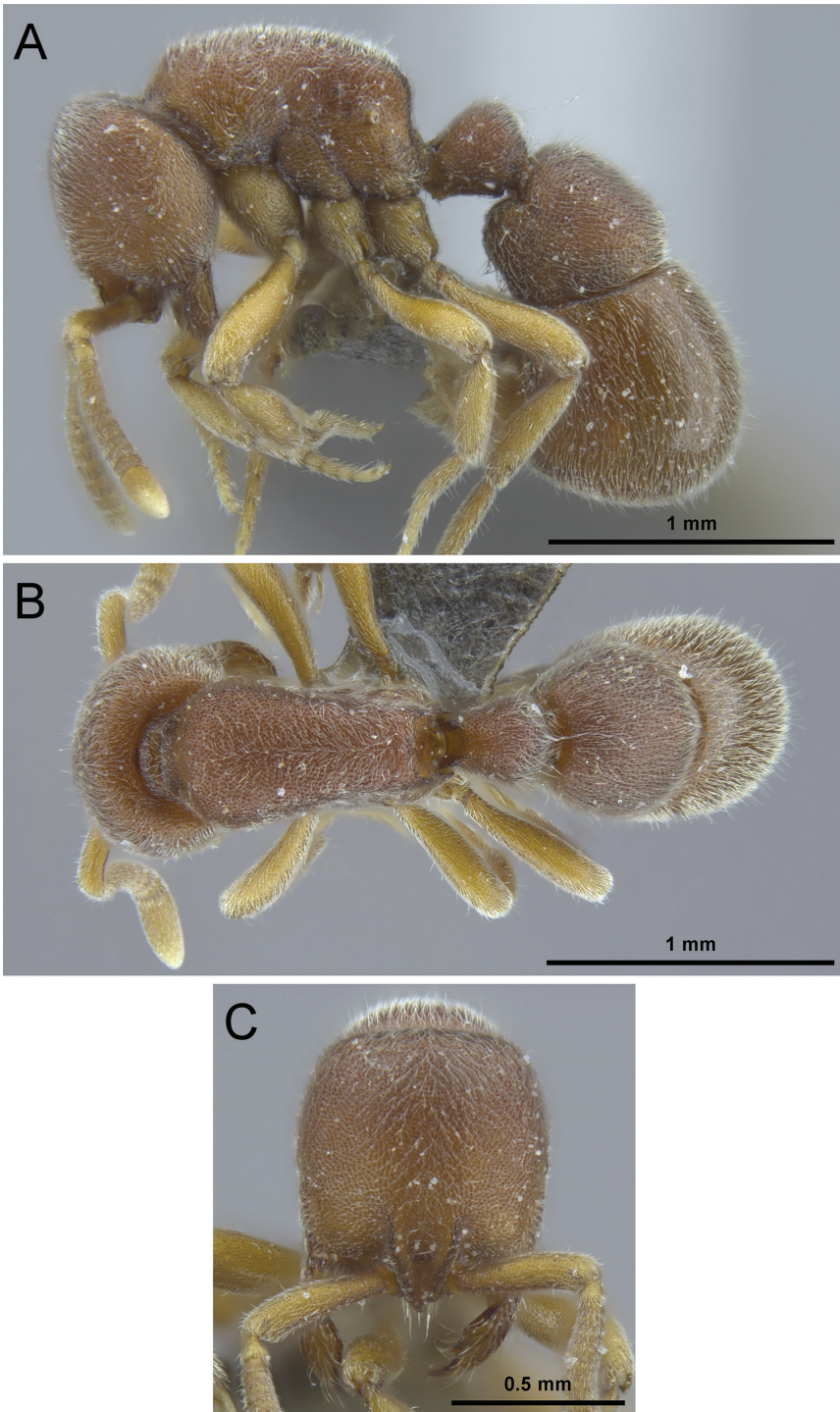


Figure 10. *Proceratium itoi* non-type worker (OKENT0016142). **A** Body in profile **B** Body in dorsal view **C** Head in full-face view.

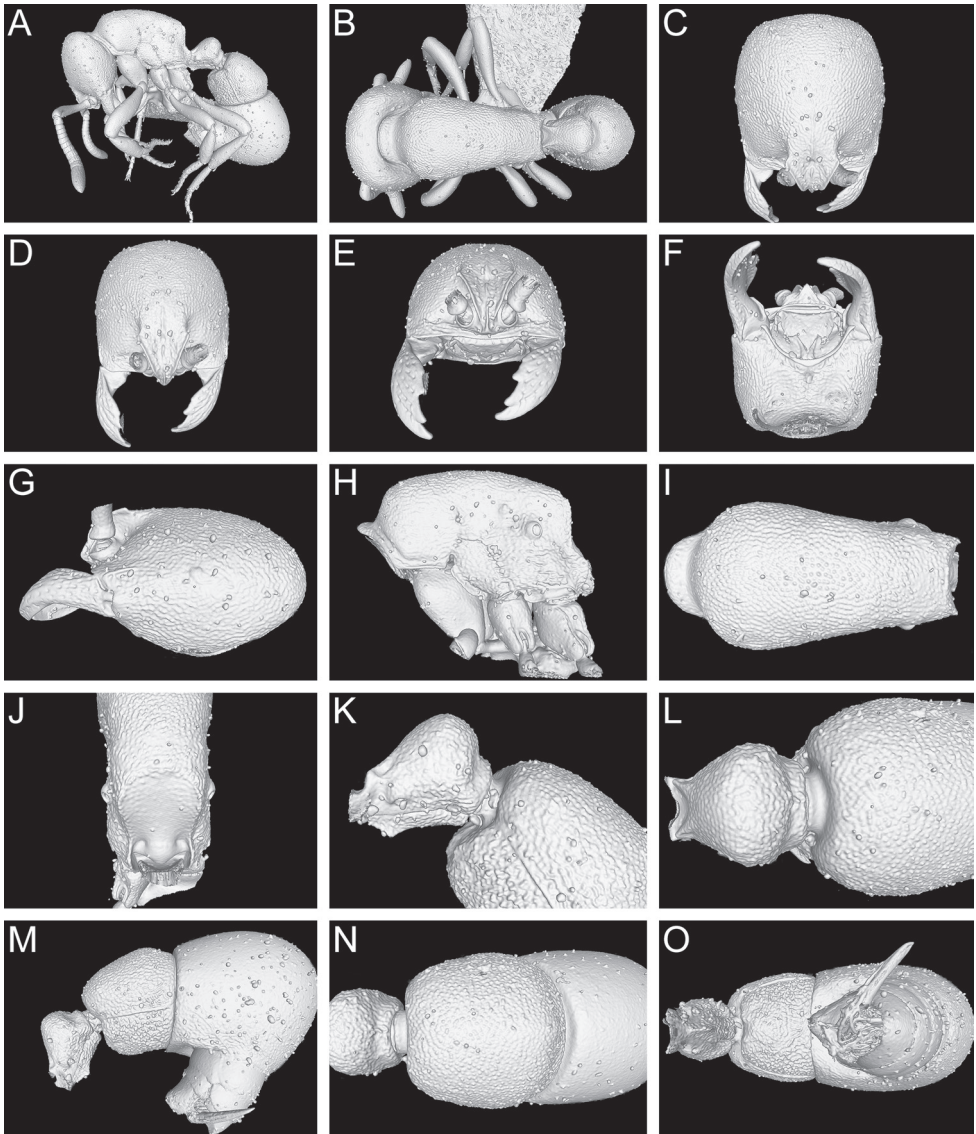


Figure 11. Still images from surface display volume renderings of 3D model of *Proceratium itoi* non-type worker (OKENT0016142). **A** Body in profile **B** Body in dorsal view **C** Head in dorsal view **D** Head in anterodorsal view **E** Head in anterior view **F** Head in ventral view **G** Head in profile **H** Mesosoma in profile **I** Mesosoma in dorsal view **J** Propodeum in posterodorsal view **K** Abdominal segment II and parts of III in profile **L** Abdominal segment II and parts of III in dorsal view **M** Abdominal segments II–VII in profile **N** Abdominal segment III and parts of II and IV in dorsal view **O** Abdominal segments II–VII in ventral view.

(WL 0.71–0.90) with a broadly rounded vertex (weakly convex, almost straight in *P. itoi*) and a broadly rounded petiolar node in profile (posterior face of petiolar node in profile steeper than anterior face in *P. itoi*).

***Proceratium kepingmai* Staab, Xu & Hita Garcia sp. n.**

<http://zoobank.org/0233F3AD-8F60-4CBB-B64B-B0A48857CBFF>

Figs 5B, 7A, 7C, 12, 13, 24

Type material. Holotype. Pinned worker from CHINA, Jiangxi Province, near the village Xingangshan, ca. 15 km SE of Wuyuan, 29°7'28"N / 117°54'40"E, 270 m asl, secondary subtropical mixed forest, Winkler leaf litter extraction, 26-III-2015, leg. Michael Staab, label "MS1836" (CASENT0790031), deposited in SWFU.

Paratype. Pinned worker from CHINA, Zhejiang Province, Gutianshan National Nature Reserve, ca. 30 km NW of Kaihua, 29°14'50"N / 118°8'10"E, 665 m asl, secondary subtropical mixed forest, Winkler leaf litter extraction, 27-IV-2015, leg. Merle Noack, label "MS1859" (CASENT0790032), deposited in ZMBH.

Cybertype. Volumetric raw data (in DICOM format), 3D rotation video (in .mp4 format, see Suppl. material 5: Video 3), still images of surface volume rendering, and 3D surface (in PLY format) of the physical holotype (CASENT0790031) in addition to montage photos illustrating head in full-face view, profile and dorsal views of the body. The data is deposited at Dryad (Staab et al. 2018, <http://dx.doi.org/10.5061/dryad.h6j0g4p>) and can be freely accessed as virtual representation of the type. In addition to the cybertype data at Dryad, we also provide a freely accessible 3D surface model of the holotype at Sketchfab (<https://skfb.ly/6txMy>).

Diagnosis. *Proceratium kepingmai* differs from the other members of the *P. itoi* clade by the following character combination: large species (TL 4.39–4.54); sides of head weakly convex, broadest at level of eyes and gently narrowing anteriorly and stronger posteriorly; vertex almost straight; very reduced eyes (OI 2–3) consisting of a single minute ommatidium; frontal carinae well developed, with large lamellae that extend laterally above the antennal insertions; frontal furrow darker than the surrounding anterior cephalic dorsum; posterodorsal corners of the propodeum broadly angular; propodeal declivity densely punctured, mostly opaque; posterior face of petiolar node in profile steeper than anterior face and about half as long as anterior face; apex of petiolar node distinctly broader than long in dorsal view; in addition to dense pubescence, erect hairs present on scapes and dorsal surface of body, longest of those hairs at most as long as the maximum dorsoventral diameter of metafemur.

Worker measurements. Holotype. TL 4.39; EL 0.02; SL 0.57; HL 0.92; HLM 1.08; HW 0.86; WL 1.14; MFeL 0.71; MTiL 0.60; MBaL 0.44; PeL 0.45; PeW 0.36; LT3 0.64; LS4 0.32; LT4 1.08; OI 2; CI 92; SI 60; MFeI 83; MTiI 70; MBaI 51; DPeI 80; IGR 0.30; ASI 169.

Paratype. TL 4.54; EL 0.03; SL 0.59; HL 0.98; HLM 1.14; HW 0.90; WL 1.24; MFeL 0.79; MTiL 0.65; MBaL 0.48; PeL 0.46; PeW 0.37; LT3 0.65; LS4 0.34; LT4 1.05; OI 3; CI 93; SI 62; MFeI 88; MTiI 72; MBaI 53; DPeI 80; IGR 0.33; ASI 161.

Worker description. In full-face view, head slightly longer than broad (CI 92–93), sides weakly convex, broadest at the eye level and gently narrowing anteriorly and (stronger) posteriorly, vertex weakly convex, almost straight. Clypeus reduced and

narrow, with a broadly triangular median anterior projection. Frontal carinae relatively short, moderately separated, slightly covering antennal insertions, constantly diverging posteriorly, lateral expansions of anterior part of frontal carinae developed as broad lamellae, raised, conspicuously and broadly extending laterally above antennal insertions; frontal area convex; frontal furrow well developed as a raised carina, starting at the clypeal projection and extending over the anterior 2/5 of the cephalic dorsum, with a short gap at the level where the lamellae of frontal carinae are broadest. Eyes reduced, minute (OI 2–3), consisting of a single ommatidium and located on midline of head. Antennae 12-segmented, scapes short (SI 60–62), not reaching posterior head margin and thickening apically. Mandibles elongate and triangular, masticatory margin with four teeth in total, apical tooth long and acute, the other teeth smaller and decreasing in size from second to fourth tooth, gap between second and third tooth larger than between other teeth.

Mesosoma in profile slightly convex and slightly longer than maximum head length including mandibles (WL 1.14–1.24 vs. HLM 1.08–1.14). Lower mesopleurae (katepisterna) with well-demarcated sutures, upper mesopleurae (anepisterna) with inconspicuous sutures, no other sutures developed on lateral and dorsal mesosoma; lower mesopleurae weakly inflated posteriorly; posterodorsal corner of propodeum broadly angular, propodeal lobes weakly developed as bluntly rounded lamellae; propodeal declivity almost vertical, slightly inclined anteriorly; in posterodorsal view sides of propodeum separated from declivity by distinct lamellate margins; in profile propodeal spiracle rounded, at mid height, opening of spiracle slightly facing posteriorly. Legs moderately long; all tibiae with a pectinate spur; calcar of strigil without a basal spine; pretarsal claws simple; arolia present.

Petiolear node in profile high, nodiform, with a straight and sloping anterior face, dorsum of node broadly rounded, posterior face half as long and steeper than anterior face; petiole in dorsal view longer than broad but apex of node clearly broader than long; ventral process moderately developed on anterior petiole, with a relatively indistinct rectangular projection.

In dorsal view abdominal segment III anteriorly much broader than petiole; its sides convex; abdominal sternite III anteriomedially with a conspicuous depression marked by a thin rim. Constriction between abdominal segments III and IV deep. Abdominal segment IV very large, recurved (IGR 0.30–0.33) and posteriorly strongly rounded, with a lamella on its anterior border around the constriction to abdominal segment III, this lamella thicker ventrally than dorsally; abdominal tergum IV 1.6–1.7× longer than abdominal tergum III (ASI 161–169); remaining abdominal tergites and sternites inconspicuous and projecting anteriorly. Sting large and extended.

Whole body covered with dense mat of short, decumbent to suberect pubescent hairs; additionally, the dorsal surfaces of body interspersed with significantly longer suberect and erect hairs, such hairs also present on abdominal sterna III + IV, scapes (anterior faces of scapes with many hairs, posterior faces with single hairs), and legs

(ventral faces of femora and tibiae with many hairs, dorsal faces with single hairs); the longest hairs on dorsal surface of body at most as long as the maximum dorsoventral diameter of metafemur. Mandibles striate; entire body including propodeal declivity densely punctate; on sides of pronotum punctures aligned in diffuse lines, appearing striate; punctures on antennae, legs, and abdominal segment IV finer than on rest of body, abdominal segments V–VII very superficially punctured and shiny. Body color uniformly orange brown to reddish brown, vertex of head slightly darker, frontal furrow conspicuously darker than surrounding cephalic dorsum, legs, antennal funiculus, and abdominal segments V–VII yellowish brown.

Etymology. The species epithet is a patronym in honor of the Chinese botanist Prof. Keping Ma and his efforts in establishing the BEF-China project and promoting biodiversity research and nature conservation in China. All specimens of this species were collected in old-growth subtropical forest, an ecosystem Prof. Ma has investigated in detail.

Distribution and ecology. Both specimens were collected in secondary mixed evergreen broadleaved forest of relatively advanced age, as indicated by the presence of large trees. The paratype was collected within the Gutianshan National Nature Reserve (Yu et al. 2001, Bruelheide et al. 2011, Staab 2014), one of the larger remaining fragments of subtropical broadleaved forest in southeast China. The forest at this locality (the type locality is a similar but much smaller forest fragment) is on sloped land and rich in plant species; more than 250 woody species have been recorded on about 8000 ha. Approximately 50% of the woody species are deciduous but the tree layer is dominated by evergreen species including *Castanopsis eyrei* (Fagaceae) (Champ. ex Benth.) Tutch., *Cyclobalanopsis glauca* (Fagaceae) (Thunb.) Oerst., *Machilus thunbergii* (Lauraceae) Sieb. et Zucc., and *Schima superba* (Theaceae) Gardn. et Champ. No direct observations of biology and natural history are available for *P. kepingmai*.

Taxonomic notes. *Proceratium kepingmai* is the largest (WL 1.14–1.24) member of the *P. itoi* clade and has, even for eye-bearing *Proceratium*, very minute eyes (OI 2–3). From each of the species in the clade with very similar body proportions (particularly indices) that also have erect hairs on the dorsal surface of the body (*P. itoi*, *P. longmenense*, *P. malesianum*, *P. bruelheidei*; no erect hairs, only dense pubescence in *P. williamsi*, *P. zhaoi*) it can safely be separated by one or more characters. In *P. kepingmai* the posterodorsal corner of the propodeum is angular (rounded in *P. itoi* and *P. malesianum*), which is also the case for *P. longmenense* and *P. bruelheidei*. However, *P. longmenense* lacks erect hairs on the scape (at least some erect hairs present in *P. kepingmai* and *P. bruelheidei*), has a relatively narrower head (CI 85) with longer scapes (SI 68) (CI 92–93 and SI 60–62 in *P. kepingmai*), and frontal carinae that touch each other at their anteriormost level (clearly separated in *P. kepingmai* and *P. bruelheidei*). With *P. bruelheidei*, the most similar species, *P. kepingmai* also shares the broad frontal carinae that have large lamellae and are conspicuously extended laterally above the antennal insertions (not extended and narrower in *P. longmen-*

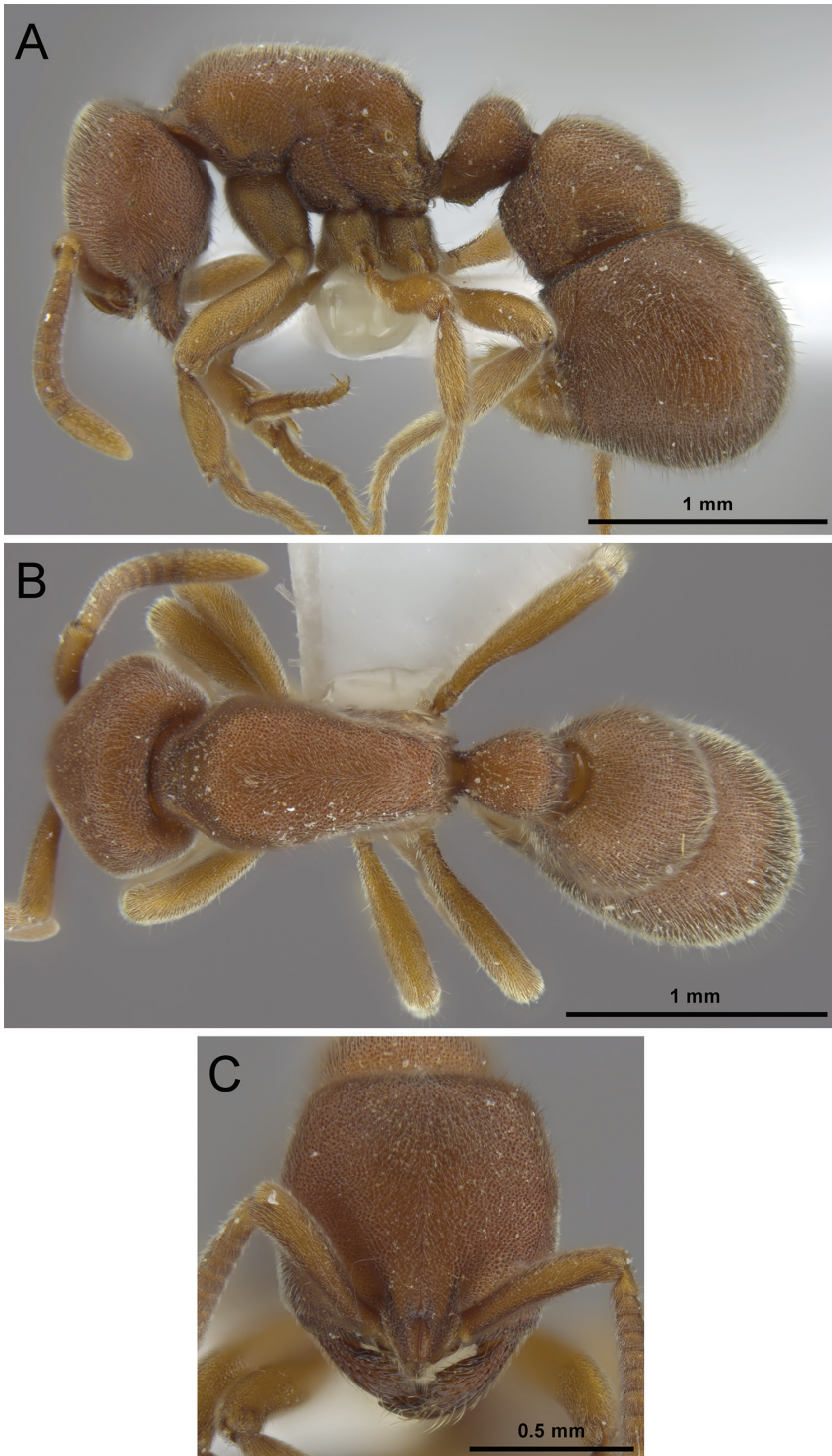


Figure 12. *Proceratium kepingmai* sp. n. holotype worker (CASENT0790031). **A** Body in profile **B** Body in dorsal view **C** Head in full-face view.

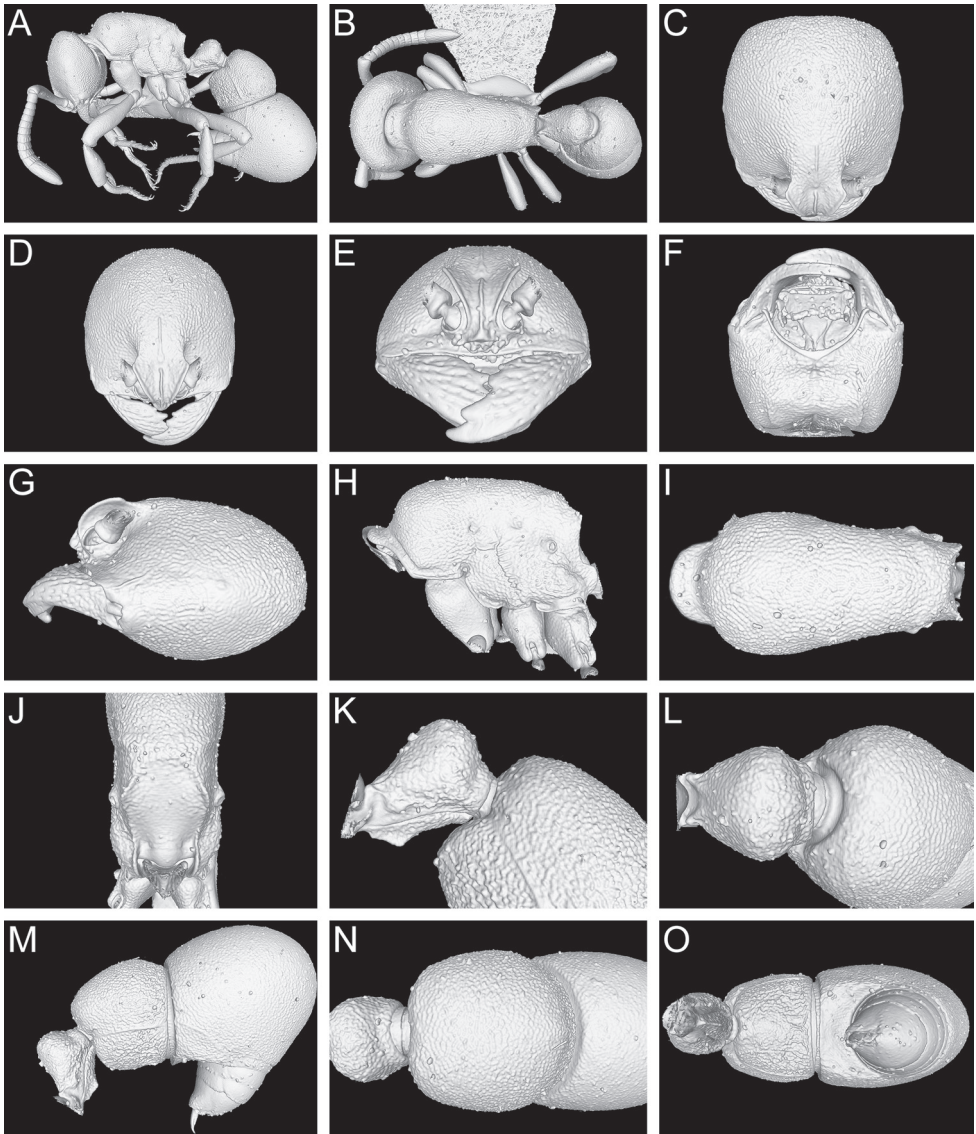


Figure 13. Still images from surface display volume renderings of 3D model of *Proceratium keepingmai* sp. n. holotype worker (CASENT0790031). **A** Body in profile **B** Body in dorsal view **C** Head in dorsal view **D** Head in anterodorsal view **E** Head in anterior view **F** Head in ventral view **G** Head in profile **H** Mesosoma in profile **I** Mesosoma in dorsal view **J** Propodeum in posterodorsal view **K** Abdominal segment II and parts of III in profile **L** Abdominal segment II and parts of III in dorsal view **M** Abdominal segments II–VII in profile **N** Abdominal segment III and parts of II and IV in dorsal view **O** Abdominal segments II–VII in ventral view.

ense). In contrast, *P. keepingmai* differs from *P. bruelheidei* by the shape of the head in full-face view that has convex sides, which are broadest at the level of the eyes and narrow weakly anteriorly and more strongly posteriorly towards to almost straight vertex (sides straight, not narrowing anteriorly and vertex convex in *P. bruelheidei*),

the densely punctured and mostly opaque propodeal declivity (sparsely and superficially punctured and very shiny in *P. bruelheidei*), the conspicuous frontal furrow that is darker than the rest of the surrounding anterior cephalic dorsum (inconspicuous and of same color in *P. bruelheidei*), the posterior face of petiolar node in profile steeper than the anterior face of the node and about half as long as the anterior face (posterior face as steep as anterior face and less than half as long in *P. bruelheidei*), the apex of the petiolar node that is clearly broader than long in dorsal view (less broad than long in *P. bruelheidei*), and relatively fewer and shorter erect hairs (see *P. bruelheidei* for details).

Variation. Apart from the small difference in body size (WL 1.14 vs. 1.24) there is no observable variation between the two specimens.

Proceratium longmenense Xu, 2006

Figs 6A, 14, 25

Proceratium longmenense Xu, 2006: 154 (w.), China

Type material. Holotype. Pinned worker from CHINA, Yunnan Province, Kunming City, Xishan Mountain Forest Park, Longmen, subtropical evergreen broadleaf forest, 2050 m asl, 5-V-2001, leg. Zhenghui Xu, No. A00514 (in SWFU) [examined].

Diagnosis. *Proceratium longmenense* differs from the other members of the *P. itoi* clade by the following character combination: medium-sized species (TL 3.2); sides of head and vertex weakly convex, almost straight; head (CI 85) and scapes (SI 68) relatively long; frontal carinae developed, their lateral lamellae relatively narrow, touching each other at their anteriormost level, not conspicuously broader above antennal insertions; posterodorsal corners of the propodeum broadly angular; posterior face of petiolar node in profile shorter and steeper than anterior face; petiole almost as broad as long (DPeI 91); subpetiolar process developed, roughly trapezoid; in addition to dense pubescence erect hairs present on dorsal surface of body, but only sparsely on head, scapes without erect hairs.

Distribution and ecology. This species is only known from the holotype that was collected in subtropical evergreen broadleaved forest at 2050 m asl. No direct observations of biology and natural history are available for *P. longmenense*.

Taxonomic notes. The unique hair patterns separate *P. longmenense* from the other species of the *P. itoi* clade. *Proceratium williamsi* and *P. zhaoi* have no erect hairs that protrude from the dense pubescence on the dorsal surface of body (hairs present in *P. longmenense*, but relatively sparsely, especially on head). All other species (*P. bruelheidei*, *P. itoi*, *P. kepingmai*, *P. malesianum*) have also such hairs on the scapes (absent on scapes in *P. longmenense*). In addition to hairs, which may be worn down in old specimens, *P. longmenense* is unique by the relatively long scapes (SI 68) combined with the relatively narrow head (CI 85). Among the other Chinese *P. itoi* clade species, it differs furthermore from *P. zhaoi* in size (WL 0.97; WL < 80 in *P. zhaoi*), from

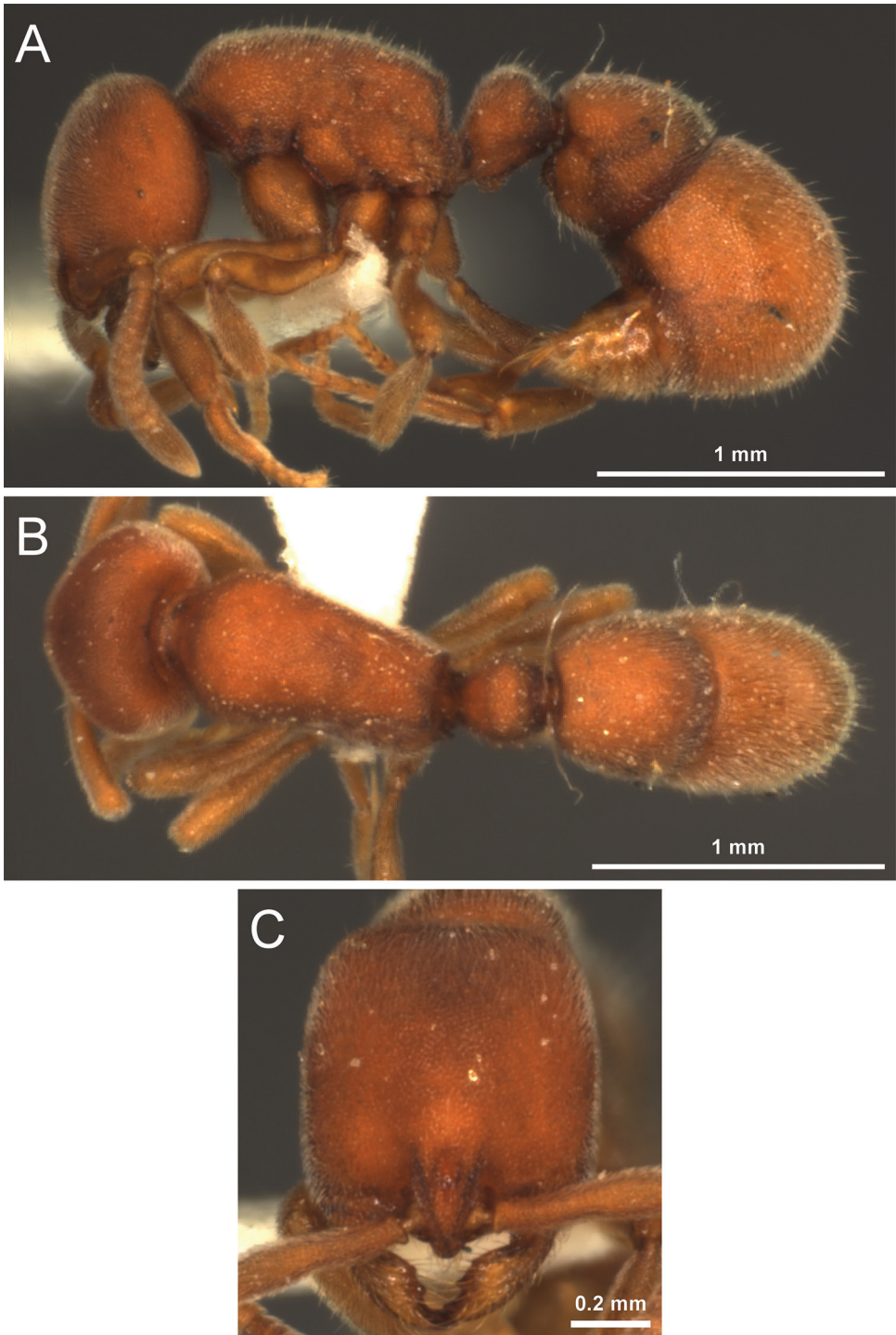


Figure 14. *Proceratium longmenense* holotype worker. **A** Body in profile **B** Body in dorsal view **C** Head in full-face view.

P. itoi by the shape of the posterodorsal corners of the propodeum (broadly angular; rounded in *P. itoi*), and from *P. bruelheidei*, *P. itoi*, and *P. kepingmai* by the lamellae of the frontal carinae (touching each other at their anteriormost level; separated in the other three species).

***Proceratium zhaoi* Xu, 2000**

Figs 4A, 15, 16, 17, 25

Proceratium zhaoi Xu, 2000: 435 (w.q.), China

Proceratium nujiangense Xu, 2006: 153 (w.q.), China, **syn. n.**

Type material. Of *P. zhaoi*: Holotype. Pinned worker from CHINA, Yunnan Province, Menghai County, Meng'a Town, Papo Village, 1280 m asl, deciduous broad-leaved forest, soil sample, 10-IX-1997, leg. Zheng-Hui Xu, No. A97-2338 (in SWFU) [examined].

Paratypes. Six pinned workers and 24 alate females; one worker with same data as holotype; all other paratypes with same data as holotype but No. A97-2380 (CASENT0235334 in CASC; CASENT0790671 and all other paratypes in SWFU) [all examined].

Of *P. nujiangense*: Holotype. Pinned worker from CHINA, Yunnan Province, Baoshan City, Lujiang Town, Bawan, 1500 m asl, *Pinus yunnanensis* forest on east slope of Nujiang River Valley, 11-VIII-1998, leg. Qizhen Long, label "A98-1964" (in SWFU) [examined].

Paratypes. Seven pinned workers and 10 queens with same data as holotype but No. A98-1995, No. A98-1997, No. A98-2010, No. A98-2016, No. A98-2029 (CASENT0790672 and all other paratypes in SWFU) [all examined].

Virtual dataset. Volumetric raw data (in DICOM format), 3D rotation videos (in .mp4 format, see Suppl. material 6: Video 4 for *P. zhaoi* and Suppl. material 7: Video 5 for *P. nujiangense*), still images of surface volume rendering, and 3D surfaces (in PLY format) of a paratype of *P. zhaoi* (CASENT07900671) and a paratype of *P. nujiangense* (CASENT0790672) in addition to montage photos illustrating head in full-face view, profile and dorsal views of the body. The data is deposited at Dryad (Staab et al. 2018, <http://dx.doi.org/10.5061/dryad.h6j0g4p>) and can be freely accessed as virtual representations of the species. In addition to the data at Dryad, we also provide freely accessible 3D surface models at Sketchfab (<https://skfb.ly/6txOT> and <https://skfb.ly/6txOL>).

Diagnosis. *Proceratium zhaoi* differs from the other members of the *P. itoi* clade by the following character combination: small species (TL 2.0–2.8, WL 0.66–0.80; measurements and indices use data from the original descriptions); of head weakly convex, broadest at level of eyes and gently narrowing anteriorly and posteriorly, posterior head margin weakly concave to almost straight; frontal carinae developed,

their lateral lamellae relatively narrow, not extending over antennal insertions; posterodorsal corners of propodeum bluntly angled; posterior face of petiolar node, in profile, shorter and steeper than anterior face, dorsum of node broadly rounded, petiole as long as broad or broader than long (DPEI 98–110), subpetiolar process developed, relatively variable, varying in size and shape (from rectangular to triangular to acutely toothed); only dense pubescence, no erect hairs on dorsum of body, head, and scapes.

Distribution and ecology. This species is only known from two locations at mid elevation in forests of southern and western Yunnan Province. The original description reported 45 workers in the type colony (Xu 2000) and no other data on natural history have been published. However, the relatively short legs suggest a purely hypogeic life style, which conforms to the fact that specimens were extracted from soil samples.

Taxonomic notes. Even though at the beginning of this study we treated *P. nujiangense* and *P. zhaoi* as distinct species, thorough examinations combining traditional microscopy with micro-CT scans proved that there are no morphological characters separating them. The virtual comparisons of type specimens of both taxa showed that there are no morphological differences, a fact that is not easy to observe by comparing physical specimens. The types are hairy, dirty, and mounted in ways that hide most important characters, as it is typical for most *Proceratium* specimens. Furthermore, the main character used by Xu (2006) to separate the species was the subpetiolar process, which has been used for species diagnostics in previous studies (Baroni Urbani and de Andrade 2003, Hita Garcia et al. 2014, 2015). However, these works either had very little material for the assessment of intraspecific variation and/or treated different clades of *Proceratium*. Our study shows that the subpetiolar process is extremely variable within the *P. itoi* clade and refrain from using it for species delimitations. As a matter of fact, the variation of the subpetiolar process was already noted in the description of *P. zhaoi* (Xu 2000). Reexamination of all type specimens of both species also revealed a comparatively high degree of variation and overlap in the form of the posterodorsal corner of the propodeum and the width of the propodeal node. In addition, the morphometric ranges of *P. nujiangense* and *P. zhaoi* overlap and form a continuum, and there are no significant differences in proportions since all indices are identical. Considering these similarities in light of the newly available images and micro-CT data, we propose treating *P. nujiangense* as a junior synonym of *P. zhaoi*.

This species was not mentioned in the revision of Baroni Urbani and de Andrade (2003), potentially because the authors were not aware of its description shortly before the completion of their monograph. Despite some size variation (TL 2.0–2.8), the relative body proportions of *P. zhaoi* are constant (CI 84–90, SI 61–66). *Proceratium zhaoi* is the smallest (WL 0.66–0.80) member of the *P. itoi* clade. It can be distinguished from all other *P. itoi* clade species (except for *P. williamsi*) by the absence of erect hairs that protrude through the dense pubescence on the dorsal body surface. *Proceratium williamsi* also lacks hairs on the dorsal body surface, but is larger (WL 0.80–0.92), has

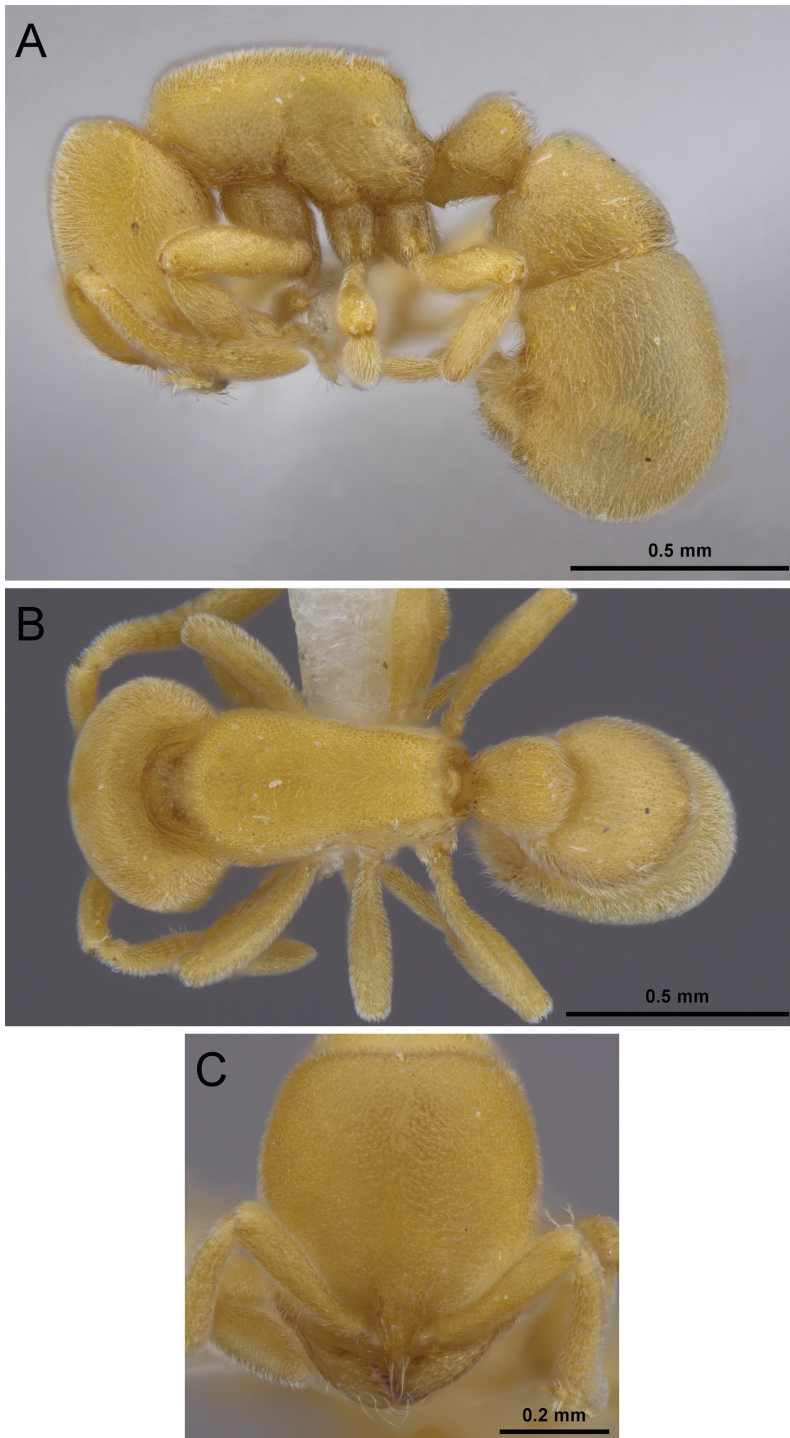


Figure 15. *Proceratium zhaii* paratype worker (CASENT0790671). **A** Body in profile **B** Body in dorsal view **C** Head in full-face view.

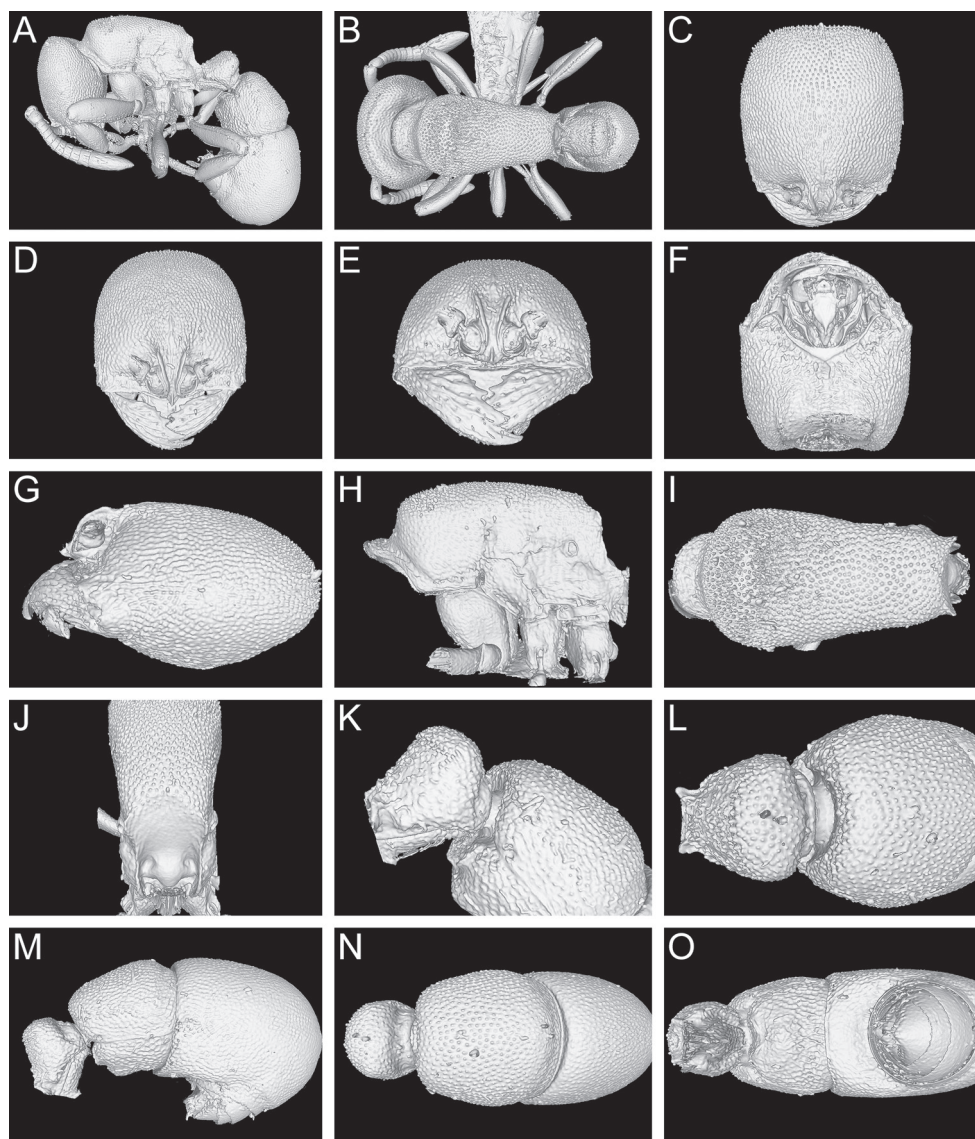


Figure 16. Still images from surface display volume renderings of 3D model of *Proceratium zhaii* paratype worker (CASENT0790671). **A** Body in profile **B** Body in dorsal view **C** Head in dorsal view **D** Head in anterodorsal view **E** Head in anterior view **F** Head in ventral view **G** Head in profile **H** Mesosoma in profile **I** Mesosoma in dorsal view **J** Propodeum in posterodorsal view **K** Abdominal segment II and parts of III in profile **L** Abdominal segment II and parts of III in dorsal view **M** Abdominal segments II–VII in profile **N** Abdominal segment III and parts of II and IV in dorsal view **O** Abdominal segments II–VII in ventral view.

stronger developed frontal carinae and relatively more slender and longer legs. The relatively weakly developed frontal carinae and the short legs (MFel <80, MTil <65, MBal <40) make *P. zhaii* also unique among the Chinese *P. itoi* clade species.

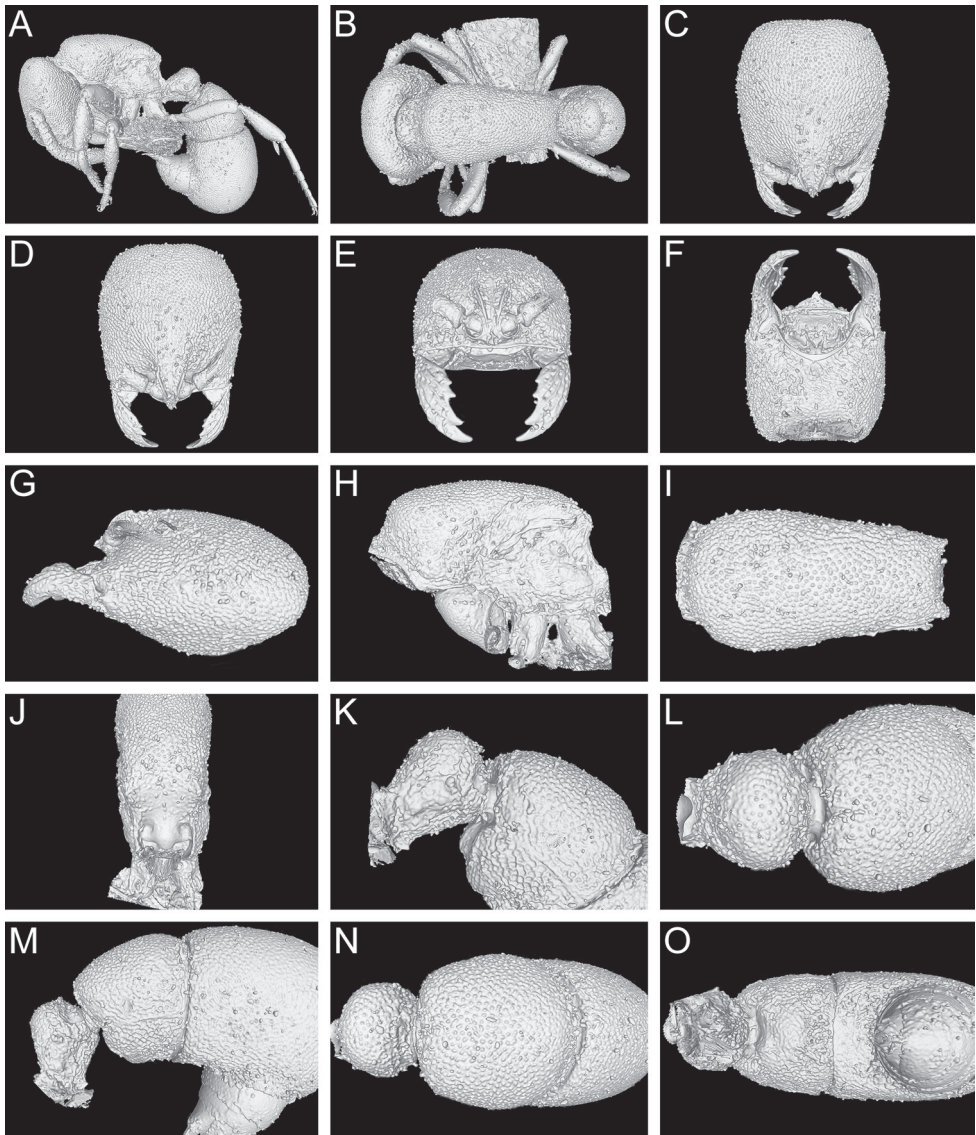


Figure 17. Still images from surface display volume renderings of 3D model of *Proceratium zhai* paratype worker of *P. nujiangense* (CASENT0790672). **A** Body in profile **B** Body in dorsal view **C** Head in dorsal view **D** Head in anterodorsal view **E** Head in anterior view **F** Head in ventral view **G** Head in profile **H** Mesosoma in profile **I** Mesosoma in dorsal view **J** Propodeum in posterodorsal view **K** Abdominal segment II and parts of III in profile **L** Abdominal segment II and parts of III in dorsal view **M** Abdominal segments II–VII in profile **N** Abdominal segment III and parts of II and IV in dorsal view **O** Abdominal segments II–VII in ventral view.

Proceratium silaceum clade

Definition. Workers of this clade can be distinguished by a moderately squamiform petiolar node that narrows only little from base to apex (extremely squamiform in the

Fiji archipelago, Hita Garcia et al. 2015) and by an almost straight to weakly concave anterior clypeal margin (definition follows Baroni Urbani and de Andrade 2003).

Comments. The *P. silaceum* clade sensu Baroni Urbani and de Andrade (2003) is, with more than 30 species, the most speciose and widespread clade within the genus. Numerous species occur in, respectively, Borneo and Australia. Species of this clade have been reported from all continents and several have reached oceanic islands. From China and east Asia only two species, *P. japonicum* and *P. longigaster*, are known.

***Proceratium japonicum* Santschi, 1937**

Figs 1A, 2B, 18, 19, 24

Proceratium japonicum Santschi, 1937: 362 (w.), Japan (see also Baroni Urbani and de Andrade 2003: 368, Onoyama and Yoshimura 2002: 38)

Proceratium formosicola Terayama, 1985: 406 (w.q.), Taiwan (junior synonym, see Onoyama 1991: 695)

Proceratium japonicum – Onoyama and Yoshimura 2002: 35 (q.m.), Japan

Type material. Of *P. japonicum*: Syntypes. Three pinned workers from JAPAN, Honshu, Oshima, Iya, Honshiu, 10.VI.28, leg. K. Sato (CASENT0915312, in NHMB) [images examined].

Of *P. formosicola*: Holotype. TAIWAN, Nantou Hsien, Lushan, ca. 100 m asl, 15-VIII.1980, leg. M. Terayama. (in NIAES) [not examined].

Paratypes. Two pinned workers and one queen with same data as holotype; one pinned worker from TAIWAN, Nantou Hsien, Puli, 4-VIII.1981, leg. M. Terayama (TARI) [not examined].

Non-type material examined. JAPAN: Okinawa, Ishigaki Island, Mt. Omoto, 1-IV-1975, leg. M. Tanaka (CASENT0281854, in BMNH); JAPAN, Okinawa, Irimote Island, Shirahama, 6-V-2000, leg. M. Yoshimura (OKENT0019995; OKENT0019996, both in OIST); JAPAN, Kanagawa, Odawara, Minazurimisaki, 27-VII-2000, leg. M. Yoshimura (CASENT0790834; OKENT0019998; OKENT0019999; OKENT0020000, all in OIST).

Virtual dataset. Volumetric raw data (in DICOM format), 3D rotation video (in .mp4 format, see Suppl. material 8: Video 6), still images of surface volume rendering, and 3D surface (in PLY format) of a non-type specimen (CASENT0790834) in addition to montage photos illustrating head in full-face view, profile and dorsal views of the body. The data is deposited at Dryad (Staab et al. 2018, <http://dx.doi.org/10.5061/dryad.h6j0g4p>) and can be freely accessed as virtual representation of the species. In addition to the data at Dryad, we also provide a freely accessible 3D surface model at Sketchfab (<https://skfb.ly/6txNO>).

Diagnosis. *Proceratium japonicum* differs from the other east Asian members of the *P. silaceum* clade by the following character combination: medium-sized species (WL 0.72–1.00); sides of head convex, broadest above the level of eyes; anterior clypeal margin not protruding and slightly notched; frontal carinae well developed and widely

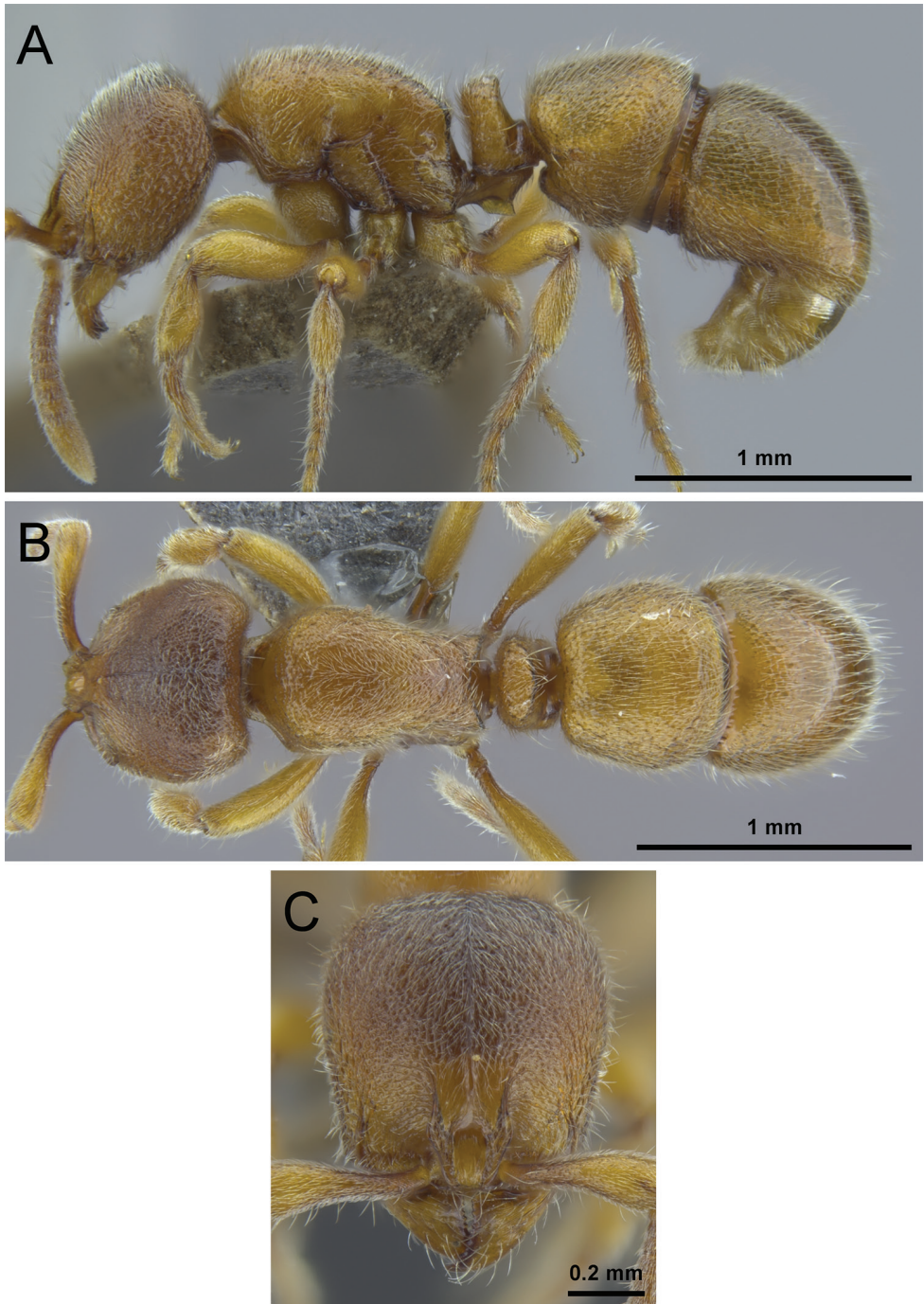


Figure 18. *Proceratium japonicum* non-type worker (CASENT0790834). **A** Body in profile **B** Body in dorsal view **C** Head in full-face view.

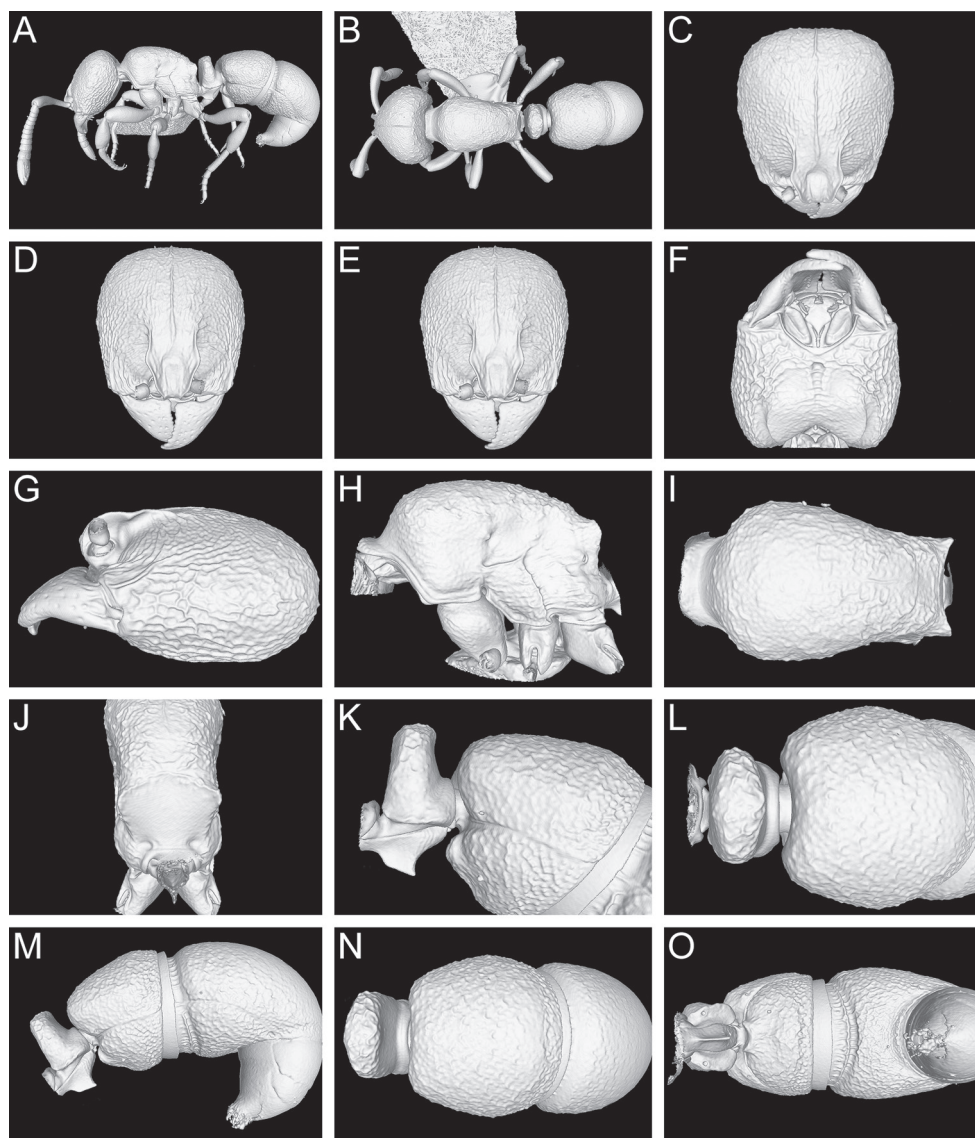


Figure 19. Still images from surface display volume renderings of 3D model of *Proceratium japonicum* non-type worker (CASENT0790834). **A** Body in profile **B** Body in dorsal view **C** Head in dorsal view **D** Head in anterodorsal view **E** Head in anterior view **F** Head in ventral view **G** Head in profile **H** Mesosoma in profile **I** Mesosoma in dorsal view **J** Propodeum in posterodorsal view **K** Abdominal segment II and parts of III in profile **L** Abdominal segment II and parts of III in dorsal view **M** Abdominal segments II–VII in profile **N** Abdominal segment III and parts of II and IV in dorsal view **O** Abdominal segments II–VII in ventral view.

separated, with large lamellae that extend laterally above the antennal insertions and reach posteriorly almost to the level of eyes; frontal furrow strongly developed; petiole squamiform, in profile not or only weakly narrowing dorsally, the base as or almost as

broad as the apex, in dorsal view relatively narrow (DPeI <150); subpetiolar process developed, subtriangular, directing backwards; sculpture not deeply impressed, on abdominal segment III granulate and relatively regular; in addition to dense pubescence, some suberect to erect hairs present on scapes and dorsal surface of body.

Distribution and ecology. This species is common from Japan (except Hokkaido) to Taiwan and usually collected in forests of relatively low elevation. It has also been reported from Yunnan Province in China. Thus, it is not unlikely that more records from the southern and eastern Chinese mainland will appear in the future if sampling effort is increased. No direct biological observations from China are available. In Japan, nests are typically found in deadwood in evergreen broadleaved forest (Onoyama and Yoshimura 2002). Colony size can reach over 150 workers and larval haemolymph feeding has been observed (Masuko 1986).

Taxonomic notes. According to Baroni Urbani and de Andrade (2003) *P. japonicum* is most similar to *P. numidicum* Santschi, 1912, which is, however, a geographically widely separated species occurring in the eastern Mediterranean and northern Africa. We were not able to examine *P. japonicum* material from China. In Japan, specimens from the Ryukyu and Yaeyama islands are smaller than from the main islands (Onoyama and Yoshimura 2002, Baroni Urbani and de Andrade 2003), explaining the relatively large variation in body size.

From *P. longigaster*, the only other *P. silaceum* clade species in China and east Asia, *P. japonicum* can be separated by the shape of the petiole in profile that not or only weakly narrows dorsally (clearly narrowing dorsally, broader on the base than on the apex in *P. longigaster*). Also, the petiole in dorsal view is narrower in *P. japonicum* (DPeI <150) than in *P. longigaster* (DPeI ≥155). Furthermore, the frontal carinae in *P. japonicum* reach posteriorly almost to the level of eyes (shorter and ending well below the level of eyes in *P. longigaster*). *Proceratium japonicum* has only relatively few suberect to erect hairs that protrude from the dense pubescence on the dorsal body; those hairs are straight (never shaggy) and do not conspicuously project from LT3 over the constriction between LT3 and LT4 (many shaggy hairs projecting in *P. longigaster*); if single longer hairs are present, then they are not shaggy.

Proceratium longigaster Karavaiev, 1935

Figs 2A, 20, 21, 25

Proceratium longigaster Karavaiev, 1935: 59 (w.), Vietnam (see also Xu 2000: 436, Baroni Urbani and de Andrade 2003: 438)

Type material. Holotype. VIETNAM, Central Annam, close to Tourane, Bana, 1400 m asl, 30-IX.1931, leg. K. Davydov (CASENT0916806, in SIZK) [images examined].

Non-type material examined. CHINA, Zhejiang Province, Gutianshan National Nature Reserve, ca. 30 km NW of Kaihua, 29°15'3"N, 118°8'34"E, 890 m asl, secondary subtropical mixed forest, Winkler extraction of a rotten log, 27-IV-

2015, leg. Merle Noack, all with label 'MS1857' (CASENT0790844 in CASC; CASENT0790673 and CASENT0790843 in SWFU; CASENT0790845 in BMNH; CASENT0790846 in ZMBH).

Virtual dataset. Volumetric raw data (in DICOM format), 3D rotation video (in .mp4 format, see Suppl. material 9: Video 7), still images of surface volume rendering, and 3D surface (in PLY format) of a non-type specimen (CASENT0790673) in addition to montage photos illustrating head in full-face view, profile and dorsal views of the body. The data is deposited at Dryad (Staab et al. 2018, <http://dx.doi.org/10.5061/dryad.h6j0g4p>) and can be freely accessed as virtual representation of the species. In addition to the data at Dryad, we also provide a freely accessible 3D surface model at Sketchfab (<https://skfb.ly/6txOA>).

Diagnosis. *Proceratium longigaster* differs from the other east Asian members of the *P. silaceum* clade by the following character combination: medium-sized species (WL 0.75–0.89); sides of head slightly convex, broadest directly above the level of eyes; anterior clypeal margin not protruding and slightly notched; frontal carinae well developed and widely separated, with large lamellae that extend laterally above the antennal insertions and reach posteriorly about half the distance to the level of eyes; frontal furrow strongly developed; petiole squamiform; in profile, narrowing dorsally, the base clearly broader than the apex; in dorsal view, relatively wide (DPeI ≥ 155); subpetiolar process developed, subtriangular, directing backwards and relatively acute; sculpture deeply impressed, on abdominal segment III irregularly granular to reticulate (more so on dorsum); very hairy species; in addition to dense pubescence, many appressed to erect hairs present on entire body; abundant, long appressed, shaggy hairs project from LT3 distinctly over the constriction between LT3 and LT4.

Worker measurements. (n=5). TL 2.66–3.10; EL 0.03–0.04; SL 0.42–0.46; HL 0.65–0.70; HLM 0.71–0.92; HW 0.60–0.66; WL 0.75–0.89; MFeL 0.43–0.54; MTiL 0.35–0.42; MBaL 0.26–0.29; PeL 0.20–0.22; PeW 0.31–0.34; LT3 0.43–0.49; LS4 0.28–0.30; LT4 0.56–0.63; OI 5; CI 92–98; SI 65–66; MFeI 71–83; MTiI 58–65; MBaI 42–45; DPeI 155–157; IGR 0.47–0.50; ASI 123–138.

Distribution and ecology. The type locality is at ca. 1400 m asl in the Bà Nà hills close to Đà Nẵng city (referred to as Tourane in the original description), central Vietnam. The species is also known from Nangongshan Mountain, Mengla County, Yunnan Province (Xu 2000) (1525 m asl) and from Hunan Province (Guénard and Dunn 2012). In the places where it is known, specimens were collected from the ground in evergreen broadleaved forest. The new record from the Gutianshan National Nature Reserve, Zhejiang Province, is no exception in being from the same forest type albeit at lower elevation (890 m asl) and marks the easternmost distribution of the species. Thus, *P. longigaster* seems to be widespread in suitable forest habitats in south and east China and adjacent countries. No direct observations of biology and natural history are available.

Taxonomic notes. This is a poorly known species. Since the single type specimen was not available for examination, Baroni Urbani and de Andrade (2003) were unable to formally treat it in their monograph. Karavaiev's (1935) type specimen is lodged in the Schmalhausen Institute of Zoology (Kiev, Ukraine) and cannot be obtained as

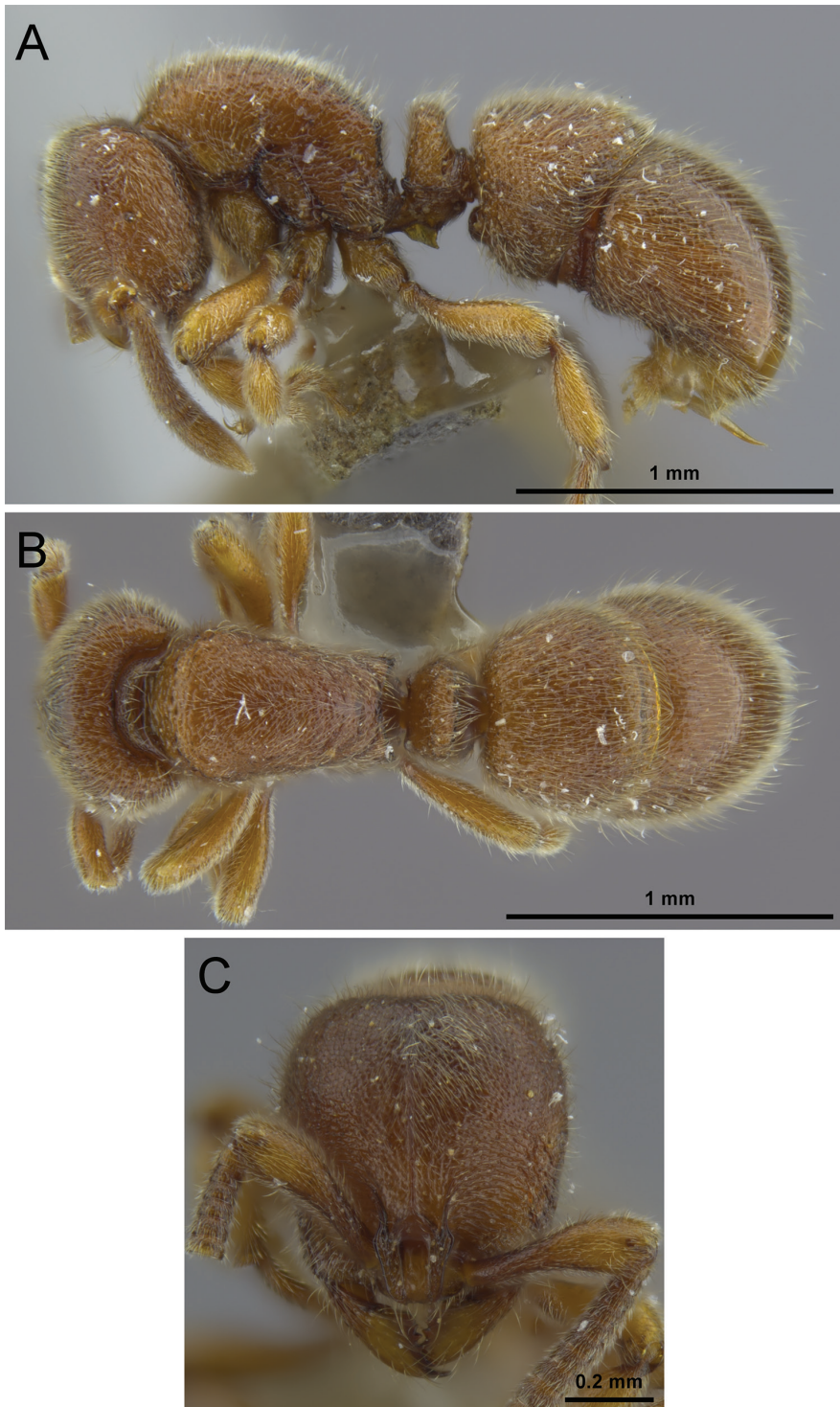


Figure 20. *Proceratium longigaster* non-type worker (CASENT0790673). **A** Body in profile **B** Body in dorsal view **C** Head in full-face view.

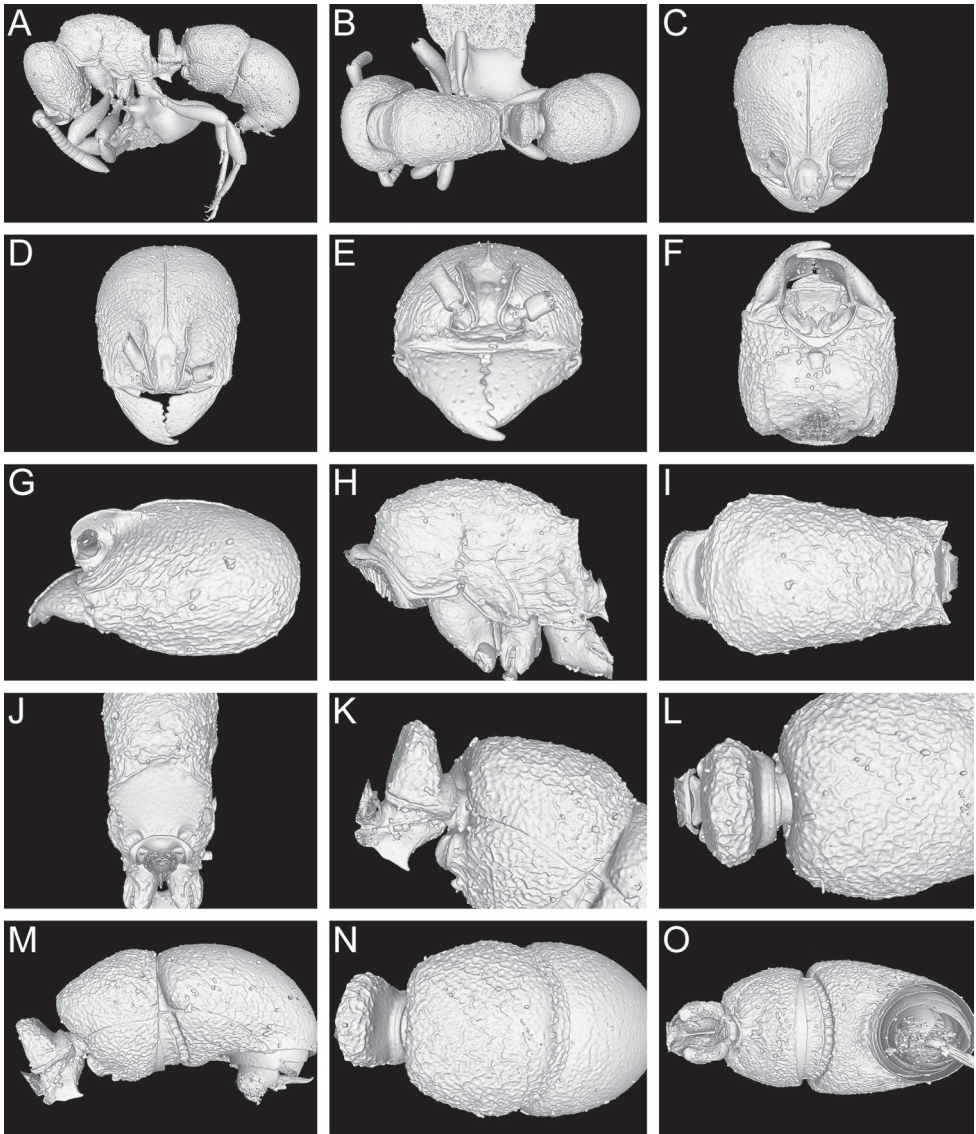


Figure 21. Still images from surface display volume renderings of 3D model of *Proceratium longigaster* non-type worker (CASENT0790673). **A** Body in profile **B** Body in dorsal view **C** Head in dorsal view **D** Head in anterodorsal view **E** Head in anterior view **F** Head in ventral view **G** Head in profile **H** Mesosoma in profile **I** Mesosoma in dorsal view **J** Propodeum in posterodorsal view **K** Abdominal segment II and parts of III in profile **L** Abdominal segment II and parts of III in dorsal view **M** Abdominal segments II–VII in profile **N** Abdominal segment III and parts of II and IV in dorsal view **O** Abdominal segments II–VII in ventral view.

a loan. Fortunately, though, it has recently been imaged and the montage photos are available on AntWeb (CASENT0916806). Our new specimens agree with the type and the accounts of Xu (2000). Thus, with a note of caution, we feel confident enough to treat the specimens from Zhejiang Province as *P. longigaster*.

The only other *P. silaceum* clade species known from China and east Asia is *P. japonicum*, from which *P. longigaster* can be separated by the shape of the petiolar node, the frontal carinae, and the pilosity, among other characters (see the accounts for *P. japonicum* above).

***Proceratium stictum* clade**

Definition. Worker of this clade can be separated from all other *Proceratium* by the combination of calcar of strigil with a basal spine and clypeus distinctly and broadly notched (definition follows Baroni Urbani and de Andrade 2003).

Comments. This is an exclusively tropical clade with species occurring in Africa, Australia, Madagascar, the Mascarene Islands, Mesoamerica, and tropical southeast Asia. Eleven extant species are known, of which *P. deelemani* Perrault, 1981, *P. foveolatum* Baroni Urbani and de Andrade, 2003, *P. stictum* Brown, 1958, and the newly described *P. shobei* are known from the oriental zoogeographic region. *Proceratium shobei* is the only species known from China.

***Proceratium shobei* Staab, Xu & Hita Garcia sp. n.**

<http://zoobank.org/09C9335F-C01F-4B6A-B289-1E6B9611E96F>

Figs 3A, 3C, 22, 23, 25

Type material. Holotype. Pinned worker from CHINA, Yunnan Province, Xishuangbanna, Kilometer 55 station, 21.964°N / 101.202°E, 820 m asl, rain forest, Winkler leaf litter extraction, 13-VI-2013, leg. Benoit Guénard, Benjamin Blanchard & Cong Liu, label '#05121' (CASENT0717686), deposited in SWFU.

Cybertype. Volumetric raw data (in DICOM format), 3D rotation video (in mp4 format, see Suppl. material 10: Video 8), still images of surface volume rendering, and 3D surface (in PLY format) of the physical holotype (CASENT0717686) in addition to montage photos illustrating head in full-face view, profile and dorsal views of the body. The data is deposited at Dryad (Staab et al. 2018, <http://dx.doi.org/10.5061/dryad.h6j0g4p>) and can be freely accessed as virtual representation of the type. In addition to the cybertype data at Dryad, we also provide a freely accessible 3D surface model of the holotype at Sketchfab (<https://sketchfab.com/models/0dd8217041274f268fae8897958d9b6a>).

Diagnosis. *Proceratium shobei* differs from the other oriental members of the *P. stictum* clade by the following character combination: head broadest at the level of eyes, sides and vertex of head weakly convex, almost straight; scapes relatively long (SI 72); frontal carinae relatively broad and slightly convex; posterodorsal corners of propodeum with broad teeth that project over less than half of the propodeal lobes in profile; petiole in dorsal view longer than broad; petiolar node relatively compressed dorsoventrally, subpetiolar process inconspicuous, a lamellae only, without a projec-

tion; LS3 with a straight ventral outline; abdominal segment IV strongly recurved and broadly rounded, LS4 reduced (IGR not measurable); head, mesosoma, petiole, and LT3 foveolate; LT4 smooth and shiny, dorsally without sculpture, laterally superficially punctured.

Worker measurements. Holotype. TL 4.15; EL 0.09; SL 0.71; HL 0.99; HLM 1.13; HW 0.89; WL 1.25; MFeL 0.89; MTiL 0.71; MBaL 0.56; PeL 0.47; PeW 0.44; LT3 0.64; LS4 n.a.; LT4 0.66; OI 10; CI 90; SI 72; MFeI 100; MTiI 80; MBaI 63; DPeI 94; IGR n.a.; ASI 103.

Worker description. In full-face view, head slightly longer than broad (CI 90), sides and vertex weakly convex, almost straight. Clypeus relatively broad, surrounding antennal insertions and protruding anteriorly, anterior clypeal margin with a distinct notch. Frontal carinae relatively short, broadly separated from each other, constantly diverging posteriorly and not covering antennal insertions, lateral expansions of frontal carinae slightly concave in full-face view; frontal area convex; frontal furrow absent. Genal carinae strongly developed; ventral face of head (gular area) concave. Eyes relatively large (OI 10), consisting of one convex ommatidium, located slightly anterior to the midline of head. Antennae 12-segmented, scapes comparatively long (SI 72), not reaching posterior head margin and thickening apically. Mandibles elongate and triangular, masticatory margin with three teeth in total, apical tooth large and acute, the other teeth smaller and decreasing in size from second to third tooth that is followed by a series of minute blunt denticles.

Mesosoma in profile convex and longer than maximum head length including mandibles. Lower mesopleurae (katepisterna) with demarcated sutures, upper mesopleurae (anepisterna), and promesonotum with inconspicuous and very shallow sutures; lower mesopleurae inflated posteriorly; posterodorsal corners of propodeum with broad teeth that project over less than half of the propodeal lobes in profile, propodeal lobes strongly developed as broadly triangular teeth protruding dorsolaterally; propodeal declivity almost vertical, slightly inclined anteriorly; in posterodorsal view, sides of propodeum separated from declivity by lamellate margins; propodeal spiracle relatively small, located above mid height; in profile, opening ellipsoid and facing posteriorly. Legs comparatively long; all tibiae with a pectinate spur; calcar of strigil with a basal spine; pretarsal claws simple; arolia present.

Petiole in dorsal view longer than broad, sides consistently diverging posteriorly, anterior border with a thick margin that is distinctly angulate on each side; in profile, petiolar node relatively compressed dorsoventrally, its anterior face slightly sloping; dorsum of node relatively flat, weakly convex; ventral face inconspicuous with a thin lamella and no projection.

In dorsal view, abdominal segment III anteriorly much broader than petiole, its sides weakly convex; abdominal sternite III extended ventrally, its outline straight, anteriomedially with a conspicuous depression marked by a broad rim. Constriction between abdominal segments III and IV deep. Abdominal segment IV very large, very strongly recurved (abdominal sternum IV reduced and IGR not measurable) and posteriorly rounded, with a thin lamella on its anterior border; abdominal tergum IV

slightly longer than abdominal tergum III (ASI 103), remaining abdominal tergites and sternites inconspicuous and projecting anteriorly. Sting large and extended.

Whole body covered with dense relatively short decumbent to erect hairs; additionally significantly longer suberect to erect hairs abundant on the whole body, including legs and scapes; such hairs also present on funicular joints, but shorter and relatively thicker; dense appressed to decumbent pubescence on the funiculus only; mandibles striate; head, mesosoma, petiole, and abdominal segment III foveolate with superimposed punctures and granules, the foveae relatively deep, large, and irregular; abdominal segment IV smooth and shiny, dorsally without sculpture, laterally superficially punctured; scapes and legs densely punctured. Body color uniformly dark ferruginous-brown, antennae, legs, and abdominal segments V–VII orange brown.

Etymology. This species is named in honor of Dr. Shohei Suzuki (1979–2016), a Japanese marine biologist whose life was tragically lost in a diving accident while conducting coral reef research in Okinawa.

Distribution and ecology. No direct observations of biology and natural history are available. The type specimen was collected from rain forest leaf litter. Like many other ant species occurring in the tropical rain forest of Xishuangbanna, the species probably also occurs in adjacent countries such as Laos or Thailand.

Taxonomic notes. In Liu et al. (2015b) this species was erroneously listed as *P. deelemani*, a species known from Borneo, peninsular Malaysia, and Thailand (see Baroni Urbani and de Andrade 2003). However, a careful reexamination of the specimen from Yunnan and comparisons with images of the holotype of *P. deelemani* (CASENT0915370) and further *P. deelemani* specimens from Borneo (CASENT0790842, CASENT0790847, CASENT0790848; see Suppl. material 2: Figure S1 for micro CT images of CASENT0790842 and see Suppl. material 11: Video 9 for a 3D rotation video of the same specimen) revealed considerable morphological differences that convinced us to separate both species and to describe *P. shohei* as new. Among the other species of the *P. stictum* clade occurring in the oriental zoogeographic region (*P. deelemani*, *P. foveolatum*, *P. stictum*), *P. shohei* is unsurprisingly most similar to *P. deelemani*, but both species can be safely and easily separated. *Proceratium shohei* has an indistinct subpetiolar process without a median anterior projection (subpetiolar process with a distinct tooth in *P. deelemani*; opposed to the *P. itoi* clade, the subpetiolar process is an informative character in the *P. stictum* clade). Also, *P. shohei* has relatively longer scapes (SI 72) (SI 58–68 in *P. deelemani*), the posterodorsal corner of the propodeum with relatively shorter teeth that project over less than half of the length of the propodeal lobes in profile (at least projecting over half of propodeal lobes in *P. deelemani*), a very reduced LS4 so that IGR cannot be measured (LS4 also reduced but IGR 0.23–0.29 in *P. deelemani*), a straight ventral outline of LS3 (with a depression in *P. deelemani*), and slightly convex frontal carinae (slightly concave in *P. deelemani*). Superficially, *P. shohei* also resembles *P. stictum* and *P. foveolatum*. From *P. stictum* it can be distinguished by the subpetiolar process without a median anterior projection (subpetiolar process with a distinct tooth in *P. stictum*), the longer teeth on the posterodorsal corners of the propodeum that project straightly backwards (short

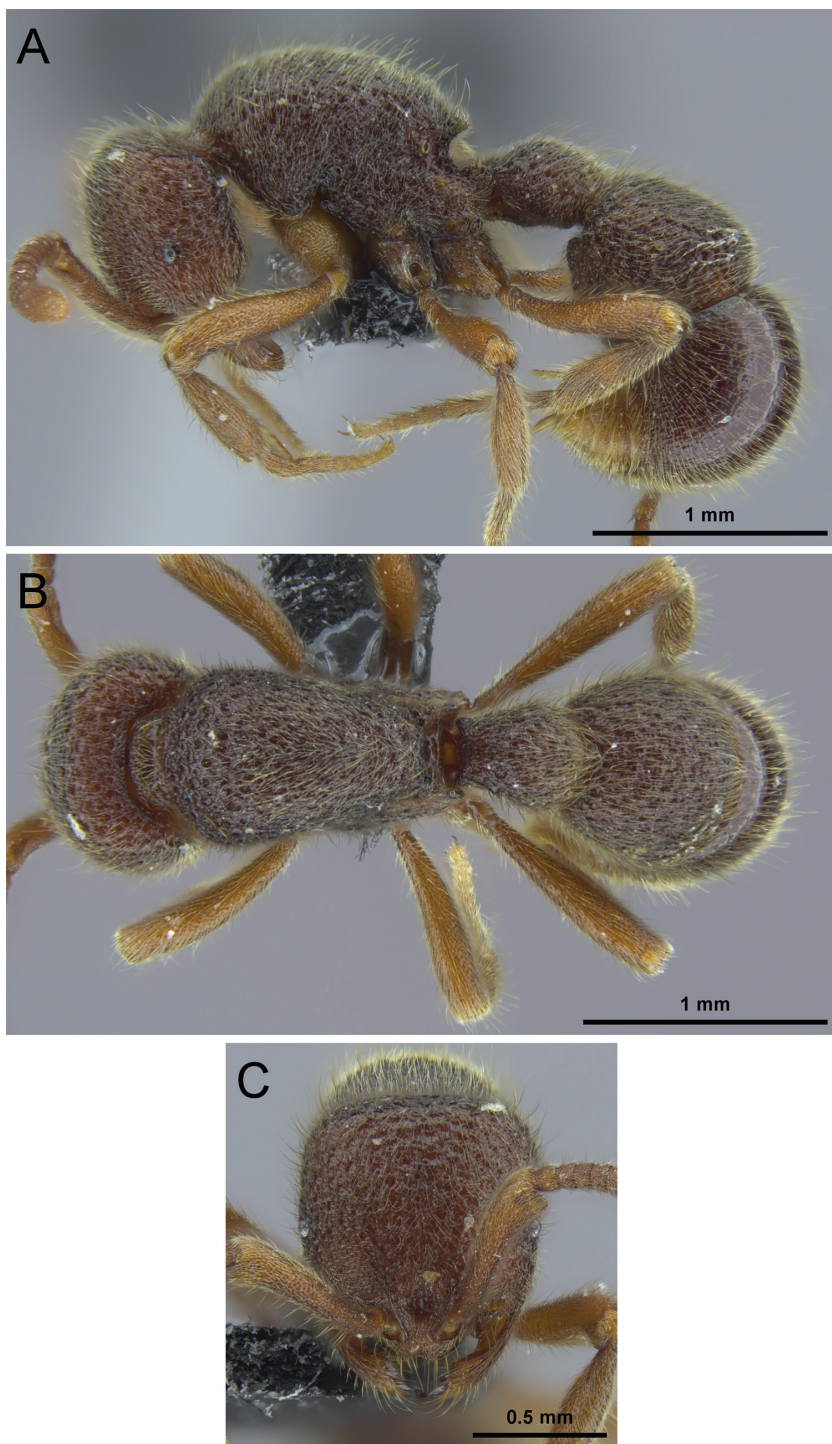


Figure 22. *Proceratium shobei* sp. n. holotype worker (CASENT0717686). **A** Body in profile **B** Body in dorsal view **C** Head in full-face view.

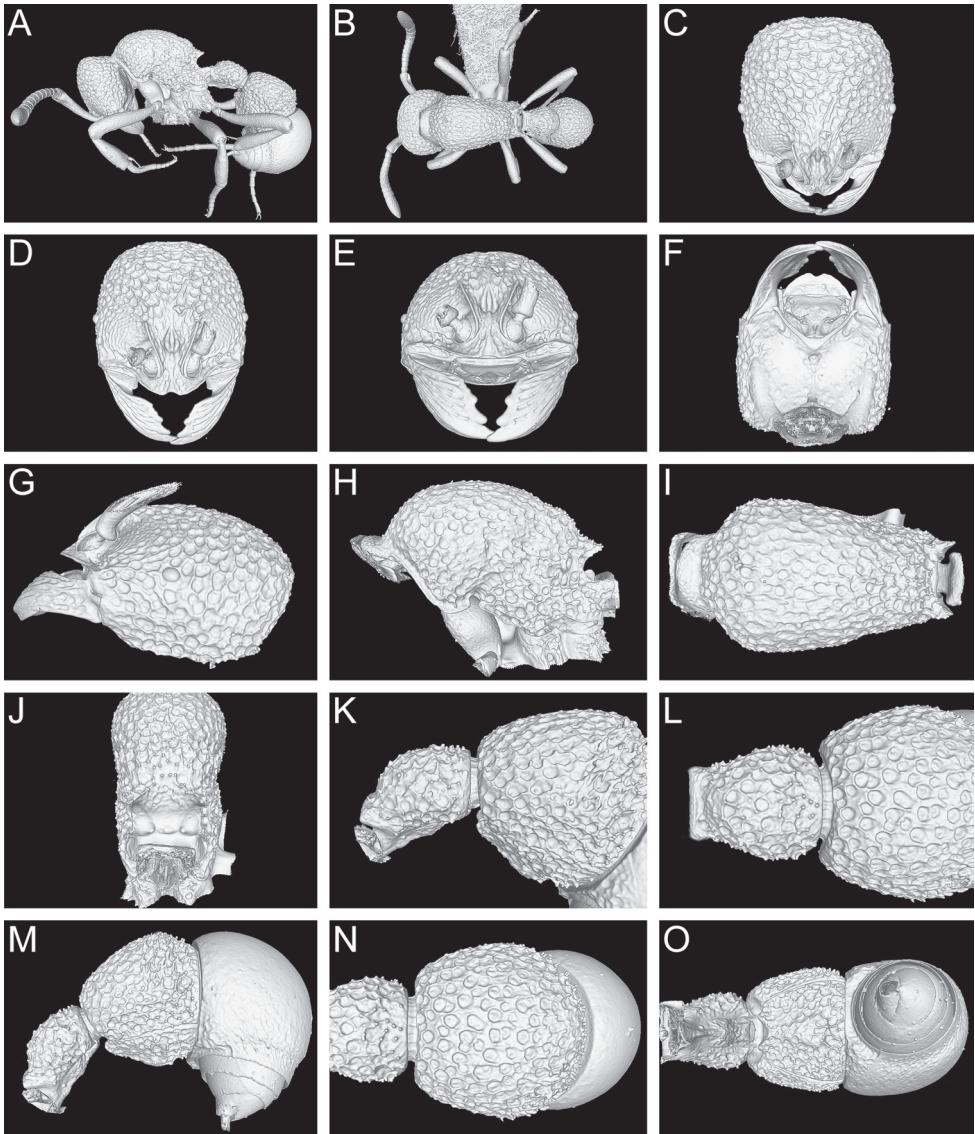


Figure 23. Still images from surface display volume renderings of 3D model of *Proceratium shobei* sp. n. holotype worker (CASENT0717686). **A** Body in profile **B** Body in dorsal view **C** Head in dorsal view **D** Head in anterodorsal view **E** Head in anterior view **F** Head in ventral view **G** Head in profile **H** Mesosoma in profile **I** Mesosoma in dorsal view **J** Propodeum in posterodorsal view **K** Abdominal segment II and parts of III in profile **L** Abdominal segment II and parts of III in dorsal view **M** Abdominal segments II–VII in profile **N** Abdominal segment III and parts of II and IV in dorsal view **O** Abdominal segments II–VII in ventral view.

and blunt, projecting slightly dorsally in *P. stictum*), and the foveolate sculpture of the head, mesosoma, petiole, and LT3 (coarsely granulate with superimposed fovea in *P. stictum*). The sculpture of the integument likewise easily distinguishes *P. shobei* from

P. foveolatum, which has the entire integument including LT4 covered with large, deep, regular, and clearly demarcated fovea (fovea smaller and shallower, at most superficial punctures but no fovea on LT4 in *P. shohei*). Also, in *P. foveolatum* LT4 is extended posteriorly and forms a broad, strong angle while LT4 is not as extended and broadly rounded in *P. shohei*.

Variation. Since this species is known only from the holotype there is no available information about intraspecific variation.

Discussion

The genus *Proceratium* in China

As for most other regions in which *Proceratium* occur, collection records and distributional information for the Chinese fauna is very limited, which is likely a consequence of the species' cryptobiotic and partly subterranean lifestyle. This is especially true for the *P. itoi* clade that based on currently available information seems to be restricted to east and southeast Asia (Baroni Urbani and de Andrade 2003, Guénard et al. 2017). All species of this clade except *P. malesianum* (Peninsular Malaysia) and *P. williamsi* (Buthan; India) have been recorded from China but are generally only known from few locations. Further collections targeting leaf litter and soil (Wong and Guénard 2017) will be necessary to clarify species-specific distribution ranges. It is expected that several species of the genus, of which some might also be new to science, occur in the large areas in south and southeast China that lack records so far (Guénard et al. 2017). Increased specimen availability will also allow associating queens and males to workers, as both reproductive castes are only known for *P. itoi* and *P. japonicum* (Onoyama and Yoshimura 2002, Baroni Urbani and de Andrade 2003), while for *P. zhaoi* queens have been described (Xu 2000).

Recently, Liu et al. (2015b) recorded *P. deelemani* Perrault, 1981, a conspicuous large-bodied species originally described from Borneo, from the tropical rain forests of Xishuangbanna, Yunnan Province. After careful reexamination of the single available specimen, we find that this species differs in several important characters from *P. deelemani* and describe it as *P. shohei*. The species belongs to the *P. stictum* clade and represents the northernmost record of this tropical clade in Asia.

With the exception of *P. bruelheidei*, which type habitat is an early successional tree plantation with relatively open soil and comparatively little litter cover, all other Chinese species have only been collected from old-growth forests. Unfortunately, forests in tropical and subtropical China have been heavily transformed and fragmented (e.g. Zhang and Song 2006, Li et al. 2009), which has largely unknown but likely negative consequences for native ant assemblages (e.g. Liu et al. 2016).

Direct observations of ecology and natural history are very rare for Chinese *Proceratium*. To the best of our knowledge, the nest size of 45 individuals for the type colony of *P. zhaoi* given by Xu (2000) is the only published information on that mat-

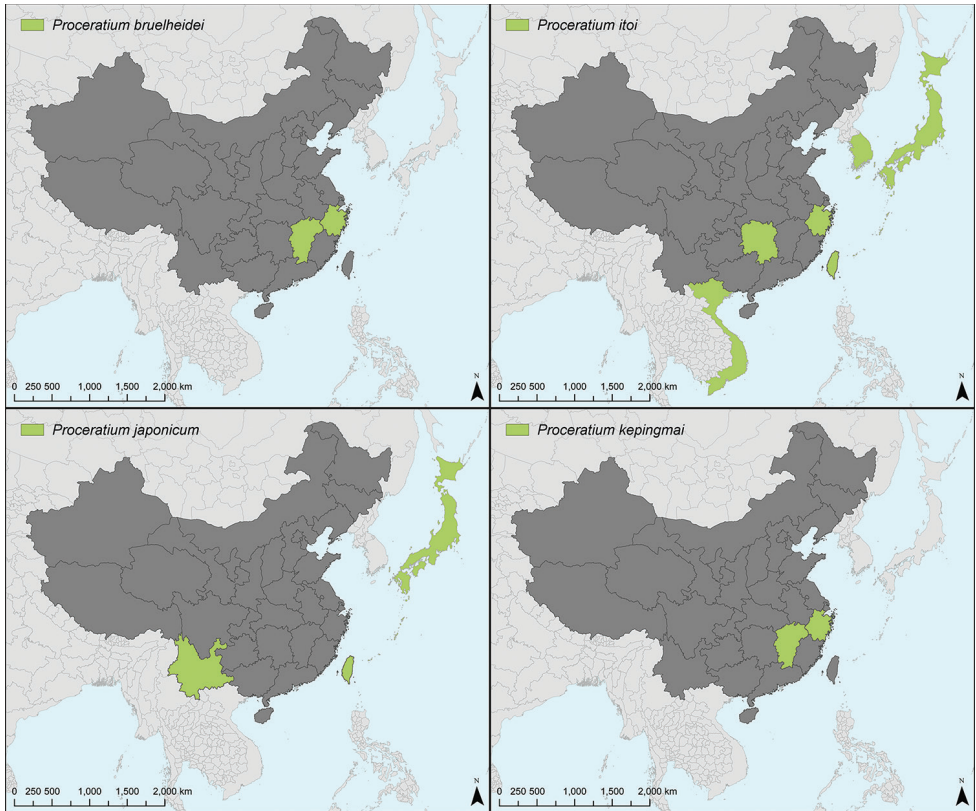


Figure 24. Maps of China (country is shown in dark grey with highlighted country and province borders) and South East Asia displaying known species distribution ranges (in green) of *P. bruelheidei*, *P. itoi*, *P. japonicum*, and *P. kepingmai*.

ter. We assume that the general natural history of the Chinese species conforms to the observations from other parts of the world outlined above (Baroni Urbani and de Andrade 2003). This life history is also documented for the Japanese populations of *P. japonicum* and *P. itoi* (Masuko 1986, Onoyama and Yoshimura 2002), two species that occur in China. As for distribution ranges and habitat preferences, further observations and collections will be necessary to extend our knowledge on natural history.

Microtomography

One problem encountered by Hita Garcia et al. (2017b) was the poor recovery of pilosity in the 3D reconstructions due to insufficient voxel resolution, which was resolved in Hita Garcia et al. (2017a) by scanning single body parts at higher resolutions. Nevertheless, in this study, we aimed to turn this handicap into an advantage. Like most proceratiines, the Chinese species of *Proceratium* are very hairy and covered in a thick

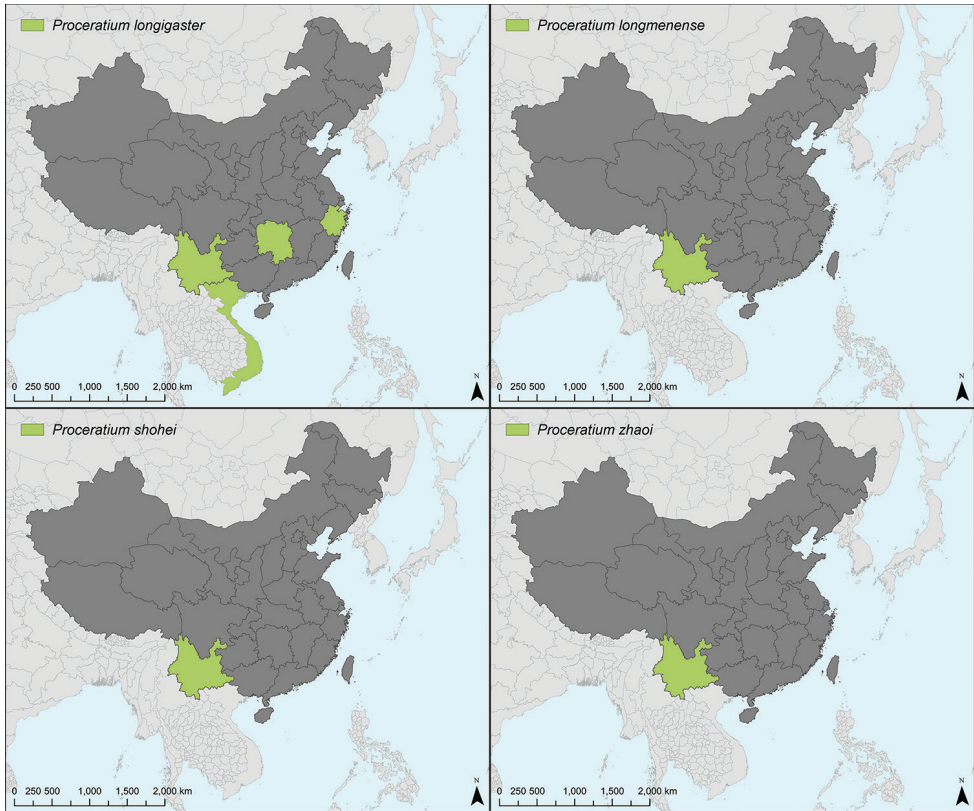


Figure 25. Maps of China (country is shown in dark grey with highlighted country and province borders) and South East Asia displaying known species distribution ranges (in green) of *P. longigaster*, *P. longmenense*, *P. shobei*, and *P. zhaoi*.

pelt, which makes morphological examinations challenging. The furry coats cover and hide important character states, such as surface sculpture, and, to make things worse, many specimens are extremely dirty due to numerous soil particles caught within the hairs. Furthermore, potentially harmful cleaning or dissections of specimens are out of the question since, as is typical for the genus in general, the available Chinese material is way too scarce and valuable.

By applying micro-CT scanning and virtually “shaving” the specimens, we were able to examine proceratiine morphology in more detail resulting in clearer diagnostic character definitions and species delimitations without causing any physical harm to the few available specimens. This approach might also be useful for morphological examinations of other very hairy groups of ants, such as *Discothyrea* Roger or many species of *Tetramorium* Mayr (previously grouped in the genus *Triglyphothrix* Forel). For those ants it could complement high-resolution montage images illustrating specimens including pilosity and hairs, which can be diagnostic characters and useful for species identifications, as illustrated with the present study.

Acknowledgements

We thank the administration of the Gutianshan National Nature Reserve for granting research permissions for the forests under their management. The land of the BEF-China Main Experiment is owned by the Xingangshan Forestry Company, which is gratefully acknowledged for allowing research on their property. Merle Noack, Andreas Schuldt, Benoit Guénard, Benjamin Blanchard, and Masashi Yoshimura collected or provided specimens. We thank Adam Khalife for his assistance with processing the videos and Kenneth Dudley for the generation of the maps used in this study. The work of Michael Staab in China was funded by the German Research Foundation (DFG FOR 891/3, KL 1849/6-2), with travel support from the Sino German Center for Research Promotion (GZ 1146). Cong Liu, Francisco Hita Garcia, and Evan Economo were supported by subsidy funding from the Okinawa Institute of Science and Technology Graduate University.

References

- Agavekar G, Hita Garcia F, Economo EP (2017) Taxonomic overview of the hyperdiverse ant genus *Tetramorium* Mayr (Hymenoptera, Formicidae) in India with descriptions and X-ray microtomography of two new species from the Andaman Islands. PeerJ 5: e3800. <https://doi.org/10.7717/peerj.3800>
- Akkari N, Enghoff H, Metscher BD (2015) A new dimension in documenting new species: high-detail imaging for myriapod taxonomy and first 3D cybertype of a new millipede species (Diplopoda, Julida, Julidae). PLoS ONE 10: e0135243. <https://doi.org/10.1371/journal.pone.0135243>
- Barden P, Grimaldi D (2012) Rediscovery of the bizarre Cretaceous ant *Haidomyrmex* Dlussky (Hymenoptera: Formicidae), with two new species. American Museum Novitates 3755: 1–16. <https://doi.org/10.1206/3755.2>
- Baroni Urbani C, de Andrade ML (2003) The ant genus *Proceratium* in the extant and fossil record (Hymenoptera: Formicidae). Museo Regionale di Scienze Naturali Monografie (Turin) 36: 1–492.
- Berry RP, Ibbotson MR (2010) A three-dimensional atlas of the honeybee neck. PLoS ONE 5: e10771. <https://doi.org/10.1371/journal.pone.0010771>
- Beutel RG, Ge S-Q, Hörschemeyer T (2008) On the head morphology of *Tetraphalerus*, the phylogeny of Archostemata and the basal branching events in Coleoptera. Cladistics 24: 270–298. <https://doi.org/10.1111/j.1096-0031.2007.00186.x>
- Blanchard BD, Moreau CS (2017) Defensive traits exhibit an evolutionary trade-off and drive diversification in ants. Evolution 71: 315–328. <https://doi.org/10.1111/evo.13117>
- Bolton B (2018) An online catalog of the ants of the world. <http://antcat.org> [Accessed 01 February 2018]
- Borowiec ML, Rabeling C, Brady SG, Fisher BL, Schultz TR, Ward PL (2017) Compositional heterogeneity and outgroup choice influence the internal phylogeny of the ants. bioRxiv 173393. <https://doi.org/10.1101/173393>

- Brady SG, Schultz TR, Fisher BL, Ward PS (2006) Evaluating alternative hypotheses for the early evolution and diversification of ants. *Proceedings of the National Academy of Sciences of the United States of America* 103: 18172–18177. <https://doi.org/10.1073/pnas.0605858103>
- Brown WL (1957) Predation of arthropod eggs by the ant genera *Proceratium* and *Discothyrea*. *Psyche* 64: 115. <https://doi.org/10.1155/1957/45849>
- Brown WL (1958) Contributions toward a reclassification of the Formicidae. II. Tribe Ecatommini (Hymenoptera). *Bulletin of the Museum of Comparative Zoology at Harvard College* 118: 173–362.
- Brown WL (1979) A remarkable new species of *Proceratium*, with dietary and other notes on the genus (Hymenoptera: Formicidae). *Psyche* 86: 337–346. <https://doi.org/10.1155/1979/78461>
- Bruelheide H, Böhnke M, Both S, Fang T, Assmann T, Baruffol M, Bauhus J, Buscot F, Chen XY, Ding BY, Durka W, Erfmeier A, Fischer M, Geissler C, Guo DL, Guo LD, Härdtle W, He JS, Hector A, Kröber W, Kühn P, Lang AC, Nadrowski K, Pei KQ, Scherer-Lorenzen M, Shi XZ, Scholten T, Schuldt A, Trogisch S, von Oheimb G, Welk E, Wirth C, Wu YT, Yang XF, Zeng XQ, Zhang SR, Zhou HZ, Ma KP, Schmid B (2011) Community assembly during secondary forest succession in a Chinese subtropical forest. *Ecological Monographs* 81: 25–41. <https://doi.org/10.1111/2041-210x.12126>
- Bruelheide H, Nadrowski K, Assmann T, Bauhus J, Both S, Buscot F, Chen XY, Ding BY, Durka W, Erfmeier A, Gutknecht JLM, Guo DL, Guo LD, Härdtle W, He JS, Klein AM, Kühn P, Liang Y, Liu X, Michalski S, Niklaus PA, Pei KQ, Scherer-Lorenzen M, Scholten T, Schuldt A, Seidler G, Trogisch S, von Oheimb G, Welk E, Wirth C, Wubet T, Yang XF, Yu MJ, Zhang SR, Zhou HZ, Fischer M, Ma KP, Schmid B (2014) Designing forest biodiversity experiments: general considerations illustrated by a new large experiment in subtropical China. *Methods in Ecology and Evolution* 5: 74–89. <https://doi.org/10.1111/2041-210x.12126>
- Carbayo F, Lenihan JW (2016) Micro-computed tomography scan and virtual histological slide data for the land planarian *Obama otavioi* (Platyhelminthes). *GigaScience* 5: 1–6. <https://doi.org/10.1186/s13742-016-0119-4>
- Carbayo F, Francoy TM, Giribet G (2016) Non-destructive imaging to describe a new species of *Obama* land planarian (Platyhelminthes, Tricladida). *Zoologica Scripta* 45: 566–578. <https://doi.org/10.1111/zsc.12175>
- Csósz S (2012) Nematode infection as significant source of unjustified taxonomic descriptions in ants (Hymenoptera: Formicidae). *Myrmecological News* 17: 27–31.
- Deans AR, Mikó I, Wipfler B, Friedrich F (2012) Evolutionary phenomics and the emerging enlightenment of arthropod systematics. *Invertebrate Systematics* 26: 323–330. <https://doi.org/10.1071/IS12063>
- Evenhuis NL (2018) The insect and spider collections of the world website. <http://hbs.bishop-museum.org/codens/> [Accessed 01 February 2018]
- Faulwetter S, Vasileiadou A, Kouratoras M, Dailianias T, Arvanitidis C (2013) Micro-computed tomography: introducing new dimensions to taxonomy. *ZooKeys* 263: 1–45. <https://doi.org/10.3897/zookeys.335.6030>
- Fernández R, Kvist S, Lenihan J, Giribet G, Ziegler A (2014) Sine systemate chaos? A versatile tool for earthworm taxonomy: Non-destructive imaging of freshly fixed and museum speci-

- mens using micro-computed tomography. PLoS ONE 9: e96617. <https://doi.org/10.1371/journal.pone.0096617>
- Fischer G, Sarnat E, Economo EP (2016) Revision and microtomography of the *Pheidole knowlesi* group, an endemic ant radiation in Fiji (Hymenoptera, Formicidae, Myrmicinae). PLoS ONE 11: e0158544. <https://doi.org/10.1371/journal.pone.0158544>
- Fisher BL (2005) A new species of *Discothyrea* Roger from Mauritius and a new species of *Proceratium* Roger from Madagascar (Hymenoptera: Formicidae). Proceedings of the California Academy of Sciences 56: 657–667.
- Forel A (1918) Etudes myrmécologiques en 1917. Bulletin de la Société Vaudoise des Sciences Naturelles 51: 717–727. [in French]
- Friedrich F, Beutel RG (2008) Micro-computer tomography and a renaissance of insect morphology. Proceedings SPIE 2008 7078: 70781U. <https://doi.org/10.1117/12.794057>
- Friedrich F, Matsumura Y, Pohl H, Bai M, Hörschemeyer T, Beutel RG (2014) Insect morphology in the age of phylogenomics: innovative techniques and its future role in systematics. Entomological Science 17: 1–24. <https://doi.org/10.1111/ens.12053>
- Guénard B, Dunn RR (2012) A checklist of the ants of China. Zootaxa 3558: 1–77.
- Guénard B, Weiser MD, Gomez K, Narula N, Economo EP (2017) The Global Ant Biodiversity Informatics (GABI) database: synthesizing data on the geographic distribution of ant species (Hymenoptera: Formicidae). Myrmecological News 24: 83–89.
- Hita Garcia F, Hawkes PG, Alpert GD (2014) Taxonomy of the ant genus *Proceratium* Roger (Hymenoptera, Formicidae) in the Afrotropical region with a revision of the *P. arnoldi* clade and description of four new species. ZooKeys 447: 47–86. <https://doi.org/10.3897/zookeys.447.7766>
- Hita Garcia F, Sarnat EM, Economo EP (2015) Revision of the ant genus *Proceratium* Roger (Hymenoptera, Proceratiinae) in Fiji. ZooKeys 475: 97–112. <https://doi.org/10.3897/zookeys.475.8761>
- Hita Garcia F, Fischer G, Liu C, Audisio TL, Economo EP (2017a) Next-generation morphological character discovery and evaluation: an X-ray micro-CT enhanced revision of the ant genus *Zasphectus* Wheeler (Hymenoptera, Formicidae, Dorylinae) in the Afrotropics. ZooKeys 693: 33–93. <https://doi.org/10.3897/zookeys.693.13012>
- Hita Garcia F, Fischer G, Liu C, Audisio TL, Alpert GD, Fisher BL, Economo E (2017b) X-Ray microtomography for ant taxonomy: An exploration and case study with two new *Terataner* (Hymenoptera, Formicidae, Myrmicinae) species from Madagascar. PLoS ONE 12: e0172641. <https://doi.org/10.1371/journal.pone.0172641>
- Hörschemeyer T, Beutel RG, Pasop F (2002) Head structures of *Priacma serrata* Leconte (Coleoptera, Archostemata) inferred from X-ray tomography. Journal of Morphology 252: 298–314. <https://doi.org/10.1002/jmor.1107>
- Janicki J, Narula N, Ziegler M, Guénard B, Economo EP (2016) Visualizing and interacting with large-volume biodiversity data using client–server web-mapping applications: the design and implementation of antmaps.org. Ecological Informatics 32: 185–193 <https://doi.org/10.1016/j.ecoinf.2016.02.006>
- Karavaiev W (1935) Neue Ameisen aus dem Indo-Australischen Gebiet nebst Revision einiger Formen. Treubia 15: 57–117. [In German]

- Li H, Ma Y, Liu W, Liu W (2009) Clearance and fragmentation of tropical rain forest in Xishuangbanna, SW, China. *Biodiversity and Conservation* 18: 3421–3440. <https://doi.org/10.1007/s10531-009-9651-1>
- Liu C, Fischer G, Economo EP (2015a) A rare ant on Samoa: first record of the cryptic subfamily Proceratiinae (Hymenoptera, Formicidae) and description of a new *Proceratium* Roger species. *Journal of Hymenoptera Research* 46: 35–44. <https://doi.org/10.3897/jhr.46.5849>
- Liu C, Guénard B, Hita Garcia F, Yamane S, Blanchard B, Yang D-R, Economo E (2015b) New records of ant species from Yunnan, China. *ZooKeys*: 17–78. <https://doi.org/10.3897/zookeys.477.8775>
- Liu C, Guénard B, Blanchard B, Peng YQ, Economo EP (2016) Reorganization of taxonomic, functional, and phylogenetic ant biodiversity after conversion to rubber plantation. *Ecological Monographs* 86: 215–227. <https://doi.org/10.1890/15-1464.1>
- Masuko K (1986) Larval hemolymph feeding – a nondestructive parental cannibalism in the primitive ant *Amblyopone silvestrii* Wheeler (Hymenoptera, Formicidae). *Behavioral Ecology and Sociobiology* 19: 249–255. <https://doi.org/10.1007/bf00300639>
- Masuko K (2010) Nest density and distribution of subterranean ants in an evergreen broadleaf forest in Japan with special reference to *Amblyopone silvestrii*. *Entomological Science* 13: 191–198. <https://doi.org/10.1111/j.1479-8298.2010.00383.x>
- Mathew R, Tiwari RN (2000) Insecta: Hymenoptera: Formicidae. *Zoological Survey of India, State Fauna Series 4: Fauna of Meghalaya, Part 7*: 251–409.
- Michalik P, Ramírez MJ (2013) First description of the male of *Thaïda chepu* Platnick, 1987 (Araneae, Austrochilidae) with micro-computed tomography of the palpal organ. *ZooKeys* 352: 117–125. <https://doi.org/10.3897/zookeys.352.6021>
- Moreau CS, Bell CD, Vila R, Archibald SB, Pierce NE (2006) Phylogeny of the ants: diversification in the age of angiosperms. *Science* 312: 101–104. <https://doi.org/10.1126/science.1124891>
- Noack M (2016) Leaf litter as template for ant communities in a tree diversity experiment. MSc Thesis. Stuttgart, Germany: University of Hohenheim. 35 pp.
- Ogata K (1987) A generic synopsis of the poneroid complex of the family Formicidae in Japan (Hymenoptera). Part I. Subfamilies Ponerinae and Cerypachyinae. *ESAKIA* 25: 97–132.
- Onoyama K (1991) A new synonym of the ant *Proceratium japonicum* (Hymenoptera, Formicidae). *Japanese Journal of Entomology* 59: 695–696.
- Onoyama K, Yoshimura M (2002) The ants of the genus *Proceratium* (Hymenoptera: Formicidae) in Japan. *Entomological Science* 5: 29–49.
- Perrault GH (1981) *Proceratium deelemani*, nouvelle espèce de Kalimantan. *Nouvelle Revue d'Entomologie* 11: 189–193. [In French]
- Roger J (1863) Die neu aufgeführten Gattungen und Arten meines Formiciden-Verzeichnisses nebst Ergänzung einiger früher gegebenen Beschreibungen. *Berliner Entomologische Zeitschrift* 7: 131–217. <https://doi.org/10.1002/mmnd.18630070116> [In German]
- Santschi F (1912) Nouvelles fourmis de Tunisie. *Bulletin de la Société d'Histoire Naturelle de l'Afrique du Nord* 3: 172–175. [In French]
- Santschi F (1937) Fourmis du Japon et de Formose. *Bulletin et Annales de la Société Entomologique de Belgique* 77: 361–388. [In French]

- Sarnat E, Fischer G, Economo E (2016) Inordinate spinescence: taxonomic revision and microtomography of the *Pheidole cervicornis* species group (Hymenoptera, Formicidae). PLoS ONE 11: e0156709. <https://doi.org/10.1371/journal.pone.0156709>
- Sartori M, Kubiak M, Michalik P (2016) Deciphering genital anatomy of rare, delicate and precious specimens: first study of two type specimens of mayflies using micro-computed X-ray tomography (Ephemeroptera; Heptageniidae). Zoosymposia 11: 28–32. <https://doi.org/10.11646/zoosymposia.11.1.7>
- Simonsen TJ, Kitching IJ (2014) Virtual dissections through micro-CT scanning: a method for non-destructive genitalia ‘dissections’ of valuable Lepidoptera material. Systematic Entomology 39: 606–618. <https://doi.org/10.1111/syen.12067>
- Staab M (2014) A new species of the *Aenictus wroughtonii* group (Hymenoptera, Formicidae) from South-East China. ZooKeys 391: 65–73. <https://doi.org/10.3897/zookeys.391.7213>
- Staab M, Schuldt A, Assmann T, Bruelheide H, Klein AM (2014) Ant community structure during forest succession in a subtropical forest in South-East China. Acta Oecologica 61: 32–40. <https://doi.org/10.1016/j.actao.2014.10.003>
- Staab M, Fornoff F, Klein A-M, Blüthgen N (2017) Ants at plant wounds: a little-known trophic interaction with evolutionary implications for ant-plant interactions. American Naturalist 190: 442–450. <https://doi.org/10.1086/692735>
- Staab M, Hita Garcia F, Liu C, Xu Z-H, Economo EP (2018) Data from: Systematics of the ant genus *Proceratium* Roger (Hymenoptera, Formicidae, Proceratiinae) in China – with descriptions of three new species based on micro-CT enhanced next-generation-morphology. Dryad Digital Repository. <https://doi.org/10.5061/dryad.h6j0g4p>
- Stoev P, Komerički A, Akkari N, Liu S, Zhou X, Weigand AM, Hostens J, Hunter CI, Edmunds SC, Porco D, Zapparoli M, Georgiev T, Mietchen D, Roberts D, Faulwetter S, Smith V, Penev L (2013) *Eupolybothrus cavernicolus* Komerički & Stoev sp. n. (Chilopoda: Lithobiomorpha: Lithobiidae): the first eukaryotic species description combining transcriptomic, DNA barcoding and micro-CT imaging data. Biodiversity Data Journal 1: e1013. <https://doi.org/10.3897/BDJ.1.e1013>
- Terayama M (1985) Description of a new species of the genus *Proceratium* Roger from Taiwan (Hymenoptera, Formicidae). Kontyû 53: 406–408
- Wong MKL, Guénard B (2017) Subterranean ants: summary and perspectives on field sampling methods, with notes on diversity and ecology (Hymenoptera: Formicidae). Myrmecological News 25: 1–16.
- Xu Z-H (2000) A systematic study of the ant genus *Proceratium* Roger from China (Hymenoptera: Formicidae). Acta Zootaxonomica Sinica 25: 434–437.
- Xu Z-H (2006) Three new species of the ant genera *Amblyopone* Erichson, 1842 and *Proceratium* Roger, 1863 (Hymenoptera: Formicidae) from Yunnan, China. Myrmecological News 8: 151–155.
- Yu MJ, Hu ZH, Yu JP, Ding BY, Fang T (2001) Forest vegetation types in Gutianshan Natural Reserve in Zhejiang. Journal of Zhejiang University (Agriculture and Life Science) 27: 375–380. [In Chinese]
- Zhang Y, Song C (2006) Impacts of afforestation, deforestation, and reforestation on forest cover in China from 1949 to 2003. Journal of Forestry 104: 383–387.

Supplementary material 1

Table S1

Authors: Michael Staab, Francisco Hita Garcia, Cong Liu, Zheng-Hui Xu, Evan P. Economo

Data type: species data

Explanation note: Overview of specimens of non-Chinese *Proceratium* species examined in this study.

Copyright notice: This dataset is made available under the Open Database License (<http://opendatacommons.org/licenses/odbl/1.0/>). The Open Database License (ODbL) is a license agreement intended to allow users to freely share, modify, and use this Dataset while maintaining this same freedom for others, provided that the original source and author(s) are credited.

Link: <https://doi.org/10.3897/zookeys.770.24908.suppl1>

Supplementary material 2

Figure S1.

Authors: Michael Staab, Francisco Hita Garcia, Cong Liu, Zheng-Hui Xu, Evan P. Economo

Data type: multimedia

Explanation note: Still images from surface display volume renderings of 3D model of *Proceratium deelemani* non-type worker (CASENT0790842). **A** Body in profile **B** Body in dorsal view **C** Head in dorsal view **D** Head in anterodorsal view **E** Head in anterior view **F** Head in ventral view **G** Head in profile **H** Mesosoma in profile **I** Mesosoma in dorsal view **J** Propodeum in posterodorsal view **K** Abdominal segment II and parts of III in profile **L** Abdominal segment II and parts of III in dorsal view **M** Abdominal segments II–VII in profile **N** Abdominal segment III and parts of II and IV in dorsal view **O** Abdominal segments II–VII in ventral view.

Copyright notice: This dataset is made available under the Open Database License (<http://opendatacommons.org/licenses/odbl/1.0/>). The Open Database License (ODbL) is a license agreement intended to allow users to freely share, modify, and use this Dataset while maintaining this same freedom for others, provided that the original source and author(s) are credited.

Link: <https://doi.org/10.3897/zookeys.770.24908.suppl2>

Supplementary material 3

Video 1

Author: Francisco Hita Garcia

Data type: (Video file (.mp4))

Explanation note: *Proceratium bruelheidei* sp. n. holotype worker (CASENT0790023).
3D rotation video based on volumetric surface rendering of full body..

Copyright notice: This dataset is made available under the Open Database License (<http://opendatacommons.org/licenses/odbl/1.0/>). The Open Database License (ODbL) is a license agreement intended to allow users to freely share, modify, and use this Dataset while maintaining this same freedom for others, provided that the original source and author(s) are credited.

Link: <https://doi.org/10.3897/zookeys.770.24908.suppl3>

Supplementary material 4

Video 2

Author: Francisco Hita Garcia

Data type: (Video file (.mp4))

Explanation note: *Proceratium itoi* non-type worker (OKENT0016142). 3D rotation video based on volumetric surface rendering of full body.

Copyright notice: This dataset is made available under the Open Database License (<http://opendatacommons.org/licenses/odbl/1.0/>). The Open Database License (ODbL) is a license agreement intended to allow users to freely share, modify, and use this Dataset while maintaining this same freedom for others, provided that the original source and author(s) are credited.

Link: <https://doi.org/10.3897/zookeys.770.24908.suppl4>

Supplementary material 5

Video 3

Author: Francisco Hita Garcia

Data type: (Video file (.mp4))

Explanation note: *Proceratium kepingmai* sp. n. holotype worker (CASENT0790031).
3D rotation video based on volumetric surface rendering of full body.

Copyright notice: This dataset is made available under the Open Database License (<http://opendatacommons.org/licenses/odbl/1.0/>). The Open Database License (ODbL) is a license agreement intended to allow users to freely share, modify, and use this Dataset while maintaining this same freedom for others, provided that the original source and author(s) are credited.

Link: <https://doi.org/10.3897/zookeys.770.24908.suppl5>

Supplementary material 6

Video 4

Author: Francisco Hita Garcia

Data type: (Video file (.mp4))

Explanation note: *Proceratium zhaoi* paratype worker (CASENT0790671). 3D rotation video based on volumetric surface rendering of full body.

Copyright notice: This dataset is made available under the Open Database License (<http://opendatacommons.org/licenses/odbl/1.0/>). The Open Database License (ODbL) is a license agreement intended to allow users to freely share, modify, and use this Dataset while maintaining this same freedom for others, provided that the original source and author(s) are credited.

Link: <https://doi.org/10.3897/zookeys.770.24908.suppl6>

Supplementary material 7

Video 5

Author: Francisco Hita Garcia

Data type: (Video file (.mp4))

Explanation note: *Proceratium nujiangense* syn. n. paratype worker (CASENT0790672). 3D rotation video based on volumetric surface rendering of full body.

Copyright notice: This dataset is made available under the Open Database License (<http://opendatacommons.org/licenses/odbl/1.0/>). The Open Database License (ODbL) is a license agreement intended to allow users to freely share, modify, and use this Dataset while maintaining this same freedom for others, provided that the original source and author(s) are credited.

Link: <https://doi.org/10.3897/zookeys.770.24908.suppl7>

Supplementary material 8

Video 6

Author: Francisco Hita Garcia

Data type: (Video file (.mp4))

Explanation note: *Proceratium japonicum* non-type worker (CASENT0790834). 3D rotation video based on volumetric surface rendering of full body.

Copyright notice: This dataset is made available under the Open Database License (<http://opendatacommons.org/licenses/odbl/1.0/>). The Open Database License (ODbL) is a license agreement intended to allow users to freely share, modify, and use this Dataset while maintaining this same freedom for others, provided that the original source and author(s) are credited.

Link: <https://doi.org/10.3897/zookeys.770.24908.suppl8>

Supplementary material 9

Video 7

Author: Francisco Hita Garcia

Data type: (Video file (.mp4))

Explanation note: *Proceratium longigaster* non-type worker (CASENT0790673). 3D rotation video based on volumetric surface rendering of full body.

Copyright notice: This dataset is made available under the Open Database License (<http://opendatacommons.org/licenses/odbl/1.0/>). The Open Database License (ODbL) is a license agreement intended to allow users to freely share, modify, and use this Dataset while maintaining this same freedom for others, provided that the original source and author(s) are credited.

Link: <https://doi.org/10.3897/zookeys.770.24908.suppl9>

Supplementary material 10

Video 8

Author: Francisco Hita Garcia

Data type: (Video file (.mp4))

Explanation note: *Proceratium shohei* sp. n. holotype worker (CASENT0717686). 3D rotation video based on volumetric surface rendering of full body.

Copyright notice: This dataset is made available under the Open Database License (<http://opendatacommons.org/licenses/odbl/1.0/>). The Open Database License (ODbL) is a license agreement intended to allow users to freely share, modify, and use this Dataset while maintaining this same freedom for others, provided that the original source and author(s) are credited.

Link: <https://doi.org/10.3897/zookeys.770.24908.suppl10>

Supplementary material 11

Video 9

Author: Francisco Hita Garcia

Data type: (Video file (.mp4))

Explanation note: *Proceratium deelemani* non-type worker (CASENT0790842). 3D rotation video based on volumetric surface rendering of full body.

Copyright notice: This dataset is made available under the Open Database License (<http://opendatacommons.org/licenses/odbl/1.0/>). The Open Database License (ODbL) is a license agreement intended to allow users to freely share, modify, and use this Dataset while maintaining this same freedom for others, provided that the original source and author(s) are credited.

Link: <https://doi.org/10.3897/zookeys.770.24908.suppl11>

Two new species of *Brusqueulia* Razowski & Becker, 2000 from the Neotropics, with comments on the systematic position of the genus in relation to the *Apolychrosis* Amsel, 1962 group of genera (Lepidoptera, Tortricidae, Cochylini)

Jose V. Pérez Santa-Rita¹, Joaquin Baixeras¹

¹ *Cavanilles Institute of Biodiversity and Evolutionary Biology, University of Valencia, Calle Catedrático José Beltrán, 2, 46980-Valencia, Spain*

Corresponding author: *Joaquin Baixeras* (joaquin.baixeras@uv.es)

Academic editor: *E. van Nieuwerkerken* | Received 16 February 2018 | Accepted 4 April 2018 | Published 4 July 2018

<http://zoobank.org/7ACAE33B-E062-40A3-AB1F-5EBF3CC3CFA3>

Citation: Pérez Santa-Rita JV, Baixeras J (2018) Two new species of *Brusqueulia* Razowski & Becker, 2000 from the Neotropics, with comments on the systematic position of the genus in relation to the *Apolychrosis* Amsel, 1962 group of genera (Lepidoptera, Tortricidae, Cochylini). ZooKeys 770: 193–210. <https://doi.org/10.3897/zookeys.770.24281>

Abstract

Two new species of the neotropical genus *Brusqueulia* Razowski & Becker, 2000, are described and illustrated: *B. yunkensis* Pérez Santa-Rita & Baixeras, **sp. n.** from Bolivia and *B. araguensis* Pérez Sant-Rita & Baixeras, **sp. n.** from Venezuela. The systematic position and diagnostic characters of the genus are reviewed, resulting in the synonymy of *Pinhaisania* Razowski & Becker, 2000, with *Brusqueulia*, and the combination *B. crispula* (Razowski & Becker, 2000), **comb. n.** New characters of the female genitalia are discussed.

Keywords

Brusqueulia araguensis, *Brusqueulia yunkensis*, Euliina, South America, subpapillar sclerite, systematics, taxonomy

Introduction

Tortricoidea are a monophyletic and rather homogeneous superfamily of Lepidoptera that includes the single family Tortricidae, containing more than 10,800 described species (Gilligan et al. 2014). Nineteen tribes organised in three subfamilies are cur-

rently recognised. The tribe Cochylini includes more than 2,150 species assigned to 246 genera, of which 1,041 species and 169 genera belong to the subtribe Euliina (Gilligan et al. 2014). Euliini was proposed by Kuznetsov and Stekolnikov (1977) as the monophyletic sister group (subtribe Euliae) to Cochylini (Cochyliae), with the former subsequently elevated to tribal level by Powell (1986). Molecular evidence (Regier et al. 2012) strongly supports the monophyly of Cochylini s. str., but leaves Euliini as a paraphyletic taxon. Cochylini has nomenclatorial priority but for practical reasons, it has been recommended that the two hypothetical subtribes Euliina and Cochyliina be retained (Gilligan et al. 2014, Gilligan and Brown 2016, Pérez Santa-Rita and Baixeras 2017). We follow that convention in this paper.

Horak (1998) suggested that the loss of forewing CuP, the loss of uncus and gnathos in the male genitalia, and the ill-defined signum in female genitalia are diagnostic characters for Cochyliina. Monsalve et al. (2011) found a two-bristled female frenulum is also a common condition in the group. However, these characters are reductive trends shared with Euliina, not true autapomorphic characters (Brown and Powell 1991). The presence of one or more large non-deciduous, laterobasally attached, aciculate, capitate cornuti with a microdentate vesica is also evidence of the relationship between the two subtribes (Anzaldo et al. 2014). Extreme morphological variation, especially in the genitalia, contributes to the difficulty of defining Cochylini (Pérez Santa-Rita and Baixeras 2017) and makes it difficult to establish boundaries between the taxa. In fact, more than half of the genera of the subtribe Euliina are monotypic, mostly from the Neotropics. In this taxonomic and morphological scenario, how Cochyliina is nested within Euliina remains unresolved.

The Neotropical genus *Brusqueulia* Razowski & Becker, 2000 (originally placed in Euliina), is an interesting example of a mixture of euliine and cochyline characters that is in agreement with the transitional role which the molecular data indicate for Euliina. Brown and Powell (1991) recognised a group of genera organised around *Apolychrosis* Amsel, 1962 to be basal with respect to a well-defined *Chrysoxena* Meyrick, 1912 group of genera. Brown and Adamski (2003) detailed the systematic composition of the *Apolychrosis* group, one of the few groups of Euliina for which a phylogeny has been proposed. The study of two new species of *Brusqueulia* shows evidence of the connection of this genus with the *Apolychrosis* group and allows speculation regarding relationships within Cochylini.

Materials and methods

Specimens were obtained by light trapping in Bolivia (different localities) by the second author (JB) and from museum collections (listed below). See supplementary file 1: material_examined.xls for a detailed account of the material examined. Dissection procedures follow Robinson (1976) and Zlatkov (2011), and were performed under a Leica MZ8 stereomicroscope. Adults and genitalia were photographed using a Leica Z16 microscope, equipped with a CF500 camera and LAS 4.9 (Leica) image capture

software. Z-stacks followed by extended depth of field application was extensively used to produce final images. When the level of pressure on the genitalia preparation is considered to change the shape of the valvae, the value of the thickness of the preparation is determined by the z-range during the acquisition and is indicated in Figures 2B and C. Methods for scanning electron microscope (SEM) preparation and observation follow Lincango et al. (2013). All images were edited using Photoshop CS3 (Adobe). Terminology of the genitalia follows Horak (1984) and Anzaldo et al. (2014); terminology for elements of the forewing pattern follows R. Brown and Powell (1991) as modified by Baixeras (2002). Forewing measurements were taken along a straight line from the base of the wing to the apex (including fringe). Range, mean (\bar{x}), and number (n) of specimens measured are indicated throughout the text.

DNA extraction was performed from an abdomen according to NucleoSpin XS Tissue purification procedure (Macherey-Nagel Duren, Germany). COI was amplified by PCR using LepF1 / LepR1 primers (Hebert et al. 2004). The selected PCR products were purified following High Pure PCR Product Roche Purification protocol. DNA labeling was performed with BigDye Terminator v3.1 Cycle Sequencing Ready Reaction ABI PRISM (Applied Biosystems). Amplicons were sequenced by Sanger method (Sanger and Coulson 1975) in an ABI 3730 DNA sequencing equipment (Applied Biosystems). Reading and assembly of the 658 bp sequence was assisted by STADEN software Package (Staden 1999). Finally, the sequence was tested against GenBank by BLAST.

A phylogenetic analysis was conducted to determine the relative position of the newly described taxa within the *Apolychrosis* group of genera. The character matrix of Brown and Adamski (2003) was used as the starting point (i.e., 25 morphological characters), to which we added character states for the two new species of *Brusqueulia*. However, as discussed below, the group of *Punctapinella niphastra* was finally excluded from the analysis in order to improve resolution. We converted two of the 25 original characters from binary to multi-state: the vesica of the phallus in male genitalia and the sterigma in female genitalia [characters 21 and 22, respectively, in Brown and Adamski (2003). Character 21 adds a character state “2” referring to the presence of two types of cornuti (aciculate + microspinulate). Character 22 adds a character state “2” referring to the sterigma complex. Brown and Adamski (2003) assumed that the ductus seminalis (Character 25) originated from the ductus bursae in *Eubetia* Brown, 1999. However, re-examination of this character (J. Brown, personal communication) confirmed that the intersection of the ductus seminalis and the bursa copulatrix is really in the cervix and consequently part of the corpus bursae. This character state has been changed accordingly in the data matrix. The data matrix is included as supplementary file 2: character_matrix. Characters were coded and subjected to parsimony analysis using the TnT version 1.5 (Goloboff and Catalano 2016). Each character was added one by one in the taxa analyzed. We used “Traditional Search” method with 1000 random addition sequences (RAS), each with the option tree bisection reconnection (TBR) branch-swapping (Goloboff et al. 2008).

Abbreviations

- MNKM** Museo de Historia Natural Noel Kempff Mercado, Universidad Autónoma Gabriel René Moreno, Santa Cruz de la Sierra, Bolivia.
- USNM** National Museum of Natural History, Smithsonian Institution, Washington D.C., United States.
- ICBiBE** Institut Cavanilles de Biodiversitat i Biologia Evolutiva, Universitat de València, Spain.

Taxonomy

Brusqueulia Razowski & Becker, 2000

Brusqueulia Razowski & Becker, 2000, SHILAP Revista de Lepidopterología 28: 386; type-species: *Brusqueulia sebastiani* Razowski & Becker, 2000

Pinhaisania Razowski & Becker, 2000, SHILAP Revista de Lepidopterología 28: 387; type-species: *Pinhaisania crispula* Razowski & Becker, 2000 – **syn. n.**

Diagnosis. Venation typically for Cochyliina (Fig. 1). Forewing (based on two slides) without costal fold; discal cell ca. 0.6 times length of wing, no M-stem, chorda obsolescent ca. 0.25 times length of wing, cross veins vestigial; all veins present except CuP; R_4 to the costa near apex, R_5 to the termen; distances between pairs of veins R_5 – M_1 , M_1 – M_2 and M_2 – M_3 on termen similar; distances between M_3 – CuA_1 , CuA_1 – CuA_2 and CuA_2 – $1A+2A$ similar; CuA_2 opposite on discal cell ca. 0.3–0.5 the distance between R_1 and R_2 on the cell, approximately coincident with the point where the chorda meets R_s ; anal loop ca. 0.3 times length of $1A+2A$. Hindwing with $Sc+R_1$ somewhat parallel to R_s basally, length ca. 0.8 times length of wing; M_1 and R_s stalked in basal half; M_2 , M_3 and CuA_1 obsolescent basally; M_3 and CuA_1 connate; CuA_2 well developed, CuP reduced, present only in distal portion; $1A+2A$ and $3A$ developed, anal loop ca. 0.4 times length of $1A+2A$. Frenulum in males with one single bristle, three bristles in females. Male genitalia with transtilla broad and well developed; gnathos as two arms fused distally forming a short process, resulting in a plicate terminal plate; characteristic valva, elongate; cucullus with a more or less developed disc of hair like scales; sacculus with a free terminal process. Phallus with two distinctive sets of non-deciduous cornuti, one set as a ventral band of rather large aciculate cornuti basally attached; a second set in the inner part of vesica formed by microspinulate cornuti. Female genitalia with lobular lamella antevaginalis and postvaginalis; ventral spinous subpapillar sclerite on the 8-9 intersegmental membrane at the level of the ventral lobes of the anal papillae.

Diversity and distribution. Fifteen species have been described from Brazil and one from Ecuador (Razowski and Becker 2000, 2011). To that we add one species

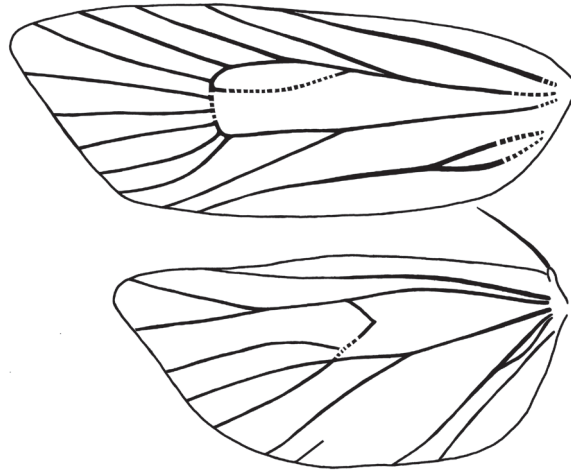


Figure 1. Venation in *Brusqueulia yunkensis*. Based on slides JBA20815 and JBA20836. Dashed lines indicate obsolete veins.

from Bolivia and another from Venezuela. Given the broad geographical and elevational range (from near sea level to ca. 2000 m), we suspect that *Brusqueulia* includes additional undiscovered species.

Checklist of species

- Brusqueulia araguensis* Pérez Santa-Rita & Baixeras, 2018 – **sp. n.**
Brusqueulia atrocentra Razowski & Becker, 2011
Brusqueulia atrograpta Razowski & Becker, 2011
Brusqueulia baeza Razowski & Becker, 2011
Brusqueulia bonita Razowski & Becker, 2011
Brusqueulia caracagena Razowski & Becker, 2011
Brusqueulia ceriphora Razowski & Becker, 2011
Brusqueulia costispina Razowski & Becker, 2011
Brusqueulia crispula (Razowski & Becker, 2000) (*Pinhaisania*) – **comb. n.**
Brusqueulia guaramiranga Razowski & Becker, 2011
Brusqueulia jacupiranga Razowski & Becker, 2011
Brusqueulia monoloba Razowski & Becker, 2011
Brusqueulia sebastiani Razowski & Becker, 2000
Brusqueulia signifera Razowski & Becker, 2000
Brusqueulia tineimorpha Razowski & Becker, 2011
Brusqueulia tripuncta Razowski & Becker, 2000
Brusqueulia uncicera Razowski & Becker, 2011
Brusqueulia yunkensis Pérez Santa-Rita & Baixeras, 2018 – **sp. n.**

***Brusqueulia yunkensis* sp. n.**

<http://zoobank.org/1BFCD272-BD76-4312-9804-7E65744802E8>

Figures 2, 4A, C

Type material. Holotype: ♂, Bolivia, Santa Cruz Department, Florida Province, Pampa Grande Municipality, locality of Hueco de la Pascana, 1575 m, 18°7.09'S; 64°3.58'W, 25 Jan 2011, J. Baixeras, A. Valdivia and G. Fernández (MNKM).

Paratypes: (15♂, 6♀). Bolivia: Santa Cruz Department, Florida Province, Mairana Municipality, locality of Yunga de Mairana, Rasete, 2000 m, 18°04'S; 63°54'W, 4 Nov 2005 (6♂, 3♀), J. Baixeras, A. Valdivia and I. García (GS USNM 124290, USNM 124291); Yunga de Mairana, ca. Bosque de Helechos, 2150 m, 18°03'S; 63°55'W, 02 Nov 2005 (1♂), J. Baixeras, A. Valdivia and I. García (GS 20724); locality of Pampa Grande, Hueco de la Pascana, 18°7.09'S; 64°3.58'W, 10 Nov 2001 (1♂), A. Valdivia and J. Baixeras; Pampa Grande, La Hoyada, 1600 m, 17°57'S; 64°06'W, 07 Nov 2005 (1♂, 1♀), J. Baixeras, A. Valdivia and I. García (GS 20727, 20728); Pampa Grande, Agua Clarita, 1554 m, 17°56.74'S; 64°7.97'W 27 Jan 2011 (5♂, 2♀), J. Baixeras, A. Valdivia and G. Fernández; Pampa Grande, El Milu, 1534 m, 17°59.36'S; 64°3.23'W, 28 Jan 2011 (1♂), J. Baixeras, A. Valdivia and G. Fernández. Paratypes deposited in MNKM, USNM, and ICBiBE.

Material examined not included in the type series. Bolivia: Santa Cruz Department, Florida Province, Mairana Municipality, locality of Yunga de Mairana, Rasete, 2000 m, 18°04'S; 63°54'W, 4 Nov 2005 (1♂, 1♀), J. Baixeras, A. Valdivia and I. García (GS JBA20684, JBA20815, SEM stub JBA193); Pampa Grande, Agua Clarita, 1554 m, 17°56.74'S; 64°7.97'W 27 Jan 2011 (2♂), J. Baixeras, A. Valdivia and G. Fernández (GS JBA20836, JBA20844, JBA20864). Deposited in ICBiBE.

Molecular characterisation. We were able to obtain partial COI sequence data (i.e., the DNA barcode) for a single specimen (GENBANK accession number MG951753), and comparison of the sequence against Genbank did not render any useful information. Interestingly, sequencing of a second sample revealed the presence of DNA related to the entomopathogenic trypanosomatid genus *Crithidia* Léger, 1902 (phylum Euglenozoa; GENBANK accession number MH118295).

Diagnosis. The habitus of *B. yunkensis* (Fig. 2A) does not ensure discrimination from similar species of *Brusqueulia* (e.g., *B. baeza* or *B. uncicera*) or species of the closely related genus *Limeulia* Razowski & Becker, 2000. An examination of the available literature suggests that the crescent-shaped blotch of the forewing costa is present in all the species of the genus *Brusqueulia* and related genera. The distinctive characters at the species level are associated with the male and female genitalia. *Brusqueulia yunkensis* can be distinguished by the unusual configuration of the transtilla in males (Figure 2B). The transtilla is well developed in most species of *Brusqueulia* and in associated genera, but a transtilla projecting posteriorly into a flat spinulose area is found only in *B. crispula* and presumably in *B. monoloba*. However, in *B. yunkensis* the spinulose area occupies ca. 0.2 of the total length of the transtilla, whereas in *B. crispula* and *B. monoloba* it occupies ca. 0.3 of the total length. The impression is a longer, more

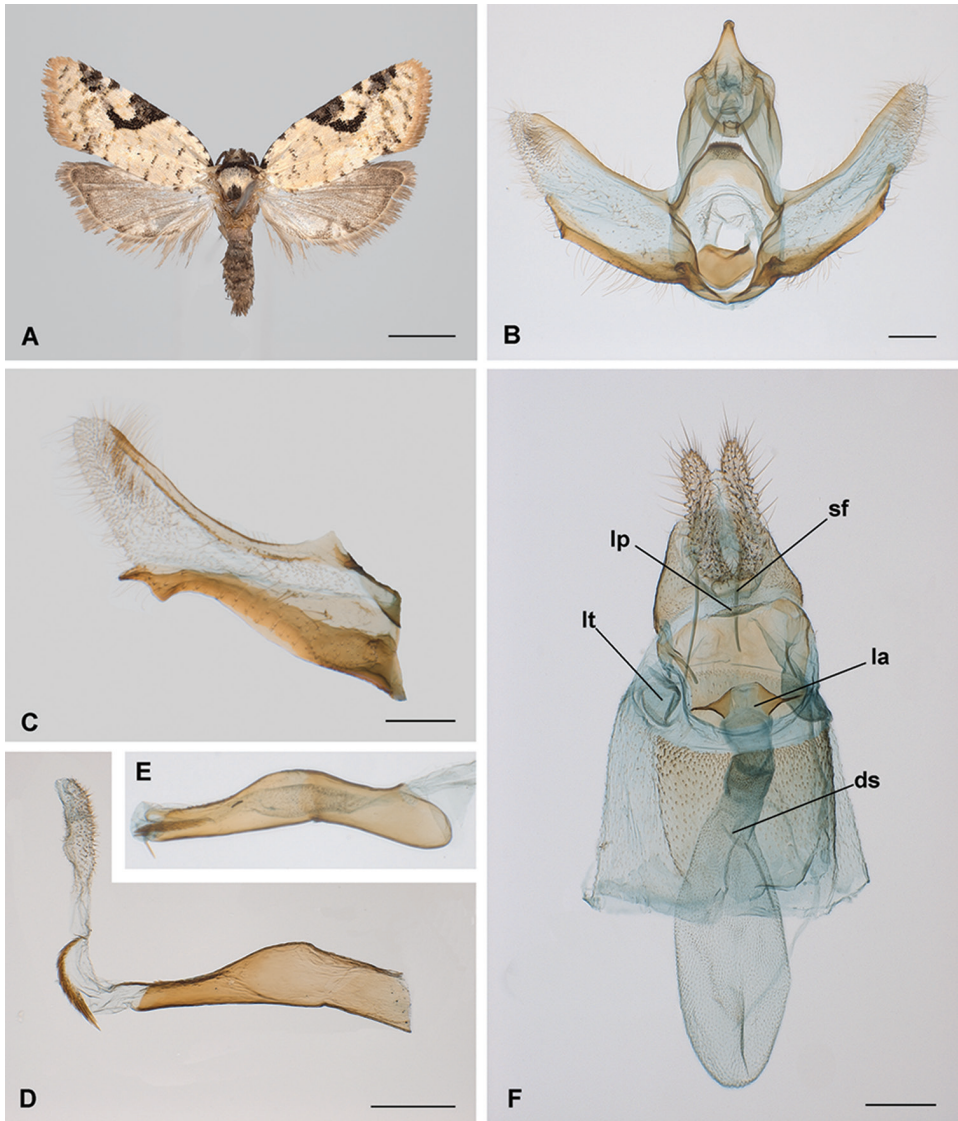


Figure 2. Morphological characters of *Brusqueulia yunkensis* sp. n. **A** habitus (Paratype, male, Bolivia, Santa Cruz, Pampagrande, 25 January 2011, ICBiBE) **B** male genitalia, phallus removed (GS JBA20728, $z = 161 \mu\text{m}$) **C** male genitalia left valva completely extended (GS JBA20684, $z = 83 \mu\text{m}$) **D** phallus with everted vesica (caecum removed, GS JBA20844) **E** phallus uneverted (GS JBA20728, same scale as D) **F** female genitalia (GS JBA20727). Abbreviations. ds: ductus seminalis connection to the bursa; la, lamella antevaginalis; lp, sclerite on the lamella postvaginalis; lt, lateral pocket; sf, ventral spinous field of segment 8. Scale bars: 2 mm (**A**); 200 μm (**B, C, D, F**).

protruding transtilla in *B. yunkensis* than in the other two species. *Brusqueulia crispula* has a distinctive pillous disc on the cucullus that is present but only weakly developed in *B. yunkensis*; no disc is apparent in *B. monoloba*. There is wide variation in the de-

velopment of the uncus in *Brusqueulia* species, from thin projections, as in *B. bonita*, *B. baeza*, and *B. araguensis* sp. n., to relatively broad finger-like projections, as in *B. crispula* and *B. tripuncta*. *Brusqueulia yunkensis* has a moderate development similar to that of *B. teneimorpha* and *B. guarimiranga*. A rugous spatulate projection of the gnathos has never been described in species of the group and could be a unique character. An inward curved sacculus distally projecting into a pointed process (Fig. 2C) is similar to that found in some species such as *B. baeza*, *B. monoloba* and even *B. crispula*, but the shape of the terminal process is diagnostic in every species of the group. Finally, the phallus of *B. yunkensis* seems to be a simplified organ with respect to the typical stout structure in its relatives, more elongate and without any distal ventral process. The presence of denticles on the dorsal distal part of the phallus (Fig. 2E) together with slender terminal cornuti (Fig. 2D) has been reported only in *B. sebastiani*. The presence of microspinulation on the inner part of the vesica is unknown in other species of the genus. So far, morphological details of the females of *Brusqueulia* are limited owing to the paucity of material. The only female described is *B. caracagena*, a species for which the male is unknown. The latter can be easily distinguished from *B. yunkensis* by the ductus bursae (Fig. 2F) – extremely short in *B. caracagena*, longer and partially sclerotised in *B. yunkensis*. The spinous subpapillar sclerite (Fig. 4B and D) on the intersegmental membrane, present in *B. yunkensis*, is absent in *B. caracagena*.

Description. *Head:* Vertex with long brownish scales protruding anteriorly and dorsally, fan-shaped, between antennae. Frons slightly convex covered with some whitish scales. Antennae dark brown, length ca. 0.5 as long as forewing costa, dorsally scaled, ventrally ciliated, two rows of scales per flagellomere. Palpus labialis porrect, length (all three segments combined) ca. 1.4 times diameter of compound eye, uniformly scaled; first segment short, slightly upcurved, with brown scales, second segment long, straight with mixed brown scales laterally and whitish scales dorsally, third segment short and slightly upcurved with whitish scales basally and apically and brown scales medially; opening of organ of vom Rath in apical position. Haustellum well developed. Ocelli and chaetosemata well developed.

Thorax: Upperside with pronotum, anterior half-part of mesoscutum, and tegulae covered by dark brown scales and posterior half-part of mesoscutum and metanotum covered by white scales; smooth-scaled including tegulae, without scales tufts. Under-side, including legs, whitish, male foreleg hairpencil absent. Forewing length 5.0–6.6 mm (\bar{x} = 6.1; n = 19) in males, 5.8–7.3 mm (\bar{x} = 6.7; n = 7) in females. Forewing with typical venation of Cochyliina, details described for the genus. Forewing pattern not sexually dimorphic (Fig. 2A). Forewing upperside with ground colour whitish with brownish-grey marking; most marks concentrated in costal area; system of pairs of strigulae vaguely recognisable, presumably concolourous with background, only through inter strigular dark marks; some scattered marks at basal fourth of costa; marks at level of Sc fused to produce a distinctive crescent shape brownish-grey blotch projected discally in a rather conspicuous coma-like patch confluent with R2–R3; single marks between Sc and R1, R1 and R2, R2 and R3, no marks beyond R3; some scattered grey scales between marks; striae strongly fragmented; dorsal marking ill-

defined; fasciae undetectable; fringe ochreous; forewing underside uniformly brownish ochreous with some pale strigulae at radial level on the costa; overlapping area whitish. Hindwing upperside and underside, including fringe, uniformly brownish-ochreous; male costal fold absent; cubital pecten not detected.

Abdomen: Dorsad greyish, paler ochreous cephalad. Segment 8 unmodified. Male genitalia (based on four preparations; Fig. 2B, C, D, E) with tegumen well developed, laterally straight; uncus developed, basally confluent with top of tegumen, progressively narrowed distally; socii membranous, conspicuous, moderately developed, hairy; gnathos as two arms distally fused distally into a short process, moderately expanded distally in a central spinous molar-like sclerite; transtilla broad, strong, with a distal moderately flat area densely covered by short strong spines; valva elongate, variable in shape (Fig. 2B and C), costa slightly concave, sclerotised; cucullus moderately lobed, membranous, slightly sclerotised, with a central area densely hairy; sacculus internally concave, well sclerotised, distally projected in a finger-like structure, with triangular ventral subdistal process; pulvinus present; vinculum well developed; juxta strongly sclerotised in a rather pentagonal plate; ampulla present; phallus with coecum penis straight, central part strongly curved down, distal part straight, presence of dorsal teeth; vesica with two clusters of non-deciduous cornuti, one proximal oriented ventrally, consisting of aciculate cornuti, basally attached, arranged in a single longitudinal band, another distal consisting of an irregular patch of microspinulate cornuti. Segment 7 in females without modified scaling (corethogyne) but with two lateral, somewhat dorsal pockets on the 7-8 intersegmental membrane. Female genitalia (based on three preparations; Fig. 2F) with sterigma broad; lamella antevaginalis as a simple but evident lobe; ostium in a short funnel like antrum; lamella postvaginalis moderately sclerotised, smooth, broad, with a distinct ventrally prominent distal lobe as a transversal plate; ductus bursae as long as corpus bursae, moderately sclerotised in proximal half, double folded (in Z) when not extended; corpus bursae subspherical, moderately covered internally by acanthae and ctenidia in variable degree of development; no signum or other specially sclerotised area; a long ductus seminalis connected ventrally to cervix, no bulla seminalis; a large globular spermatophore extracted in one of the dissections; anterior apophysis fairly short, projected internally; ventral area of segment 8 behind the sterigma heavily covered by acanthae (spinous field) continuous with distal sclerotised plate of the lamella postvaginalis; a spiny star-shaped ventral subpapillar sclerite on the 8-9 intersegmental membrane at level of ventral lobes of anal papillae (Fig. 4B and D); posterior apophysis simple, approximately same length as papillae; egg pore broad between anal papillae.

Biology and distribution. The early stages are unknown. Adults were collected in January (n = 11) and November (n = 14) at middle elevations (1554-2150 m) in Bolivia, Santa Cruz Department, Florida Province in municipalities of Mairana, El Rasete, and Pampagrande, localities of Agua Clarita, Hueco de la Pascana, and La Hoyada. The collecting sites include transition from dry to cloud forest.

Etymology. The specific epithet refers to the Quechuan word *yun-ka*, which translates as warm valley, a band of forest on the slopes of the Andes Mountains. This zone is of enormous interest from a conservation perspective.

***Brusqueulia araguensis* sp. n.**

<http://zoobank.org/B86EF700-AFC8-4DF3-9BF2-55DE23D8F8FB>

Figures 3, 4B, D

Type material. Holotype: ♂, Venezuela, Aragua State, locality of Rancho Grande, 10°7'N; 67°20.63'W, 10–21 Feb 1969, D. Duckworth and E. Dietz (GS USNM 69274).

Paratypes: (4♀). Venezuela, Aragua State, locality of Rancho Grande, 1100 m, 10°7'N; 67°20.63'W, 24–31 Oct 1966 (1♀) (SEM stub JBA202); 22–31 Jul 1967 (3♀), R.W. Poole (GS USNM 85011).

Diagnosis. The habitus of *B. araguensis* (Fig. 3A) has more extensive dark brown scaling in the wing pattern compared to *B. yunkensis*, resulting in a more diffuse and ill-defined pattern. A similar pattern is found in *B. teneimorpha* and *B. caracagena*. Species more closely related to *B. yunkensis* (e.g., *B. baeza* and *B. uncicera*) have a more defined, contrasting pattern. The forewing costal crescent-shaped blotch allows clear discrimination between the two species (well defined in *B. yunkensis* and diffuse in *B. araguensis*), but in the context of the genus, these differences could be assumed to represent variation. More diagnostic characters are associated with the male and female genitalia. *Brusqueulia araguensis* can be distinguished by the extremely narrow uncus, the narrowest in the genus, even compare to closely related species such as *B. bonita* and *B. baeza*. The transtilla and gnathos are well developed in *B. araguensis*, similar to most species in *Brusqueulia*, and it is not diagnostic. Teeth or lobes are developed in the distal part of the sacculus coincident with the ventral part of the cucullus in most, if not all, species of the genus. Among congeners, *B. araguensis*, *B. costispina*, and *B. tripuncta* all have several teeth, but their development in *B. araguensis* is moderate compared to the other two species. Finally, the phallus in *B. araguensis* is simpler than in most species of the genus. So far, morphological features of the females of *Brusqueulia* are limited by the paucity of material. The only females available are *B. caracagena*, *B. yunkensis*, and *B. araguensis* (the last two described in this paper). Both share a broad sterigma, but *B. araguensis* and *B. yunkensis* are definitely more closely related to each other than either is to *B. caracagena*, even though differences between them are conspicuous. Both *B. caracagena* and *B. yunkensis* lack the spiny cushion-like asymmetrical areas on the lamella antevaginalis found in *B. araguensis*. *B. caracagena* can be easily distinguished from *B. araguensis* and *B. yunkensis* by the ductus bursae, short in *B. caracagena*, long and convoluted in *B. araguensis* and *B. yunkensis*. The position of the ductus seminalis is clearly different in *B. yunkensis* (from cervix) and *B. araguensis* (from mid-corpus bursae); no information about the ductus seminalis in *B. caracagena* is available. The subpapillar spiny sclerite of the 8–9 intersegmental membrane is pointed in *B. yunkensis* and truncate in *B. araguensis*.

Description. Head: Vertex with long whitish scales protruding anteriorly and dorsally, fan-shaped, between antennae. Frons slightly concave covered with a whitish scales. Antenna dark brown, length ca 0.4 as long as forewing costa, dorsally scaled, ventrally ciliated, two rows of scales per flagellomere. Labial palpus porrect, length (all three segments combined) ca. 1.3 times diameter of compound eye, uniformly scaled; first segment short, slightly upcurved with ochreous scales, second segment

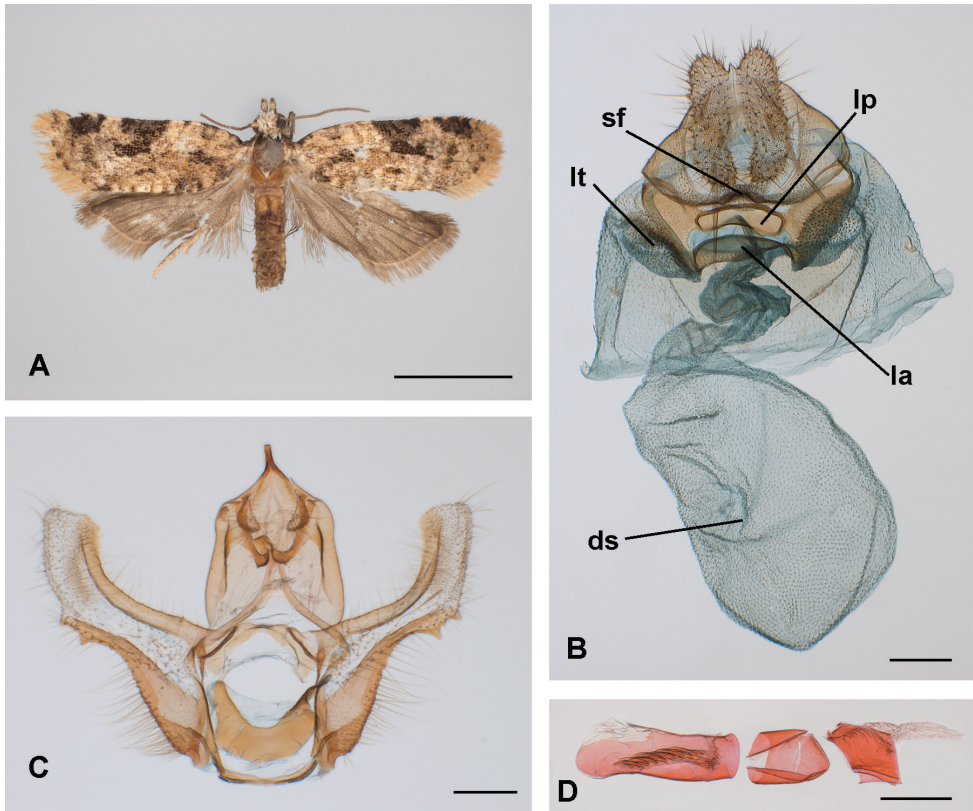


Figure 3. Morphological characters of *Brusqueulia araguensis*. **A** habitus (Paratype, female, Venezuela, Rancho Grande, 22–31 August 1967, USNM) **B** female genitalia (GS USNM85011) **C** male genitalia (GS USNM69274) **D** phallus (fragments photographically assemblage, may not correspond to the real order or orientation) (GS USNM6274). Abbreviations. ds: ductus seminalis connection to the bursa; la, lamella antevaginalis; lp, sclerite on the lamella postvaginalis; lt, lateral pocket; sf, ventral spinous field of segment 8; sp, subpapillar sclerite. Scale bars: 3 mm (**A**); 200 μ m (**B, C, D**).

long, straight with ochreous scales, third segment short, slightly upcurved with a mixed of dominant ochreous scales and a few whitish scales only basally; opening of organ of vom Rath in apical position. Haustellum well developed. Ocelli and chaetosemata well developed.

Thorax: Dorsum whitish ochreous with a dorso-apical dark brownish band. Smooth scaled including tegulae, with no tufts. Legs whitish, unmodified, male foreleg hair-pencil absent. Forewing length 5.7 mm ($n = 1$) in males, 5.7–6.2 mm ($\bar{x} = 5.9$; $n = 4$) in females. Forewing pattern (Fig. 3A) not sexually dimorphic. Forewing upperside general background colour whitish with scattered greyish-brown marks; marking ill defined; pairs of strigulae ill defined, concolourous with general background, vaguely detectable, with variable degree of suffusion; basal and subbasal fasciae poorly developed, median fascia as an irregular costal blotch projected tornally, with a small group

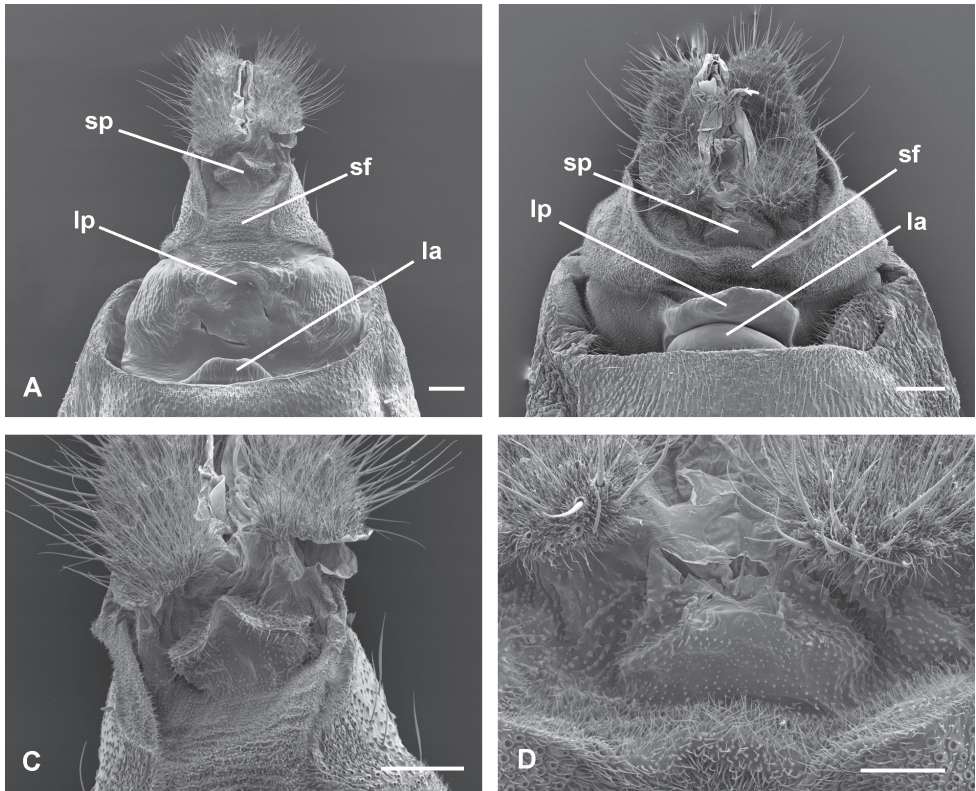


Figure 4. Female terminalia of *Brusqueulia yunkensis* and *B. araguensis*, ventral view, under scanning electron microscopy. **A** *B. yunkensis* **B** *B. araguensis* **C** subpapillar sclerite of *B. yunkensis* **D** same in *B. araguensis*. Abbreviations; la, lamella antevaginalis; lp, lamella postvaginalis; sf, ventral spinous field of segment 8; sp, subpapillar sclerite. Scale bars 100 μ m.

of dark scales at the level of cubital cell; some coma-like marks on the costa as postmedian and preterminal fasciae; fringe concolourous with general background; forewing underside uniformly brownish ochreous with some pale strigulae on the costa; overlapping area whitish. Hindwing upperside and underside, including fringe, uniformly brownish-ochreous; male costal fold absent; cubital pecten not detected.

Abdomen: Dorsally greyish, pale ochreous cephalad. Segment 8 unmodified in males. Male genitalia (based on one preparation; Fig. 3C) with tegumen well developed, laterally straight; uncus slender, straight, basally confluent with top of tegumen to drastically slimmed distally; socii membranous, hairy, obvious, moderately developed; gnathos as two arms distally fused and projected in a short process distally spatulate; transtilla broad, naked; appreciable pulvinus, valva elongate, costa concave, moderately sclerotised, cucullus subrectangular, membranous ventrally, costal area slightly sclerotised, central area densely hairy, sacculus basally convex, distally concave, well sclerotised, transition area of sacculus to cucullus with several tooth like distal process, one of them larger and basal clearly associated to the sacculus, the distal one assign-

able to the cucullus, a variable number of smaller teeth in between; vinculum broad but rather weakly developed; juxta strongly sclerotised horseshoe shaped; phallus (Fig. 3D) (fragmented in three pieces in the slide) presumably straight with simple caecum, central part broken; no teeth detected on the external surface; vesica simple with two clusters of cornuti, one distal (vesica not evaginated) consisting of non-deciduous (not detected in female corpus bursae) cornuti arranged in a single longitudinal band, another proximal consisting in an irregular patch of microspinulate cornuti. Segment 7 in females without modified scaling (corethogyne) but with two inconspicuous latero-dorsal pockets on the 7–8 intersegmental membrane. Female genitalia (based on two preparations; Fig. 3B) with sterigma broad, complex, slightly asymmetrical, ostium simple, slightly on the right; sterigma broad extended laterally in pockets ventrally covered by acanthae continuous laterally with two asymmetrical membranous cushion-shaped areas densely covered by acanthae (Fig. 4A); lamella antevaginalis with a moderately sclerotised convex plate; lamella postvaginalis moderately sclerotised, broad, with a distinct ventrally prominent but smooth dome like plate; ductus bursae rugose, sinuous, posterior half more sclerotised, internally covered by ctenidia continuous with internal vestiture of corpus bursae; corpus bursae subglobular, densely internally covered by ctenidia; no signum or any other sclerotised area detected; ductus seminalis from central area of corpus bursae; no bulla seminalis detected; no spermatophore found; anterior apophysis short projected internally; behind the sterigma the ventral area of segment 8 as a densely spiny lobe; 8–9 intersegmental membrane densely covered by acanthae; densely spiny crescent shape ventral sclerite on the 8–9 intersegmental membrane at the level of the ventral lobes of the anal papillae; posterior apophysis simple, approximately as long as anal papillae; presence of evident broad egg pore between anal papillae.

Biology and distribution. The early stages are unknown. Adults have been collected in February (n = 1), July (n = 2), August (n = 1), and October (n = 1) at middle elevation (1100 m) in Aragua State, Venezuela.

Etymology. The specific epithet refers to the state of Aragua in Venezuela.

Phylogenetic results

The phylogenetic analysis resulted in five trees of similar topology when using the complete matrix. Small differences are present in the relative position of the *P. niphastra* group with respect to other terminal taxa (the *P. conchitis*, *Seticosta tholeraula*, and *S. homosacta* groups) probably due to the lack of information about the males for the *P. niphastra* group. However, the position of the two new species of *Brusqueulia* remained stable. The consensus trees (including Nelson's method) rendered a polytomy for the whole *Apolychrosis* group. Nevertheless, removing the *P. niphastra* group from the matrix improved the resolution of the analysis producing a single cladogram (Fig. 5) basically similar to Brown and Adamski (2003). *Brusqueulia* is positioned as sister group of the *Apolychrosis* group in all the analysis.

Discussion

Based on three species, Razowski and Becker (2000) proposed the following autapomorphies of *Brusqueulia*: a well-developed transtilla, the presence of non-deciduous cornuti, and the configuration of the gnathos. Eleven species were later added (Razowski and Becker 2011) based on males and one more based exclusively on a single female. Although no formal relationships have been proposed, several genera are recognised as having a strong affinity with *Brusqueulia* by Razowski (2016): *Pinhaisania*, *Limeulia*, *Marcelina* Razowski & Becker, 2000, *Saopaulista* Razowski & Becker, 2000, *Crocotaenia* Razowski & Becker, 2003, and *Ibateguara* Razowski & Becker, 2011. All of these share a common appearance and some morphological features of the male genitalia, including the gnathos (with distally joined arms projected into a process) and the valva (with a terminal process in sacculus and a group of slender setae on the cucullus). Among these genera, the relation between *Brusqueulia* and *Pinhaisania* is most conspicuous. Unfortunately, very little information is available about the females of either.

The discovery of two new species including both males and females allows some detailed analysis of characters and rearrangements. The two new species are assigned to *Brusqueulia* on the basis of the characters mentioned above, although *B. yunkensis* could be assigned to *Pinhaisania* based on the conspicuous development of a spinulous transtilla. However, a set of remarkable characters relate *B. yunkensis* to *B. araguensis*, and presumably to other species of *Brusqueulia*, including the absence of CuP in the forewing, two types of non-deciduous cornuti in the vesica of the male genitalia, a characteristic ventral subpapillar sclerotised plate on female segment 9, and the position of the ductus seminalis never associated with the ductus bursae in the female genitalia. Based on this evidence, we propose *Pinhaisania* as a new synonym of *Brusqueulia* and consequently *B. crispula* as a new combination. It would not be surprising if this combination of characters were shared with other genera related to *Brusqueulia* (see above); however, the paucity of material, especially females, does not allow a detailed character analysis.

Among the *Apolychrosis* group of genera (Brown and Adamski 2003), the presence of a characteristic neck in the valva, a subapical process of the sacculus, and the absence of a CuP on the forewing are remarkable defining characters. The two species described in this paper share a robust series of characters consistent with the *Apolychrosis* group of genera. A re-analysis of the character matrix used by Brown and Adamski (2003) including the species here described placed them as a sister group of *Apolychrosis* group.

Molecular evidence already revealed that Cochyliina is nested with in Euliina, but the exact point of this connection is still unclear. Our research allows us to suggest a close relationship between Cochyliina and the group of genera around *Apolychrosis*. The absence of a CuP on the forewing, the presence of microspinulate areas combined or not with non-deciduous cornuti in the phallus, and a displacement of the ductus seminalis to positions associated to the corpus bursae would be derived characters, all of them putative of Cochyliina (Horak and Brown 1991; Horak 1998). A lamella postvaginalis as a central sclerite, and the 8–9 intersegmental membrane covered by acanthae especially remarkable at the sternal level of segment 8 (spinous field by some authors) is also frequent among

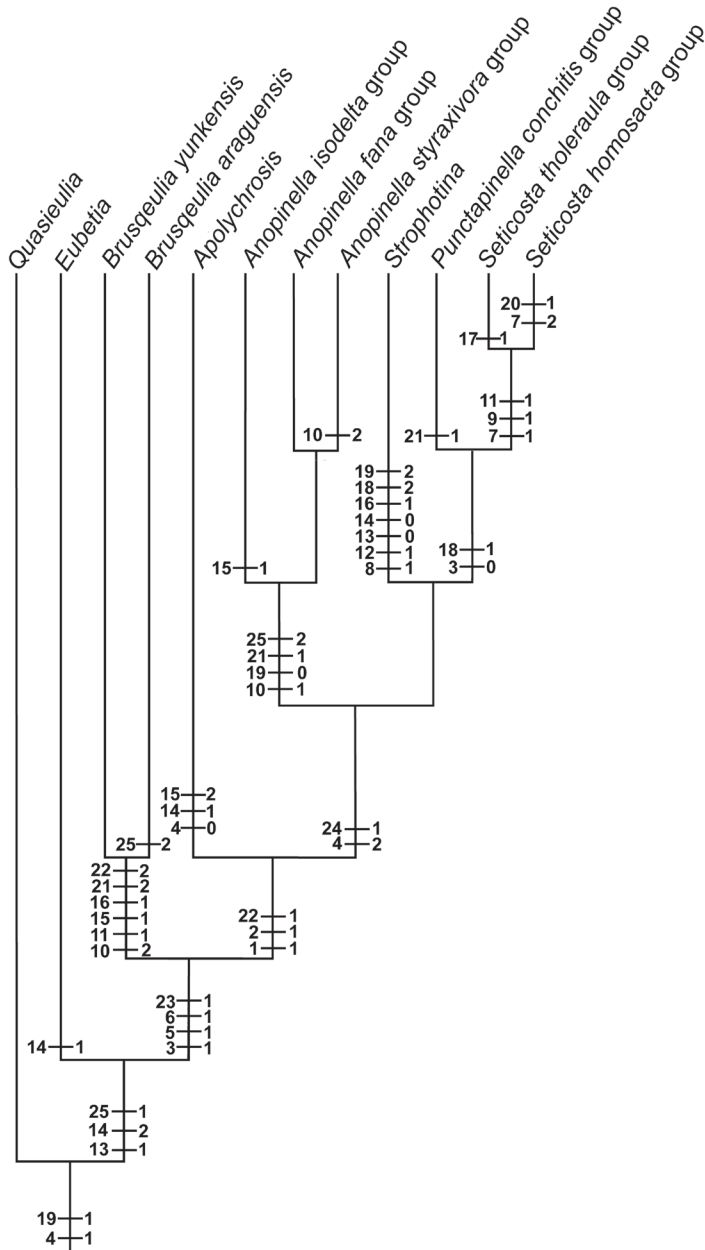


Figure 5. Hypothesis of phylogenetic relationships in the *Apolychrosis* group. *Brusqueulia* is positioned as sister group of the *Apolychrosis* group. The *P. niphastra* group has been excluded from the analysis.

Cochylina. In *Brusqueulia* there is an additional sclerite just at the ventral base of the anal papillae. A survey of some selected Cochylina did not reveal the presence of this subpapillar sclerite on the female genitalia. However, given the difficult observation of this character and its superficial confluence with the lamella postvaginalis, a more detailed examination of related genera seems necessary to clarify the taxonomic limits of this character.

Acknowledgements

We are indebted to the entomology laboratory of the MNKM and especially its head, Julieta Ledezma, for collaboration and for providing local support for fieldwork in Bolivia. Local and regional authorities provided collecting permissions. Guillermo Fernández (UVEG), Alejandra Valdivia, Ivan García, Ivan Royano, and Andres Langer (MNKM) collaborated in field work. We extend our gratitude to John Brown (USNM) for critical review and linguistic assistance during preparation of the manuscript and to Todd Gilligan (USDA, USA) and Pasquale Trematerra (University of Molise, Campobasso, Italy) for reviewing the manuscript. Financial support was provided by grants CGL2008-00605 and BFU2015-64322-C2-1-R (co-financed by FEDER funds and the Ministerio de Economía y Competitividad, Spanish Government). SEM observation and DNA Sanger sequencing were conducted at the Electron Microscopy and Genomic Services of the University of Valencia.

References

- Anzaldo S, Dombroskie J, Brown JW (2014) Morphological variation, taxonomic distribution, and phylogenetic significance of *cornuti* in Tortricinae (Lepidoptera: Tortricidae). *Proceedings of the Entomological Society of Washington* 116: 1–31. <https://doi.org/10.4289/0013-8797.116.1.1>
- Baixeras J (2002) An overview of genus level taxonomic problems surrounding *Argyroplote* Hübner (Lepidoptera, Tortricidae), with descriptions of a new species. *Annals of the Entomological Society of America* 95: 422–431. [https://doi.org/10.1603/0013-8746\(2002\)095\[0422:A0OGLT\]2.0.CO;2](https://doi.org/10.1603/0013-8746(2002)095[0422:A0OGLT]2.0.CO;2)
- Brown JW, Adamski D (2003) Systematic revision of *Anopinella* Powell (Lepidoptera: Tortricidae: Euliini) and phylogenetic analysis of the *Apolychrosis* group of genera. *Zootaxa* 200: 1–94. <https://doi.org/10.11646/zootaxa.200.1.1>
- Brown JW, Powell J (1991) Systematics of the *Chrysoxena* group of genera (Lepidoptera: Tortricidae: Euliini). *University of California Publications in Entomology* 111: 1–87.
- Brown RL, Powell, J (1991) Description of a new species of *Epiblema* (Lepidoptera: Tortricidae: Olethreutinae) from costal redwood forest in California with an analysis of the forewing pattern. *Pan-Pacific Entomologist* 67: 107–114.
- Gilligan TM, Baixeras J, Brown JW, Tuck KR (2014) T@RTS: Online World Catalogue of the Tortricidae (Ver. 2.0). <http://www.tortricid.net/catalogue.asp/> [accessed 25 March 2018]
- Gilligan TM, Brown JW (2016) A new genus for *Tortrix druana* Walsingham, 1914 and a new species from the northern Neotropics (Lepidoptera: Tortricidae: Cochylini: Euliina). *Journal of the Lepidopterists' Society* 70: 139–144. <https://doi.org/10.18473/lepi.70i2.a9>
- Goloboff PA, Catalano SA (2016) TNT version 1.5, including a full implementation of phylogenetic morphometrics. *Cladistics* 32: 221–238. <https://doi.org/10.1111/cla.12160>

- Goloboff PA, Farris JS, Nixon KC (2008) TNT, a free program for phylogenetic analysis. *Cladistics* 24: 774–786. <https://doi.org/10.1111/j.1096-0031.2008.00217.x>
- Hebert PDN, Penton EH, Burns J, Janzen DJ, Hallwachs W (2004) Ten species in one: DNA barcoding revealed cryptic species in the neotropical skipper butterfly, *Astraptes fulgerator*. *Proceedings of the National Academy of Sciences of the United States of America* 101: 14812–14817. <https://doi.org/10.1073/pnas.0406166101>
- Horak M (1984) Assessment of taxonomically significant structures in Tortricinae (Lep., Tortricidae). *Mitteilungen der Schweizerischen Entomologischen Gesellschaft* 57: 3–64.
- Horak M (1998) The Tortricoidea. In: Kristensen NP (Ed.) *Handbook of Zoology, 4 Arthropoda: Insecta, 35: Lepidoptera, Moths and Butterflies, 1: Evolution, Systematics and Biogeography*. Walter de Gruyter, Berlin, New York, 199–215.
- Horak M, Brown RL (1991) Taxonomy and Phylogeny. In: van der Geest LPS, Evenhuis HH (Eds) *Tortricid Pest*. Elsevier, Amsterdam, 23–48.
- Kuznetsov VI, Stekolnikov AA (1977) Functional morphology of the male genitalia and phylogenetic relationships of some tribes in the family Tortricidae (Lepidoptera) fauna of the Far East. *Trudy Zoologicheskogo instituta Akademii nauk SSSR* 70: 65–97. [In Russian]
- Lincago P, Fernández G, Baixeras J (2013) Microstructure and diversity of the bursa copulatrix wall in Tortricidae (Lepidoptera). *Arthropod Structure and Development* 42: 246–256. <https://doi.org/10.1016/j.asd.2013.01.003>
- Monsalve S, Dombroskie JJ, Lam WHY, Rota J, Brown JW (2011) Variation in the Female Frenulum in Tortricidae (Lepidoptera). Part 3. Tortricinae. *Proceedings of the Entomological Society of Washington* 113(3): 335–370. <https://doi.org/10.4289/0013-8797.113.3.335>
- Pérez Santa-Rita J, Baixeras J (2017) Description of a new genus of Euliina with unique coupling adaptations of the male and female (Lepidoptera: Tortricidae: Cochylini). *Zootaxa* 4227 (1): 135–143. <https://doi.org/10.11646/zootaxa.4227.1.9>
- Powell JA (1986) Synopsis of the classification of Neotropical Tortricinae, with descriptions of new genera and species (Lepidoptera: Tortricidae). *Pan-Pacific Entomologist* 62: 372–398.
- Razowski J (2016) Diagnoses and remarks on the genera of Tortricidae (Lepidoptera). Part 4. Cnephasiini, Ceracini, Atterini, Sparganothini and Euliini. *Acta zoologica cracoviensia* 59: 90–149. https://doi.org/10.3409/azc.59_2.89
- Razowski J, Becker VO (2000) Description of six Brazilian genera of Euliini and their species (Lepidoptera: Tortricidae). *SHILAP Revista de Lepidopterologia* 28: 385–393.
- Razowski J, Becker VO (2011) New species of *Hynhamia* Razowski and other genera close to *Toreulia* Razowski and Becker (Lepidoptera: Tortricidae). *Polskie Pismo Entomologiczne* 80: 53–82. <https://doi.org/10.2478/v10200-011-0006-3>
- Regier JC, Brown JW, Mitter C, Baixeras J, Cho S, Comings MP, Zwick A (2012) A molecular phylogeny for the leaf-roller moths (Lepidoptera: Tortricidae) and its implications for classification and life history evolution. *PLoS One* 7: e35574. <https://doi.org/10.1371/journal.pone.0035574>
- Robinson GS (1976) The preparation of slides of Lepidoptera genitalia with special reference to the Microlepidoptera. *Entomologist's Gazette* 27: 127–132.

- Sanger F, Coulson AR (1975) A rapid method for determining sequences in DNA by primed synthesis with DNA polymerase. *Journal of Molecular Biology* 94: 441–448. [https://doi.org/10.1016/0022-2836\(75\)90213-2](https://doi.org/10.1016/0022-2836(75)90213-2)
- Staden R (1999) Staden Package. MRC Laboratory of Molecular Biology, Cambridge, England. Available from http://staden.sourceforge.net/manual/master_unix_brief.html [accessed September 2015]
- Zlatkov B (2011) A preliminary study of everted vesicae of several leafrollers (Tortricidae). *Nota lepidopterologica* 33(2): 285–300.

Supplementary material 1

Material examined

Authors: Jose V. Pérez Santa-Rita, Joaquín Baixeras

Data type: (Data table)

Explanation note: Collection data of the voucher material examined.

Copyright notice: This dataset is made available under the Open Database License (<http://opendatacommons.org/licenses/odbl/1.0/>). The Open Database License (ODbL) is a license agreement intended to allow users to freely share, modify, and use this Dataset while maintaining this same freedom for others, provided that the original source and author(s) are credited.

Link: <https://doi.org/10.3897/zookeys.770.24281.suppl1>

Supplementary material 2

Character matrix

Authors: Jose V. Pérez Santa-Rita, Joaquín Baixeras

Data type: (Phylogenetic matrix)

Explanation note: Data matrix for phylogenetic analysis.

Copyright notice: This dataset is made available under the Open Database License (<http://opendatacommons.org/licenses/odbl/1.0/>). The Open Database License (ODbL) is a license agreement intended to allow users to freely share, modify, and use this Dataset while maintaining this same freedom for others, provided that the original source and author(s) are credited.

Link: <https://doi.org/10.3897/zookeys.770.24281.suppl2>

A new species of *Kurixalus* from western Yunnan, China (Anura, Rhacophoridae)

Guohua Yu^{1,*}, Hong Hui^{1,*}, Dingqi Rao¹, Junxing Yang¹

¹ State Key Laboratory of Genetic Resources and Evolution, Kunming Institute of Zoology, Chinese Academy of Sciences, 32 Jiaochang Donglu, Kunming, Yunnan 650223, China

Corresponding author: Junxing Yang (yangjx@mail.kiz.ac.cn); Dingqi Rao (raodq@mail.kiz.ac.cn)

Academic editor: A. Crottini | Received 11 January 2018 | Accepted 6 May 2018 | Published 4 July 2018

<http://zoobank.org/3246F1C2-905B-4325-8F39-253959A3C1B3>

Citation: Yu G, Hui H, Rao D, Yang J (2018) A new species of *Kurixalus* from western Yunnan, China (Anura, Rhacophoridae). *ZooKeys* 770: 211–226. <https://doi.org/10.3897/zookeys.770.23526>

Abstract

A new species of the genus *Kurixalus* (Anura: Rhacophoridae) is described from western Yunnan, China. Genetically the new species, *Kurixalus yangi* **sp. n.**, is closer to *Kurixalus naso* than to other known congeners. Morphologically the new species is distinguished from all other known congeners by a combination of the following characters: smaller ratios of head, snout, limbs, IND, and UEW to body size; male body size larger than 30 mm; curved canthus rostralis; weak nuptial pad; brown dorsal color; absence of large dark spots on surface of upper-middle abdomen; presence of vomerine teeth; gold brown iris; single internal vocal sac; serrated dermal fringes along outer edge of limbs; granular throat and chest; rudimentary web between fingers; and presence of supernumerary tubercles and outer metacarpal tubercle.

Keywords

China, *Kurixalus yangi* sp. n., new species, Western Yunnan

Introduction

The genus *Kurixalus* Ye, Fei, & Dubois in Fei (1999) distributes widely in eastern India, Indochina, Sunda Islands, Philippine archipelago, montane forests of southern China, and adjacent continental islands, and currently contains 15 species (Frost 2018). Owing

* These authors contributed equally to this work.

to its morphological conservativeness, the taxonomy and systematics of *Kurixalus* were once very confusing (Yu et al. 2017a). For instance, *Kurixalus hainanus* (Zhao, Wang, & Shi in Zhao et al. 2005) was once thought to be a synonym of *Kurixalus odontotarsus* (Ye & Fei in Ye et al. 1993) by some authors (e.g., Fei et al. 2010) or a synonym of *Kurixalus bisacculus* (Taylor, 1962) by Yu et al. (2010). On the basis of broad sampling, recently Yu et al. (2017a) suggested that *K. hainanus* is valid and revealed six lineages that might represent undescribed species in the genus *Kurixalus*, one of which occurs in western Yunnan, China and northern Myanmar and is genetically closer to *Kurixalus naso* (Anandale, 1912) than to other known congeners with a divergence of 6.18% estimated from COI sequences (clade C, Fig. 1).

Here we further describe the lineage consisting of specimens from western Yunnan, China as a new species. Morphological comparisons demonstrate that the new species is distinctive from *K. naso* and other known congeners and therefore warrants taxonomic recognition.

Materials and methods

Sampling. Specimens were collected during fieldwork in Dehong Autonomous Prefecture, western Yunnan, China in June and July, 2014 (Fig. 2). They were euthanized with diethyl ether anesthesia and fixed by 90% ethanol before being stored in 70% ethanol. Liver tissues were preserved in 99% ethanol. Specimens were deposited at Kunming Institute of Zoology, Chinese Academy of Sciences.

Morphology. Morphometric data were taken using digital calipers to the nearest 0.1 mm. Morphological terminology follows Fei (1999). Measurements include:

SVL	snout-vent length (from tip of snout to vent);
HL	head length (from tip of snout to rear of jaws);
HW	head width (width of head at its widest point);
SL	snout length (from tip of snout to anterior border of eye);
IND	internarial distance (distance between nares);
IOD	interorbital distance (minimum distance between upper eyelids);
UEW	upper eyelid width (maximum width of upper eyelid);
ED	eye diameter (diameter of exposed portion of eyeball);
TD	tympanum diameter (the greater of vertical or horizontal diameter of tympanum);
DNE	distance from nostril to eye (from posterior border of nostril to anterior border of eye);
FLL	forelimb length (distance from elbow to tip of third finger);
THL	thigh length (distance from vent to knee);
TL	tibia length (distance from knee to heel);
FL	foot length (distance from proximal end of inner metatarsal tubercle to tip of fourth toe);
TFL	length of foot and tarsus (distance from tibiotarsal joint to tip of fourth toe).

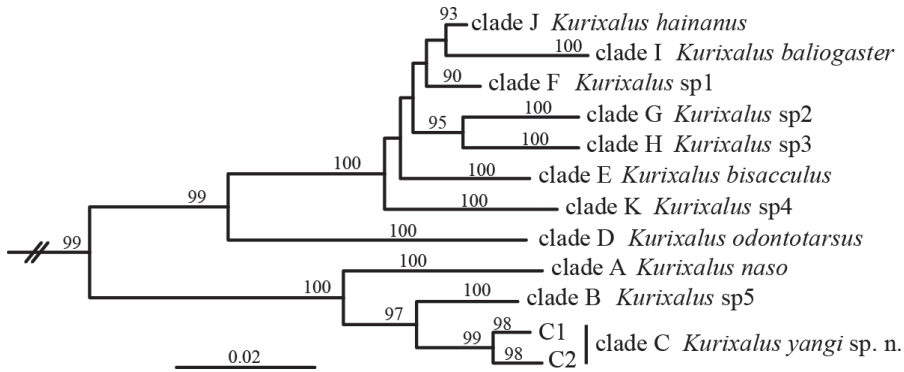


Figure 1. Simplified Neighbor-joining tree of the *Kurixalus odontotarsus* species group reproduced from Yu et al. (2017a).

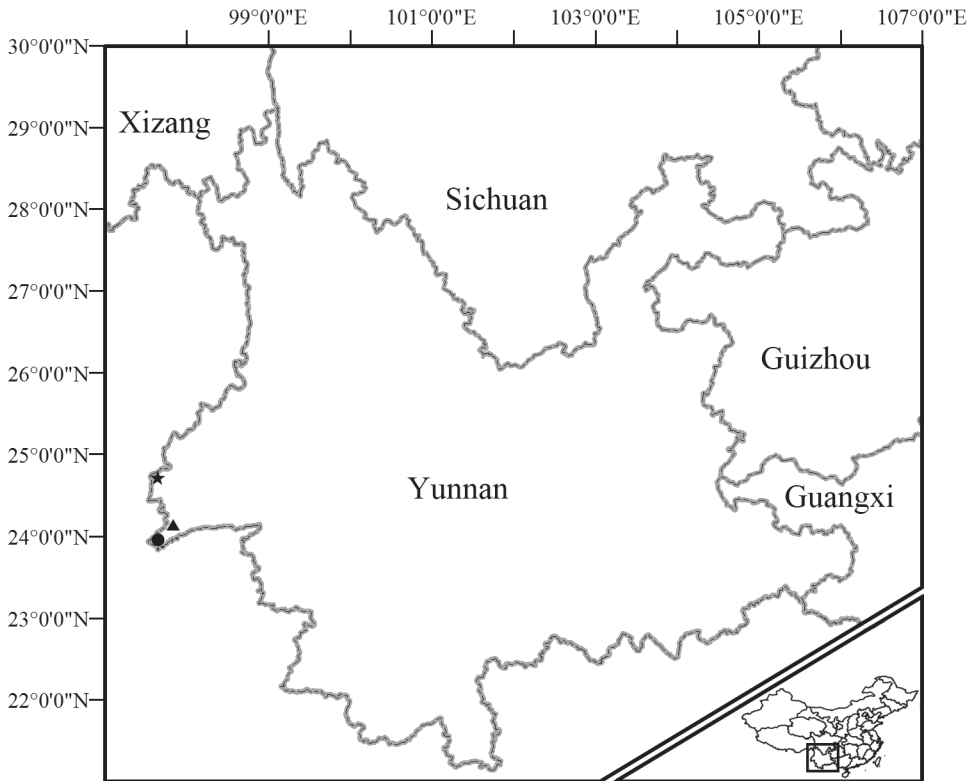


Figure 2. Collection sites of *Kurixalus yangi* sp. n. from western Yunnan, China. Star indicates the type locality, triangle indicates Nanjingli Village, and circle indicates Dengga Village.

A multivariate principal component analysis (PCA) was conducted using SPSS 17.0 (SPSS Inc.) based on a correlation matrix of size-standardized measurements (all measurements divided by SVL). Scatter plots of the scores of the first two factors

of the PCA were used to examine the differences between the new species and *K. naso*. Additionally, the differences between the new species and its two congeners known from Yunnan, China (*K. odontotarsus* and *K. hainanus*) were also similarly examined based on morphometric data.

Results

Morphometric data of the new species and *K. naso* are summarized in Table 1. We retained the first two principal components which accounted for 63.03% of the total variance and had eigenvalues above 2.0 (Table 2). Loadings for PC 1, which accounted

Table 1. Measurements of *Kurixalus yangi* sp. n. and *Kurixalus naso*. Abbreviations defined in text.

	Voucher no	SVL	HL	HW	SL	IND	IOD	UEW	ED	TD	DNE	FLL	THL	TL	TFL	FL
<i>Kurixalus yangi</i> sp. n.	KIZ 14102901	32.2	9.8	11.7	4.6	3.2	3.4	2.9	4.0	2.1	2.5	15.5	15.3	15.6	22.0	14.3
	KIZ 14102902	33.4	10.2	11.9	4.9	3.2	3.4	2.9	3.9	2.3	2.6	16.5	15.9	16.8	23.3	15.1
	KIZ 14102904	33.7	10.2	12.0	4.6	3.0	3.3	2.8	4.6	2.0	2.6	16.7	15.8	15.9	22.1	14.2
	KIZ 14102905	34.7	10.7	12.7	5.0	3.2	3.5	3.3	4.6	2.6	2.4	16.5	15.9	16.7	23.1	14.5
	KIZ 14102906	31.6	9.7	11.7	4.4	3.0	3.1	3.0	4.3	2.2	2.4	15.5	14.9	14.2	20.4	13.0
	KIZ 14102908	34.0	9.7	12.2	4.7	3.3	3.4	2.6	4.5	2.0	2.4	16.7	16.4	16.6	22.9	15.3
	KIZ 14102911	32.2	9.8	11.6	4.8	3.2	3.3	2.8	3.9	1.9	2.4	15.8	15.5	16.0	21.9	14.4
	KIZ 14102912	33.3	9.9	12.1	4.8	3.1	3.1	3.3	4.4	2.0	2.5	16.7	16.2	16.4	21.8	14.7
<i>Kurixalus naso</i>	KIZ 14102913	33.6	9.9	12.3	4.4	3.3	2.8	3.5	4.2	1.6	2.6	16.4	16.3	16.7	22.5	14.8
	KIZ 180001R	31.6	10.3	11.3	5.0	3.3	3.2	3.4	4.3	1.6	2.1	15.9	16.1	16.0	21.7	13.9
	KIZ 180002R	31.9	10.1	11.9	5.1	3.2	2.9	3.1	4.3	1.4	2.4	16.1	15.8	16.2	22.0	14.1
	KIZ 180003R	32.5	11.1	12.0	5.3	3.7	3.2	3.7	4.7	2.1	2.5	17.7	16.5	16.5	23.2	15.4
	KIZ 180004R	30.9	10.5	11.3	4.8	3.3	3.0	3.3	4.0	1.7	2.4	16.0	15.6	15.7	21.5	14.4
	KIZ 180005R	31.4	10.5	11.3	5.1	3.4	3.1	3.3	4.3	1.8	2.3	16.1	16.1	16.2	21.8	13.9
	KIZ 180006R	29.3	10.3	10.6	4.8	3.2	3.0	3.2	4.0	1.7	2.4	15.0	15.1	14.7	20.2	12.7

Table 2. Factor loadings of the first two principal components of 14 size-adjusted morphometric characteristics of males of *Kurixalus yangi* sp. n. and *Kurixalus naso*. Absolute values of loading greater than 0.70 in boldface. Abbreviations defined in text.

Character	PC 1	PC 2
Eigenvalue	6.817	2.008
% variation	48.691	14.339
HL	0.866	0.000
HW	0.187	-0.706
SL	0.885	0.135
IND	0.947	0.069
IOD	0.001	0.776
UEW	0.783	-0.384
ED	0.423	-0.486
TD	-0.388	0.367
DNE	0.182	-0.094
FLL	0.882	-0.111
THL	0.927	-0.050
TL	0.788	0.251
FTL	0.827	0.413
FL	0.658	0.330

for 48.69% of the total variance, were all positive except for TD and were most heavily loaded on HL, SL, IND, UEW, FLL, THL, TL, and TFL (Table 2). Differentiation was found along the PC 1 axis between *K. naso* and the new species (Fig. 3). This result indicates that the new species differs from *K. naso* by a series of characters associated with the head and limbs such as shorter HL, shorter SL, narrower IND, narrower UEW, shorter FLL, shorter THL, shorter TL, and shorter TFL. The second principal component (PC 2) accounted for 14.34% of the total variance and loaded heavily and positively on IOD and negatively on HW (Table 2), but no clear separation was observed along this axis between the new species and *K. naso* (Fig. 3). In addition, the new species can be separated from *K. odontotarsus* and *K. hainanus* by having smaller ratio of head length to body size (Fig. 4).

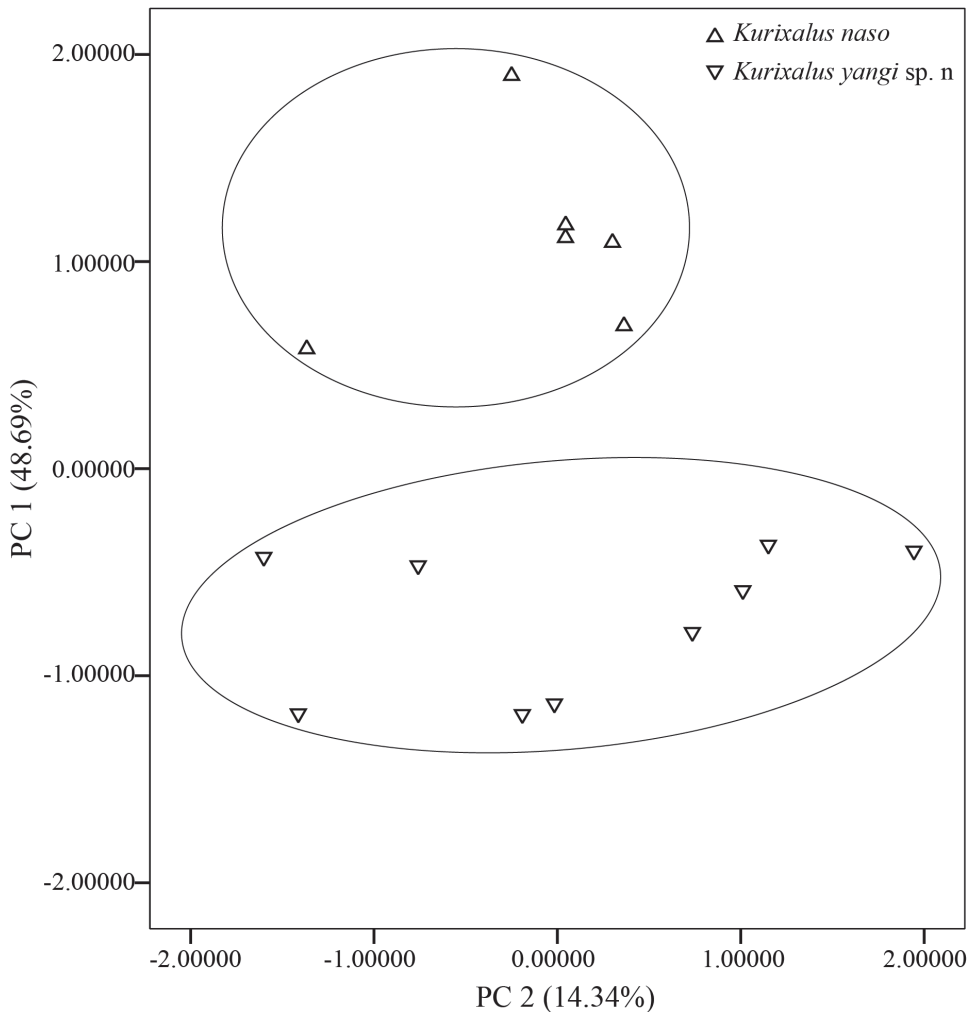


Figure 3. Scatterplot of principal components 1 and 2 of size-adjusted morphometric data for males of *Kurixalus yangi* sp. n and *Kurixalus naso*.

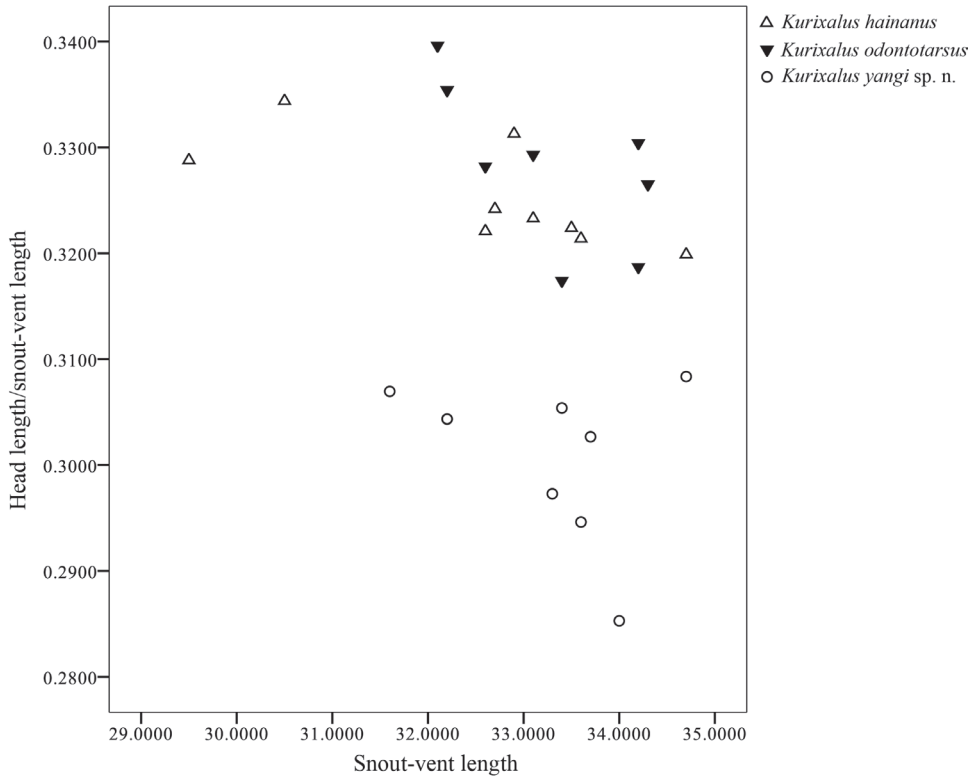


Figure 4. Scatterplot of ratio of head length against snout-vent length for males of *Kurixalus yangi* sp. n., *Kurixalus hainanus*, and *Kurixalus odontotarsus*.

Kurixalus yangi sp. n.

<http://zoobank.org/DBB82038-0DCD-48E0-AADB-FE66C31B1A7A>

Figs 5–7

Holotype. KIZ 14102911, an adult male, collected at 21:10 on 30 June 2014 by Hong Hui from Nabang (24°46'12.03"N, 97°34'28.03"E, 354 m elevation; Fig. 2), Yingjiang County, Dehong Autonomous Prefecture, Yunnan, China.

Paratype. Eight adult males: KIZ 14102901 and KIZ 14102902 collected at 20:40 on 10 July 2014 by Hong Hui from Dengga Village (23°59'21.05"N, 97°35'13.03"E, 868 m elevation; Fig. 2), Longdao Township, Ruili City, Dehong Autonomous Prefecture, Yunnan, China; KIZ 14102904–14102906 collected at 21:10 on 9 July 2014 by Hong Hui from Nanjingli Village (24°05'52.07"N, 97°50'30.07"E; 1366 m elevation; Fig. 2), Ruili City, Dehong Autonomous Prefecture, Yunnan, China, and KIZ 14102908, KIZ 14102912, and KIZ 14102913 collected at 21:10 on 30 June 2014 by Hong Hui from the type locality.

Etymology. The species name is dedicated to Professor Datong Yang from Kunming Institute of Zoology, Chinese Academy of Sciences for his outstanding contribution to herpetofauna research of Yunnan, China.

Diagnosis. The new tree frog species is assigned to the genus *Kurixalus* based on a combination of the following characters: tips of digits enlarged to discs, bearing circum-marginal grooves; small body size (SVL range of 31.6–34.7 mm in adult males; Table 1); finger webbing poorly developed and toe webbing moderately developed; serrated dermal fringes along outer edge of forearm and tarsus; an inverted triangular-shaped dark brown mark between eyes; dorsal brown “(” (“ saddle-shaped marking; and coarse dorsal and lateral surfaces with small, irregular tubercles (Nguyen et al. 2014a, Nguyen et al. 2014b, Yu et al. 2017b). Our previous molecular study placed the new species in *Kurixalus* with other known congeners (Yu et al. 2017a).

Kurixalus yangi sp. n. can be distinguished from its congeners by a combination of the following characters: male body size larger than 30 mm; smaller ratio of head length to body size; curved canthus rostralis; weak nuptial pads; brown dorsal color; absence of large dark spots on upper-middle abdomen; presence of vomerine teeth; gold brown iris; single internal vocal sac; serrated dermal fringes along outer edge of limbs; granular throat and chest; interorbital space longer than upper eyelid; rudimentary web between fingers; and presence of supernumerary tubercles and thenar tubercle.

Description of holotype. A small rhacophorid; HL shorter than HW; snout pointed, no dermal prominence on tip, projecting beyond margin of lower jaw in ventral view; canthus rostralis blunt and curved; lore region oblique, slightly concave; nostril oval, slightly protuberant, closer to tip of snout than eye; IND slightly narrower than IOD; pineal spot absent; pupil oval, horizontal; tympanum distinct, rounded, slightly less than half ED; supratympanic fold distinct, curving from posterior edge of eye to insertion of arm; vomerine teeth in two oblique patches, touching inner front edges of oval choanae; tongue notched posteriorly; single internal vocal sac.

Relative length of fingers is $I < II < IV < III$. Tips of all four fingers expanded into discs with circum-marginal and transverse ventral grooves; relative width of discs is $I < II < IV < III$; nuptial pad present on first finger; fingers weakly webbed at base; lateral fringes on free edges of all fingers; subarticular tubercles prominent and rounded, formula 1, 2, 2, 1; supranumerary tubercles present; two metacarpal tubercles present; series of white tubercles forming serrated fringe along outer edge of forearm.

Heels overlapping when legs at right angle to body; relative length of toes is $I < II < III < V < IV$; tips of toes expanded into discs with circum-marginal and transverse ventral grooves; toe discs smaller than finger discs; relative size of discs is $I < II < III < V < IV$; webbing moderate on all toes, webbing formula is $I1.5-2II1-2III1-2IV2-1V$ following Myers and Duellman (1982); subarticular tubercles prominent and rounded, formula 1, 1, 2, 3, 2; supernumerary tubercles present; inner metatarsal tubercle distinct, oval; outer metatarsal tubercle absent; series of tubercles forming serrated dermal fringe along outer edge of tarsus and fifth toe.

Numerous small to large tubercles scattered on top of head, upper eyelids, dorsum, and flanks; patch of white tubercles below vent; white tubercles on tibiotarsal articulation; throat and chest finely granulated and abdomen coarsely granulated; dorsal surface of limbs smooth with tubercles and ventral surface of thighs granulated.

Color of holotype in life. Iris golden brown; dorsal surface brown, mottled with green patches and a dark brown saddle-shaped mark on dorsum behind eye; a dark

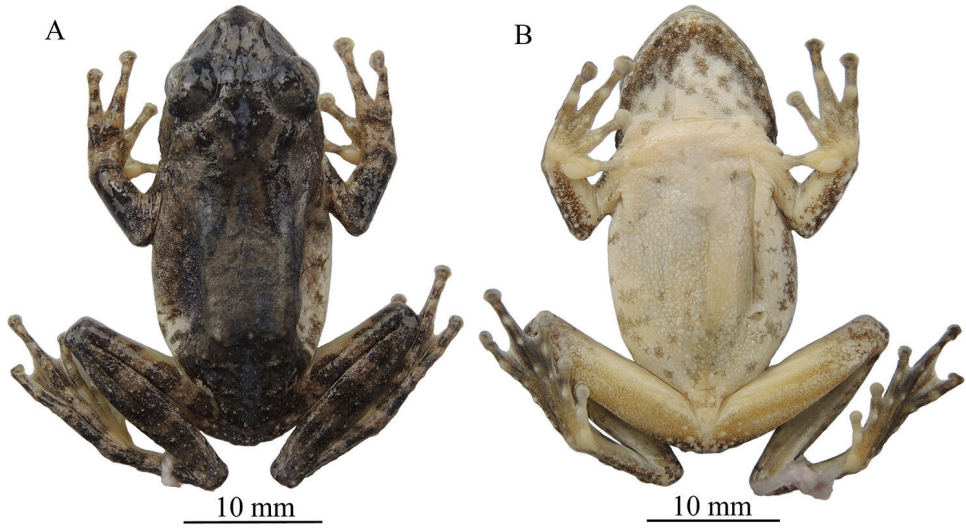


Figure 5. Dorsal (A) and ventral (B) views of the holotype of *Kurixalus yangi* sp. n. in preservative.



Figure 6. Ventral view of hand (A) and foot (B) of the holotype of *Kurixalus yangi* sp. n. in preservative.

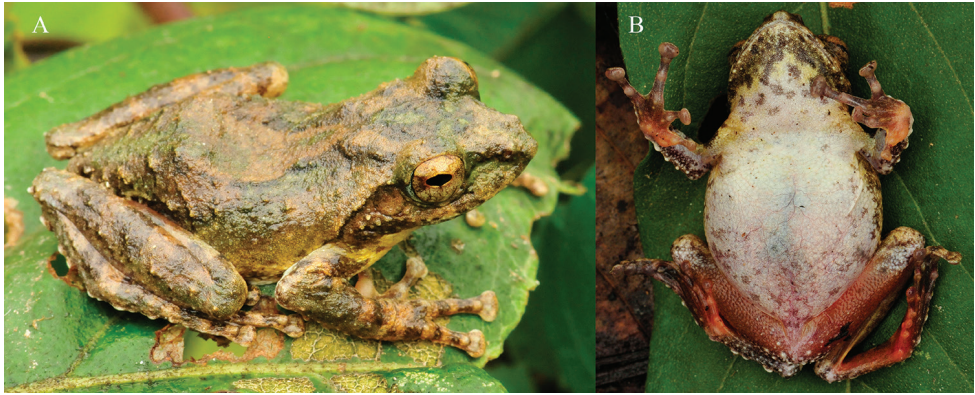


Figure 7. lateral-dorsal (A) and ventral (B) views of the holotype of *Kurixalus yangi* sp. n. in life.

brown inverted triangular-shaped mark between eyes, posterior of which extends to and touches the saddle-shaped mark; lateral head and tympanic region brown, mottled with green patches below canthus and dark brown spots on edge of upper jaw; flank light yellow, mottled with green and brown patches; limbs dorsally brown with three clear dark brown bands, mottled with green; palm of hand light red; rear, anterior, and venter of thigh red; inner side of tarsus and foot red; chest and abdomen white, fringed with yellow and mottled with small brown spots; chin clouded with dark brown and mottled with yellow patches.

Color of holotype in preservative. In preservative, green, yellow, and red faded. Dorsal ground color brown, pattern same as in life. Flank white with brown patches; margin of lower jaw clouded with dark brown; chin, chest, and abdomen white with scattered brown spots; palm of hand dirty white; anterior, posterior, and venter of thigh dirty white, with many fine brown speckling scattered on venter of thigh; inner side of tarsus and foot dirty white.

Variations. Because the holotype and paratypes of the new species are all male, sexual dimorphism could not be determined. IND is smaller than IOD in holotype and most paratypes, but IND is larger than IOD in paratype KIZ 14102913 (Table 1). In addition, IOD is larger than UEW in holotype and most paratypes, but IOD is smaller than UEW in paratypes KIZ 14102912 and KIZ 14102913 (Table 1). Additionally, color pattern of paratype KIZ 14102912 also differs from other specimens in that its chin has much less spotting.

Distribution and natural history. The new species is known from border region with northern Myanmar in western Yunnan, China (Fig. 2) and northern Myanmar according to Yu et al. (2017a). At the type locality, the new species was found calling on leaves of bushes adjacent to a road at night (Fig. 8). Specimens from the other two sites were found calling on broad leaves at the edge of an evergreen forest. Tadpoles, eggs and females were not found.

Comparisons. The new species, *Kurixalus yangi* sp. n., is genetically closer to *K. naso* than to other known members of *Kurixalus* according to our previous work (Yu

et al. 2017a), but morphologically it can be separated from *K. naso* by having smaller ratios of head, snout, IND, UEW, and limbs divided by SVL (Table 2 and Fig. 3). The smaller IND and UEW ratios in the new species can be observed when comparing these distances with the IOD, which is generally larger in the new species but smaller in *K. naso* (Table 1).

Currently, three *Kurixalus* species (*K. odontotarsus*, *K. hainanus*, and *K. lenquanensis* Yu, Wang, Hou, Rao, & Yang, 2017) are recognized in Yunnan, China (Yu et al. 2017a, Yu et al. 2017b). The new species differs from *K. odontotarsus* and *K. hainanus* by having smaller ratio of head length to body size and no large dark spots on abdomen (versus larger ratio of head length to body size and large dark spots on entire abdomen; Figs 4, 9) and from *K. lenquanensis* by larger body size (SVL of 31.6–34.7 mm in adult males), more pointed snout, and presence of green coloration on dorsal surface and lateral side of head and body (versus smaller body size [SVL of adult males less than 30 mm], somewhat rounded snout, and absence of green coloration on dorsum; Fig. 9, Yu et al. 2017b).

The new species is distinguished from *Kurixalus idiotocus* (Kuramoto & Wang, 1987) by larger body size, absence of a pair of symmetrical large dark patches on chest, and single internal vocal sac (versus smaller body size [SVL of adult males less than 30 mm], presence of a pair of symmetrical large dark patches on chest, and single external vocal sac; Yu et al. 2017a); from *Kurixalus berylliniris* Wu, Huang, Tsai, Li, Jhang, & Wu, 2016 by gold brown irises, weak nuptial pads, and coarsely granular abdomen (versus emerald to light green irises, greatly expanded nuptial pads, and smooth abdomen; Wu et al. 2016); from *Kurixalus wangi* Wu, Huang, Tsai, Li, Jhang, & Wu, 2016 by larger body size, weak nuptial pads, and presence of supernumerary tubercles on foot (versus smaller body size [SVL of 28.6–31.6 mm in adult males], greatly expanded nuptial pads, and absence of supernumerary tubercles on foot; Wu et al. 2016); and from *Kurixalus eiffingeri* (Boettger, 1895) by weak nuptial pads, oblique loreal region, and curved canthus rostralis (versus greatly expanded nuptial pads, vertical loreal region, and straight canthus rostralis; Wu et al. 2016).

In addition, *Kurixalus yangi* sp. n. differs from *Kurixalus baliogaster* (Inger, Orlov, & Darevsky, 1999) by having serrated dermal fringes on limbs, tuberculate dorsum, tubercles on eyelids, and absence of large dark spots on venter (versus no serrated dermal fringes on limbs, dorsum smooth, tubercles on eyelids absent, and large dark spots scattered on entire venter; Inger et al. 1999); from *Kurixalus banaensis* (Bourret, 1939) by having larger body size and vomerine teeth (versus smaller body size [SVL of 26.2–33.2 mm in adult males] and vomerine teeth absent; Nguyen et al. 2014b, Bossuyt and Dubois 2001); from *Kurixalus viridescens* Nguyen, Matsui, & Duc, 2014 by having brown dorsal color, dark markings on dorsum and limbs, and vomerine teeth (versus uniformly greenish dorsal color with no dark markings on dorsum and limbs, and vomerine teeth absent; Nguyen et al. 2014a); and from *Kurixalus motokawai* Nguyen, Matsui, & Eto, 2014 by having larger body size and vomerine teeth (versus smaller body size [SVL of 23.2–28.4 mm in adult males] and vomerine teeth absent; Nguyen et al. 2014b).



Figure 8. Habitat of *Kurixalus yangi* sp. n. at the type locality.

Kurixalus yangi sp. n. can be distinguished from *Kurixalus ananjevae* Matsui & Orlov, 2004 by having vomerine teeth, serrated dermal fringes on limbs, and finely granular throat surface (versus vomerine teeth absent, serrated dermal fringes absent, and throat surface smooth; Matsui and Orlov 2004); from *Kurixalus verrucosus* (Boulenger, 1893) by granular throat and chest and interorbital space longer than upper eyelid (versus throat and chest smooth and interorbital space as broad as upper eyelid; Boulenger 1893); from *K. bisacculus* by having single internal vocal sac (versus paired external lateral vocal sacs; Taylor 1962); and from *Kurixalus appendiculatus* (Günther, 1858) by having rudimentary web between fingers, supernumerary tubercles, and outer metacarpal tubercle (versus one third web between fingers, supernumerary tubercles absent, and outer metacarpal tubercle absent; Günther 1858, Brown and Alcalá 1994).

Discussion

Species diversity of the genus *Kurixalus* seems to be underestimated, with at least five unnamed lineages in the *K. odontotarsus* species group, with the exception of the new species described here, remaining to be described according to our earlier work (Yu et al. 2017a; Fig. 1). Taxonomic confusion in the *K. odontotarsus* species group mainly involved *K. bisacculus*. Of the remaining five clades that might represent unnamed species, four (clades F, G, H, and K; Fig. 1) were placed in *K. bisacculus* (Stuart and Emmett 2006, Thy et al.

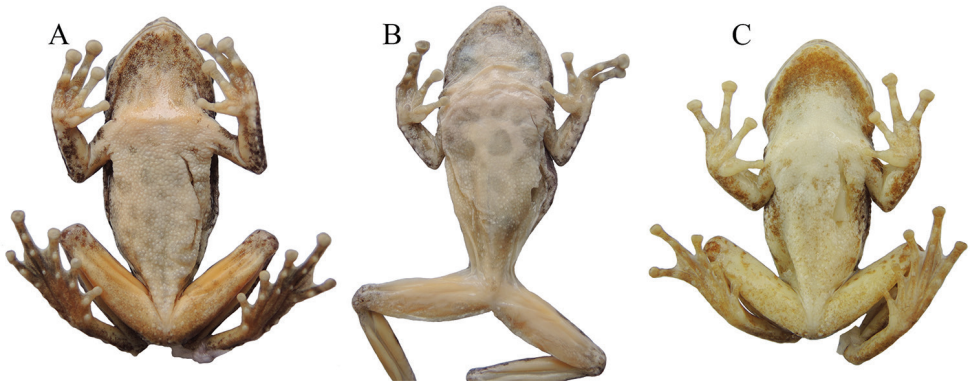


Figure 9. Ventral views of **A** *Kurixalus odontotarsus* (KIZ 180019Y) **B** *Kurixalus hainanus* (KIZ 180007R), and **C** *Kurixalus lenquanensis* (KIZ 170184Y; from Yu et al. 2017b).

2010, Yu et al. 2010, Nguyen et al. 2014a, Nguyen et al. 2014b). Even *K. hainanus* (clade J) was considered a synonym of *K. bisacculus* (Yu et al. 2010). A reason for this situation is the relatively low divergence of 16S rRNA sequences between *K. bisacculus* and these clades, which resulted in these lineages being considered conspecific though morphological differences exist between them (e.g., Yu et al. 2010). Another source of taxonomic confusion in the *K. odontotarsus* species group involves *K. verrucosus*, as specimens from northern Myanmar (*Kurixalus* sp5; Fig. 1) and *Kurixalus naso* from southern Tibet (clade A, Fig. 1) had been wrongly treated as *K. verrucosus* in previous molecular studies (Yu et al. 2010, Yu et al. 2013, Li et al. 2013, Nguyen et al. 2014a, Nguyen et al. 2014b) according to Yu et al. (2017a). Additionally, with the exceptions of those unnamed lineages revealed by Yu et al. (2017a), cryptic species likely also exist in Philippine populations of *K. appendiculatus* according to Gonzalez et al. (2014). In short, combination of the two recent molecular studies based on broad sampling (Gonzalez et al. 2014, Yu et al. 2017a) has provided a relatively clear genetic framework for the taxonomy of *Kurixalus* and more morphological studies will be necessary to verify the specific status of those lineages.

Phylogenetically, the *K. odontotarsus* species group is comprised of two clades; one contains *K. yangi* sp. n., *K. naso*, and *K. sp5* and one contains other species from Indochina and southern China (Fig. 1). *Kurixalus yangi* sp. n. is known from western Yunnan, China and northern Myanmar, *K. naso* is known from southern Tibet and northeastern India, and *K. sp5* is known from northern Myanmar. This pattern suggests that frogs of *Kurixalus* might have colonized the Indian subcontinent from northern Indochina.

Key to the new species and its congeners

- | | | |
|---|---|---|
| 1 | Limbs without serrated dermal fringes | 2 |
| – | Limbs with serrated dermal fringes | 3 |

- 2 Dorsum smooth; many dark spots scattered on ventral surface *K. baliogaster*
 *K. baliogaster*
- Dorsum with small tubercles, no dark spots on ventral surface *K. ananjevae*
- 3 Dorsal color uniformly greenish..... *K. viridescens*
- Dorsal color not uniformly greenish, generally brownish mixed with dark marking 4
- 4 Iris emerald to light green *K. berylliniris*
- Iris golden..... 5
- 5 Nuptial pad greatly expanded 6
- Nuptial pad slight 7
- 6 Tubercles on lateral margin of finger IV connected with dermal fringe; venter whitish with very little pigmentation; loreal region oblique; canthus rostralis curved..... *K. wangi*
- Tubercles on lateral margin of finger IV separated from each other; venter with numerous fine brownish dots, especially in the gular region; loreal region vertical; canthus rostralis straight *K. eiffingeri*
- 7 Vomerine teeth absent 8
- Vomerine teeth present 9
- 8 Snout tip less markedly pointed; lateral fringes on limbs and infra-cloacal tubercles less developed; lateral sides areolate *K. motokawai*
- Snout tip markedly pointed; lateral fringes on limbs and infra-cloacal tubercles developed; flanks smooth *K. banaensis*
- 9 Smaller body size (adult male SVL less than 30 mm) 10
- Bigger body size (generally adult male SVL greater than 30 mm)..... 11
- 10 Snout obtusely pointed with no prominence on tip; absence of a pair of symmetrical large dark patches on chest; single internal vocal sac *K. lenquanensis*
 *K. lenquanensis*
- Snout pointed with a small prominence on tip; a pair of symmetrical large dark patches present on chest; single external vocal sac *K. idiootocus*
- 11 Snout rounded or somewhat pointed; chin and breast smooth... *K. verrucosus*
- Snout obviously pointed; chin and breast granular..... 12
- 12 Paired external lateral vocal sacs *K. bisacculus*
- Single internal vocal sac 13
- 13 Outer metacarpal tubercles absent *K. appendiculatus*
- Outer metacarpal tubercles present 14
- 14 Ventral surface shaded posteriorly with dark spots 15
- Whole ventral surface shaded with large dark spots..... 16
- 15 Longer head, snout, and limbs; interorbital distance narrower than internarial distance and upper eyelid width *K. naso*
- Shorter head, snout and limbs; generally interorbital distance wider than internarial distance and upper eyelid width *K. yangi* sp. n.
- 16 Omosternum unforked..... *K. odontotarsus*
- Omosternum forked *K. hainanus*

Comparative material examined

Kurixalus naso: KIZ 180001R–180003R (field number: Rao 06304–06306), KIZ 180004R (field number: Rao 06308), KIZ 1800005R (field number: Rao 06309), KIZ 180006R (field number: Rao 06311), Motuo, Tibet, China. The sampling locality of these specimens is close to the type locality of *K. naso* (Egar stream between Renging and Rotung, Motuo, Tibet, China [in area claimed by India]) and morphological evidence provided in Yu et al. (2017a) indicates that the clade consisting of these specimens (clade A; Fig. 1) is most likely *K. naso*.

Kurixalus hainanus: KIZ 180007R (field number: Rao 14111303), KIZ 180008R (field number: Rao 14111304), Diaoluo Mt., Hainan, China (type locality of the species); KIZ 180009Y–180011Y (field number: YGH 090266, YGH 090268, YGH 090269), Nanning, Guangxi, China; KIZ 180012Y–180015Y (field number: YGH 090201, YGH 090202, YGH 090204, YGH 090205), Longmeng, Guangdong, China. These specimens were grouped in clade J (Fig. 1; Yu et al. 2017a) and morphologically differ from *K. bisacculus* (where they were previously placed in synonymy) by having single internal vocal sac (versus paired external lateral vocal sacs; see Yu et al. 2017a).

Kurixalus odontotarsus: KIZ 180016Y–180023Y (field number: YGH 090130–090137), Caiyanghe, Puer, Yunnan, China. The sampling locality of these specimens is close to the type locality of this species (Mengyang, Jinghong, Yunnan; ca. 75 KM) and genetically these specimens were grouped together with *K. odontotarsus* from the type locality according to previous studies (clade D in Yu et al. 2017a, clade II in Yu et al. 2010).

Acknowledgements

Thanks go to Xinqiang Song, Yan He, and Wenjing Jiang for their assistances with the field work. This study was supported by the National Natural Science Foundation of China (No. 31301870) and CAS “Light of West China” Program to G. Yu.

References

- Annandale N (1912) Zoological results of the Abor expedition. Part I. Batrachia. Records of the Indian Museum 8: 7–36. <https://doi.org/10.5962/bhl.part.1186>
- Boettger O (1895) Neue Frösche und Schlangen von den Liukiu-Inseln. Zoologischer Anzeiger 18: 266–270.
- Bossuyt F, Dubois A (2001) A review of the frog genus *Philautus* Gistel, 1848 (Amphibia, Anura, Ranidae, Rhacophoridae). Zeylanica 6: 1–112.
- Boulenger GA (1893) Concluding report on the reptiles and batrachians obtained in Burma by Signor L. Fea, dealing with the collection made in Pegu and the Karin Hills in 1887–1888. Annali del Museo Civico di Storia Naturale di Genova Serie 2 13: 304–347.

- Bourret R (1939) Notes herpétologiques sur l'Indochine française. XVII. Reptiles et batraciens reçus au Laboratoire des Sciences Naturelles de l'Université au cours de l'année 1938. Descriptions de trois espèces nouvelles. Annexe au Bulletin Général de l'Instruction Publique 6: 13–34.
- Brown WC, Alcalá AC (1994) Philippine frogs of the family Rhacophoridae. Proceedings of the California Academy of Sciences 10: 185–220.
- Fei L (1999) Atlas of Amphibians of China. Henan Publishing House of Science and Technology, Zhengzhou, China, 432 pp.
- Fei L, Ye C, Jiang J (2010) Colored Atlas of Chinese Amphibians. Sichuan Publishing House of Science and Technology, Chengdu, China, 519 pp.
- Frost DR (2018) Amphibian Species of the World: and Online Reference. Version 6.0. American Museum of Natural History, New York, USA. <http://research.amnh.org/herpetology/amphibia/index.html> [accessed 16 April 2018]
- Gonzalez P, Su YC, Siler CD, Barley AJ, Sanguila MB, Diesmos AC, Brown RM (2014) Archipelago colonization by ecologically dissimilar amphibians: Evaluating the expectation of common evolutionary history of geographical diffusion in co-distributed rainforest tree frogs in islands of Southeast Asia. Molecular Phylogenetics and Evolution 72: 35–41. <http://doi.org/10.1016/j.ympev.2013.12.006>
- Günther ACLG (1858) Neue Batrachier in der Sammlung des britischen Museums. Archiv für Naturgeschichte 24: 319–328. <https://doi.org/10.5962/bhl.part.5288>
- Inger RF, Orlov N, Darevsky I (1999) Frogs of Vietnam: a report on new collections. Fieldiana Zoology, New Series 92: 1–46.
- Kuramoto M, Wang C (1987) A new rhacophorid treefrog from Taiwan, with comparisons to *Chirixalus eiffingeri* (Anura, Rhacophoridae). Copeia 1987: 931–942. <https://doi.org/10.2307/1445556>
- Li J, Li Y, Klaus S, Rao D, Hillis DM, Zhang Y (2013) Diversification of rhacophorid frogs provides evidence for accelerated faunal exchange between India and Eurasia during the Oligocene. Proceedings of the National Academy of Sciences of the United States of America 110: 3441–3446. <https://doi.org/10.1073/pnas.1300881110>
- Matsui M, Orlov NL (2004) A new species of *Chirixalus* from Vietnam (Anura: Rhacophoridae). Zoological Science 21: 671–676. <https://doi.org/10.2108/zsj.21.671>
- Myers CW, Duellman WE (1982) A new species of *Hyla* from Cerro Colorado, and other tree frog records and geographical notes from western Panama. American Museum Novitates 2752: 1–32.
- Nguyen TT, Matsui M, Duc HH (2014a) A new tree frog of the genus *Kurixalus* (Anura: Rhacophoridae) from Vietnam. Current Herpetology 33: 101–111. <https://doi.org/10.5358/hsj.33.101>
- Nguyen TT, Matsui M, Eto K (2014b) A new cryptic tree frog species allied to *Kurixalus banaensis* (Anura: Rhacophoridae) from Vietnam. Russian Journal of Herpetology 21: 295–302.
- Stuart BL, Emmett DA (2006) A collection of Amphibians and Reptiles from the Cardamom Mountains, Southwestern Cambodia. Fieldiana Zoology 109: 1–27. [https://doi.org/10.3158/0015-0754\(2006\)187\[1:TNSOFA\]2.0.CO;2](https://doi.org/10.3158/0015-0754(2006)187[1:TNSOFA]2.0.CO;2)
- Taylor EH (1962) The amphibian fauna of Thailand. University of Kansas Science Bulletin 43: 265–599. <https://doi.org/10.5962/bhl.part.13347>

- Thy N, Grismer LL, Onn CK, Grismer JL, Wood jr. PL, Youmans TM (2010) First report on the herpetofauna of Dalai Mountain in Phnom Samkos Wildlife Sanctuary, southwestern Cardamom Mountains, Cambodia. *Cambodian Journal of Natural History* 2: 127–143.
- Wu S, Huang C, Tsai C, Lin T, Jhang J, Wu S (2016) Systematic revision of the Taiwanese genus *Kurixalus* members with a description of two new endemic species (Anura, Rhacophoridae). *ZooKeys* 557: 121–153. <https://doi.org/10.3897/zookeys.557.6131>
- Ye C, Fei L, Hu S (1993) Rare and Economic Amphibians of China. Sichuan Publishing House of Science and Technology, Chengdu, China, 412 pp.
- Yu G, Rao D, Matsui M, Yang J (2017a) Coalescent-based delimitation outperforms distance-based methods for delineating less divergent species: the case of *Kurixalus odontotarsus* species group. *Scientific Reports* 7: 16124. <https://doi.org/10.1038/s41598-017-16309-1>
- Yu G, Wang J, Hou M, Rao D, Yang J (2017b) A new species of the genus *Kurixalus* from Yunnan, China (Anura, Rhacophoridae). *Zookeys* 694: 71–93. <https://doi.org/10.3897/zookeys.694.12785>
- Yu G, Zhang M, Yang J (2010) A species boundary within the Chinese *Kurixalus odontotarsus* species group (Anura: Rhacophoridae): New insights from molecular evidence. *Molecular Phylogenetics and Evolution* 56: 942–950. <https://doi.org/10.1016/j.ympev.2010.05.008>
- Yu G, Zhang M, Yang J (2013) Molecular evidence for taxonomy of *Rhacophorus appendiculatus* and *Kurixalus* species from northern Vietnam, with comments on systematics of *Kurixalus* and *Gracixalus* (Anura: Rhacophoridae). *Biochemical Systematics and Ecology* 47: 31–37. <https://doi.org/10.1016/j.bse.2012.09.023>
- Zhao E, Wang L, Shi H, Wu G, Zhao H (2005) Chinese rhacophorid frogs and description of a new species of *Rhacophorus*. *Sichuan Journal of Zoology* 24: 297–300.

Carnivore distribution across habitats in a central-European landscape: a camera trap study

Klára Pyšková^{1,2}, Ondřej Kauzál^{1,2}, David Storch^{1,3},
Ivan Horáček⁴, Jan Pergl², Petr Pyšek^{1,2}

1 Department of Ecology, Faculty of Science, Charles University, Viničná 7, CZ-12844 Prague 2, Czech Republic
2 Institute of Botany, Department of Invasion Ecology, The Czech Academy of Sciences, CZ-25243 Průhonice, Czech Republic
3 Center for Theoretical Study, Charles University and The Czech Academy of Sciences, Jiřská 1, CZ-11000, Prague 1, Czech Republic
4 Department of Zoology, Faculty of Science, Charles University, Viničná 7, CZ-12844 Prague 2, Czech Republic

Corresponding author: Klára Pyšková (klarapyskova@hotmail.com)

Academic editor: J. Maldonado | Received 27 November 2017 | Accepted 21 May 2018 | Published 4 July 2018

<http://zoobank.org/AE2AA1B0-460C-4471-AC8D-20C317748F90>

Citation: Pyšková K, Kauzál O, Storch D, Horáček I, Pergl J, Pyšek P (2018) Carnivore distribution across habitats in a central-European landscape: a camera trap study. ZooKeys 770: 227–246. <https://doi.org/10.3897/zookeys.770.22554>

Abstract

Quantitative data on local variation in patterns of occurrence of common carnivore species, such as the red fox, European badger, or martens in central Europe are largely missing. We conducted a study focusing on carnivore ecology and distribution in a cultural landscape with the use of modern technology. We placed 73 automated infra-red camera traps into four different habitats differing in water availability and canopy cover (mixed forest, wetland, shrubby grassland and floodplain forest) in the Polabí region near Prague, Czech Republic. Each habitat was represented by three or four spatially isolated sites within which the camera traps were distributed. During the year of the study, we recorded nine carnivore species, including the non-native golden jackal. Habitats with the highest numbers of records pooled across all species were wetland (1279) and shrubby grassland (1014); fewer records were made in mixed (876) and floodplain forest (734). Habitat had a significant effect on the number of records of badger and marten, and a marginally significant effect on fox. In terms of seasonal dynamics, there were significant differences in the distribution of records among seasons in fox, marginally significant in least weasel, and the occurrence among seasons did not differ for badger and marten. In the summer, fox and marten were more active than expected by chance during the day, while the pattern was opposite in winter when they were more active during the night. Our findings on habitat preferences and circadian and seasonal activity provided the first quantitative data on patterns whose existence was assumed on the basis of conventional

wisdom. Our study demonstrates the potential of a long-term monitoring approach based on infra-red camera traps. Generally, the rather frequent occurrence of recorded species indicates that most carnivore species are thriving in current central-European landscapes characterized by human-driven disturbances and urbanization.

Keywords

camera trap, Elbe River catchment, central Bohemia, circadian activity, ecology, seasonal dynamics

Introduction

In the last decade, field research of mammals has principally changed with the invention of automated camera traps, which are now becoming a standard monitoring tool (O'Connell et al. 2011, Burton et al. 2015). With the rapid technological advances, camera traps have been gaining more attention and popularity as they allow for the non-intrusive observation of animals and rapid and efficient collection of large data sets that are both unique and high quality. Mammals, and particularly carnivores, are a group of animals that are not easy to monitor due to their mobility and mostly nocturnal and crepuscular activity, and their intelligence and shyness. Camera traps allow insight into this hidden world without disturbing the observed organisms.

While most studies using camera traps have focused on a particular species, habitat type, activity or behaviour (e.g. Ahumada et al. 2011, Manzo et al. 2011, Braczkowski et al. 2016), complex studies addressing diversity, species composition and behaviour across habitat types are missing. In the Czech Republic, most attention has been paid to large and rare carnivore species, such as the Eurasian lynx (*Lynx lynx*) and the gray wolf (*Canis lupus*), iconic representatives of a charismatic group of animals and the focus of nature conservation (Baruš et al. 1989, Kutal et al. 2016, Kutal 2017). These carnivores began returning to this country in the 1990s from neighbouring regions and have established viable populations. In addition, camera traps proved useful for discovering and monitoring the presence and behaviour of species spreading from other regions, such as the golden jackal, *Canis aureus* (Pyšková et al. 2016). However, the more common carnivore species (such as martens, weasels, foxes and badgers) are largely neglected and to date have never become a target of systematic quantitative investigation using camera traps over a long period of time. Within the temperate zone such data are lacking completely not only for the Czech Republic, but for Europe as a whole. Moreover, the majority of literature sources on carnivore ecology and distribution in the Czech Republic are rather outdated (e.g. Mazák 1964, Baruš and Zejda 1981), based on information that is often anecdotal, and much of the quantitative data on these species' distributions come from hunting statistics or questionnaires, which can suffer from various biases. Data on habitat preferences, seasonal and circadian activity, and presence of common carnivore species in the changing landscapes of central Europe are lacking. We know little about how these animals adapt to the heavily inhabited modern environment.

To contribute towards closing this gap and to provide the first basic quantitative insights into the patterns of carnivore distribution in typical central-European habitats, we (i) recorded the species richness and composition of carnivores in a typical temperate mosaic landscape, (ii) quantitatively compared carnivore presence in different habitats along the moisture and canopy-cover gradients, (iii) analysed the seasonal and circadian activity of the species in the course of a whole year, and (iv) identified any non-native species in the area studied.

Methods

Study area

The study area was located ~30–40 km east of Prague in the Elbe River catchment, in the districts of Nymburk and Mladá Boleslav (Fig. 1). The area is quite heavily inhabited (114 and 123 inhabitants per km², respectively; Český statistický úřad 2016) and agriculturally dense (70.2% of the central Bohemia district is covered by agricultural land, 23.9% by forest, 4.6% by artificial surfaces and 0.7% by water bodies; Corine Land Cover 2012, version 18.5.1 – CENIA 2012). We chose this region because it contains various types of habitats and represents a typical central-European landscape, consisting of a mosaic of human-made and seminatural habitats. The majority of the study area is at an altitude of < 200 m a.s.l., with a warm mild climate, annual average temperature of 8.5–9.0 °C and annual precipitation of 550 mm. The size of the study area, expressed as the landscape sections over which the 13 sites were distributed was ~200 km². From the botanical perspective, the area belongs to thermophyticum, district of thermophilous flora with vegetation cover formed by oak and hornbeam forest, dry grassland and xerophilous shrub (Kaplan 2012). Recently, part of the area was used for reintroduction of ungulates that were driven to extinction by past human activities, such as a breed of domestic cattle resembling the auroch (*Bos primigenius*), the Exmoor pony as a breed resembling the wild horse (*Equus ferus*), and European bison (*Bison bonasus*; Stokstad 2015).

Habitats

The habitats chosen for this project were wetland, floodplain forest, mixed forest and a shrubby grassland (steppe), forming a distinct moisture- and canopy-openness gradient (see Fig. 2):

- (i) Wetland habitat, the wetter alternative of the open biotope, had a high ground-water level or was located in close proximity to water courses, or abandoned meanders and oxbow lakes. The dominant vegetation types are mostly sedge- and moor-grass meadows, reed beds, and willow patches along streams.

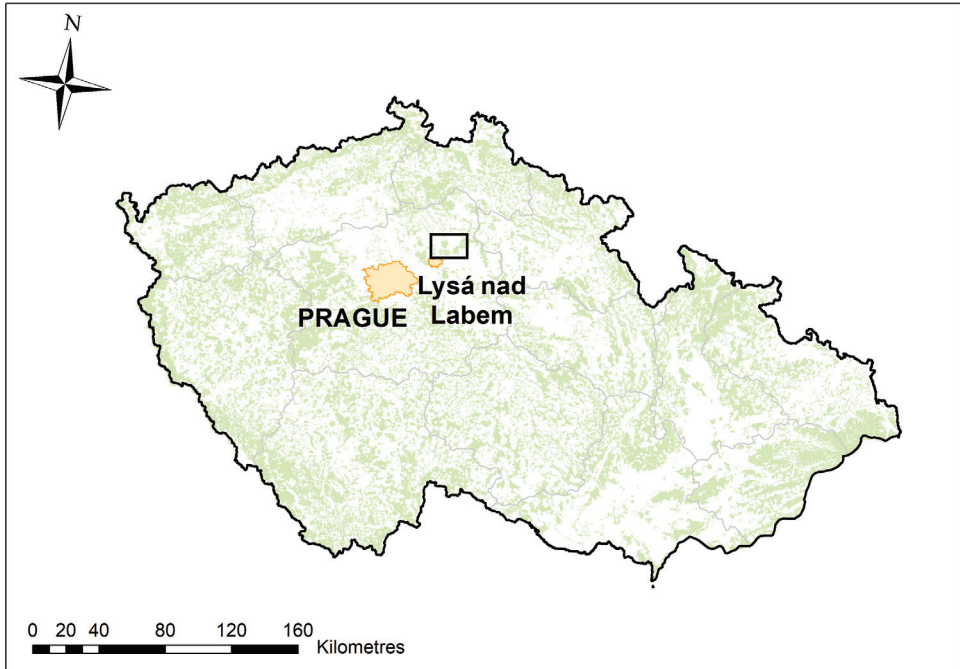


Figure 1. Location of the study area in central Bohemia, western part of the Czech Republic (black rectangle).



Figure 2. Habitat types studied. **A** wetland **B** floodplain forest **C** mixed forest **D** shrubby grassland (see text for description). Photo credits: Klára Pyšková

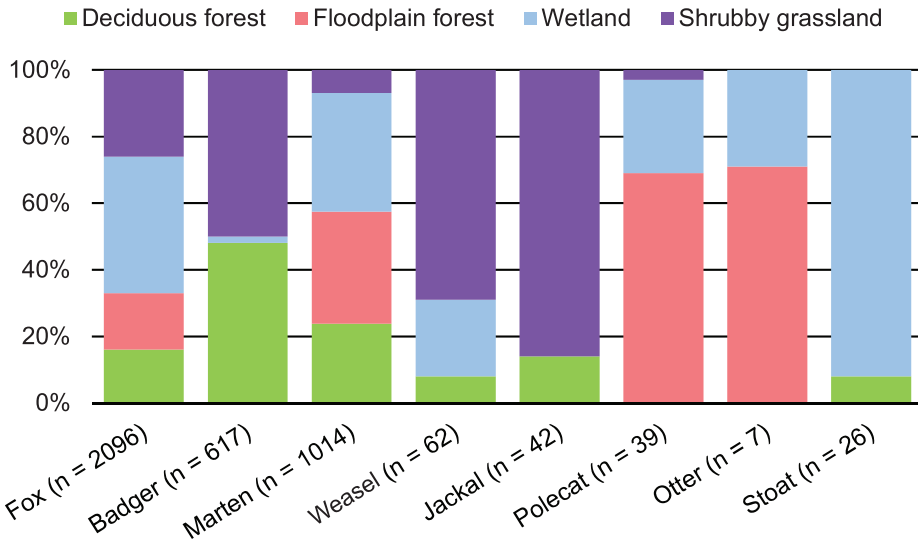


Figure 3. Habitat preferences of the carnivores studied; the figures are percentages of the total number of standardized daily records as recorded in each habitat.

- (ii) Floodplain forest was located along the Elbe river, in sites with high groundwater level and regular flood cycles, forming a mosaic of wetter and drier patches. Prevailing trees are oak, poplar, elm and ash; typical plant communities are alder carrs and willow carrs, with treeless patches covered by reed and tall-sedge beds and wet meadows. Presence of seasonal and perennial pools or creeks by the banks of the Elbe River is typical of this habitat, which represents the wet side of the moisture gradient with closed canopy.
- (iii) Mixed forest, the dry variant of the closed-canopy habitat, with oak- and oak-hornbeam woodlands; the other dominant species of these communities were lime, birch, spruce and pine.
- (iv) Shrubby grassland was a savanna-like dry alternative of the open habitat. This habitat was dominated by grasses with scattered shrubs, mostly blackthorn and hawthorn (Fig. 3).

Data collection

Each habitat type was represented by 3–4 spatially isolated sites, giving the total of 13 sites: wetland (4), floodplain forest (3), mixed forest (3), and shrubby grassland (3). The sites were located on average 3 km from one another. In each site we placed 4–10 camera traps, depending on the area of the site; each habitat was therefore monitored by 15–20 camera traps in total as follows: wetland (18), floodplain forest (19), mixed forest (15), and shrubby grassland (21). We used 73 UOVision type UV 535 Panda

camera traps with infrared flash. The minimal distance between the traps within a site was 200 m and they were distributed so as to cover the range of conditions represented at a site, from the margins to the interior of the given habitat. The particular placement spots for the traps were chosen with consideration of the expected carnivores' occurrence, i.e. mainly along animal trails, near water, along terrain depressions, etc. The traps were placed on trees approximately 0.5–1 m above the ground and we also had to consider possible human presence, so we chose places where we expected the least movement of people. The project started at the beginning of June 2015 and the results from the first complete year, until the end of May 2016, are reported here. The camera traps were in the field non-stop and data collection (photo downloading) was done at all sites approximately once a month. In total, we gathered over 900,000 photographs with the majority of them being empty or of non-target animal groups (such as ungulates, rodents, or occasionally birds).

Data standardization

Because it was not possible to identify individual animals (especially on the night photographs, which were black and white because of the infrared flash), in order to infer data on abundances we standardized the data as follows. First, if the same animal was recorded as moving around on a series of subsequent photographs taken over less than two minutes, we considered this as one record. If such an individual was present for a long period of time without leaving the spot in front of the camera trap, for example resting, feeding or sleeping, we also considered that as one record. The data standardized in this way (termed 'standardized records'), making up the total of 5011 records, were used for the analysis of patterns in daily activity.

For other analyses that addressed seasonal dynamics and habitat preferences, we used another standardization procedure. To reduce the possibility of bias caused by the repeated presence of an individual animal at the same camera trap, we only counted the presence of a particular species at each camera trap in a given day, disregarding the number of records (further termed as 'standardized daily records'). After this standardization we were left with 3903 records of carnivores (i.e. 78.9% of the total number of 5011 records).

Statistical analysis

Differences in the numbers of species among habitats were tested by using GLM models with Poisson distribution of errors. The effect of habitat and season on the number of standardized daily records of individual species was statistically tested only for those species with > 50 records (fox, marten, badger, least weasel), using a linear model with normal errors. Because the numbers of records at individual sites were divided by the numbers of camera traps taking pictures at the given time (accounting for the fact

that some might not be functioning between two samples due to technical problems or theft until replaced), we could not use a GLM model with Poisson distribution of errors. The models were tested by step-wise removal of interactions or factors (Crawley 2007). The sites ($n = 13$) were treated as a random factor, and the factor 'season' was nested within the site to eliminate the effect of pseudoreplication.

The significance of interaction between the number of standardized records during day vs. night and season was tested by using GLM model with Poisson distribution of errors (Crawley 2007), and the significance of differences between cells according to Řehák and Řeháková (1986). There were two tests carried out for each species, one on standardized data as recorded, and the other one on the data related to the duration of day and night in particular seasons (using the ratio of absolute number of records in a season to the proportional length of the day in that season, averaged across the three months).

Results

Carnivore species richness

In total we recorded nine carnivore species in our study area: red fox (*Vulpes vulpes*), European badger (*Meles meles*), pine marten (*Martes martes*) and stone marten (*Martes foina*; these two species were merged into one group "marten", due to the difficulty of recognizing them especially on the nocturnal black and white photographs), stoat (*Mustela erminea*), least weasel (*Mustela nivalis*), European polecat (*Mustela putorius*), European otter (*Lutra lutra*) and golden jackal (*Canis aureus*). The highest numbers of species occurred in wetland (7), followed by mixed forest and shrubby grassland (6), and the least in the floodplain forest (4), but these differences were not significant (GLM model with Poisson distribution of errors; $df = 3$, $dev. = 2.09$, $P = 0.55$). The most frequently recorded species were fox ($n = 2069$), marten ($n = 1014$) and European badger ($n = 617$), the species with the lowest number of records was otter ($n = 7$). Standardized numbers of species in respective habitats are shown in Table 1.

Habitat preferences

Habitats with the highest standardized numbers of daily records pooled across all species were wetland (1279) and shrubby grassland (1014); fewer records were made in mixed (876) and floodplain forest (734) (Table 1).

Since we were interested in how the numbers of standardized daily records of the common carnivore species were affected by habitat and season, we first tested for the interaction of these two factors. This interaction was not significant for any of the species (fox: $F = 0.41$; badger: $F = 0.39$; marten: $F = 1.05$; least weasel: $F = 1.64$; $df = 36, 45$); therefore we tested for the effect of habitat and season separately. Habitat had a significant effect on the number of records of badger and marten, and marginally

Table 1. Standardized numbers of carnivore records in particular habitats in the four seasons. Data are summary numbers of records from all camera traps located in a given habitat, captured in a particular season.

	Spring	Summer	Autumn	Winter	Total
Mixed forest	220	256	250	150	876
fox	68	60	115	82	325
badger	92	89	86	31	298
marten	60	107	40	33	240
jackal			2	4	6
weasel			5		5
stoat			2		2
Floodplain forest	173	123	234	204	734
fox	39	53	140	130	362
marten	124	60	87	69	340
polecat	8	10	5	4	27
otter	2		2	1	5
Wetland	230	269	372	408	1279
fox	143	173	244	295	855
marten	76	72	106	107	361
stoat	1	9	12	2	24
weasel	3	3	6	2	14
badger	7	3	2		12
polecat		8	2	1	11
otter		1		1	2
Shrubby grassland	214	286	287	227	1014
fox	100	163	156	135	554
badger	85	96	76	50	307
marten	25	11	19	18	73
weasel	3	3	21	16	43
jackal	1	12	15	8	36
polecat		1			1
Total (all habitats)	837	934	1143	989	3903
fox	350	449	655	642	2096
marten	285	250	252	227	1014
badger	184	188	164	81	617
weasel	6	6	32	18	62
jackal	1	12	17	12	42
polecat	8	19	7	5	39
stoat	1	9	14	2	26
otter	2	1	2	2	7

significant on fox (Table 2). Foxes were most often recorded in wetland (41% of all standardized daily records) and this difference was statistically significant ($P < 0.05$). Of all species, the red fox had the most even distribution among habitats. The records of marten were also evenly distributed, with the exception of shrubby grassland, where it was significantly less represented (Fig. 3). Badgers were only present in the dry habitats, shrubby grassland and mixed forest, with only 2% of records from wetland. Least

Table 2. Effect of habitat and season on the numbers of standardized daily records of the four species with sufficient number of records. Tested by using linear regression with normal distribution of errors ($df = 3, 48$); n.s., not significant.

Species	Factor	F	P
fox	Habitat	2.15	< 0.1
	Season	2.92	< 0.05
badger	Habitat	12.07	< 0.001
	Season	0.53	n.s.
marten	Habitat	5.79	< 0.05
	Season	0.24	n.s.
least weasel	Habitat	5.79	< 0.05
	Season	2.60	< 0.1

weasel had the strongest, statistically significant preference for shrubby grassland with 69% of the records (both these species were missing from the floodplain forest). All the remaining species, for which the habitat preferences were not statistically tested due to a small number of records, revealed a strong preference for a certain habitat, stoat in floodplain forest (92%), jackal in shrubby grassland (86%) and otter (71%) and polecat (69%) in floodplain forest (Fig. 3).

Seasonal dynamics

The total numbers of standardized daily records pooled across species and habitats were rather evenly distributed over seasons, reaching the highest values in the autumn (1143), lowest in spring (837), being very similar in summer and winter (934 and 989, respectively, Table 1). There were significant differences in the distribution of records of fox, marginally significant for least weasel, and these numbers did not significantly differ for badger and marten (Table 2). The number of red fox records increased throughout the year, from spring minima through stable numbers in summer and beginning of autumn, towards the highest numbers of records in November and December. The numbers of badger records fluctuate, with maxima in April and later on October and November, and markedly, but non-significantly, reduced activity over winter. Least weasel's activity is greatest in autumn and very low in spring and summer. Marten was the only species with no obvious seasonal pattern (Fig. 4).

Circadian activity

Using exact time data recorded by the camera traps we analysed the circadian activity of all the species. Fox and marten were more often recorded during the day in the summer (with 33% and 34% of records, respectively), while in winter they were more active during the night (with only 8% and 1% of records recorded during the day).

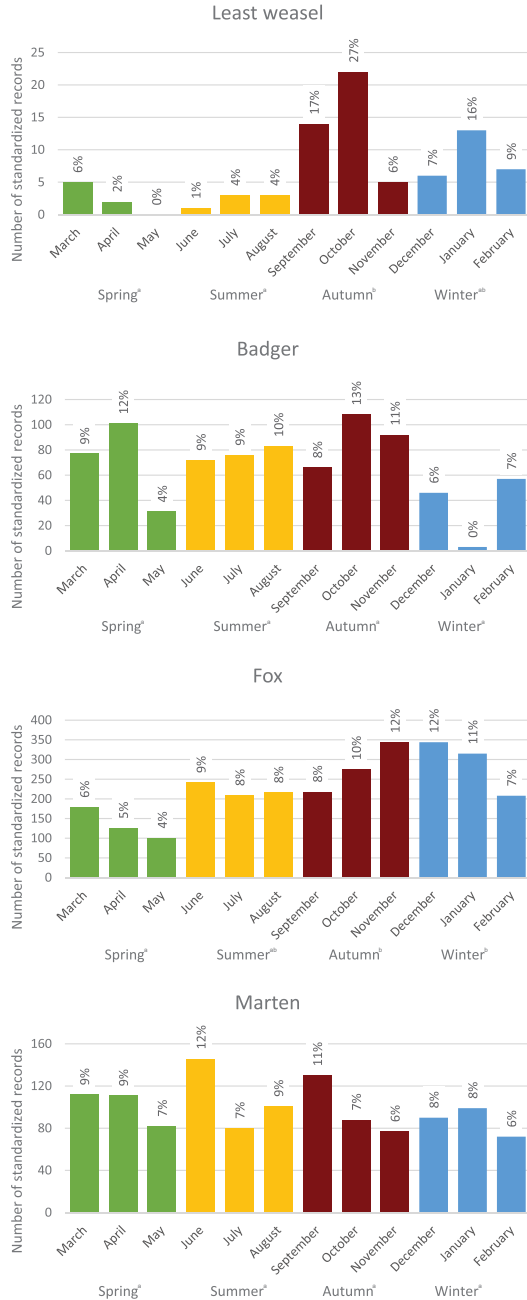


Figure 4. Seasonal dynamics shown for the carnivore species commonly occurring in the study area (with > 50 standardized daily records). The data were collected from June 2015 to May 2016, and the seasons are arranged in annual sequence for better illustration of seasonal dynamics. Seasons bearing the same letter are not significantly different from each other, based on linear model testing differences in the total number of records over the three months within the season. Values on top of the bars are percentages of the total number of records for a given species.

Table 3. Interaction between season and the number of standardized records collated in daylight vs night, presented for the three most common carnivore species studied. The data were tested on contingency tables following Crawley (2007), with $df = 3$ for all tests; n.s., not significant. The analysis is based on the numbers of records standardized by the length of the day in particular seasons (using the ratio of absolute number of records in a season to the proportional length of the day in that season, averaged across the three months). Note that the least weasel is not included in the test because the number of records ($n = 62$) was too low for robust analysis.

Species	χ^2	P
fox	19.08	< 0.001
marten	8.32	< 0.05
badger	1.89	n.s.

Badgers were only rarely photographed in the daylight (2%, 5% and 4% of records in spring, summer and autumn, respectively, and none in winter, Fig. 5). For these three most common species we tested, using the numbers of records standardized by the seasonal variation in day length, whether the percentage of records from day and night differed depending on the season. The differences observed for fox and marten were statistically significant, while those for badger were not (Table 3).

Discussion

Methodological assumptions

Most studies using camera traps focus on particular species, habitat type or topic. The majority of studies are on carnivores in forest habitats and most studies focus on population densities (McCallum 2013). While there are hundreds of studies based on camera traps published each year (over 200 papers in Web of Science categories ‘ecology’, ‘zoology’ and ‘conservation’ for 2016; WoS search as of 21 June 2017) papers quantitatively comparing the occurrence of carnivores in a range of habitats representing different levels of moisture and canopy openness are, to best of our knowledge, non-existent for temperate Europe. Our study started in June 2015 and covered all seasons with the traps permanently present throughout the year. We investigated species composition and structure in a range of habitats, representing the current central European landscape, the seasonal and circadian dynamics of all the species in all habitats and their habitat preferences.

Because it was not possible to identify individual animals on photographs, we did not attempt to estimate population densities and the quantitative comparisons were rigorously tested only interspecifically. We assumed that individuals of the same species behave in a similar way in different habitats or seasons, therefore the frequencies of captures do not systematically differ among these factors. Based on this assumption, we expect that a species with significantly more records in certain habitat or season is indeed more abundant in the respective habitat or season.

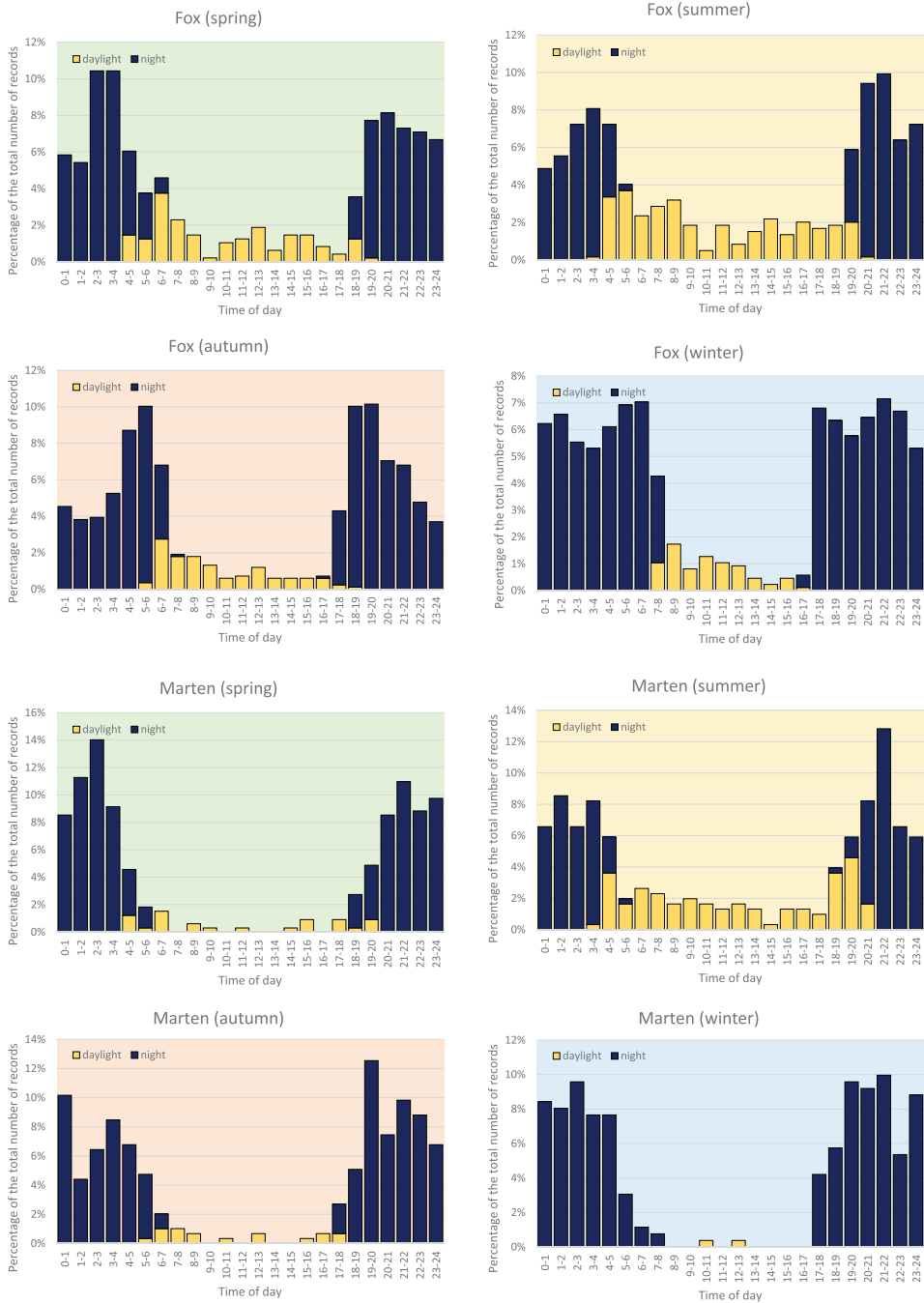


Figure 5. Circadian activity of fox and marten shown by season, expressed as the percentage of standardized records photographed at daylight and in the night. For badger, a whole-year summary is shown as the significant differences among seasons are due to it not occurring at daylight in winter.

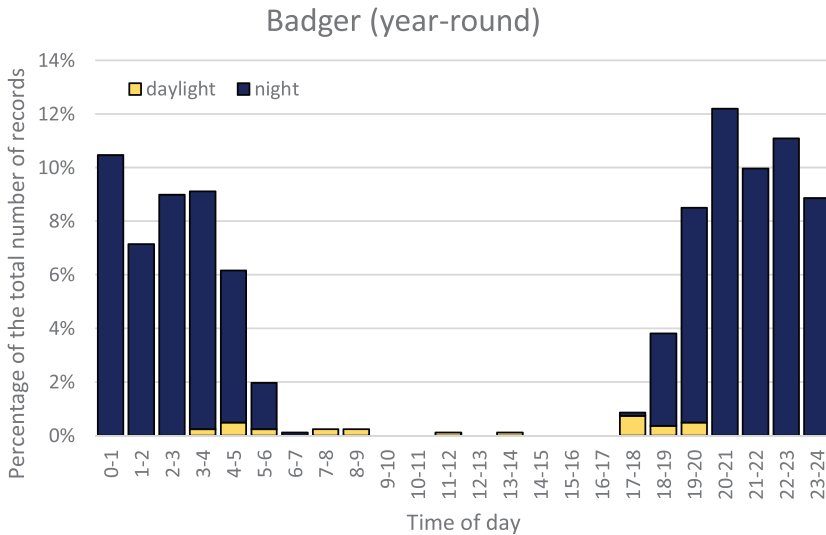


Figure 5. Continued.

To estimate population densities, the capture-recapture technique is necessary (Karanth 1995, Karanth and Nichols 1998) if individual recognition is not possible (Wilson and Delahay 2001, Jennelle et al. 2002). However, in our study the capture-recapture method was not feasible for logistic reasons, including difficulties with obtaining permits for this kind of animal handling. While we were able to recognize some individuals repeatedly visiting locations of particular camera traps, we could not do so with certainty for different camera traps within- or among sites. With some other species such as badgers, individual recognition, which is crucial for abundance- and population-densities estimates (Trolle and Kery 2003), was not possible especially on black and white photos. Some authors argue that mathematical models can overcome the need for individual recognition (Rowcliffe et al. 2008, Shulman et al. 2016), but other authors invalidate these assumptions (Sollmann et al. 2013) and warn about a number of pitfalls (Foster and Harmsen 2012). Indeed, our data for one species suggest that population density estimates based on the number of records would really be biased – the 47 records of a golden jackal probably capture just one individual (Pyšková et al. 2016).

Distribution and abundance of carnivore species in the Czech Republic

Out of 13 native carnivore species (notwithstanding the extinct European mink *Mustela lutreola* and four alien species) hitherto recorded in the Czech Republic (Anděra and Červený 2009, Pyšková 2017) eight were recorded in our study. Four of the native species that are absent from our record have rather restricted distribution in the country: gray wolf (*Canis lupus*), European lynx (*Lynx lynx*), wild cat (*Felis silvestris*)

and brown bear (*Ursus arctos*); the latter species was recently repeatedly reported to cross the Polish or Slovakian borders (Anděra and Červený 2009). The remaining species, steppe polecat (*Mustela eversmanii*), is known from few records dispersed in the lowland regions of the country (Anděra and Gaisler 2012) and although it cannot be excluded at least in two areas of our study, until now it was not recorded. The majority of information on the distribution of carnivores comes from questionnaires and hunting statistics, compiled in approximately 10-year intervals (Anděra and Hanzal 1996, Anděra 2017a). The hunting data are not collected systematically, therefore their quality varies from one region to another, yet they provide a broad overall picture of how common individual carnivore species are in the Czech Republic.

The red fox and European badger are the most common carnivore species throughout the whole country and their occurrence is stable. The same holds for stoat and least weasel. The European polecat is also present in most grid cells, but its population densities have been declining slowly, and nowadays it is becoming rare or even extinct in some regions. Our results, with only 39 records of European polecat across all habitats throughout the year, seem to reflect this declining population trend reported by IUCN, which is also happening in neighbouring countries, Austria and Germany (Skumatov et al. 2016). Both species of marten are also common, forming stable populations. One species undergoing a significant change is the otter – it has become more common again in the past decades (Anděra and Hanzal 1996, Anděra and Červený 2009).

In our study, the most common species was the red fox. The data allow for quantifying the probability of its occurrence in a certain spot throughout the duration of the study. In total, there were 2096 standardized daily records of fox (i.e. 68% of all 3903 records pooled across species); taking into account that the maximum number of daily records from 62 camera traps over the whole year is 22,692 (the maximum number of daily records is reduced due to the possible malfunction of camera traps or theft between two sampling dates before replacement), there is a ~9% probability that the fox would be observed in a place where a camera was placed at least once a day. The red fox is not protected by law and can be hunted throughout the year without any restrictions in the Czech Republic (Regulation MZe ČR 245/2002 Sb). After eradication of rabies in the mid-2000s (Matouch et al. 2006, 2007), hunting represents the only means of regulating fox populations; however, this need not necessarily lead to lower population densities because foxes are reported to respond to hunting pressure by increasing their reproduction rate (Lozano et al. 2013).

Martens were the second most frequently captured carnivores. Since the hunting statistics utilize the same species merging (pine and stone marten) methodology as we did, our results are directly comparable and support the belief that these species are common in the Czech Republic. The same holds for badger, another frequently recorded species in our area; it is considered very common, widespread and with the population tending to increase in the country (Anděra and Červený 2009).

As for other species, the weasel and stoat are also considered to be common, but data on animals that had been shot are missing since neither species is on the hunted species list. The fairly low numbers of records of these species (Table 1) can be due to several factors. First, weasels and stoats travel shorter distances, their home ranges are

smaller and show more restricted habitat preferences (stoats prefer wetter habitats, weasels open ones; Fig. 3; Hunter 2011, McDonald et al. 2016), which eliminates some of our trapping locations. Second, a small body size can cause the animal to be less visible, allowing it to pass by uncaptured by the camera trap, including walking through bushes rather than on a path which is preferred by larger animals. It is therefore likely that the recording bias was higher for these species and the captures may reflect less reliably their true population trends. This is, however, not caused by the inability of the traps to capture them due to their small body size because the traps were activated by even smaller animals such as mice or even larger insects.

Alien species

The only non-native species recorded in the study area is the golden jackal. The status of this species is unclear, as it cannot be considered invasive, but we also do not consider it native because its historical range in Europe never reached these latitudes at least during the Holocene (Pyšková et al. 2016). Of the invasive species of carnivores in the Czech Republic – raccoon (*Procyon lotor*), raccoon dog (*Nyctereutes procyonoides*) and American mink (*Neovison vison*) – none were recorded during the year. This was not surprising for the raccoon, which is not widespread in the country as yet, but it was surprising for the American mink, which started spreading rapidly in the 1990s and is now reported as widespread throughout all regions of the Czech Republic. Similarly, raccoon dogs, also reported as widespread by national grid mapping (Anděra and Červený 2009, Anděra 2017b), are believed to be opportunistic generalists colonizing almost any location where water, food and resting opportunities are available. The absence of raccoon dog in our study area is unlikely to be caused by interspecific competition with foxes and badgers as these species were shown to permanently coexist in many regions of their syntopic occurrence (Sidorovich et al. 2000, Drygala and Zoller 2013). One feasible explanation could be the shyness of the species. While in Japan they wander close to human settlements, in Europe they tend to avoid them (Kauhala 1995, Drygala et al. 2008, Kauhala and Salonen 2012). Moreover, raccoon dog inhabits middle elevations in the Czech Republic and is quite rare below 200 m a.s.l, i.e. the altitude of our study area (Anděra and Gaisler 2012). The obvious contradiction between the widespread occurrence in grid cells at the national scale and absence from our local records raises the question to what extent can we extract the information on carnivores from the traditional sources (hunting statistics and questionnaires).

Habitat preferences, seasonal dynamics and circadian activity of the carnivore species studied

The red fox preferred wetlands in our study, but it is a habitat generalist, with other habitats represented almost equally. This agrees with the fact that fox was the most

common carnivore in our study. It is not restricted by particular habitat preferences, therefore it can prosper anywhere, even in cities, where their population densities sometimes reach higher numbers than in natural habitats (Bateman and Fleming 2012). The opportunistic omnivore diet of this species allows for a low level of habitat specialization, especially in the Czech cultural landscape with plentiful food sources (for example numerous records of hares in our camera traps). Martens were represented equally in all habitats except shrubby grassland, reflecting the pine marten's preference for more wooded areas (Anděra and Horáček 2005). Based on habitat preferences of the marten species occurring in the Czech Republic, we assume that most of the animals were individuals of the pine marten. Badgers were mainly present in the dry habitats and avoided wetlands and floodplain forests where they cannot dig their deep burrows in wet soils. Only a few records of badgers were made in wetlands, but we assume the individual animals were just passing through, not being permanent residents, as they were not photographed repeatedly. The weasel was mostly present in the shrubby grassland, reflecting its preference for open habitats (McDonald et al. 2016). As for the other species whose habitat affiliations were not tested statistically due to the low number of records, all of them occurred in supposed habitats typical for them, confirming they prefer certain environmental conditions.

The quantitatively documented patterns in the seasonal circadian activity were most pronounced in the red fox and can be related to reproductive period. Foxes were recorded with a significantly lower frequency in the spring, which is the season of cub rearing, when the mother spends more time in the den with the young, and the father staying nearby to help with care of the cubs (Macdonald 1979). During the rest of the year the activity of foxes was quite evenly distributed and increased again in November and December – this could be related to a greater effort needed to secure food. Quite the opposite results were shown for the badger, which were not active at all during heavy snowfall and frost. This is because in harsh conditions badgers retire to winter sleep (Matyáščík et al. 2000). Martens do not show any significant variation in seasonal dynamics, since they are habitat and food generalists and thus are active throughout the year; lower numbers in May can be also related to the rearing of the young.

Most of our carnivores have crepuscular or nocturnal activity (Anděra and Červený 2009). Foxes were most active early in the morning (4–5) and evening (19–22) hours, but the pattern varied with respect to season. In summer, the foxes are more active during the daylight – this is caused by the fact that when the female is rearing the cubs, she stays out longer to hunt (Harris and Yalden 2008). It also needs to be noted that for all species except the red fox, the differences in proportions of records taken at daylight vs. night disappear, or are smaller, if the different length of the day in particular seasons is taken into account. The fox is not strictly nocturnal in any season, unlike the badger, which was captured in daylight in only 2% of all the records. Martens were more nocturnal than foxes, although in the summer they were also more active during the day (about one third of the records), while in winter they were almost exclusively active at

night. The weasel and stoat were both more active during the day, confirming common knowledge (Anděra and Horáček 2005, Samson and Raymond 2009), the polecat was recorded mostly at night, although not entirely, and the golden jackal was most active early in the morning (Pyšková et al. 2016).

Conclusions

Our study is the first that provides systematically collected quantitative data, made possible by employing a relatively new technology, to assess the frequency of occurrence of central-European carnivore species. In general, our results confirm the known historical, largely anecdotal information on the ecology of the species as reported in the faunal literature. Although there are no quantitative historical data to which our results can be compared, it appears that ecological preferences of the carnivores in our study system have not changed much, if at all, while the central-European landscape has changed immensely in the past century due to human activities. The landscape has turned into a mosaic of human settlements, infrastructure, industrial or agricultural land and patches of semi-natural habitats, with even the latter not free from the influence of people in the form of management or tourism.

The results presented in our study further indicate that carnivores are fairly frequent in such a modern landscape, and the majority of species successfully adapted to the changes that have occurred over the last century. Since the industrial revolution, agricultural production, as well as urbanization and other human-related disturbances, have significantly increased. However, in last few decades these trends were complemented by decreasing direct human pressure (including hunting) driven by the decline of the traditional rural way of life and increasing areas of forests and shrubs due to decreasing needs for food production in less fertile regions. It is possible that due to these changes, the landscape was becoming increasingly more suitable for wildlife. More studies are needed for confirmation of the broader generalizations of these trends, but that the mesocarnivores are successfully inhabiting the open landscape is good news, even considering the limitations of our regional-scale study.

Acknowledgements

The research was supported by long-term research development project RVO 67985939 (The Czech Academy of Sciences) and from Praemium Academiae award from The Czech Academy of Sciences to PP. We thank Barbora Pyšková, Jana Pyšková, Markéta Stránská, Pavel Vebr, Jakub Žák, Adam Tureček and Karolína Majerová for accompanying the first author on some of the field trips. Pavel Pipek kindly helped with sorting camera-trap images. We thank Laura Meyerson for improving our English, and two anonymous reviewers for their valuable comments.

References

- Ahumada JA, Silva CEF, Gajapersad K, Hallam C, Hurtado J, Martin E, McWilliam A, Mugerwa B, O'Brien T, Rovero F, Sheil D, Spironello WR, Winarni N, Andelman SJ (2011) Community structure and diversity of tropical forest mammals: data from a global camera trap network. *Philosophical Transactions of the Royal Society London B* 366: 2703–2711. <https://doi.org/10.1098/rstb.2011.0115>
- Anděra M (2017a) Mapování druhů. Savci v České republice. Biological Library – BioLib. <http://www.biolib.cz>
- Anděra M (2017b) Mapa rozšíření *Nyctereutes procyonoides* v České republice. In: Zicha O (Ed.) Biological Library – BioLib. <http://www.biolib.cz/cz/taxonmap/id50>
- Anděra M, Červený J (2009) Velcí savci v České republice. Rozšíření, historie a ochrana. 2. Šelmy (Carnivora). Národní muzeum, Praha, 216 pp.
- Anděra M, Gaisler J (2012) Savci ČR. Academia, Praha, 288 pp.
- Anděra M, Hanzal V (1996) Atlas rozšíření savců v České republice. Předběžná verze. II. Šelmy (Carnivora). Národní muzeum, Praha, 64 pp.
- Anděra M, Horáček I (2005) Poznáváme naše savce. Sobotáles, Praha, 327 pp.
- Baruš V, Bauerová Z, Kokeš J, Král B, Lusk S, Pelikán J, Sládek J, Zejda J, Zima J (1989) Červená kniha ohrožených a vzácných druhů rostlin a živočichů ČSSR. 2. Kruhoústí, ryby, obojživelníci, plazi, savci. Státní zemědělské nakladatelství, Praha, 136 pp.
- Baruš V, Zejda J (1981) The European otter (*Lutra lutra*) in the Czech Socialistic Republic. *Acta Scientiarum Naturalium / Academiae Scientiarum Bohemicae* Brno 22: 1–33.
- Bateman PW, Fleming PA (2012) Big city life: carnivores in urban environments. *Journal of Zoology* 287: 1–23. <https://doi.org/10.1111/j.1469-7998.2011.00887.x>
- Braczkowski AR, Balme GA, Dickman A, Fattebert J, Johnson P, Dickerson T, Macdonald DW, Hunter L (2016) Scent lure effect on camera-trap based leopard density estimates. *PLoS ONE* 11: e0151033. <https://doi.org/10.1371/journal.pone.0151033>
- Burton AC, Neilson E, Moreira D, Ladle A, Steenweg R, Fisher JT, Bayne E, Boutin S (2015) Wildlife camera trapping: a review and recommendations for linking surveys to ecological processes. *Journal of Applied Ecology* 52: 675–685. <https://doi.org/10.1111/1365-2664.12432>
- CENIA (2012) CORINE Land Cover 2012. Česká agentura životního prostředí, <http://www1.cenia.cz/www/node/595>
- Český statistický úřad (2016) Počet obyvatel v regionech soudržnosti, krajích a okresech České republiky k 1. 1. 2016. <https://www.czso.cz/csu/czso/pocet-obyvatel-v-obcích>
- Crawley MJ (2007) *The R book*. Wiley and Sons, Chichester. <https://doi.org/10.1002/978-0470515075>
- Drygala F, Stier N, Zoller H, Boegelsack K, Mix HM, Roth M (2008) Habitat use of the raccoon dog (*Nyctereutes procyonoides*) in north-eastern Germany. *Mammalian Biology* 73: 371–378. <https://doi.org/10.1016/j.mambio.2007.09.005>
- Drygala F, Zoller H (2013) Spatial use and interaction of the invasive raccoon dog and the native red fox in Central Europe: competition or coexistence? *European Journal of Wildlife Research* 59: 683–691. <https://doi.org/10.1007/s10344-013-0722-y>
- Foster RJ, Harmsen BJ (2012) A critique of density estimation from camera-trap data. *Journal of Wildlife Management* 76: 224–236. <https://doi.org/10.1002/jwmg.275>

- Harris S, Yalden D (2008) Mammals of the British Isles: handbook. Fourth edition. The Mammal Society, London, 799 pp.
- Hunter L (2011) Carnivores of the world. Princeton University Press, Princeton, 240 pp.
- Jennelle CS, Runge MC, MacKenzie DI (2002) The use of photographic rates to estimate densities of tigers and other cryptic mammals: a comment on misleading conclusions. *Animal Conservation* 5: 119–120. <https://doi.org/10.1017/S1367943002002160>
- Kaplan Z (2012) Flora and phytogeography of the Czech Republic. *Preslia* 84: 505–573.
- Karanth KU (1995) Estimating tiger *Panthera tigris* populations from camera trap data using capture–recapture models. *Biological Conservation* 71: 333–338. [https://doi.org/10.1016/0006-3207\(94\)00057-W](https://doi.org/10.1016/0006-3207(94)00057-W)
- Karanth KU, Nichols JD (1998) Estimation of tiger densities in India using photographic captures and recaptures. *Ecology* 79: 2852–2862. [https://doi.org/10.1890/0012-9658\(1998\)079\[2852:EOTDII\]2.0.CO;2](https://doi.org/10.1890/0012-9658(1998)079[2852:EOTDII]2.0.CO;2)
- Kauhala K (1995) Changes in distribution of the European badger *Meles meles* in Finland during the rapid colonization of the raccoon dog. *Annales Zoologici Fennici* 32: 183–191. <http://www.sekj.org/PDF/anzf32/anz32-183-191.pdf>
- Kauhala K, Salonen L (2012) Does a non-invasive method – latrine surveys – reveal habitat preferences of raccoon dogs and badgers? *Mammalian Biology* 77: 264–270. <https://doi.org/10.1016/j.mambio.2012.02.007>
- Kutal M (2017) Pozvolný návrat vlků a dalších šelem. *Fórum ochrany přírody* 2017/1: 33–36.
- Kutal M, Váňa M, Bojda M, Turbaková B, Krojerová J, Hulva P, Černá Bolfíková B, Woznicová V, Pospíšková J, Beneš J, Kutalová L, Kristianová J, Machková J, Flousek J, Šimurda J, Kafka P, Žák L, Tomášek V, Romportl D (2016) Monitoring velkých šelem a kočky divoké ve vybraných lokalitách soustavy Natura 2000. Hnutí DUHA, Olomouc. <http://monitoring.selmy.cz/data/publications/studie-monitoring-n2000-final.pdf>
- Lozano J, Casanovas JG, Virgós E, Zorilla JM (2013) The competitor release effect applied to carnivore species: how red foxes can increase in numbers when persecuted. *Animal Biodiversity and Conservation* 36.1: 37–46.
- Macdonald DW (1979) Helpers in fox society. *Nature* 282: 69–71. <https://doi.org/10.1038/282069a0>
- Manzo E, Bartolommei P, Rowcliffe JM, Cozzolino R (2011) Estimation of population density of European pine marten in central Italy using camera trapping. *Acta Theriologica* 57: 165–172. <https://doi.org/10.1007/s13364-011-0055-8>
- Matouch O, Vitásek J, Semerád Z, Malena M (2006) Elimination of rabies in the Czech republic. *Developmental Biology* 125: 141–143.
- Matouch O, Vitásek J, Semerád Z, Malena M (2007) Rabies-free status of the Czech republic after 15 years of oral vaccination. *Revue Scientifique et Technique* 26: 577–584. <https://doi.org/10.20506/rst.26.3.1762>
- Matyáščík T, Bičík V, Řehák L (2000) Jezevec lesní, jeho biologie a význam v ekosystému. Venator, Praha, 191 pp.
- Mazák V (1964) Několik poznámek o rodu *Lutreola* Wagner 1841 v Československu. *Lynx* 3: 17–29.
- McCallum J (2013) Changing use of camera traps in mammalian field research: habitats, taxa and study types. *Mammal Review* 43: 196–206. <https://doi.org/10.1111/j.1365-2907.2012.00216.x>

- McDonald RA, Abramov AV, Stubbe M, Herrero J, Maran T, Tikhonov A, Cavallini P, Kranz A, Giannatos G, Kryštufek B, Reid F (2016) *Mustela nivalis*. The IUCN Red List of Threatened Species 2016, e.T70207409A45200499.
- O'Connell AF, Nichols JD, Karanth KU (2011) Camera traps in animal ecology. Methods and analyses. Springer, New York, 271 pp. <https://doi.org/10.1007/978-4-431-99495-4>
- Preisler J (1998) Sarkoptový svrab u divoce žijících lišek obecných (*Vulpes vulpes*) na území České republiky. *Lynx* 29: 99–100.
- Pyšková K (2017) Nepůvodní druhy šelem v České republice. *Forum ochrany přírody* 2017/3: 44–45.
- Pyšková K, Storch D, Horáček I, Kauzál O, Pyšek P (2016) Golden jackal (*Canis aureus*) in the Czech Republic: the first record of a live animal and its long-term persistence in the colonized habitat. *Zookeys* 641: 151–163. <https://doi.org/10.3897/zookeys.641.10946>
- Řehák J, Řeháková B (1986) Analýza kategorizovaných dat v sociologii. Academia, Prague, 397 pp.
- Rowcliffe JM, Field J, Turvey ST, Carbone C (2008) Estimating animal density using camera traps without the need for individual recognition. *Journal of Applied Ecology* 45: 1228–1236. <https://doi.org/10.1111/j.1365-2664.2008.01473.x>
- Samson C, Raymond M (2009) Daily activity pattern and time budget of stoats (*Mustela erminea*) during summer in southern Québec. *Mammalia* 59: 501–510. <https://doi.org/10.1515/mamm.1995.59.4.501>
- Shulman B, Wagner BD, Grunwald GK, Engeman RM (2016) Evaluation of estimation quality of a general paradigm for indexing animal abundance when observations are counts. *Ecological Informatics* 32: 194–201. <https://doi.org/10.1016/j.ecoinf.2016.02.004>
- Sidorovich VE, Polozov AG, Lauzhel GO, Krasko DA (2000) Dietary overlap among generalist carnivores in relation to the impact of the introduced raccoon dog *Nyctereutes procyonoides* on native predators in northern Belarus. *Zeitschrift für Säugetierkunde – International Journal of Mammalian Biology* 65: 271–285.
- Skumatov D, Abramov AV, Herrero J, Kitchener A, Maran T, Kranz A, Sándor A, Saveljev A, Saviour-Soubelet A, Guinot-Ghestem M, Zuberogoitia I, Birks JDS, Weber A, Melisch R, Ruetten S (2016) *Mustela putorius*. In: The IUCN Red List of Threatened Species 2016: e.T41658A45214384.
- Sollmann R, Mohamed A, Samejima H, Wilting A (2013) Risky business or simple solution: relative abundance indices from camera-trapping. *Biological Conservation* 159: 405–412. <https://doi.org/10.1016/j.biocon.2012.12.025>
- Stokstad E (2015) Bringing back the aurochs. *Science* 350: 1144–1147. <https://doi.org/10.1126/science.350.6265.1144>
- Trolle M, Kery M (2003) Estimation of ocelot density in the Pantanal using capture–recapture analysis of camera trapping data. *Journal of Mammalogy* 84: 607–614. [https://doi.org/10.1644/1545-1542\(2003\)084<0607:EOODIT>2.0.CO;2](https://doi.org/10.1644/1545-1542(2003)084<0607:EOODIT>2.0.CO;2)
- Wilson G, Delahay RJ (2001) A review of methods to estimate the abundance of terrestrial carnivores using field signs and observation. *Wildlife Research* 28: 151–164. <https://doi.org/10.1071/WR00033>